University of Southampton

Faculty of Medicine, Health and Life Science

School of Medicine

The role of relaxin in the regulation of human liver and kidney fibrosis

Annette Louise Hayden M.Sc.

Submitted for the degree of Doctor of Philosophy

April 2009

UNIVERSITY OF SOUTHAMPTON

ABSTRACT

SCHOOL OF MEDICINE

FACULTY OF MEDICINE, HEALTH AND LIFE SCIENCES

Doctor of Philosophy

The role of relaxin in the regulation of human liver and kidney fibrosis

by Annette Hayden M.Sc.

Liver fibrosis has a range of aetiologies and is a global cause of mortality. A critical effect of liver fibrosis which also increases mortality is portal hypertension. The hepatic stellate cell is accepted as a major progenitor of liver myofibroblasts, which have been shown to be a major source of collagen and extracellular matrix proteins that disrupt liver architecture and function. Relaxin is a hormone involved in remodelling of extracellular matrix in the uterus and cervix and is known to increase renal blood flow in pregnancy. It has been implicated in the regulation of fibrosis in animal models and to modify the cell biology of hepatic stellate cells in vitro. I have demonstrated the profile of expression of relaxin receptors in primary human stellate cells (HSC), showing them to express RXFP-1, 3 and 4. Using a cAMP assay I confirm these receptors to be functional, with RXFP-1 positively and RXFP-3 and 4 negatively coupling to cAMP. The expression of RXFP-1 is coupled with the level of activation, demonstrating a possible role for H2-relaxin in the regulation of HSC. I have established a dynamic regulation of fibrotic mediators and HSC activation markers, including a reduction in α-SMA, TIMP-1 and TGF-β with increases in MMP-1 and MMP-2, consistent with H2-relaxin having potentially therapeutic antifibrotic effects by increasing the fibrolytic phenotype. In addition through the use of gel contraction assays I demonstrate that H2-relaxin reduces serum or endothelin-1 induced HSC contraction. Through the use of siRNA I have confirmed that H2-relaxin mediates its regulation of fibrotic mediators and HSC activation markers as well as the inhibition of gel contraction through the relaxin receptor RXFP-1. I have evidence to suggest that the inhibition of contraction may in part be via nitric oxide release in HSC. In conclusion I propose that RXFP-1 is a potential therapeutic target in end stage human liver disease, targeting fibrosis and portal blood hypertension via both resolution of the phenotypic collagen deposition and vascular constriction associated with the human hepatic stellate cell.

List of Contents

List of Figures

List of Tables

National and international presentations arising from this thesis

Hayden.A.L, Foster.B.E, Smart.D, Collins.J.E, Iredale.J.P, Princivalle.M. Relaxin reduces the fibrotic phenotype of LX-2 and primary hepatic stellate cells (HSC) in culture.

- Oral presentation at the **British Association for the Study of Liver disease,** London 2007.

Hayden.A.L, Smart.D, Iredale.J.P, Collins.J.E, Yea.C, Princivalle.M. Investigation of Relaxin in fibrotic liver disease.

- Poster presentation at the **American Association for the Study of Liver disease,** Boston 2006.

Declaration of Authorship

I, Annette Louise Hayden

declare that the thesis entitled

The role of relaxin in the regulation of human liver and kidney fibrosis

and the work presented in this thesis is my own, and has been generated by me as the result of my own original research. I confirm that:

- this work was done wholly or mainly while in canditure for a research degree at this university;
- where any part of this thesis has previously been submitted for a degree or any other qualification at this university or any other institution, this has been clearly stated;
- where I have consulted the published work of others, this is always clearly attributed;
- where I have quoted from the work of others, the source is always given. With the exception of such quotations, this thesis is entirely my own work;
- I have acknowledged all main sources of help;
- Where the thesis is based on work done by myself jointly with others, I have made clear exactly what was done by others and what I have contributed myself;
- None of this work has been published before submission.

Signed: ……...

Date: ……...

Acknowledgements

First and foremost I would like to thank my supervisors Dr Marc Princivalle, Dr Jane Collins and Professor John Iredale who have not only given me the opportunity to carry out this PhD but given support and guidance along the way. I would also like to make a particular mention to Dr Jane Collins for not only agreeing to take on my supervision half way through the project but for giving me so much good sound advice and Dr Marc Princivalle for being a friend and not just my boss!

I would like to thank everybody in the lab at Ferring and in the liver group, especially Becky, Dave, Lucy, Jess, Anne, Jane, Gayle, Sara, Tim, Mannish and Andy for being helpful colleagues and good friends who made the lab a brighter place to be, although I won't miss your singing Jess! I would also like to thank the histology unit and Dr Paul Bass for their help with immunohistochemistry techniques and interpreting these results.

I would like to make a special mention to John for putting up with me for the last few years, for always being understanding, supportive and letting me take over the office and crashing your computer more times then I care to remember! Last but by certainly no means least I would like to thank my family, in particular mum and dad, whom without I simply could not have done it. Having you guys there for me unconditionally, has given me the confidence to take on new challenges.

Abbreviations

ADH- Antidiruetic Hormone

ADAM protein- A Disintegrin and Metalloproteinase-domain protein

ALD- Alcoholic Liver Disease

Ang- Angiotensin

α-SMA- Alpha Smooth Muscle Actin

AP-1- Activator Protein-1

ATP- Adenosine Triphosphate

AVP- Vasopressin

BDNF- Bone Derived Neurotrophic Factor

cAMP- 3'-5' cyclic adenosine monophosphate

CAMs- Cell Adhesion Molecules

CCl_4- Carbon Tetrachloride

CD8- Cluster of Differentiation 8

C-FOS- Cellular Finkel-biskis-jinkins murine OsteoSarcoma viral (v-fos) oncogene homolog

cGMP- cyclic Guanosine Monophosphate

C-JUN- cellular jun oncogene

CKD- Chronic Kidney Disease

CLD- Chronic Liver Disease

C-MYC- Cellular- Myelocytomatosis

CREB- cAMP response element binding proteins

CTGF- Connective Tissue Growth Factor

CSF-Colony Stimulating Factor

CYP2E1- Cytochrome P450 family 2, subfamily E, polypeptide 1

CXCR4- CXC Chemokine Receptor 4

DAG- Diacylglycerol

DISC- Death Inducing Signaling Complex

DMEM- Dulbecco's Modified Eagle's Medium

D-CDK4- Cyclin Dependent Kinase 4

DNA- Deoxyribonucleic acid

DSRS- Distal Splenorenal Shunts

EC_{50}- half maximal effective concentration

E-CDK2- Cyclin Dependent Kinase 2

ECM- Extra-Cellular Matrix

EDRF- Endothelial Derived Relaxing Factor

EMA- Epithelial Membrane Antigen

EMT- Epithelial Mesenchymal Transition

ET-1- Endothelin-1

ET_A- Endothelin receptor A

ET_B- Endothelin Receptor B

FADD- Fas-associated Death Domain

FasL- Fas Ligand

FBS- Fetal Bovine Serum

FGF- Fibroblast Growth Factor

FSGS- Focal Segmental Glomerularsclerosis

FLT-3- Fms-related tyrosine kinase 1 (vascular endothelial growth factor/vascular permeability factor receptor) 3

GAGs- Glycosaminoglycans

GAPDH- Glyceraldehyde 3-phosphate dehydrogenase

GBM- Glomerular Basement Membrane

GFR- Glomerular Filtration Rate

GFR- Growth Factor Reduced

GR- Glucocorticoid Receptors

GRE- Glucocorticoid Response Elements

GSH- Glutathione

HA- Hyaluronic Acid

HAV- Hepatitis A Virus

HBV- Hepatitis B Virus

HBSS- Hanks Buffered Salt Solution

HCV- Hepatitis C Virus

HCC- Hepatocellular carcinoma

HDV- Hepatitis D Virus

HEV- Hepatitis E Virus

H+E- Haematoxylin and Eosin

HGV- Hepatitis G Virus

HFE- Hemochromatosis protein

HLA- Human Leukocyte Antigen

HSC- Hepatic Stellate Cell

IL-1- Interleukin 1

IL-2- Interleukin 2

IL-4- Interleukin 4

IL-6- Interleukin 6

IL-13- Interleukin 13

INF-γ- Interferon gamma

INSL3- Insulin-Like 3 receptor

INSL4- Insulin-Like 4 receptor

INSL5- Insulin-Like 5 receptor

INSL6- Insulin-Like 6 receptor

IP_3- Inositol triphosphate

IP-10/CXCL-10- Chemokine (C-X-C-motif) Ligand 10

LDH- Lactose Dehydrogenase

LDLa- Low Density Lipoprotein class-A

L-NAME- N-Nitro-L-Arginine Methyl Ester

LTA- Lotus Tetregonolobus Antigen

MAPCs- multipotent adult progenitor cells

MAPK- Mitogen Activated Protein Kinase

MCD- Minimal Change Disease

MGN- Membranous Glomerulonephritis

MHC- Major Histocompatibility Complex

MLCK- Myosin Light Chain Kinase

MMP- Matrix Metalloproteinase

mRNA- messenger Ribonucleic Acid

MTS- 3(4,5-dimethylthiazol-2-yl)-5-(3-carboxymethoxyphenyl)-2-(4-sulfophenyl)-2H-tetrazolium, inner salt

NAD/NADH- nicotinamide adenine dinucleotide

NAFLD- Non-alcoholic fatty liver disease

NASH- Non-alcoholic steatohepatitis

NF-κB – Nuclear Factor-kappa B

NGF- Nerve Growth Factor

NK- Natural Killer

NT-4- Neurotrophic Factor 4

OSCR- Oil Supported Collagen Retraction

PARP 1- Poly (ADP-ribose) polymerase family, member 1

PBS- Phosphate Buffered Saline

PDGF- Platelet derived growth factor

PKA- Protein Kinase A

PKC- Protein Kinase C

PKG- Protein Kinase G

PLC- Phospholipase C

PTX- Pertussis Toxin

qRT-PCR- Quantitative Reverse Transcription Polymerase Chain Reaction

RACK- Receptor Activated C-Kinase

RANTES/CCL5- Chemotactic Cytokine 5

RNA- Ribonucleic Acid

ROS- Reactive Oxygen Species

RT-PCR- Reverse Transcription Polymerase Chain Reaction

RXFP- Relaxin Family Peptide Receptor

SDF- Stromal Derived Factor

siRNA- short interfering ribonucleic acid

SMAD- Small Mothers Against Decapentaplegics

STAT-3- Signal Transducer and Activator of Transcription 3

sFasL- Souble Fas Ligand

TGF- Transforming Growth Factor

Tie 1- Tyrosine Kinase with immunoglobulin-like and EGF-like domains 1

Tie 2- Tyrosine Kinase with immunoglobulin-like and EGF-like domains 2

TIMP- Tissue Inhibitor of Matrix Metalloproteinase

TNF- Tumour Necrosis Factor

TIPS- Transjugular Intraheptic Portosystemic Shunting

Trk- Tyrosine Kinase

VE-Cadherin- Vascular Endothelial Cadherin

VEGF- Vascular Endothelial Growth Factor

Vmax- Concentration where maximal response is reached

Chapter 1

Introduction

1.1 The burden of chronic liver disease, a worldwide 'epidemic'

Chronic Liver disease (CLD) is a worldwide public health problem. In the UK deaths from CLD have increased eight times in men and seven times in women over the last three decades (Chief medical officer's report, 2001). The disease burden of CLD in the UK, encompassing a number of aspects including frequency, longevity, morbidity, mortality, quality of life and finance, is likely to be underestimated at the present time and is only set to increase in the coming decades. CLD is characterised by chronic damage to the liver, which can lead to irreversible scarring eventually impairing its normal function. The extent of injury increases over time with the persistence of injurious stimuli and ultimately leads to liver failure and the need to transplant if left untreated. This is associated with serious physical and psychological morbidity and mortality and cost to the National Health Service. CLD has many different aetiologies ranging from viral hepatitis to autoimmune diseases.

In the UK mortality rates from CLD are eleven per one hundred thousand and rising. In the year 2000 over seventeen percent of deaths due to CLD were from alcoholic liver disease (ALD) but increasingly non-alcoholic fatty liver disease (NAFLD), as a result of the relatively recent epidemic of obesity and increasing levels of type 2 diabetes, is fast becoming a major problem. The group with the poorest outcome also represent the patients with alcoholic liver disease (ALD), especially if this is combined with hepatitis C infection and obesity, and consequently these patients are more likely to have secondary complications. The five year survival rate for patients without complications given a transplant is 75% but if they develop secondary complications it is reduced to less then 50% (Roderick, 2004). In the US between 1997 and 2002, seventy two people per one hundred thousand were diagnosed with CLD which made it the tenth leading cause of death. Hepatitis C and alcoholic cirrhosis made up over 80% of the diagnosed cases (Kim, 2002).

The scale of the problem is almost certainly being underplayed by these statistics as the number of cases that are not diagnosed is still relatively high. Many people are asymptomatic for many years due to the time it takes from initial injury, e.g. Hepatitis C infection, to evolution to cirrhosis leaving the disease undetected for many years. Many patients only present at clinic with advanced fibrosis or cirrhosis when much of the function and regenerative capacity of the liver has been lost. The largest groups of people that develop end stage chronic liver disease are traditionally the 'hard to reach patients' such as intravenous drug users and may go undiagnosed even after death (Roderick et al., 2004).

There is clear evidence that better diagnostics and treatments that can slow the progression of the disease are urgently needed, as there is already a shortage of donor organs and this treatment does not come without its own risks and complications.

1.2 The causes of liver disease

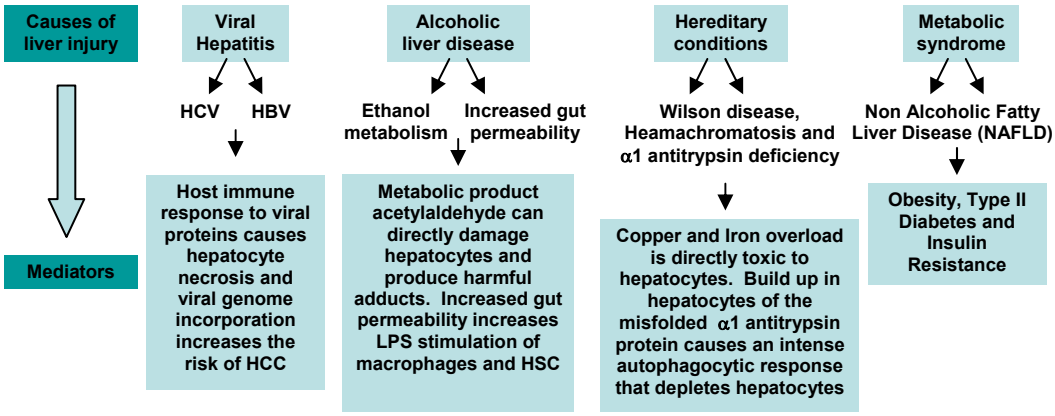

Figure 1.1. Flow diagram outlining the main causes of liver disease which will be discussed in further detail below.

1.2.1 Persistent Viral Infection

The term viral hepatitis is used to encompass the infection of the liver by a group of viruses that have particular affinity for the liver. At present there are six hepatitis viruses known to infect humans and they have been classed A-G. Hepatitis B and C are the most common cause of chronic liver disease and cirrhosis worldwide. There are other systemic viral infections that can affect the liver, for example yellow fever and the Epstein Barr virus, but these do not carry a chronic risk of liver damage (Kumar et al., 2005).

Hepatitis A virus (HVA) is self limiting disease with an incubation period of 2-6 weeks. It is spread by ingesting contaminated food or water and outbreaks are usually in areas where people live in close contact and in unsanitary conditions. The HVA infectious agent is a small non-enveloped single stranded RNA picornavirus that occupies its own genus, ultrastructurally it is a icosahedral capsid around 27 nm in diameter and does not cause chronic hepatitis (Cuthbert, 2001). Hepatitis E virus (HEV) is similar to HAV due to transmission being through water-borne infection. A characteristic of HEV is a high mortality rate among pregnant women, which approaches 20%. HEV is an un-enveloped single stranded RNA virus with an average incubation period of around 6 weeks. The RNA genome is around 7.6 kb and the active infection can cause acute hepatitis but is not persistent or chronic (Mast and Krawczynski, 1996). Hepatitis D virus (HDV) is a unique single stranded RNA virus that is replication defective and will only cause infection if co-infected with HBV. The virus is then encapsulated by the hepatitis B surface antigen and is then dependent on the genetic information provided by the HBV virus for multiplication and infectivity. The co-infection can increase the risk of developing fulminant disease then with HBV alone. The co-infection can also cause acute severe hepatitis in previously healthy carriers of HBV and chronic progressive disease culminating in cirrhosis develops in 80% of patients (Hoofnagle, 1989;Lai, 1995). Hepatitis G virus (HGV) bears similarity to HCV.

It is a single stranded RNA virus that is transmitted through contaminated blood or possibly sexual contact. In 75% of infection HGV is cleared from the plasma, the remaining cases become chronic. The site of replication is more likely to be the mononuclear cells and therefore has been inappropriately named. Infection does not cause damage to the liver and in fact to date no pathological effects of the virus have been found. It is commonly co-infected with HIV and surprisingly can show some protective affects against the HIV disease (Pomerantz and Nunnari, 2004).

Hepatitis B virus (HBV) is a particular problem when considering liver fibrosis. A member of the hepadanavirus family containing semi-double stranded circular DNA, the mature HBV is a 42 nm spherical double layered Dane particle that has an outer surface envelope of protein, lipid and carbohydrate which encloses an electron dense core. The DNA molecule comprises 3200 nucleotides and all of the HBV genome encodes protein (Ganem and Prince, 2004). HBV is a major global problem, there are around 350 million chronic hepatitis B carriers worldwide and it is estimated that the virus has infected over 2 billion individuals alive today at some point in their life. In the UK the rate of infection is around 1 in 1000. 75% of all chronic carriers live in Asia and the Pacific Rim but in the United States there are an estimated 185,000 new infections per year (Kim, 2002). HBV has a prolonged incubation of 4-26 weeks and the virus remains in the blood during all active episodes of acute or chronic hepatitis. HBV is a hardy virus and can be transmitted not only through blood and body fluids but also secretions such as semen, saliva, sweat, tears and breast milk. There is an effective vaccination against the virus due to the circulating host antibodies effectively neutralising HBV. The vaccine has been effective at reducing prevalence in endemic areas and in people at risk such as health care professionals. HBV can cause acute hepatitis with resolution, chronic hepatitis that may go on to develop cirrohsis and/or hepatocellular carcinoma (HCC), fulminant hepatitis with massive hepatocyte necrosis and is also the backdrop for Hepatitis D infection (Chisari, 2000). HBV infection of the hepatocyte goes

through two phases. The proliferative phase, when the virus is actively replicating inside the hepatocyte, causes a massive influx of lymphocytes (CD8 + cytotoxic T cells), activation of the immune response and increase necrosis/destruction of the hepatocytes. The next phase is the integrative phase where hepatocytes that were infected but not destroyed by the cytotoxic T cells incorporate the viral DNA into the host genome. This reduces the immune response due to the cessation of viral replication and the damage to the liver subsides, but now there is an increased risk of developing HCC (Chisari, 2000).

Hepatitis C virus (HCV) is also a major cause of fibrosis, it is an enveloped virus carrying a positive strand RNA genome, an estimated 3% of the worlds population carry the virus around 200 million (70%) of these chronically (Mast et al., 1999). It is transferred via blood-blood contact, around 60-90% of intravenous drug users carry the virus. There is no vaccination available for HCV unlike HBV (Fabris et al., 1999). These statistics make HCV the most common of all blood-borne infections and accounts for around half of all chronic liver disease patients in the United States (Kim et al., 2002). HCV is closely related to the Hepatitis G virus (HGV), they are both hepacivirus in the flaviviradae family. HCV is an RNA virus with a genome of 9kb that encodes for a single poly-protein of about 3010 amino acids in one single open reading frame. This single protein then undergoes post translational processing to produce functional highly conserved proteins and six less conserved proteins with unknown function. The HCV virus genome is inherently unstable which enables mutations to take place and this gives rise to many different subtypes of the virus. This is why there is no vaccine to the HCV virus unlike the HBV virus which is a more stable DNA virus (Farci P, 2008). The initial incubation period for HCV is 2-26 weeks. The initial infection is usually less severe then HBV infection but due to the HCV ability to evade the hosts immune system, persistent reinfection and chronic hepatitis is more common in HCV affected patients and cirrhosis may develop 5-20 years after the initial acute infection. Over the next decade HCV may become the leading cause of chronic liver

disease in the western world (Farci P, 2008). Hepatitis, particularly HCV, can lead to chronic liver injury resulting in fibrosis. Regardless of aetiology fibrosis can become progressive and lead to cirrhosis. Therefore combining viral therapies with antifibrotic therapies such as H2-relaxin, may augment the benefit previously observed from removing the cause of liver damage.

1.2.2 Alcohol and Toxic Damage

Excessive alcohol consumption is currently the number one cause of liver disease in the western world. This highlights the major differences in lifestyle between westernised society and the rest of the world, when considering liver disease. There are three forms of alcoholic liver disease, hepatic steatosis (fatty liver), alcoholic hepatitis and alcoholic cirrhosis. Steatosis and hepatitis can be independent from one another but cirrhosis represents the end stage of either of the first two conditions. Ethanol and its metabolites can cause fatty change through the increased catabolism of fat by peripheral tissues causing increased delivery of free fatty acids to the liver causing massive enlargement. Ethanol and its metabolites are also believed to be directly toxic to hepatocytes (Tsukamoto and Lu, 2001;Lands, 1995b). This toxicity is understood to be mediated by glutathione depletion, mitochondrial injury, altered metabolism of methionine and cytokine release from Kupffer cells, which then activates HSC. Ethanol is believed to cause damage at the site of metabolism from ethanol to acetylaldehyde. This metabolism is performed by nicotinamide adenine dinucleotide (NAD+) dependent enzyme, alcohol dehydrogenase (Zakhari and Li, 2007). This reaction is performed by alchohol dehydrogenase in the cytosol of the gastric mucosa but can also be performed by cytochrome P-450 (CYP2E1) in liver microsomes and catalase in the liver peroxisomes. Induction of cytochrome P-450 and in particular CYP2E1, increases the catabolism of ethanol and other drugs such as paracetamol in the endoplasmic reticulum, increasing the levels of toxic metabolites and reactive oxygen species in the liver which causes hepatocellular damage. Aldehyde dehydrogenase converts the

toxic acetylaldehyde to acetic acid in the mitochondria and this process also requires NAD+. The consumption of large amounts of alcohol depletes the oxidised NAD+ and causes an excess of the reduced NADH in the liver causing a build up of toxic acetylaldehyde within the cytosol of the hepatocytes (Zakhari and Li, 2007). An excess of NADH over NAD not only reduces the conversion of ethanol to acetic acid but can also stimulate lipid biosynthesis and the oxidation of fatty acids by the mitochondria is decreased. Alcohol induced impaired metabolism of methionine leads to decreased intrahepatic levels of glutathione (GSH) which sensitises the liver to oxidative injury. Acetylaldehyde is toxic due to the formation of adducts with tubulin, this impairs the function of microtubules which results in the decreased transport of lipoproteins from the liver. Antibodies to these adducts have been detected in alcoholics suggesting an autoimmune component causing inflammation of the liver and immune mediated hepatocellular injury. (Adducts are the parts of a metabolised protein that may retain an electrophilic carbonyl group or neutrophilic groups that then attenuate the toxicity of the toxic stimuli within the hepatocytes) (Viitala et al., 2000;Rolla et al., 2000).

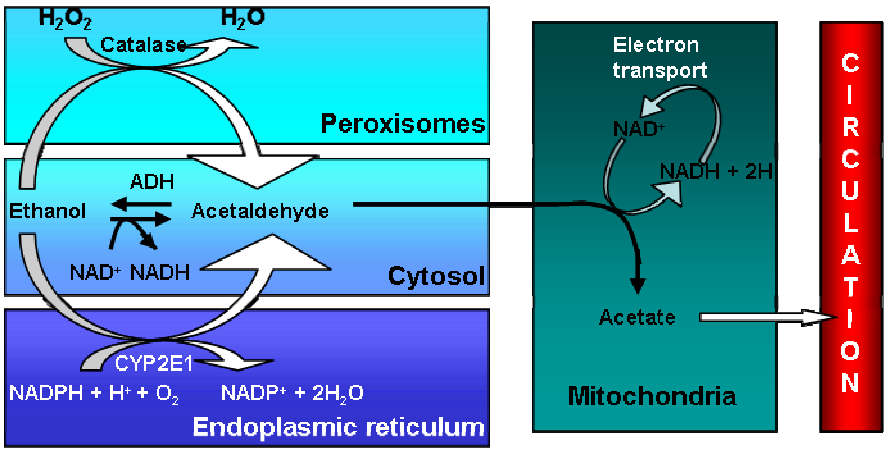

Figure 1.2. Adapted from (Zakhari and Li, 2007). Schematic showing the four compartments peroxisomes, cytosol, endoplasmic reticulum and the mitochondria as sites of ethanol metabolism in the liver. The liver has a limited capacity to oxidise acetate to $C0_2$ using acetyl coenzyme A in the mitochondria TCA cycle and therefore

during high exposure to ethanol the acetate is released into the circulation and transported to organs such as the heart, skeletal muscle and the brain, that have a high capacity to utilize the TCA cycle for this function.

Alcohol increases the permeability of the intestine to bacterial endotoxin, increasing the content in the portal circulation and therefore increasing inflammation within the liver. The inflammation is caused by the activation of Kupffer cells (liver macrophages). The activation of Kupffer cells will initiate the activation of HSC from a quiescent to myofibroblast like state. This process will exacerbate fibrosis in the liver (Thurman, 2000). Alcohol can also induce the release of endothelins from the sinusoidal endothelial cells. Endothelins are potent vasoconstrictors and the hepatic stellate cells in the Space of Disse can react to endothelin by contracting, which can reduce hepatic sinusoidal perfusion causing hypoxia to the regions of hepatocytes that are cut off from the circulation (Rockey, 2001;Rockey and Weisiger, 1996). Alcoholic liver disease is a chronic disorder that is marked by the derangement of vascular perfusion when the disease manifests to alcoholic cirrhosis. Alcohol is a source of calories and in many alcoholics can replace the intake of food, which displaces other nutrients and vitamins leading to malnutrition and vitamin deficiencies (Lands, 1995a). Alcoholic cirrhosis is similar to other forms of cirrhosis with a common feature of portal hypertension (Geerts et al., 2008). Portal hypertension is a lethal condition that leads to the development of ascites and varices which can lead to fatal infection in the oedema of the abdomen or blood loss respectively (Williams and Iredale, 1998).

1.2.3 Hereditary Conditions Leading to Fibrosis

A significant number of cases of liver fibrosis can be attributed to hereditary diseases such as Wilson disease, hemochromatosis and α_1 antitrypsin deficiency. Wilson disease is a autosomal recessive disorder resulting from the bodies inability to excrete excess copper in the bile, which leads to a toxic accumulation

in the cytoplasm of the hepatocytes (Schaefer et al., 1999;Llanos and Mercer, 2002) The disease usually presents in late childhood with viral-hepatitis like symptoms. Wilson disease also causes an accumulation of copper throughout the body but particularly in the liver, connective tissue, eye and the brain. The gene for Wilson disease, designated ATP7B, is on chromosome 12 and encodes a 7.5kb transcript for a transmembrane copper transporting ATPase, located on the hepatocyte canalicular membrane (Llanos and Mercer, 2002). Over 30 mutations of this gene have been identified and the majoritiy of patients are heterozygotes with different mutations on each allele. Defective biliary excretion leads to accumulation of copper in excess of the metallothionein-binding capacity. The accumulation becomes toxic when there is a formation of reactive oxygen species catalyzed by copper. There is usually a lag period of around 5 years before clinical symptoms of the disease appear. The most common presentation is acute or chronic liver disease with increased hepatic copper levels and increased urinary excretion but in many cases there may also be mild behavioural changes or a Parkinson disease like syndrome due to the increased deposition of copper in the brain. Early diagnosis and the long term use of copper chelation therapy has changed the outcome for many patients that in the past would have experienced a progressive chronic hepatitis and unmanageable cirrhosis with a transplant being the only treatment option (Llanos and Mercer, 2002).

Hemochromatosis can be caused by a hereditary condition that affects the absorption of dietary iron resulting in elevated levels of serum iron. This condition can lead to a progressive increase in the iron absorbed and depositied within parenchymal cells of the liver (hepatocytes) and other organs such as the pancreas and heart. Humans do not have a major iron excretory pathway and are therefore particularly susceptible to iron accumulation. In the normal body there is 2-6 grams of iron with 0.5 grams being stored in the liver and 98% of this in the hepatocytes. Fully developed cases of hereditary hemochromatosis can have as much as 50 grams of iron in the body and as much as 1/3 of this can be in the

liver. Fully developed cases can take as long as 50-60 years to develop symptoms and they will all have micronodular cirrhosis, 75-80% will have diabetes and 75-80% will have skin pigmentation (Fletcher and Halliday, 2002). The hereditary condition is due to the mutation of the HFE gene, located on chromosome 6 close to the HLA gene locus (Philpott, 2002). The HFE gene encodes a HLA-class 1 like molecule, expressed in the small intestinal crypt epithelial cells where it complexes with a transferrin receptor enabling the binding of plasma transferrin and its bound iron which is then endocytosed into the regulatory pool in the crypt cell. The mutation of the HFE protein abolishes the crypt cells ability to remove iron from the circulation. This system also acts as the sensing mechanism for systemic iron balance as well as the regulatory iron pool that can set the level of apical iron uptake required (Pietrangelo, 2002). Therefore the system that regulates dietary iron absorption is no longer regulated by the amount of iron in the systemic circulation leading to iron overload. The most common mutation found in 70-100% of cases is the C282Y mutation which substitutes a cysteine to a tyrosine in position 282 of the amino acid sequence, which inactivates the protein. Hereditary hemochromatosis is one of the most common genetic disorders but penetrance even with homozygotes for the C282Y mutation is still only 20%. Males are over 5 times more likely to develop the disease and it tends to be more severe with earlier presentation of symptoms due to women undergoing physiological loss of iron, preventing accumulation (Philpott, 2002). The disease can manifest after 20 grams of iron is stored which is thought to be directly toxic to the tissue through lipid peroxidation by iron catalysed free radicals, the stimulation of collagen synthesis and the interaction of reactive oxygen species (ROS) and iron with DNA leading to lethal injury and the increased predisposition to hepatocellular carcinoma (HCC) (Houglum et al., 1994). Secondary hemochromatosis is the name given to any condition that results in iron overload that is not through the gene mutation. Conditions such as haemolytic anemias require repeated blood transfusions. Left untreated they result in an increased level of iron (iron

overload) in the body. These conditions are classified as a secondary hemochromatosis (Chandrasoma and Taylor, 2005).

α_1 Antitrypsin is a small 394 amino acid glycoprotein, synthesized mainly by hepatocytes. Its main function is as a protease inhibitor of proteins such as elastase, cathepsin G and proteinase 3, which are normally secreted by neutrophils at the site of inflammation (Fairbanks and Tavill, 2008). α_1 Antitrypsin deficiency is an autosomal recessive disorder that manifests with low serum levels of this important protein, which can cause tissue destructive enzymes to become unregulated and this can affect the lung causing pulmonary emphysema (Fairbanks and Tavill, 2008). Patients can also be susceptible to developing liver disease, although liver disease will usually only affect neonates and young adults and has a distinct mechanism compared to the affect in the lung (Perlmutter, 2002;Fairbanks and Tavill, 2008). The gene for α_1 antitrypsin is located on chromosome 14 and is very polymorphic. Up to 75 different genotypes have been found for the protein, some that cause the deficiency and some that have no obvious phenotype. Deficiency variants exhibit a defect in the migration of the translated protein from the endoplasmic reticulum to the Golgi apparatus (Teckman et al., 2002). Only 10% of the individuals with this deficiency variant will exhibit liver disease and this is due to these individuals exhibiting a lag in the endoplasmic reticulum protein degradation pathway. This pathway is essential for quality control, detecting and degrading proteins that have been misfolded or misassembled. The accumulated protein in the hepatocytes is not toxic per se and the liver does not suffer from the lack of protease inhibitor as it is secreted into the circulation for use in other organs (Perlmutter, 2002). The cells response to the lag in the degradation pathway is to increase the autophagocytic response in the hepatocytes. This intense autophagocytic response that may affect the mitochodria of the hepatocytes is probably the cause of hepatocytoxicity in this syndrome. Neonatal hepatitis with jaundice occurs in 10-20% of patients with the deficiency. Attacks of acute

hepatitis may subside to full recovery but in a small number of patients the injury becomes chronic and may lead to cirrhosis (Teckman et al., 2002).

1.2.4 Non-alcoholic fatty liver disease (NAFLD)

Non-alcoholic steatohepatitis (NASH) has been recognised as a major cause of liver fibrosis, it is considered part of the spectrum of non-alcoholic fatty liver disease (NAFLD) (Clark et al., 2002). NASH is characterised by the presence of histological features of steatohepatitis in the absence of significant alcohol consumption. Non-alcoholic liver diseases range from steatosis to cirrhosis and can eventually lead to hepatocarcinoma. Cirrhosis is present in 10-20% of patients at diagnosis (Bataller and Brenner, 2005). NASH is a component of the metabolic syndrome, which is characterised by obesity, type-2 diabetes mellitus with insulin resistance as a common feature (Kanda et al., 2005). Men and women are equally affected and patients are largely asymptomatic. NAFLD is thought to account for 70% of chronic hepatitis of unknown cause and 10-30% of these patients will develop cirrhosis. There is also evidence that NAFLD can contribute to the progression of other liver diseases, such as HCV infection and alcoholic liver disease (Clark et al., 2002).

1.3 Normal architecture of the liver and biliary tract

1.3.1 Normal liver and biliary tract physiology

The word hepatic is often used to describe medical terms relating to the liver. Hepatic comes from the Greek word hĕpar, meaning repairable, indicating this organ can regenerate itself spontaneously in the case of a lesion. Basic anatomy divides the liver into four lobes and two ligaments (figure 1.3). The left and right anatomical lobes can be seen from the anterior side and the caudate (superior) above the quadrate lobe can be seen from the inferior side (Saxena et al., 1999). Each lobe is made up of lobules and these all contain veins that join the hepatic

vein carrying blood out of the liver. The two ligaments are the falciform and the teres ligament. The falciform ligament attaches the liver to the anterior abdominal wall and the diaphragm and the ligament teres extends from the falciform to the umbilicus. The liver is encapsulated with a network of connective tissue named the Glissons capsule (Rapport., 1958;Saxena et al., 1999).

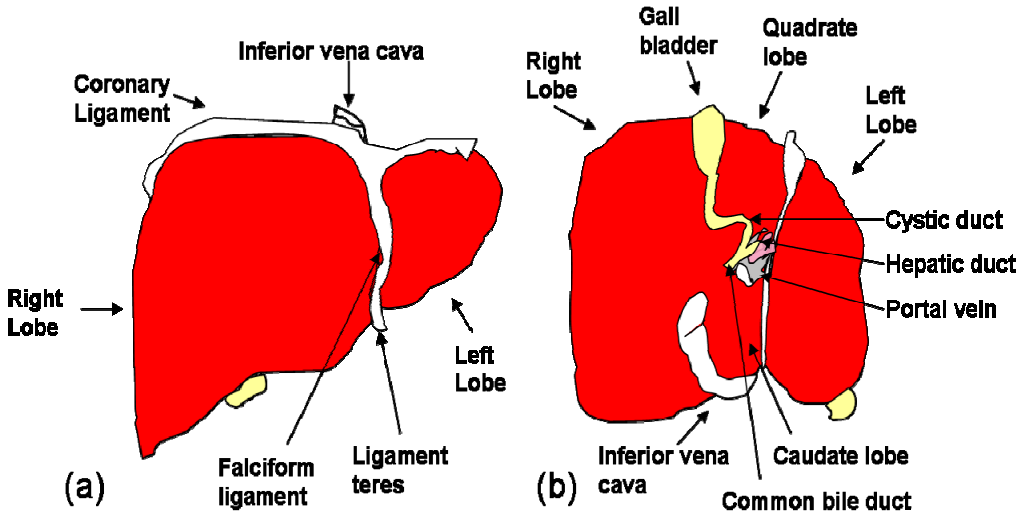

Figure 1.3. Basic anatomy of the liver (a) anterior view (b) inferior view, adapted from (Saxena et al., 1999).

The liver has a major role in regulating metabolism with many functions such as glycogen storage, decomposition of red blood cells, plasma protein synthesis, detoxification and the production of bile, which aids digestion and emulsification of lipids (Rapport., 1958;Saxena et al., 1999). At any one time the liver contains an eighth of the body's blood supply, which means it must have a good and uninterrupted circulation. 60-80% of the blood flow is from the portal venous system. The portal venous system is generated from the splenic vein joining the inferior mesenteric vein, which then joins the superior mesenteric vein forming the hepatic portal vein. This system brings venous blood from the spleen, stomach, pancreas and the small and large intestines and

the liver processes the blood for nutrients and toxins. The hepatic vein then drains directly into the inferior vena cava. The hepatic artery usually branches from the celiac trunk but can branch from the superior mesenteric artery (Saxena et al., 1999). The remaining 20-40% of the blood is supplied by the hepatic artery. The blood is transported further into the liver through portal venules and hepatic arterioles, which enter the lobules or acini, which have vessels called capillaries or sinusoids that are perforated by fenestrae. The capillaries and sinusoids separate the circulating blood from the hepatocytes (Saxena et al., 1999). The space between the sinusoid and the hepatocytes is called the Space of Disse, this is where the hepatic stellate cells reside and this is the region that allows the flow of solutes important for hepatic function to and from the hepatocytes (figure 1.4a). This flow is extremely important for the normal function of the liver and in some disease states the flow is disrupted through the build up extra cellular matrix causing the fenestrae of the epithelial layer to be become blocked (figure 1.4b) (RAPPAPORT, 1958;Saxena et al., 1999).

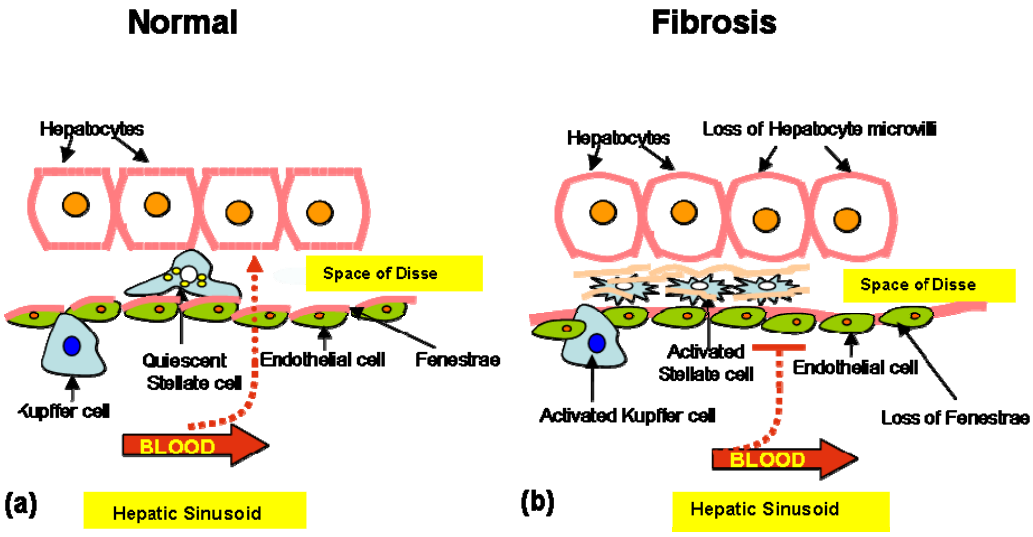

Figure 1.4. Schematic representation of the blood flow from the hepatic sinusoid to the hepatocytes in **(a)** normal and **(b)** fibrotic liver. Dotted line represents flow of solutes, which is blocked in the fibrotic liver.

An important role of the liver is to produce bile and this is collected in the canaliculi which merge to form bile ducts (Tsukada et al., 1995). The bile ducts run into the left and right hepatic ducts which in turn merge into the common hepatic duct. The cystic duct then merges with the common hepatic duct to form the common bile duct which drains in the duodenum or the gall bladder. In some cases of liver disease the bile ducts proliferate which can be seen very easily in biopsy specimens. The normal bile duct to portal tract ratio is 1:1, but in cases of obstruction in the biliary tract and some metabolic disorders the number of bile ducts is obviously increased (figure 1.5) (Tsukada et al., 1995;Crawford, 2002).

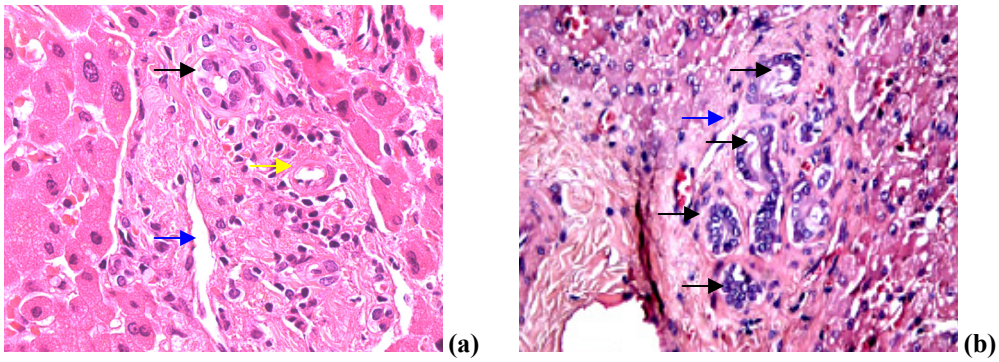

Figure 1.5. (a) A portal triad encompassing the portal vein (blue arrow), hepatic artery (yellow arrow) and a bile duct (black arrow) (b) A portal triad where the bile ducts (black arrows) have proliferated around the hepatic vein (blue arrow)

1.3.2 The cell cycle and proliferation in the liver

The cell cycle consists of G_1 (presynaptic), S (DNA synthesis), G_2 (premitotic), M (mitotic), and G_0 (quiescent) and most mature tissue will have a population of cells that occupy different phases of the cycle (figure 1.6) (Kumar et al., 2005). Adult tissue determines the cell population through the rate of cell proliferation, differentiation and death by apoptosis. Apoptosis can be induced by pathogenic stimuli, differentiation depends on the cell type and circumstance, for example neurons are terminally differentiated cells that have left the cell cycle but liver

hepatocytes are normally quiescent cells that still retain the ability to divide and cell proliferation can occur from stem cells or normally quiescent cells and can be stimulated by physiologic and pathologic conditions. Cell proliferation can become excessive in pathological conditions causing conditions such as prostatic hyperplasia (Mullauer et al., 2001). Cell proliferation is largely controlled through signals, either soluble or contact dependent. These signals can either stimulate or inhibit cell proliferation. Accelerated growth can be through excess stimulators or deficiency of inhibitors which shortens the cell cycle. The most important mechanism for repairing tissue is the conversion of resting cells (quiescent hepatocytes) in to proliferating cells (Becker and Lane, 1968;Becker, 1970). There are three main cell types that populate the body, continuously dividing for example the epithelia of the gut, quiescent cells such as hepatocytes in the liver and non dividing cells such as neurons and cardiac muscle cells. Continuously dividing cells are constantly in the cell cycle and the mature cells in most tissues are derived from stem cells which have an unlimited capacity to proliferate. Quiescent or stable cells have a low level of replication in normal conditions, they are in G_0 in the cell cycle but can be stimulated to enter G_1 and rapidly proliferate if required to repopulate damaged areas of the tissue. Non-dividing or permanent cells have left the cell cycle and cannot undergo mitotic division. Tissue that is largely made up of non-dividing cells will have little or no regenerative capacity and any repair will be through scar formation (Kumar et al., 2005).

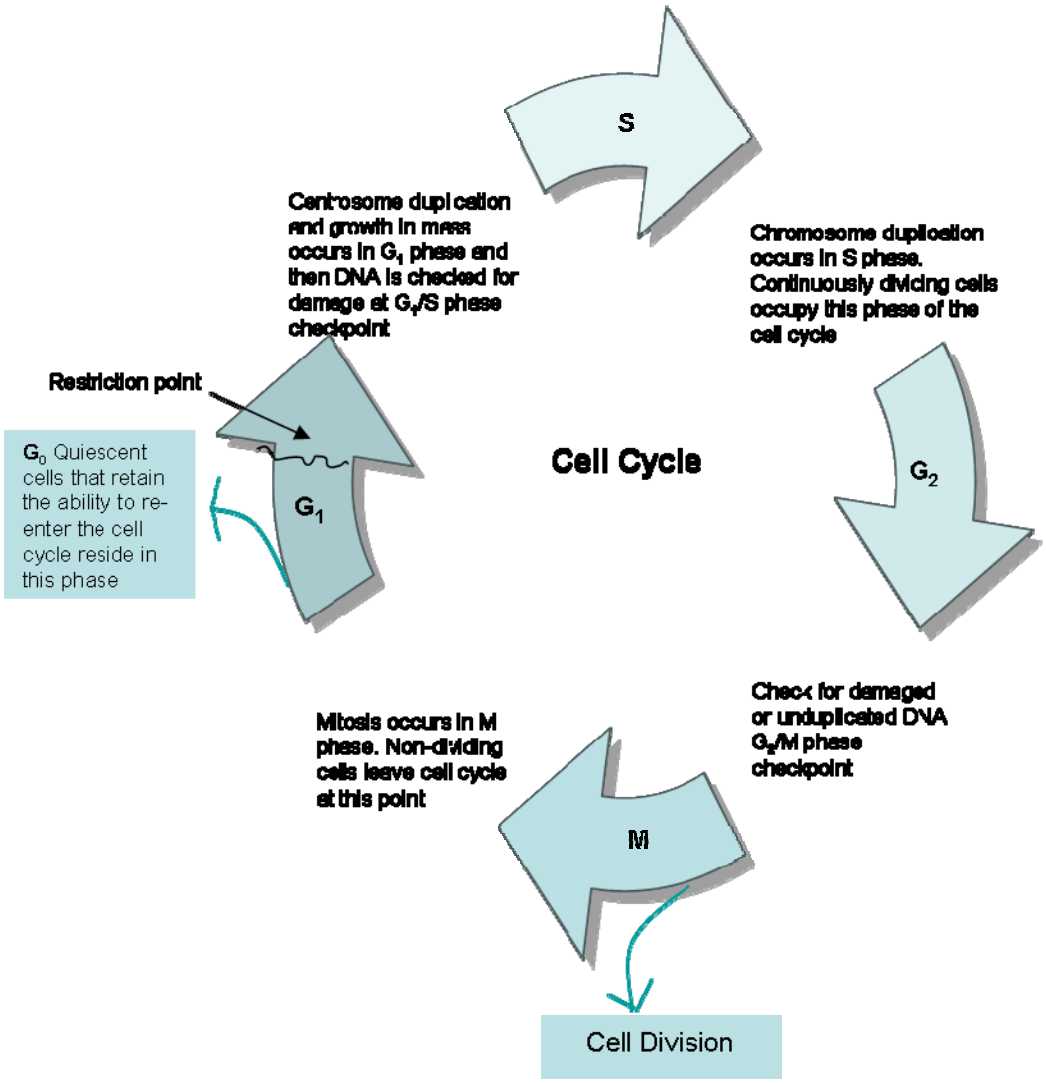

Figure 1.6. Schematic of the cell cycle adapted from (Kumar et al., 2005). Hepatocytes reside in G_0 until injury and loss of hepatocytes occurs. They are then stimulated by cytokines and growth factors released by Kupffer cells and hepatic stellate cells to re-enter the cell cycle and duplicate to repopulate the tissue. There are a number of restriction points that hepatocytes have to overcome to be able to replicate and it is only when they cannot overcome these restrictions that bone marrow and tissue derived stem cells from the canals of herring will be recruited to aid regeneration.

1.3.3 Capacity for Regeneration and Wound healing

The body's ability to replace injured or dead cells and repair tissue after inflammation is critical to survival. The injurious agent will damage the cells and affect the structure of the tissue. If the injurious agent is removed then the body must contain and repair the damage that has already occurred and therefore the surviving cells must replicate if regeneration or wound healing is to take place. Regeneration and wound healing have very different mechanisms and outcomes. Regeneration is used to describe the growth of cells and tissues to replace lost structures (Becker and Lane, 1968;Goss, 1992). It can be confused with compensatory growth that usually occurs after some of the organ has been lost for example a partial hepatectomy, when hepatocytes will be stimulated to replicate to replace the tissue and therefore stem cells are not required. Stem cells are required to replace lost tissue if hepatocyte replication is blocked (Korbling and Estrov, 2003). Regeneration requires the differentiation of stem cells to replace the cells that have undergone apoptosis. In many renewing tissue this process is occurring continuously for example the epithelia of the skin and the gut, where the cells on the outer surface are continuously replaced as long as the stem cells that generate new cells are not damaged. Wound healing is a different process that restores the original structures but will involve collagen deposition and scar formation (Clark, 1996). The most obvious example of this is a wound on the skin, but it will also occur after inflammation in internal organs and where the cells have under gone necrosis and are incapable of regenerating. To remain healthy the body must maintain a normal homeostasis and this will include the balance between the proliferation and apoptosis of cells in all tissues. In parenchymal organs such as the liver and kidney the replacement of inflammatory cell infiltrate by granulation tissue and fibrosis is called reorganisation. This may occur after any injury that causes an inflammatory response (Fausto, 2000). Regeneration requires an intact connective tissue scaffold but wound healing with scar formation occurs if the extracellular matrix framework is damaged and therefore

alters the tissue architecture. The difference in outcome of liver injury illustrates this point. After an acute injury of a single high dose of carbon tetrachloride in the rat, more then 50% of hepatocytes can be lost but regeneration and complete reversal of injury will occur. After chronic injury of multiple low doses of carbon tetrachloride over a period of time the liver will have a degree of hepatocyte necrosis but the main change will be the disruption of the extracellular matrix and normal liver architecture and all the repair will have been through fibrosis (Fausto, 2001). Extracellular matrix scaffolds are essential for wound healing because they provide the framework for cell migration and maintain the correct cell polarity for the reassembly of multilayered structures. Cells that reside in the extracellular matrix such as fibroblasts and macrophages are essential to the repair process due to their ability to release cytokines and growth factors. The liver is a highly regenerative organ that has the ability to repair itself after acute and chronic injury. The capacity of this repair mechanism means that the liver can function and regenerate to a whole liver with as little as twenty five percent of the original remaining (Chandrasoma & Taylor., 1998). The mechanism is predominantly through hepatocyte proliferation but there is evidence for bipotential stem cells populating the liver and differentiating into hepatocytes or cholangiocytes (Forbes et al., 2004). It is increasingly common for living patients to donate or have removed due to primary or secondary tumours, just part of their liver (partial hepatectomy) as it will quickly grow through compensatory mechanisms to its original size and capacity. A 70% partial hepatectomy of the rat liver elicits a growth response, the 'mini liver' can rapidly expand to its original mass after 10-14 days. The expansion occurs without regrowth of the lobes, there is only enlargement of the remaining lobes. There is a restitution of the functional mass rather then the restitution of the form (Fausto, 2001;Fausto, 2000). Hepatocytes are normally quiescent cells, residing in G_0 of the cell cycle. They can be stimulated to reenter the cell cycle and when this occurs it can take several hours for the cells to progress through G_1 and reach the S phase of DNA replication. The replication is synchronized

(all of the hepatocytes will enter S phase at the same time) and this is followed by the synchronous replication of non-parenchymal cells such as Kupffer cells, endothelial cells and stellate cells (Su et al., 2002). Proliferation of hepatocytes is triggered when the liver is injured and hepatocytes are lost. The combined factors of cytokines and polypeptide growth factors such as Transforming Growth Factor (TGF) released in an auotcrine manner by the hepatocytes themselves or cytokines such as Tumour Necrosis Factor (TNF) released in a paracrine manor by the Kupffer and stellate cells, help the hepatocytes overcome the major restriction points for replication. The two major restriction points for hepatocyte replication are G_0/G_1 transition (quiescent cells entering the cell cycle) and G_1/S phase needed for transition through the late G_1 phase restriction point. Proliferating hepatocytes have an early phase gene response (Su et al., 2002). Over 70 genes are activated including C-FOS and C-JUN which are protocogenes that dimerise to form AP-1. C-MYC, NF-κB and STAT-3 are also activated (Shaulian and Karin, 2002). C-MYC encodes for a transcription factor that regulates the expression of 15% of all genes through binding to enhancer box sequences and recruiting histone acetyltransferases. If hepatocytes are able to progress through G_1 and enter the S phase, anti-apoptotic genes are activated (Su et al., 2002). S phase starts with the formation of cyclin D-CDK4 complex and the phosphorylation of a component of the RB protein family followed by the activation of cyclin E-CDK2 complex, replication then becomes autonomous. Hepatocytes require TNF and IL-6 in G_0/G_1 transition and growth factors HGF and TGF-α are involved in cell cycle progression through G_1. TNF provides the priming signal for hepatocytes to respond to the full mitogenic affects of other growth factors. Hepatocytes only replicate once or twice once they reenter the cell cycle before returning back to G_0 in their quiescent state. The process of hepatocytes returning to G_0 is less well defined but is thought to involve the growth inhibitors Transforming Growth Factor beta (TGF-β) and activins (Michalopoulos and DeFrances, 1997).

1.3.4 Role of stem cells in liver regeneration

Stem cells are characterised by their prolonged self renewal capacity and by their asymmetric replication. Asymmetric replication describes the ability of the cell to divide. One cell retains its self renewal capacity when the other enters the differentiating pathway and is eventually converted to a mature non-dividing cell. In reality this description describes the whole population of cells, some of which differentiate and some of which self replicate (Weissman et al., 2001;Weissman, 2000). It was previously believed that stem cells existed only as embryonic stem cells in blastocytes that were pluripotent (able to differentiate into any cell or tissue type) (Martin, 1981). More recently it has been discovered that adults also have stem cell populations. The largest population is contained in the bone marrow and are called hematopoietic stem cells (Lagasse et al., 2000). It is thought that hematopoietic stem cells are usually linage specific although there have been stem cells found that have a broad differentiation potential in the bone marrow and have been named multipotent adult progenitor cells (MAPCs) (Jiang et al., 2002a). MAPCs are thought to be the adult counterparts of embryonic stem cells and their pluripotency has been demonstrated when injected into blastocyts (Hadjantonakis and Papaioannou, 2001). This technique has been used to create knockout models by manipulating the genome before injecting the cells into the blastocytes. MAPCs have the ability to differentiate into many cells types in vitro and they have been found in several tissues in the body including the muscle and brain (Jiang et al., 2002b). Stem cells are recruited to areas of injury to help regenerate the tissue. They also have a capacity to produce growth factors and cytokines that act on the tissues that they have migrated to (Lagasse et al., 2000). MAPCs that are found in various tissues in the body have been identified as having a common origin due to their similarity in gene expression profile. It has also been discovered that there are small population of stem cells that permanently reside in tissues, these cells are called tissue stem cells and have been found to have a more restricted differentiation capacity (Watt and Hogan, 2000). Tissue stem cells are

located in niches for example in the crypts of the colon and the bulge area of the hair follicle (Lavker and Sun, 2000;Marshman et al., 2002). In the liver tissue stem cells are contained in the canals of herring which is the junction between biliary ductular system and the parenchymal hepatocytes. These cells give rise to oval cells which are bipotential progenitors of hepatocytes or biliary cells and are activated when hepatocyte proliferation is blocked (Fausto and Campbell, 2003). Stem cell proliferation is prominent in patients recovering from fulminant hepatic failure, liver carcinogenesis and some cases of chronic hepatitis and cirrhosis (Libbrecht and Roskams, 2002).

Stem cells are therefore important for the regeneration of the liver but there is another side to the story. It has been found that there is a significant contribution to liver cirrhosis in humans from extra-hepatically derived myofibroblasts in liver disease of different etiology. These cells are thought to have originated from bone marrow derived stem cells (Forbes et al., 2004;Alison et al., 2004;Henderson and Iredale, 2007).

1.4 Cell – Extracellular matrix (ECM) interactions

1.4.1 ECM constituents, synthesis and function

It is now well understood that the extracellular matrix (ECM) is a vital and dynamic part of every organ in the body. There is a great deal of evidence that suggests maintaining the homeostasis of the ECM in the liver will help maintain a healthy organ, as in fibrosis this homeostasis is disrupted. The cells in any tissue must grow, migrate and differentiate and there is overwhelming evidence that all these processes are critically influenced by the intimate contact with the macromolecules surrounding the cells that constitute the ECM (Sanes, 2003). ECM is secreted locally around the cells forming a network that constitutes a significant volume in any tissue. This network of matrix serves many functions including secreting water to maintain turgidity in soft tissue and secreting

minerals to give rigidity in skeletal tissue. ECM is a reservoir for growth factors which can control the proliferation, adherence, migration and apoptosis of cells, providing a matrix where the cell form and function can be directly modulated. The synthesis and degradation of ECM accompanies morphogenesis, wound healing and fibrotic events, as well as tumour invasion and metastasis (Sanes, 2003). There are three groups of macromolecules that make up the ECM, fibrous structural proteins such as collagen and elastin, adhesive glycoproteins, and proteoglycans such as hyaluronic acid (HA). The most common protein and perhaps most relevant when considering fibrosis, in ECM is collagen but all of the components have important roles to play that can contribute to scar formation and the development of fibrosis. Proteoglycans consist of a core protein linked to one or more polysaccarides in the form of glycosaminoglycans (GAGs) (Sugahara and Kitagawa, 2000). Proteoglycans have remarkable diversity including roles in regulating connective tissue structure and permeability but also as integral membrane proteins that bind fibroblasts and growth factors which regulate cell growth and differentiation. HA is a large polysaccharide of the GAG family that consists of many repeats of a simple disaccharide molecule (Toole et al., 2002). It is found in the ECM of most tissues and has the ability to bind a large amount of water. This gives the connective tissue the capacity to resist compression forces but is also found in the matrix where migrating and proliferating cells are found where it can inhibit cell-cell adhesion which facilitates motility. HA can bind CD44, a glycoprotein expressed by leukocytes, and this function may retain T-cells in the tissue at sites of inflammation (Ponta et al., 2003). Collagen, elastin and adhesive glycoproteins will be discussed in further detail below. ECM is present in all intracellular junctions and cell surfaces and will form into two types of matrix, basement membrane and interstitial matrix. Basement membrane is produced by epithelial and mesenchymal cells and consists of largely collagen IV, laminin, heparin sulphate, proteglycan and other glycoproteins. Basement membrane is associated with the cell surface and provides the cell with a matrix that can be easily manipulated for migration and adherence purposes. In fibrosis the

basement membrane is often replaced with more fibril forming collagen molecules that form crosslinked matrixes that can inhibit the normal function of the cells that it surrounds. Interstitial matrix is located in the spaces between the epithelial and smooth muscle cells and in connective tissue. Interstitial matrix consists largely of collagen, elastin, fibronectin, proteoglycans, hyaluronate and other components that form a strong matrix essential for the structure of the tissue (Sanes, 2003).

Collagen is the most common protein in the animal world and is essential for the framework of all multicellular organisms. There are 27 different types of collagen encoded by 41 genes located on 14 different chromosomes. Collagen types 1, II, III, V, and X1 are fibrillar collagens and are highly abundant (Byers et al., 2001). Type IV collagen is non fibrillar and forms the main component of the basement membrane along with laminin. All types of collagen are produced as a triple α-helix from 3 polypeptide chains, normally a combination of α1 and α2 chains. Both α1 and α2 chains are around 1400 amino acids in length and can form a α-helix due to a small glycine residue occurring every third amino acid in the chain. The difference between fibril and non-fibril collagen comes after transcription and formation of the triple helix as the fibril forming collagens at this stage are still propeptides that require cleavage of N and C terminal peptides, which occurs after secretion from the cell to become mature fibril forming collagen whereas non-fibril forming collagen is transcribed and modified by hydroxylation of the proline and lysine residues before triple helix formation but then this is considered the mature form of the protein and is secreted from the cell without further modification (Myllyharju and Kivirikko, 2001). The collagenase domain of type IV collagen is longer then fibril collagen but is frequently interrupted with non-collagenous sequences. Most type IV collagens consist of a combination of α1 (IV) and α2 (IV) chains but combinations of α3 (IV), α4 (IV), α5 (IV) and α6 (IV) chains have been found in some basement membranes (Prockop and Kivirikko, 1995). In skeletal muscle fibrillar collagens are principally expressed by fibroblasts. Type 1 collagen

consists of two α1 chains and one α2 chain in the triple helix but collagen III is a homotrimer of three α1 chains. Fibrillar collagen is transcribed from the many different collagen genes as preprocollagen, it then undergoes hydroxylation of proline and lysine residues before the 3 chains align to form the triple helix of procollagen. Intra and inter-disulphide bonds are formed between the chains to form the tight triple α-helix of procollagen. Procollagen is then secreted from the cell where is undergoes further post-transcriptional modification. The N and C terminal domains are cleaved by proteases to produce the basic units of the fibrils that are formed by mature fibril collagen. The fibrils are formed spontaneously and will be stabilized by covalent cross-links that are generated by the conversion of some lysine and hydroxylysine residues to aldehyde derivatives by lysyl oxidase (Laurent, 1987). Vitamin C is required for the process of crosslinking which may explain the inadequate wound healing seen in cases of scurvy. Cross-linking increases the tensile strength of collagen reducing the body's ability to break it down. This is obviously a disadvantage in fibrotic diseases, when the build up of fibrillar collagen can overwhelm the tissue.

Some tissues in the body require elasticity, for example blood vessels, skin, lung and uterus. The ability to recoil is provided by elastic fibres, consisting largely of elastin which provides a central core that is surrounded by a network of microfibrils. The network of microfibrils consists mainly of fibrillin, a 350kd glycoprotein that associates with itself or other ECM proteins. These fibres can stretch to several times their length and return to their original size after the release of tension with no consequence to the tissue. The elasticity of the liver is lost during fibrosis and in cirrhosis the scar formation can restrict the expansion of blood vessels, which can lead to intrahepatic hypertension (Milewicz et al., 2000).

As described above the maintenance of homeostasis in the tissue relies on cell-matrix interactions. Essential to this process in the liver but also throughout the

body are adhesion proteins. Adhesions proteins have been given the name CAMs (cell adhesion molecules) and there are four main families of these proteins, immunoglobulin family CAMs, cadherins (calcium dependent adhesion proteins), integrins and selectins (Kumar et al., 2005). These proteins are located in the cell membrane where they can function as receptors or they are stored in the cytoplasm. CAMs provide interactions between the same (homotypic) or different cell types (heterotypic) and are responsible for many events involving adhesion, cell motility, proliferation and differentiation. Integrins have a broad specificity and will bind matrix proteins such as fibronectin and laminin (Hynes, 2002). Intergrins will facilitate the adhesion between cells and the ECM as well as other cells. Fibronectin is a large molecule that consists of two splice variants. The tissue splice variant will form fibrillar aggregates at wound healing sites and the plasma splice variant will bind fibrin forming clots at the site of injury. Laminin is an abundant glycoprotein in the basement membrane and has binding domains for ECM and cell surface receptors (Hynes, 2002). Cadherins are involved in calcium dependent homotypic interactions between cells. Cadherins and integrins together will link the cell surface with the cytoskeleton through the binding to actin and intermediate filaments. The mechanism is through not only mechanical force but through the activation of intracellular signal transduction pathways. When a ligand binds to an integrin the receptors become clustered on the cell membrane and the formation of focal adhesion complexes occurs. The complexes can act as activated receptors and may trigger MAP kinase, PKC and PI-3 kinase pathways within the cell (Stupack and Cheresh, 2002). There is a functional overlap between integrins and growth factor receptors that may cross talk via these mechanisms that are well known to regulate cell proliferation, apoptosis and differentiation. Cadherins form zonula adherins, which are spot like junctions near the apical surface of epithelial cells and desmosomes, which connect the plasma membrane of adjacent cells and are the strongest, most extensive of cadherin junctions (Hynes, 2002;Stupack and Cheresh, 2002). Adhesion proteins may also be secreted and these have implications in disease

processes. There are different classes of secreted adhesion proteins are called SPARCs (secreted protein acidic and rich in cysteine), thrombospondins, osteopontin and tenacin. SPARCs are also known as osteonectins and are important in tissue remodelling in response to injury due to their function as an angiogenesis inhibitor (Bradshaw and Sage, 2001). Thrombospondins are large multifunctional proteins that can also inhibit angiogenesis amongst other functions. Ostepontin is the ligand for the CD44 receptor which mediates leuckocyte migration and regulates calcification. Tenacins are a family of large multimeric proteins that have important functions in morphogenesis and adhesion (Sodek et al., 2002).

The ECM is therefore an important dynamic structure in the body that is vital for cellular interactions and the maintenance of homeostasis in tissues. The disruption and subsequent reorganisation of the ECM is dependent upon many different cell types, the interaction of which is fundamental for tissue remodelling and wound healing events to occur (Sodek et al., 2002).

1.4.2 Tissue remodelling and fibrosis

Resolution of fibrosis involves the restitution of tissue components with either identical components of those that were injured (regeneration), or a different process that involves a fibroproliferative response that will repair tissue with connective tissue scar formation rather then restore the original components (wound healing) (Goss, 1992). Injury can occur by a variety of mechanisms that have already been discussed in detail but the initial response of the liver to any injury is inflammation. Inflammation of the liver results in activation of macrophages and recruitment of inflammatory cells such as leuckocytes (Henry and Garner, 2003). This mechanism will remove any damaged tissue and help to clear the injurious agents such as HBV from the liver (Harty et al., 2008). Once the injurious agent has been removed the growth factors and cytokines that have been released by macrophages, HSC and ECM will initiate the proliferation and

migration of the hepatocytes and connective tissue cells, allowing spontaneous compensatory growth and/or regeneration in non cirrhotic tissue (Iredale et al., 1998;Issa et al., 2004;Tsukada et al., 1995). The first repair mechanism is to replace the damaged tissue with identical cells by hepatocyte proliferation and recruitment of stem cells. This process is called regeneration and has been described in detail above (Fausto, 2000). Compensatory growth and regeneration will only occur if the injury is acute, and once the harmful agent has been removed, it has been reported that removal of TGF-β can enhance hepatocyte proliferation (Arendt et al., 2005). The liver will regenerate if the injury is not too extensive and not chronic (Iredale, 2007;Fausto, 2000). Many tissues in the body cannot undergo regeneration like the liver and will use a wound healing mechanism to repair the tissue (Clark, 1996).

The initial process of wound healing is the same as compensatory growth and regeneration involving the recruitment of inflammatory cells and the release of growth factors and cytokines. If the damage is too extensive for regeneration to be sufficient the next stage of the wound healing process is initiated with vascular endothelial growth factor (VEGF) and other growth factors causing the formation of new blood vessels via angiogenesis and the granulation of the tissue through the proliferation of fibroblast and vascular endothelial cells which can occur as quickly as 24 hours post injury if regeneration has not occurred (Dvorak, 2000;Carmeliet, 2003). The new blood vessels that are formed via angiogenesis are permeable to plasma proteins in the presence of Nitric Oxide (NO) and VEGF, which are deposited in the ECM (Dvorak, 2000;Carmeliet, 2003). Plasma proteins in the ECM cause the in growth of fibroblast and endothelial cells. Growth factors such as TGF-β, PDGF, EGF, FGF and the cytokines IL-1 and TNF which are released by platelets, activated HSC, activated endothelium and macrophages increase the migration and proliferation of fibroblasts and endothelial cells to the site of injury (Werner and Grose, 2003). If the appropriate chemo-attractant proteins are in the tissue at the site of injury, mast cells, eosinophils and lymphocytes may accumulate in the tissue. In

this process it is believed that TGF-β is the most important growth factor due to its ability to induce fibroblast migration and proliferation, increase synthesis of collagen and fibrosis and to decrease the degradation of ECM proteins by inhibiting MMPs (Schnaper et al., 2003). Activated HSC in the liver become self sustaining by the autocrine release of TGF-β. Synthesis and deposition of ECM proteins and collagen will follow causing the remodelling of the tissue due to replacing the parenchymal cells (hepatocytes) and basement membrane of the tissue with fibril forming collagens and interstitial matrix (Gressner and Bachem, 1990;Friedman et al., 1993).

Collagen synthesis is induced by the growth factors PDGF, FGF, TGF-β and the cytokines IL-1 and IL-13 released from fibroblasts and leukocytes (Arendt et al., 2005). Tissue remodelling is also dependent on the decrease in degradation of collagen during this time allowing the granulation scaffolding to be converted into a scar composing of spindle shaped fibroblasts (activated HSC in the liver), dense collagen, fragments of elastic tissue and other ECM components. As the scar matures it undergoes vascular regression leaving an avascular scar. Tissue remodelling is dependent on the balance between ECM synthesis and degradation (Giannelli et al., 2003;Iredale, 1996). Degradation of collagen is achieved by Matrix Metalloproteinases (MMPs), which are zinc binding endopeptidases that require cleavage from a propeptide to become activated (Hemmann et al., 2007). There are over 20 MMPs in the family and they all retain the 180 residue zinc protease domain. This distinguishes them from many other proteolytic enzymes that can degrade ECM proteins that normally fall into the family of serine proteases such as fibroblast activated protein (FAP) (Gorrell et al., 2003). The family of MMPs include intersititial collagenases MMP-1, 2 and 3, which can cleave fibrillar collagens I, II and III, gelatinases MMP-2 and 9 that degrade collagen-1, IV, V, VII, X, fibronectin, laminin and elastin and stromelysins MMP-3, 10 and 11 that act on a variety of ECM proteins including proteoglycans, laminin, fibronectin and amorphous collagens (McCawley and Matrisian, 2001;Vu and Werb, 2000;Matrisian, 1990). There are also membrane

bound, surface associated MMPs and through there proteolytic activity can cleave and release extracellular domains of cell surface proteins. The cleaved proteins such as TNF and TGF-α are now active proteins that may remain associated with the cell surface or can be released (Matrisian, 1990). A large family of the membrane bound MMPs are called disintegrin and metalloproteinase-domain family (ADAM) enzymes and have been associated with the pathogenesis of bronchial asthma (Kheradmand and Werb, 2002). MMPs are synthesised by fibroblasts, macrophages, neutrophils and some epithelial cells as propeptides. They require proteolytic cleavage for activation and their secretion is regulated by PDGF, FGF, IL-1, TNF, phagocytosis and physical stress such as oxidative stress from free radical formation. MMP secretion can be inhibited by TGF-β and steroids. MMPs cleave collagen by cutting the triple helix into two unequal fragments, which makes the remaining fragments susceptible to digestion by other proteolytic enzymes (Matrisian, 1990).

MMPs are regulated by tissue inhibitors of metalloproteinases (TIMPs) which are produced by mesenchymal cells. At present there are four TIMPs in the family and they are all small 21-28 kD proteins that have a highly conserved set of six intramolecular disulphide bonds. TIMPs all have the ability to form tight, non-covalent inhibitory complexes with multiple members of the MMP family. TIMPs specifically bind the forth coordination site of the zinc molecule present in the active site domain of all MMPs. TIMP-1, 2 and 4 are inducible proteins that are secreted from the cell, whereas TIMP-3 is mainly constitutively expressed and is associated with the ECM. TIMP-1 will form a tight complex with MMP-1 and TIMP-2 is known to bind MMP-2 (Hemmann et al., 2007;Iredale, 1997). TIMPs are overexpressed by activated HSC thus preventing any collagen/matrix degradation of the fibrotic scar (Iredale et al., 1996;Benyon et al., 1996). MMPs and TIMPs are spatially and temporally regulated within scar formation and the healing wound, the balance of which is essential to the remodelling of the connective tissue and repairing the defect

once the injurious stimuli has been removed but as described above the balance can be shifted in a fibrotic situation to favour the deposition of fibril forming collagen with little or no degradation of the scar taking place. The injury and damage can persist for example in alcoholic cirrhosis or HCV infection and this can lead to chronic inflammation. This leads to tissue damage and repair occurring concurrently and the connective tissue deposition becomes fibrotic (Iredale, 1997). Fibrosis is the universal response to chronic injury and inflammation (Iredale, 2008). Over time without the removal of the injurious stimuli the fibrosis can become extensive, manifesting in excess collagen accumulation leading to cirrhosis where the scar formations link together (bridging fibrosis). This can lead to an irreversible loss of tissue function, replacing normal tissue with scar tissue which can then contract due to the nature of the collagen and cells present causing complications such as portal hypertension that will be discussed later. The underlying pathology of deep organ fibrosis remains similar in most cases, suggesting insights into the pathogenesis of scarring in one organ can lead to better understanding of fibrosis in general (Iredale, 1997).

1.4.3 Molecular mechanisms of hepatic fibrosis

Hepatic fibrosis is characterised by the excessive accumulation of extra-cellular matrix (ECM) proteins, particularly collagen type 1. These matrix proteins form a hepatic scar, which can lead to secondary complications often seen in patients presenting with advanced fibrosis and cirrhosis (Friedman, 2008). Injury to the liver causes the activation of Kupffer cells, which are the resident macrophages of the liver. As part of the inflammatory response Kupffer cells release an array of pro-inflammatory cytokines which can lead to the activation of Hepatic Stellate Cells (HSC) (Friedman and Arthur, 1989). HSC are quiescent, vitamin A storing cells but can be stimulated to re-enter the cell cycle differentiating from the quiescent into a myofibroblast-like cell (Friedman et al., 1985). This process has been called activation and is stimulated by fibrogenic cytokines and

growth factors released by the Kupffer cells, parenchymal cells and other incoming inflammatory cells. Additionally changes in cell matrix interaction are likely to contribute to HSC activation. The activation process enables HSC to become highly proliferative cells that have the ability to contribute to tissue remodelling (figure 1.7). Activated HSC lose their vitamin A (retinoid) storing capacity, up regulate α– smooth muscle actin (α-SMA) and fibril collagen synthesis. HSC are believed to be the main progenitors of fibrosis in acute and chronic liver injury (Friedman et al., 1985;Rockey et al., 1992;Friedman et al., 1993). Cytokines such as Tumour Necrosis Factor-alpha (TNF-*a*), Transforming Growth Factor-beta TGF-*b*1, angiotensin II and leptin activate HSCs (Bataller and Brenner, 2005). HSC are localised in the Space of Disse and store 80-90% of the vitamin A in the body when in their quiescent, non-activated state (figure 1.7). When activated, HSC have multifunctional characteristics in releasing retinoid, regulating synthesis and secretion of ECM components, production of MMPs and TIMPs, and the synthesis and secretion of cytokines (Li and Friedman, 1999). HSC secrete fibril forming collagens type I and III, contributing to the fibrotic changes in the ECM. Upon activation HSC secrete an array of MMPs that can breakdown a variety of collagen and ECM components. The activation of HSC in acute injury is required to clear the fibrotic scar through the production of MMPs, this enables regeneration to occur. Activated HSC will then secrete TIMPs to inhibit the MMPs, preventing excessive breakdown of the tissue (Iredale et al., 1998;Hemmann et al., 2007). If the injury becomes chronic, the persistent activation of HSC leads to constant increase in the activation of TIMPs. The TIMP-MMP balance is then shifted, inhibiting any remodelling occurring. The HSC can then continue to secrete ECM components forming fibril collagen depositions that cannot be broken down due to the inhibition of MMPs. The collagen can then over time become crosslinked forming scars that are characteristic of cirrhosis. A therapy that can reduce the expression of TIMPs and increase the expression of MMPs in HSC may contribute to tissue remodelling and resolution of fibrosis (Hemmann et al., 2007).

The progression to fibrosis means that the natural healing response becomes pathogenic. At a molecular level fibrogenic activity may become self-sustaining through the HSC expressing and releasing TGF-β, TNF-α and Platelet Derived Growth Factor (PDGF) in an autocrine manner (Gressner and Bachem, 1990;Friedman et al., 1993). There is not only a change in the composition of collagen in the fibrotic liver but also in its distribution. In normal liver HSC are located between the sinusoidal endothelial cells and the hepatic parenchymal cells, an area called the Space of Disse. HSC and their processes encircle and contact the endothelial cells and also have contact with the parenchymal cells. HSCs coexist with the three dimensional ECM components (e.g. collagen type IV and laminin) these along with the long and numerous processes of stellate cells make a complicated structure (Imai et al., 2004). The initial collagen deposition is concentrated in the sub-endothelial Space of Disse (figure 1.7). In fibrosis the matrix within the Space of Disse is transformed from a non-fibril forming basement membrane like ECM, containing type IV collagen, laminin and proteoglycans, to the fibril forming collagens type I and III, with increased ECM glyconjugates including fibronectin and hyaluronic acid (Friedman, 1993). Although initially confined to the hepatic sinusoid the accumulation of ECM proteins eventually invades vascular structures and areas of hepatocellular necrosis. This coupled with the ECM accumulation in the sinusoid causes the loss of fenestrae in the endothelial cell lining and increased pressure around the vascular structures causing a disruption in blood flow and the movement of metabolites from the sinusoid across the Space of Disse, typical in patients with advanced fibrosis and cirrhosis (McGuire et al., 1992;Friedman et al., 1992).

1.4.4 Contractility of the hepatic stellate cell

It has been postulated that HSC play a role in the control of blood flow through the liver based on anatomic location and contractile characteristics (Mallat, 1998;Rockey, 1997). HSC are located in the Space of Disse and can extend up to four cellular processes that run along the sinusoid. Secondary processes can

branch off the primary processes and these can encircle the sinusoid in a cylindrical manner (Blomhoff and Wake, 1991). HSCs possess cytosolic proteins such as calmodulin, actin and myosin that are characteristic of contractile cells (Ramadori, 1991). HSC have been found to contract in response to vasoactive mediators such as endothelin-1 (ET-1) and argenine vasopressin (AVP) (Pinzani et al., 1996;Zhang et al., 1994). ET-1 is upregulated in cirrhotic rat livers. ET-1 upregulation can increase the portal pressure by decreasing the radius of the sinusoid in regions that are co-localised with HSC (Pinzani et al., 1996;Zhang et al., 1994). ET-1 antagonists have been found to reduce portal pressure and improve hepatic blood flow in cirrhotic rats, increasing the evidence that HSC can respond to vasoactive mediators and have a vital role to play in the pathogenesis of portal hypertension (Ueno et al., 1997;Ueno and Tanikawa, 1997;Ueno et al., 2004). Substances such as ET-1, AVP, angiotensin II, substance P and thromboxan A_2 can signal through membrane receptors that can increase the intracellular calcium concentration which in turn can activate cellular contraction. It is believed this could be the mechanism of contraction in HSC (Ueno et al., 1997;Ueno and Tanikawa, 1997;Ueno et al., 2004).

In the early nineties, Rockey and co workers were interested in the link between HSC activation and contractility. They established that HSC contractility in an *in vitro* setting coincided with activation. Activation was monitored by the level of α-SMA expression and contractility was monitored by contraction of a collagen-1 lattice gel that the cells were plated on after isolation (Rockey et al., 1993). HSC were found to contract the gels when they were activated and the level of contraction was dependent on the number of cells. There was also a reduction of cell volume that was monitored by electron microscopy. No contraction was observed when hepatocytes were treated in an identical manner. Serum in the media of the HSC was a potent stimulator of contraction as was endothelins 1, 2 and 3. The affect of serum and endothelin-1 was additive. HSC were isolated from animals that had been injured with CCl_4 and from normal

controls. The cells from normal controls were found to be less contractile immediately after isolation compared to the cells isolated from the injured animals. The collagen-1 matrix predominates in the injured liver and therefore could promote contraction and activation of the HSC. Agents such as IFN-γ that can block the activation of HSC were found to inhibit the contraction of these cells (Rockey et al., 1993). These data suggest a link between the level of activation and the degree of contractility in these cells. This has important implications when considering portal hypertension. HSC are ideally situated to regulate sinusoidal blood flow and activated cells residing the Space of Disse may induce contraction of fibrotic bands leading to the physical distortion of the normal liver architecture and blood flow patterns. Activation and contraction inhibiting agents may represent potential points of therapeutic intervention for portal hypertension and chronic liver injury (Rockey et al., 1993).

1.4.5 Apoptosis of the hepatic stellate cell

Apoptosis is a form of programmed cell death in multi cellular organisms first described by Carl Vogt in 1842. A more detailed description was offered by an anatomist, Walther Flemming in 1885 but it was not until 1965 that the topic was resurrected for more detailed investigation. Dying cells were characterised by the gross condensation of cytoplasm and nuclear chromatin, which were observed to be fundamentally different from the appearance of those cells undergoing coagulative necrosis which is found in tissues damaged by noxious stimuli (Trump et al., 1965;Ginn et al., 1969). Apoptosis involves a series of biochemical events that leads to a characteristic cell morphology and death. Apoptosis was first described at the cellular level in 1972 by Kerr and colleagues. Apoptosis begins with the aggregation of nuclear chromatin, followed by the nuclear fragmentation and cytoplasmic condensation associated with prolific budding to produce membrane bound apoptotic bodies of varying sizes. A small number of apoptotic bodies are ingested by the remaining viable cells in the tissue but the vast majority are ingested and degraded by specialized

cells whose cytoplasm becomes progressively laden with telolysosomes (Kerr and Searle, 1973). Processes of disposal of cellular debris whose results do not damage the organism differentiates apoptosis from necrosis. Necrosis is a form of traumatic cell death that results from acute cellular injury (Searle et al., 1982). Apoptosis is an important process in regulating the cell population of vertebrate tissue and organs throughout the organism's life. Apoptosis complements mitosis in normal and pathological conditions ensuring the homeostatic regulation of cell kinetics (Kerr et al., 1972). A number of pathological conditions may arise if the equilibrium between mitosis and apoptosis is unbalanced, such as uncontrolled cell proliferation observed in cancer or excessive apoptosis causing hypotrophy seen in ischemic damage (Sheahan et al., 2008). Apoptosis is a tightly regulated process that is induced by different signals in various cell types. These signals may arise from the cell itself, from the surrounding tissue or from a cell that is part of the immune system. Extracellular signals such as TGF-β that either induce or inhibit apoptosis may include hormones, growth factors, nitric oxide and cytokines. Intracellular apoptotic signalling is induced as a response to stress and will ultimately result in cell suicide (Sheahan et al., 2008). Many apoptotic proteins affect the mitochondria of the cell which is essential to multicellular life. The mitochondria may be affected in different ways, for example swelling through the formation of membrane pores or the increase in non-selective permeability of the membrane that allows apoptotic proteins to leak out (Kumar et al., 2005). There is a growing body of evidence that nitric oxide is able to induce apoptosis by helping to dissipate the membrane potential of the mitochondria and therefore make it more permeable (Brune, 2003). P53 is a tumour suppressor gene that accumulates when DNA is damaged. It is a cell cycle checkpoint protein that can prevent the cell from replicating by stopping the cell cycle at G_1, or interphase which gives the cell time to repair any damage. If the damage is too extensive and cannot be repaired the cell will undergo apoptosis, therefore regulation of the p53 gene is vitally important for the life cycle of the cell (Winchester, 1983). Poly- adenosine diphosphate- ribose polymerase (PARP-1)

cleavage is used as an early marker of apoptosis in mammalian cells (Kaufmann et al., 1993). Under homeostatic conditions PARP-1 participates in genome repair, DNA replication and regulation of transcription (Quenet et al., 2008). PARP-1 catalyses the addition of long branch chains of poly adenosine diphosphate (poly ADP) to a variety of nuclear proteins using nicotinamide adenine dinucleotide (NAD^+) as a substrate. NAD^+ is broken down to nicotinamide and PAR. Cells undergoing a stress response may upregulate PARP-1 to help maintain genomic integrity (Quenet et al., 2008). Massive PARP-1 activation can however deplete the cell of NAD^+ and ATP, ultimately leading to energy failure and cell death. Massive up-regulation of PARP-1 may induce cell death through necrosis rather then apoptosis, which is associated with PARP-1 cleavage. PARP-1 is cleaved by caspase 3 from a 116 kD protein to 89 kD and 24 kD fragments rendering PARP-1 inactive (Kaufmann et al., 1993). PARP-1 cleavage not only prevents the survival of damaged DNA but will also ensure that the vital energy stores are available for the execution of apoptosis (Aikin et al., 2004). PARP-1 and PARP-1 cleavage products can be detected by western blotting and is a common method used to detect early apoptosis in cell systems (Kaufmann et al., 1993).

Apoptosis of activated stellate cells may significantly contribute to the resolution of fibrosis, acting as a mechanism for the removal of the cell population that is responsible for both producing the fibrotic matrix and protecting the matrix from degradation via the production of TIMPs (Iredale et al., 1998). In rat models of fibrosis the HSCs were found to have become activated after chronic exposure to CCl_4. In a model of progressive fibrosis the HSCs were found to have increased expression of α-SMA and TIMPs and the activity of collagenases were decreased. Once the injurious stimulus was removed the model of recovery was followed. In recovery the expression of TIMPs was reduced and the activity of the MMPs increased. The numbers of α-SMA positive cells were reduced and it is believed that the mechanism is by apoptosis rather then reversion to a quiescent, vitamin A storing cell as in the normal liver (Iredale et al., 1998).

Although recently there has been evidence to suggest senescence or reversion to quiescence of HSC also has a role to play in limiting liver fibrosis (Krizhanovsky et al., 2008). It is thought that even relatively advanced fibrosis of the rat liver can undergo remodelling with the restoration of normal liver architecture over a relatively short period of time (Iredale et al., 1998).

The hepatic stellate cell has become the focus for research into liver fibrosis, with the attention being on the development of therapies that target HSC *in vitro*. The next issue to address will then be specifically targeting activated HSC *in vivo* without affecting the surviving areas of normal liver cells (Bataller and Gines, 2002).

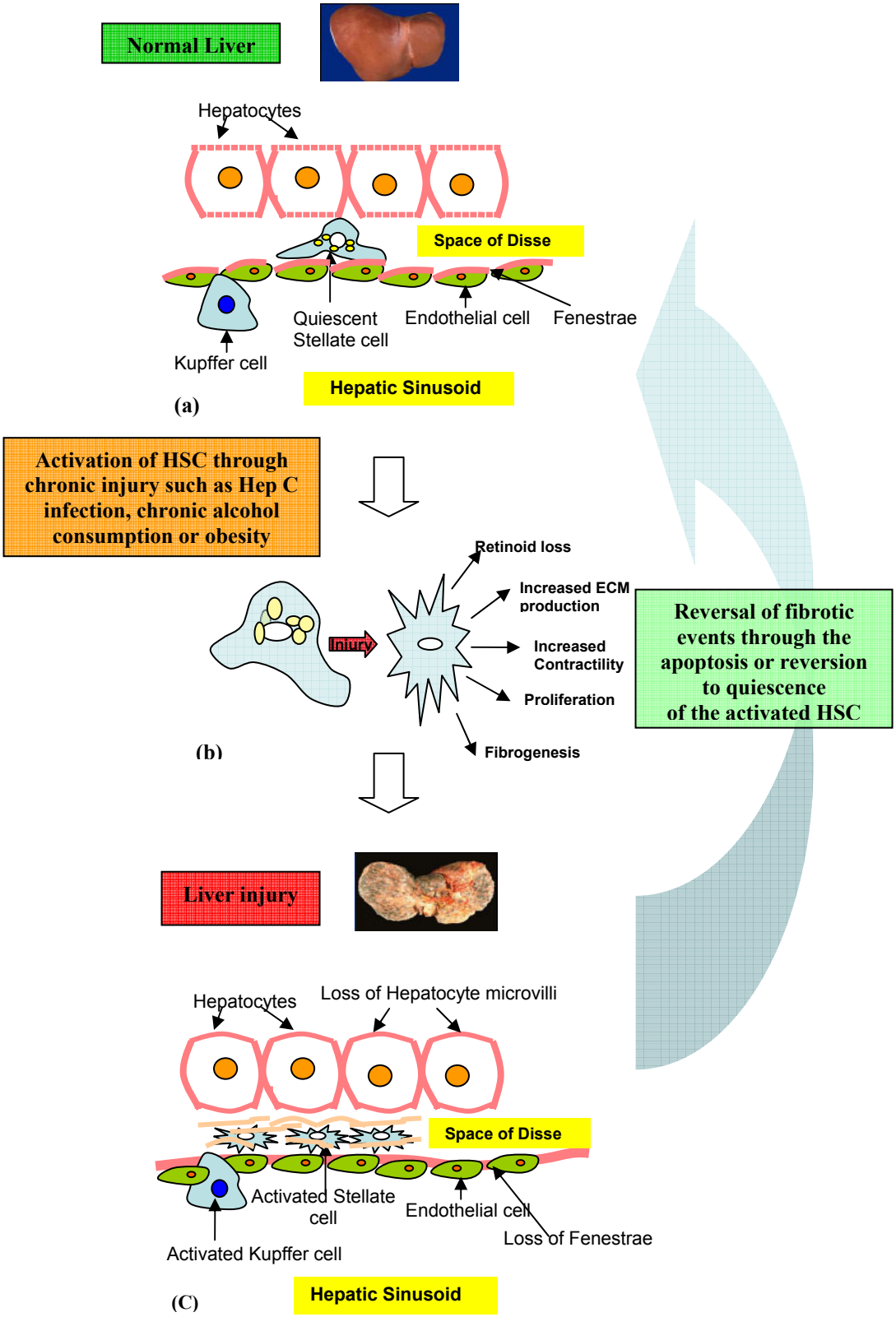

Figure 1.7. Changes in the hepatic architecture during fibrotic injury **(a)** The normal architecture of the liver before repeated injury, and associated inflammatory response

(b) activation of hepatic stellate cells through repeated/chronic injury such as Hepatitis C infection, chronic alcohol consumption and obesity **(c)** Following repeated injury, inflammatory lymphocytes infiltrate the hepatocytes causing the apoptosis of some hepatocytes, activation of Kupffer cells, which release fibrogenic cytokines/mediators. HSC proliferate and undergo the phenotypic activation associated with fibrosis, causing an increase in secretion of extracelluler matrix proteins, initially in the Space of Disse. This in turn causes the loss of fenestrae which are vital for the flow of blood through the sinusoid. This process is thought to be reversible, through the removal of activated stellate cells from the site of injury, which is the target cell for new therapies in development.

1.5 Cirrhosis and its implications in disease

1.5.1 Hepatic cirrhosis

Cirrhosis is the pathological condition, which results from end stage liver fibrosis and is one of the top ten causes of death in the western world. It is vital to appreciate when considering possible therapies that many patients that have hepatic fibrosis, which is believed to be reversible, can progress to cirrhosis after an interval of 5-20 years (Iredale, 2003). The average survival rate after five years from diagnosis of cirrhosis is only 50% (Kumar and Chandrasekharan, 1994). Cirrhosis is the result of continuous liver damage representing the late stage of progressive scarring through chronic inflammation and development of fibrosis throughout the liver. Fibrosis is the key feature of progressive damage, with the continued deposition of fibrous collagen in the Space of Disse by the hepatic stellate cells (HSC), leading to the loss of fenestrations of the endothelial cells (figure 1.7) (Iredale, 2003). This process causes the sinusoidal space to resemble a capillary rather then channel for the exchange of solutes between the hepatocytes and plasma (figure 1.4) (Le et al., 1990;Urashima et al., 1993). In particular the secretion of plasma proteins such as albumin and lipoproteins is severely impaired (Friedman, 1993). The disruption of the interface between the parenchyma and the portal tracts can lead to the destruction of the biliary

channels as well. Cirrhotic patients can develop jaundice and hepatic failure despite having a normal liver mass (Kumar et al., 2005). Characteristics of cirrhosis are parenchymal nodule formation containing proliferating hepatocytes which are encircled by fibrotic scar and bridging fibrous septae, which can take the form of delicate bands or broad scars that link the portal tracts with one another and with terminal hepatic veins. Overall this leads to a massive disruption in the normal architecture of the entire liver (Iredale, 2003). Hyperplasia of existing hepatocytes leading to the regenerative nodules described above, distorts the normal liver architecture, which leads to the disruption of the vasculature which critically alters the supply of blood to the hepatocytes causing abnormal blood flow between portal veins and hepatic arterioles (Roncalli et al., 2008). This can lead to hepatocyte necrosis and portal hypertension, which can then lead to the manifestation of varices and ascites (Chandrasoma and Taylor, 1998). Patients with cirrhosis can remain free of major complications for several years (compensated cirrhosis) but patients with decompensated cirrhosis, where the patient may have symptoms such as jaundice and one or more complications such as portal hypertension, varices and ascites, is associated with short survival and liver transplantation is often indicated as the only effective therapy (Bataller and Brenner, 2005).

The diagnosis of cirrhosis is made clinically on the basis of signs of end stage liver disease such as portal hypertension, ascites, muscle wasting, variceal bleeding, jaundice and encephalopathy (Bosch and Garcia-Pagan, 2000;Iredale, 2003). These features indicate a poor prognosis regardless of etiology due to the reversal of cirrhosis being rare. Often transplantation is seen as the only treatment for cirrhosis as the collagen fibers laid down during injury undergo extensive cross linking making the collagen much more resistant to collagenases and therefore antifibrotic therapies (Iredale, 2003;Bonis et al., 2001). Therefore any future strategy to prevent/treat liver fibrosis will have to consider the possibility patients may have advanced fibrosis/cirrhosis at presentation.

1.5.2 Secondary complications: portal hypertension, varices and ascites

Increased resistance to portal blood flow (portal hypertension) can arise in a number of circumstances that are divided into prehepatic, intrahepatic and posthepatic causes. Pre and post hepatic causes are rare but include obstructive thrombosis and narrowing of the portal vein before it connects with the liver (prehaepatic) and severe right sided heart failure, hepatic outflow obstruction and constrictive pericarditis (posthepatic) (Kumar et al., 2005). The primary intrahepatic cause is cirrhosis and results because of the increased resistance at the level of the sinusoids. There can also be compression of the terminal hepatic veins due to scarring and expansion of the parenchymal nodules in these areas. Anastomoses between the portal vein and the hepatic artery within the fibrous septa can impose extremely high pressure on the venous system. Intrahepatic causes may also include massive fatty change, sarcoidosis and disease that affect the portal microcirculation. The major clinical consequences are ascites, formation of portosystemic venous shunts, congestive splenomegaly, the development of varices and hepatic encephalopathy (Bosch and Garcia-Pagan, 2000).

Ascites is the oedema of the peritoneal cavity (Chandrasoma and Taylor, 1998). The build up of fluid is due in part to portal hypertension likely to increase hydrostatic pressure in the sinusoid, driving fluid into the Space of Disse, which is removed by the hepatic lymphatic system. The loss of liver function and the consequent decrease in plasma proteins results in the reduction of osmotic potential of the blood also increasing the level of fluid in the Space of Disse and therefore increasing the level of fluid in the hepatic lymphatic system further (Arroyo, 2002). The increase in hepatic lymphatic flow eventually exceeds the thoracic duct capacity and fluid will accumulate in the peritoneal cavity. Portal hypertension also increases the pressure in the intestinal capillaries, which will force fluid out in to the abdominal cavity and water and sodium are retained by the kidneys due to hyperaldosteronism. All these factors combined can increase

the hepatic lymphatic flow from 1000ml/day to over 20L/day in cirrhotics (Arroyo, 2002;Chandrasoma and Taylor, 1998).

Portosystemic shunts are due to the rise in portal pressure causing bypasses to develop wherever the systemic and portal circulations share capillary beds. The shunts can manifest in areas such as the rectum and the retroperitoneum but most importantly in the falciform ligament and the cardioesophageal junction producing gastric and esophageal varices respectively (Toubia and Sanyal, 2008). Gastric and esophageal varices are a serious secondary condition resulting from portal hypertension. Esophageal varices are more common, usually occurring in the lower part of the esophagus and these veins are prone to hemorrhage. If prolonged or severe, portal hypertension can induce the formation of collateral bypass channels. The portal blood is diverted into the coronary veins of the stomach into the esophageal subepithelial and submucosal veins, then into the azygos veins and eventually into the systemic circulation (Takashi et al., 1985). The build up of pressure in the esophageal plexus results in the tortuous vessels called varices. 90% of all cirrhotic patients will develop varices and they are most common in alcoholic cirrhosis. Damage to varices can be caused by chemical and mechanical damage e.g. vomiting, which can lead to fatal blood loss (Toubia and Sanyal, 2008).

Hepatic encephalopathy is regarded as a disorder of neurotransmission within the central nervous and neuromuscular systems and appears to be associated with elevated levels of ammonia in the blood and can occur in cirrhotic patients after portosystemic shunts have developed (Rogers, 1985). Ammonia levels may rise in the blood when the livers function has been impaired for any reason and its ability to remove toxins for the blood is reduced but if portal hypertension develops and there is consequent bypassing of the liver filtration system by blood travelling from the intestine due to portosystemic shunts, then the blood can travel directly to the brain without being filtered of any toxins. Elevated ammonia can impair neuronal function and promote generalized brain

edema (Rogers, 1985). There is also a risk of increased hepatic encephalopathy in patients after transjugular intraheptic portosystemic shunting (TIPS) procedure, as a therapy for portal hypertension (Nolte et al., 1998).

The management of portal hypertension is currently a much debated area. Drugs such as beta blockers in conjunction with isosorbide mononitrate are currently used as a long term treatment in the reduction of blood pressure and somatostatin analogs and antidiruetic hormones such as terlipressin are currently used as an acute treatment to inhibit splanchic blood flow thus reducing portal and variceal pressure, helping to terminate variceal bleeding (Bosch and Garcia-Pagan, 2000;Bosch et al., 2003). Some of these therapies require intravenous infusion and are not always effective. Surgical interventions may be necessary if the hypertension is severe and complications such as varices are present (Bosch and Garcia-Pagan, 2000;Bosch et al., 2003). Procedures such as transjugular intraheptic portosystemic shunting (TIPS) where a connection between the portal and venous system is created and distal splenorenal shunts (DSRS) where the distal splenic vein is connected to the left renal vein are carried out in these cases (Boyer, 2008;Boyer et al., 2008). If these procedures are unsuccessful and it has been recorded that 30% of patients that undergo a TIPS procedure develop hepatic encephalopathy, then a liver transplant may be the only effective treatment (Boyer, 2008;Boyer et al., 2008). It is clear that an effective noninvasive therapy that could treat portal hypertension at the intraheptic level by reducing blood pressure by not only relaxing the veins and contractile cells around the veins but reducing the amount of fibrosis in the liver by clearing the activated HSC would be an advantageous treatment above any existing therapies.

1.6 The history of relaxin, discovery of its receptors and its links to fibrosis

1.6.1 The identification of relaxin and relaxin-like peptides structure and function

In the early 1920's a scientist called Hisaw was investigating the physiological changes seen in the pubic symphysis in guinea pigs during pregnancy. He reported that when virgin female guinea pigs were injected with serum taken from pregnant rabbits there was a relaxation of the pubic ligaments similar to that seen to naturally occur in pregnancy. The substance responsible for the relaxation could be extracted from rabbit placenta and was found to work in conjunction with estrogen (Hisaw., 1926). In 1930, a crude extract of this substance was extracted from the corpus lutea of sows, identified as a hormone, and was given the name 'relaxin' (Fevold et al., 1930). In the 1970's three preparations of relaxin were obtained from frozen sow ovaries (Schwabe et al., 1976; Schwabe., 1977). Two peptide chains were identified and sequenced as the A and B chain of the mature form of relaxin. This led to the isolation and sequencing of relaxin from several different species including rats (John et al., 1981), mice (Evans et al., 1993) and humans (Hudson et al., 1983;Hudson et al., 1984). Humans and the four great ape species have three forms of relaxin encoded by separate genes, which is thought to be a consequence of gene duplication during primate evolution. The three relaxin genes have been designated H1 and H2 and H3-relaxin. Only H2-relaxin is known to be secreted into the blood and is therefore the main circulating form of the peptide, therefore any reference to relaxin in this thesis refers to H2-relaxin unless otherwise stated (Bathgate et al., 2006). Rodents were found to have two relaxin genes H1-relaxin and H3-relaxin, which correspond to H2-relaxin and H3-relaxin in humans respectively. H1-relaxin is the circulating form in rodents (Samuel et al., 2005). Modeling of the relaxin structure has revealed it has a primary structure very similar to insulin, comprising of two polypeptide chains (figure

1.8). The A chain has 22 amino acids (Schwabe et al., 1976) and the B chain has 32 amino acids with a combined molecular weight of around 6000 daltons (Schwabe and McDonald, 1977). The two chains are linked via two disulphide bridges, with an intra-chain disulphide bridge in the A-chain. The structure was confirmed by the x-ray crystal structure of H2-relaxin, which revealed the probable relaxin receptor binding site within the B-chain along the dimer interface. The amino acid motif that has been found to be required for relaxin receptor interaction is Arg-X-X-X-Arg-X-X-Ile/Val-X and as suggested from the crystal structure is located in the middle of the B-chain (Eigenbrot et al., 1991). Relaxin is transcribed as a prohormone that is stored in vesicles in the endoplasmic reticulum (ER). When relaxin is required the prohormone is cleaved and transported to the cell membrane where it is released into the blood stream (Gast, 1983). Therefore relaxin has been well characterised in terms of structure, and is now a well known hetrodimeric peptide hormone structurally related to the insulin family of peptides. Relaxin is an insulin-like 6 kD peptide hormone, detectable in serum during pregnancy and is produced in females by the corpus leuteum of the ovary, the breast and during pregnancy by the placenta, chorion and decidua. In males relaxin and its receptors RXFP-1 and RXFP-2 are produced by the testis and the prostate (Einspanier et al., 1997;Gunnersen et al., 1996;Filonzi et al., 2007). In women serum levels of relaxin follow the pattern of chorionic gonadotropin hormone (hCG). Relaxin levels rise after ovulation as a result of production by the corpus leuteum, in the absence of pregnancy the levels will decline at menstruation. During the first trimester of pregnancy levels of relaxin are high. The additional relaxin is produced by the decidua. The levels are maintained during the second trimester but decline in the third trimester of pregnancy and it is thought that relaxin is important in implantation and maintenance of the embryo in early development (Parry and Vodstrcil, 2007;Einspanier et al., 1999). Although in many species relaxin has been shown to be important in pregnancy, the serum level detected does not rise above 1 ng/ml in humans. The levels detected in humans are around two orders of magnitude lower than in rats, mice and pigs, where levels

of around 150 ng/ml have been detected. Relaxin widens the pubic bone facilitating labor in guinea pigs. Relaxin softens the cervix (cervical ripening) and relaxes the uterine musculature, which is why relaxin has been thought of as a hormone of pregnancy for many years (Parry and Vodstrcil, 2007). Although relaxin does have important roles in pregnancy more recently it has been found to have a diverse range of biological actions in several species (Sherwood., 2004). Relaxin can affect collagen metabolism, inhibiting its synthesis and enhancing its breakdown by increasing matrix matalloproteinases (MMPs) expression (Samuel et al., 2005a). This obviously has implications in fibrotic conditions and work has begun to investigate the role of relaxin in several fibrotic organs including the heart, lungs, kidneys and the liver (Samuel, 2005b). Relaxin enhances angiogenesis having implications in cancer and has been found to be a potent renal vasodilator which is important in pregnancy and could help protect the kidneys from hypertensive forces (Samuel and Hewitson, 2006;Jeyabalan et al., 2003;Jeyabalan and Conrad, 2007;Jeyabalan et al., 2007).

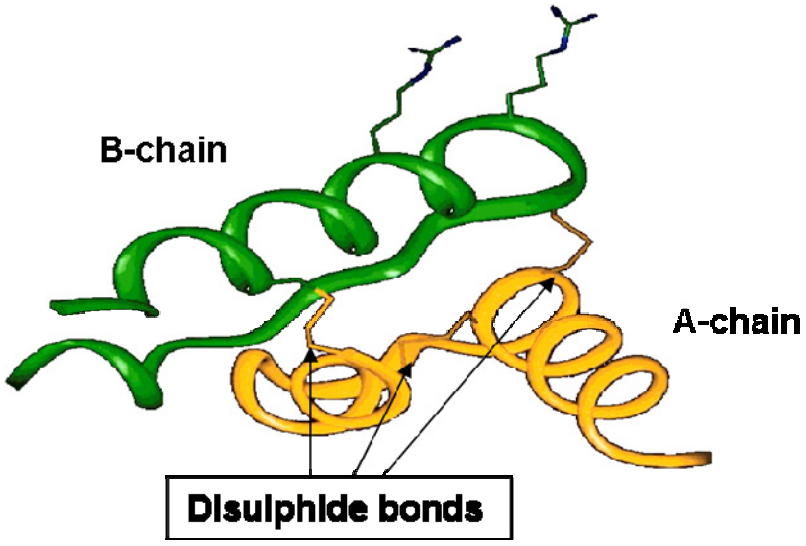

Figure 1.8. Tertiary structure of relaxin showing the A and B chain linked via two disulphide bonds and the intra-chain disulphide bond in the A-chain. (Pubmed)

In recent years the relaxin family of peptides has expanded with the discovery of five more relaxin-related peptide genes, Insulin like-3 (INSL3), Insulin like-4 (INSL4), Insulin like-5 (INSL5), Insulin like-6 (INSL6) and H3 relaxin. H3-relaxin was discovered by Bathgate and colleagues in 2002 (Bathgate et al., 2002). Orphan receptor GPCR-135 was used as bait to identify the ligand from brain extracts by HPLC. An amino acid motif in H2-relaxin was found to be highly conserved on the peptide eluted with GPCR-135 (RXFP-3), which was subsequently found to activate relaxin receptors. The peptide was identified as H3-Relaxin and was found to activate GPCR-135 (RXFP-3) with the greatest efficacy, subsequently deorphanising the receptor which has since been described as a neurotransmitter-like substance found mainly in the regions of the brain where the RXFP-3 receptors have been localized (Bathgate et al., 2002). INSL5 was discovered to bind to RXFP-3 and RXFP-4 receptors. It was subsequently found to activate RXFP-4 and by binding to RXFP-3 actually inhibits the binding of H3-relaxin to its receptor but does not activate the receptor(Liu et al., 2003;Liu et al., 2005b).

1.6.2 Relaxin receptors and signalling mechanisms

The most significant advance in relaxin biology has been the deorphanisation of the receptors for relaxin (Hsu et al., 2002). Relaxin receptors are a relatively new family of receptors causing a substantial upsurge in interest in recent years in relaxin biology. The receptors were found to contain a leucine-rich repeat domain, and a seven transmembrane region that coupled to G proteins (figure 1.9). The receptors were found to be class 1 G-protein coupled receptors (GPCRs). This was the logic behind the original nomenclature used for the receptors, leucine rich repeat containing GPCR (LGR7 and LGR8). An international union on nomenclature was agreed in 2006 (table.1) (Bathgate et al., 2006). There are four members of the relaxin receptor family. RXFP-1 and RXFP-2 are seven transmembrane receptors that have a large leucine rich extracellular domain that is essential for ligand binding (Halls et al., 2005c;Halls

et al., 2005b), and a low density lipoprotein domain that is thought to influence receptor maturation and trafficking to the membrane (Kern et al., 2007). RXFP-3 and RXFP-4 are also seven transmembrane receptors but lack the leucine rich repeat domain found in RXFP-1 and RXFP-2. RXFP-3 and RXFP-4 were originally called GPCR 135 and GPCR 142 before deorphanisation respectively. Binding to RXFP-3 and RXFP-4 is less well defined but the lack of the leucine rich repeat domain may explain the differences in ligand binding and potency of activation (Liu et al., 2005a).

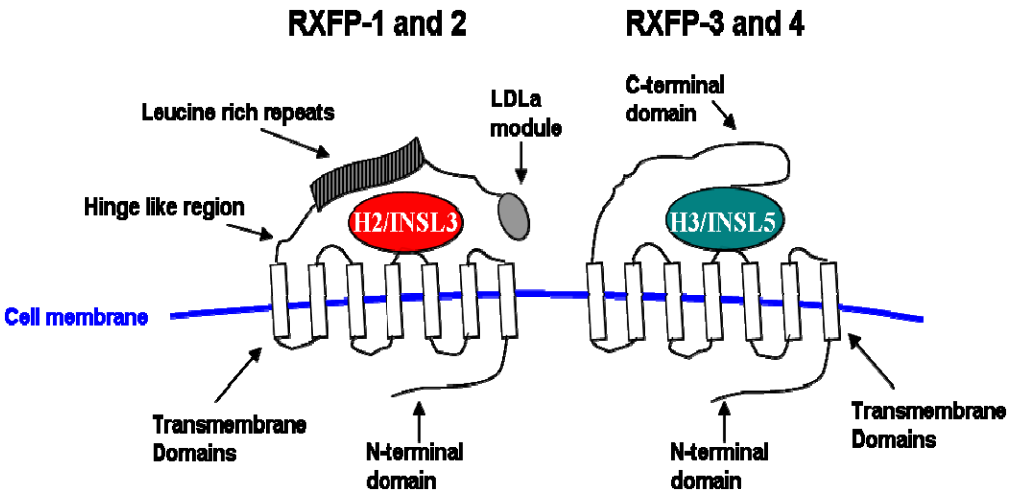

Figure 1.9. Schematic representation of the relaxin receptor structure and orientation in the cell membrane.

RXFP-1 (LGR7) is able to bind to H2-relaxin, H3-relaxin and INSL3, but its main activating ligand is H2-relaxin. H2-relaxin binds to and activates RXFP-1 with greater efficacy then any of the relaxin family peptides. RXFP-2 (LGR8 or GREAT) is able to bind to INSL3, H2 relaxin and H3 relaxin, but its main activating ligand is RXFP-2. RXFP-2 and INSL3 knockout models have the same phenotype. This was the first piece of evidence that linked these receptors, and led to the deorpahnisation of further relaxin family receptors. RXFP-3 (GPCR135 or SALPR) is able to bind to H3 relaxin and INSL5, although INSL5

acts as an antagonist at the RXFP-3 receptor. RXFP-4 (GPCR142 or GPR100) is able to bind to INSL5 and H3 relaxin, although the main activating receptor is believed to be INSL5. There have been no RXFP-4/INSL5 or RXFP-3/H3-relaxin knockout models developed to be able to study the importance of these receptors and to be able to link the receptor/ligand complex in an *in vivo* setting. The accepted nomenclature, relative ligand potencies, potential signalling mechanisms and knockout model phenotypes are described in table 1 (Bathgate et al., 2006).

Receptor	Ligand potencies	Potential Signalling Mechanism	Knockout model phenotype
RXFP-1 (LGR7)	H2-Rlx>H3 Rlx>> INSL3	↑cAMP, PI3-K, NOSII, Erk1/2	Age related heart, lung and kidney fibrosis.
RXFP-2 (LGR8)	INSL3>H2 Rlx>>H3 Rlx	↑cAMP	Cryptochirdism
RXFP-3 (GPCR135)	H3 Rlx>H3 Rlx B-Chain >>INSL5	↓cAMP	No Knockout model
RXFP-4 (GPCR142)	INSL5=H3 Rlx>>H3 Rlx B-Chain	↓cAMP	No knockout model

Table.1. The accepted receptor and ligand nomenclature (Bathgate et al., 2006).

Binding studies have been carried out to identify the region of the RXFP-1 and RXFP-2 receptors that are important for binding and activation by their respective ligands H2-relaxin and INSL3. Maximal activation of the RXFP-1 receptor requires interaction with both the ectodomain and exoloop 2 of the transmembrane domain (Halls et al., 2005b). Further studies identified the ectodomain to be the high affinity binding site and exoloop 2, the lower affinity binding site. A third region has also been discovered to be involved in the activation of these receptors; the N-terminal low density lipoprotein class-A (LDLa) module that is unique to the class C LGR's (Halls et al., 2005c;Kern et al., 2007;Bathgate et al., 2005). Stimulation of RXFP-1 and RXFP-2 receptors causes an increase in cAMP, although the coupling of these receptors still under

investigation and other potential downstream pathways have been suggested (figure 1.10) (Bathgate et al., 2005).

Much emphasis has been put on relaxin utilising the activation of cAMP accumulation pathway. The cAMP signalling pathway can be observed using simple assays, allowing the manipulation of receptor-ligand interactions in different cell types to be studied. The possible signalling pathways have been investigated through the use of reporter gene and cAMP assay in the RXFP-1 expressing THP-1 cell line and through transfecting a RXFP-1 construct into HEK293T cells (Halls et al., 2005a;Nguyen et al., 2003). The increase in cAMP has been found to be biphasic. The biphasic nature of cAMP accumulation observed in THP-1 and myometrial cells suggests the activation of adenylate cyclase may be by more then one mechanism (Dessauer and Nguyen, 2005). It is thought that the initial accumulation of cAMP is due to the classic Gs-adenylate cyclase pathway, and the delayed response may be due to the Gi-linked PI3-Kinase pathway. Further studies have also shown that the delayed response is reliant on the PI3-kinase-dependent protein kinase C (PKC) translocation to the cell membrane (Halls et al., 2006).

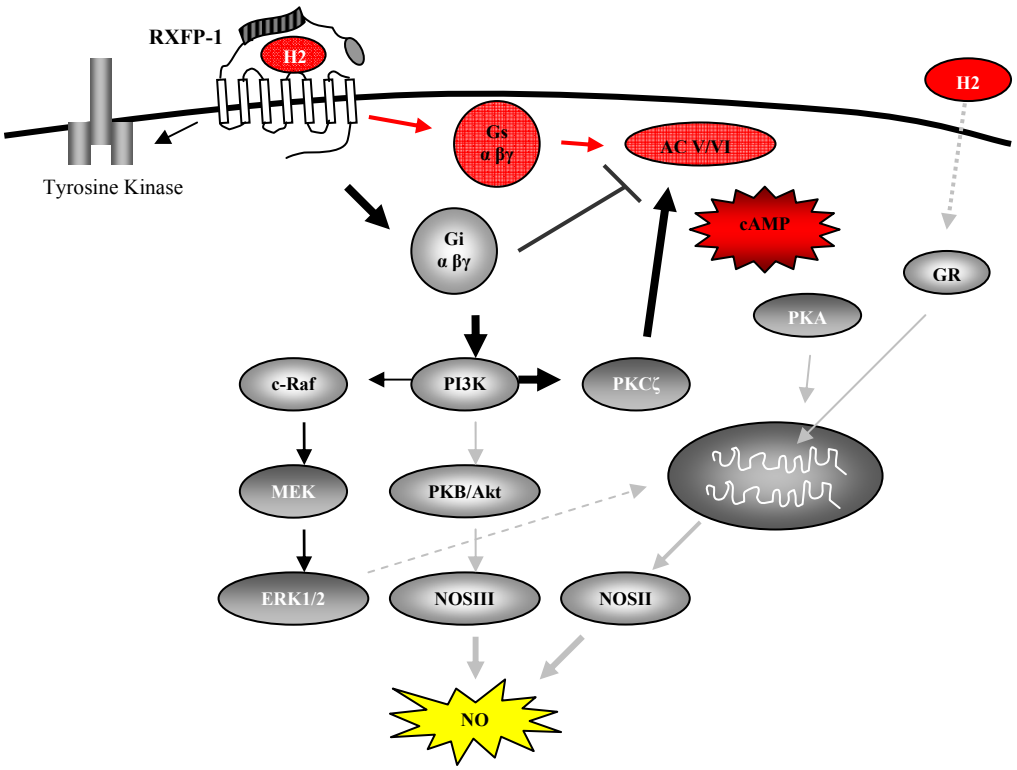

Figure 1.10. Potential signalling pathways of RXFP-1. Signalling pathways highlighted in red are used in assays to assess RXFP-1 activation, adapted from (Bathgate et al., 2005).

RXFP-3 and RXFP-4 have been less extensively studied compared to RXFP-1 and RXFP-2 but several downstream signalling mechanisms have been suggested (figure 1.11) (Bathgate et al., 2005). RXFP-3 and RXFP-4 are negatively coupled to cAMP, activation of the receptors decreases the accumulation of adenylate cyclase through the activation of G-protein Gi. The decrease in adenylate cyclase reduces the production of cAMP in the cell. In addition activation of Gi can activate PI3K and phospholipase C (PLC) and subsequently PKC, which may all have downstream affects on gene transcription and cellular responses (Zhong et al., 2005). PLC is an enzyme that hydrolyses glycerophosphatidates with the formation of diacylglycerol and a phosphorylated nitrogenous base such as choline (Long and Maguire., 1954). At the present time the down regulation of cAMP is possibly the most robust

method of detecting activation of RXFP-3 and RXFP-4 in the cell systems used in this study.

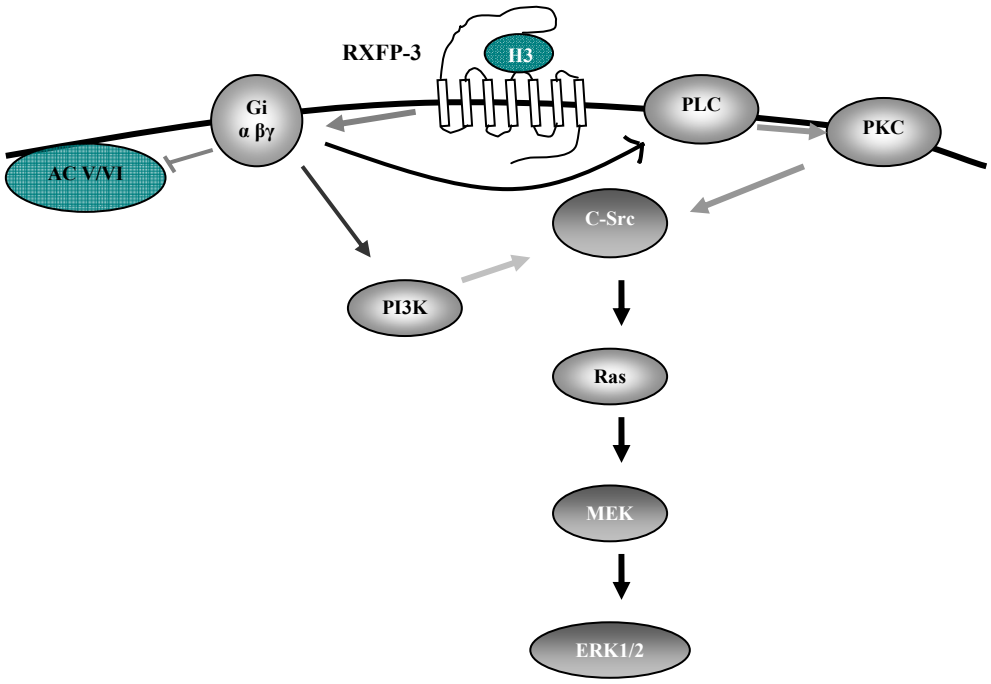

Figure 1.11. Potential signalling pathways of RXFP-3 and 4, adapted from (Bathgate et al., 2005).

PKCs are a family of protein kinases that consists of 10 isoforms in 3 subfamilies. The 3 subfamiles are divided into conventional, novel and atypical which is based on their second messenger requirements (Dempsey et al., 2000). The structure consists of a regulatory domain and a catalytic domain tethered by a hinge region. The catalytic domain is highly conserved among the different isoforms and to a lesser degree among other serine/threonine kinases (Dempsey et al., 2000). Relaxin is thought to activate the PKC zeta isoform which is an atypical PKC phosphorylated only on the activation loop and turn motif (Dessauer and Nguyen, 2005). Phosphorylation of the hydrophobic motif is unnecessary due to the presence of glutamic acid in the place of a serine which

as a negative charge acts similarly to a phosphorylated residue. Phosphorylation events are essential for the activity of the enzyme. Conventional and novel forms of PKC require Ca^{2+} and/or diacylglycerol (DAG) for activation but atypical forms such is activated by relaxin require neither Ca^{2+} or DAG but in this instance are thought to be dependent on phosphoinositde 3-kinase (PI3 Kinase) (Dempsey et al., 2000). Upon activation PKC enzymes are translocated to the plasma membrane by receptor activated C-kinase (RACK) proteins that are responsible for binding the active forms of PKC. The different isoforms of PKC use different RACK proteins as they mediate differential subcellular targeting (Csukai and Mochly-Rosen, 1999). Relaxin elicits a biphasic increase in cAMP when the RXFP-1 receptor is present. PKC proteins are known for there long term activation, and could be responsible for the second phase of the relaxin signalling response (Dessauer and Nguyen, 2005).

Relaxin has been found to stimulate protein kinase A (PKA) activity in bronchial epithelial cells and was found to activate PKA in reporter gene studies (Wyatt et al., 2002;Halls et al., 2005a). The increase in activity was 3-4 fold after 4 hours with a return to baseline after 8-10 hours. This differs from the very rapid activation of PKA through the activation of beta-adrenergic receptors (Wyatt et al., 2002). PKA also known as cAMP dependent protein kinase, which refers to a family of enzymes whose activity is dependent on the level of cAMP in the cell (Van den Berg et al., 1980). PKA is a holoenzyme consisting of two regulatory and two catalytic subunits. Under low levels of cAMP the enzyme remains intact and catalytically inactive. If the cAMP concentration increases in the cell the cAMP molecule will bind to the regulatory subunits of the PKA molecule which then undergoes a conformational change that releases the catalytic subunits, which are then free to phosphorylate other proteins in the cell. Direct protein phosphorylation by PKA can increase or decrease the activity of proteins and can be fast acting (Servillo et al., 2002). PKA can affect protein synthesis through the activation of cAMP response element binding proteins (CREB) which are transcription factors that bind cAMP response elements in

DNA, altering transcription and synthesis of proteins (Tacke et al., 2005). Proliferation of activated HSC has been reduced by the phosphoylation of CREB through a PKA mediated pathway (Houglum et al., 1997).

More recently there is evidence that relaxin can act on cells both acutely and chronically by increasing the expression and activity of nitric oxide synthase (NOS) and therefore increased processing of nitric oxide (NO) (Nistri and Bani, 2003). Nitric oxide is a secretory product present in most mammalian cells. The biological properties of nitric oxide were first widely appreciated when it was discovered that nitric oxide was endothelial derived relaxing factor (EDRF) (Furchgott and Vanhoutte, 1989;Ignarro et al., 1988). EDRF had already been described as having potent vasodilatory properties in stimulated endothelia (Furchgott and Zawadzki, 1980;Furchgott et al., 1984). NO is now recognized as being a pleiotropic biological mediator that regulates a diverse range of activites from neuronal function to immune system regulation. Upon secretion it can locally activate the host defense immune response, and has homeostatic and developmental functions by either direct stimulation or through intracellular cell signalling (Billack, 2006;Bilzer et al., 2006). NO is a gaseous free radical and is the product of five electron oxidation of the amino acid L-Argenine mediated through nitric oxide synthase (NOS). Members of the NOS family include neuronal (nNOS), endothelial (eNOS) and inducible (iNOS). nNOS is highly expressed in neurons of the central and peripheral nervous system and has been described in other cells types such as skeletal muscle myocytes, lung epithelial cells and skin mast cells. eNOS is highly expressed by endothelial cells and may also be found in neurons, dermal fibroblasts, epidermal karatinocytes, thyroid follicular cells, hepatocytes and smooth mucle cells. iNOS is expressed in a wide range of cell types including chondrocytes, epithelial cells, hepatocytes, glial cells and several cell types of the immune system. eNOS and nNOS are constitutively expressed and regulated by Ca^{2+}/calmodulin, whilst iNOS is induced by endotoxin and inflammatory cytokines and exhibits a relative insensitivity to Ca^{2+} (Alderton et al., 2001;Kone et al., 2003). NO has the

potential to mediate its effects on its target tissue via several different mechanisms, as a direct effector molecule NO can activate kinases, proteases and regulatory proteins directed by reactive oxygen intermediates. As a messenger molecule NO interacts with target molecules based on their redox potential rather then their non covalent complimentarity. Activation of the immune system is associated with an increase in macrophage nitric oxide production. NO exerts a variety of homeostatic influences as an activator of soluble guanylyl cyclase (GC), which catalyses the formation of the second messenger Guanosine 3', 5'-cyclic Monophosphate (cGMP). cGMP has a range of biological functions such as axon guidance and synaptic plasticity, cell survival and proliferation, angiogenesis, inflammation and a contraction regulator of both smooth muscle and vascular tissue. Defects in cGMP signalling have been reported in HSC from cirrhotic patients, which has been suggested contributes to the impaired NO responses in the relaxation of HSC (Perri et al., 2006). NO also has functions as an anti-tumor and anti-mircobial agent via mechanisms that include its conversion to peroxynitrite ($ONOO^-$), the formation of S-nitrosothiols, and the depletion of argenine (Bogdan, 2001). Another role for NO includes the suppression of mitochondrial respiration through the inhibition of cytochrome oxidase (Antunes et al., 2004). NO may also modify protein activity through the post-translational nitrosylation via the attachment of an NO moiety to the thiol side chain of cysteine residues (Hess et al., 2005). NO is lipid soluble and is therefore not stored but synthesized when needed and then freely diffuses across lipid membranes. NO has a very short half life *in vivo* as it is metabolized to two stable products nitrate (NO_3) and nitrite (NO_2) within a few seconds or less. The levels of these more stable metabolites can be used for indirect measurements of NO in biological fluids. Altered levels of NO have been associated with vascular disease, pregnancy related disorders, inflammatory diseases, hypoxia and cancer (Wimalawansa, 2008).

Relaxin has also been reported to act on Glucocorticoid receptors (GRs). GRs belong to a receptor superfamily that includes steroid, thyroid and retinoic acid receptor proteins. GRs function as ligand dependent transcription factors i.e. nuclear receptors. When relaxin binds the cytoplasmic GR it activates and translocates to the nucleus where it binds specific glucocorticoid response elements (GRE) of the DNA, thereby stimulating transcription of the responsive gene (Dschietzig et al., 2004;Dschietzig et al., 2005). Activated GRs can also interact with transcription factors such as NF-κB and AP-1, which then may indirectly influence gene expression. Cytoplasmic GR is complexed with different proteins such as molecular chaperones Hsp70 and Hsp90 that appear to be essential for ligand binding and receptor activation. There are two human isoforms of GRs, GR-α and GR-β (Dschietzig et al., 2004;Dschietzig et al., 2005). The two different isoforms originate from the same gene but are alternatively spliced. The GR-α form is the most abundant with GR-β hardly detectable. The function of GR-β is still under debate but it has been suggested that it is a dominant negative inhibitor of GR-α (Dschietzig et al., 2004;Dschietzig et al., 2005). Treatment with relaxin reduces the production of pro-inflammatory cytokines by human macrophages; this action is blocked by the glucocorticoid receptor antagonist RU486. Relaxin not only enters intact cells but it appears to become concentrated in the nucleus where it competes with GR agonists to activate GR receptors, and induces nuclear translocation and DNA binding. This action has been reported to be independent from the activation at RXFP1 receptors as modified relaxin unable to bind the RXFP1 receptor retains activity at the GR receptor (Bathgate et al., 2005). Relaxins role as a GR agonist and its pivotal effects in cytokine secretion by human macrophages will help our understanding of the abundant physiological actions that relaxin exerts far beyond its role in pregnancy (Dschietzig et al., 2004)

Relaxin may stimulate many different pathways in different cell types. The mechanism of this activation is important to further understanding the role of relaxin but the downstream effects regulating gene and protein expression are of

vital importance when considering relaxin receptors as a target for therapeutic intervention in humans. Studies characterising the phenotype of cells and animal models after exposure to recombinant human relaxin are required before relaxin therapies can be justified in human trials. The safety of relaxin is not in question but understanding the potency of action and effect on different cell types will ultimately influence the outcome of any trials.

1.6.3 Relaxin and fibrosis

Relaxin has been found to play an important role in the ripening of the cervix ready for parturition, inhibiting uterine contraction and softening the birth canal, which requires tissue remodelling of the cervix and the interpubic ligament. The tissue remodelling of the cervix has been studied and the effect of relaxin seems to be due to the decrease in production of collagens type 1 and III and the increase in production of collagenases (Sherwood, 2004a). One of the most consistent biological effects of relaxin is its ability to stimulate the breakdown of collagen, not only stimulating collagen remodelling in the birth canal but in cells and tissues affected by fibrosis. The use of relaxin to treat scleroderma was suggested in the 1950s (Casten and Boucek., 1958). In the late 1990s relaxin was used in clinical trials to treat scleroderma, which is a complex disorder of the connective tissue, characterised by thickening and fibrosis of the skin. Scleroderma if severe, can affect several internal organs such as the heart, lung, liver and kidneys. Relaxin treatment reduced skin thickening and increased mobility, although the efficacy end points were not reached highlighting the need to determine the potency and mechanism of action of relaxin in fibrotic disorders (Seibold et al., 2000). Relaxin was shown to inhibit collagen accumulation in a bleomycin induced model of lung fibrosis by inhibiting TGF-β-induced production of matrix proteins and stimulating MMP-induced collagen breakdown (Mookerjee et al., 2005a). Relaxin affects cardiac function and participates in the regulation of blood pressure, blood flow and fluid balance (Sherwood., 2004). Studies have been carried out showing relaxin exerting a

significant cardioprotective effect in the ischemic and reperfused rat heart. Systemic administration of relaxin results in a marked reduction of the myocardial areas damaged by post-ischemic reperfusion as well as a reduction in the occurrence of ventricular arrhythmias. Ischemic-reperfused hearts from the relaxin treated group showed a marked decrease in the recruitment of neutrophils from the circulation into the myocardium compared to the non-treated group (Bani et al., 1998). Relaxin has been studied in an animal model of liver fibrosis. Human recombinant relaxin was used to continuously treat a group of six male Sprague-Dawley rats via an osmotic pump, that were also injected (interperitoneally) with Carbon Tetrachloride (CCl_4) for a period of twenty eight days to induce hepatic fibrosis. This group was compared to a control group of six rats also being injected with CCl_4, but instead of relaxin were given PBS continuously via an osmotic pump. There was a decrease in collagen-1 synthesis and deposition as well as a decrease in liver weight in the relaxin treated group, which was repeated *in vitro* with cultured rat HSC when treated with relaxin (Williams et al., 2001a). The effect of relaxin in inhibiting collagen synthesis in the above rat model of liver fibrosis and in cultured rat HSC suggests relaxin could have similar effects in human HSC. Currently there are no data in the effect of relaxin on human HSC biology.

Relaxin knockout mice were developed, lacking H1-relaxin which is the main circulating form in rodents (Samuel et al., 2005). Endogenous relaxin is a naturally occurring inhibitor of collagen turnover, playing a role in maintaining the balance between collagen production and degradation in most major organs of the body (Samuel et al., 2005). The effect of relaxin is believed to be significant from normal growth and development, pregnancy through to aging. Male relaxin knockout mice show marked deficiencies in the reproductive tract and by 3 months of age several reproductive organs, including the prostate, testis and seminal vesicle, were significantly smaller then in age matched wild types (Samuel et al., 2005). Further studies confirmed the increase in collagen content in the prostate and testis which was associated with impaired function (Samuel

et al., 2003). Male relaxin knockout mice consistently develop organ fibrosis in the lung, heart, kidneys and prostate which led to altered tissue structure and organ dysfunction. Female relaxin knockout mice demonstrate increased fibrosis in the reproductive tract and nipples during late pregnancy which resulted in the inability of relaxin knockouts to suckle their young. Subsequent studies have connected these deficiencies to excess collagen deposition (Zhao et al., 1999;Zhao et al., 2000). Female relaxin knockout mice demonstrate delayed onset of fibrosis in the lung but did not display fibrosis in the heart and kidneys (Samuel et al., 2005). There are obvious phenotypic differences between male and female relaxin knockout mice. The presence of androgens in males has been suggested to contribute to increased fibrosis (Du, 2004) and female specific factors such as hormones, particularly estrogen may compensate for the loss of relaxin. Estrogen has been found to decrease collagen synthesis and to inhibit the profibrogenic effects of TGF-β (Neugarten et al., 1999;Negulescu et al., 2002). Treatment of relaxin knockout mice with recombinant H2-relaxin restored the normal tissue architecture in the lung, heart and kidneys particularly if applied at the early onset of the fibrotic changes (Samuel et al., 2005). RXFP-1 knockout mice were found to have a similar phenotype to the H1-relaxin knockouts (Krajnc-Franken et al., 2004). Taken together these data add further supporting evidence to the idea that relaxin is antifibrotic in many organs.

Relaxin was shown to inhibit fibroblast proliferation as early as 1989. It was demonstrated that relaxin could affect the normal course of cell division in the 3T3-L1 fibroblast cell line (Pawlina et al., 1989). Since this observation it has been shown that relaxin can directly inhibit fibroblast differentiation by inhibiting α-SMA expression and reduce cell number and proliferation in rat cortical fibroblast, rat cardiac fibroblasts, rat hepatic stellate cells and TGF-β stimulated renal fibroblasts (Masterson et al., 2004;Samuel et al., 2004;Bennett et al., 2003). Relaxin has been shown to reduce newly formed collagen secretion *in vitro* when applied to human dermal fibroblasts, human lung fibroblast, rat hepatic stellate cells, rat cortical fibroblasts and rat cardiac

fibroblasts (Unemori and Amento, 1990;Unemori et al., 1996;Williams et al., 2001b;Samuel et al., 2004). Relaxin had a marked effect even in the presence of profibrotic factors such as TGF-β1, Interleukin-1 and Angiotensin II in some cell culture models. Relaxin did not effect the basal collagen expression in any of the cells it was applied to highlighting its specificity to affect scarred tissue and not normal collagen architecture (Samuel, 2005a). The ability of relaxin to inhibit collagen deposition has been studied in numerous human and rat *in vitro* and *in vivo* models of fibrosis. It appears that relaxin can stimulate the expression and activation of several MMPs, including MMP-1, MMP-2, MMP-3, MMP-9, MMP-12 and MMP-13 in various organs and animal models (Garber et al., 2001;Lekgabe et al., 2005;Williams et al., 2001b;Mookerjee et al., 2005a). Relaxin was also documented as inhibiting the expression of TIMPs, particularly TIMP-1 and TIMP-2 (Unemori and Amento, 1990;Williams et al., 2001b). The mechanism by which relaxin down regulates collagen deposition may then in part be due to regulating the expression of MMPs and TIMPs, shifting the MMP-TIMP balance to a pro-resolution phenotype (Hemmann et al., 2007).

The most potent profibrogenic cytokines are TGF-β1 and AngII and their downstream mediators CTGF, PDGF and ET-1. TGF-β1 is a potent stimulator of ECM and collagen synthesis in fibroblasts and HSC. Relaxin has been documented as inhibiting the TGF-β1 induced secretion of ECM and collagen in human dermal, pulmonary and renal fibroblasts (Unemori and Amento, 1990;Unemori et al., 1996;Heeg et al., 2005). Relaxin was found to inhibit smad2 phosphorylation and its translocation to the nucleus which prevented smad2 forming a complex with smad3 and therefore inhibiting the action of TGF-β1. Relaxin was also found to be a potent inhibitor of TGF-β1 induced renal fibroblast activation and in a rat *in vivo* model of chronic renal disease relaxin reduced the expression of TGF-β1 (Unemori and Amento, 1990;Unemori et al., 1996;Heeg et al., 2005). There is evidence that relaxin is a functional ET-1 antagonist. Relaxin not only inhibited the stimulation of ET-1 but increased the endothelial and epithelial expression of ET_B receptors via a Raf-MEK-1-

ERK-1/2 dependent pathway that subsequently activated NF-κB (Dschietzig et al., 2003).

It is acknowledged that relaxin is an important mediator of human gestational renal adaptation. Data from rat models (Conrad et al., 2005) and human studies (Smith et al., 2005) have suggested that relaxin functions to regulate renal hemodynamic and osmoregulatory changes by decreasing the vascular resistance in the kidneys, thereby increasing the glomerular filtration rate (GFR) and cardiac output facilitating the expansion of plasma volume which stimulates renal sodium and water retention. There have been several mechanisms suggested by which relaxin has these effects. Nitric Oxide (NO) is a well known vasodilator and increased excretions of NO metabolites have been found in pregnant rats. Infusion of inhibitors to NO such as L-NAME and L-NMA were found to decrease GFR and increase vascular resistance therefore indicating a direct role for NO in renal adaptation during pregnancy (Conrad et al., 2005). The increase in NO in the cell was suggested to be through several mechanisms including increased activation of NOS II and NOS III enzymes through the activation of second messenger systems linked to RXFP-1 activation and the increased expression and activation of the endothelin B receptor (ET_B). It was hypothesised that relaxin could upregulate gelatinase activity (MMP-2) during pregnancy which increases the cleavage of big ET at the gly-leu bond to $ET_{1-32.}$ ET_{1-32} was discovered at the end of the nineties by Fernadez-Patron and colleagues (Fernandez-Patron et al., 1999) and was found to be a novel ET-1 agonist that was dependent upon MMP-2 for cleavage and activation. ET_{1-32} was found to have activity at both ET_A and ET_B receptors. Activation of ET_B can increase the activity of nitric oxide synthase enzymes (NOS) in the target tissue. NOS catalyses the reaction which produces NO from L-Arginine, NADPH and $O_{2.}$ NO induces vasodilatation through a range of second messenger systems depending on the target tissue. The traditional endothelin converting enzyme (ECE) that processes big ET to ET_{1-21} was not involved in the increased processing in the kidney during pregnancy. Therefore if the

expression of ET_B receptors was increased in the target tissue and there was increased processing of the precursor for ET_{1-32} thus increasing the activation of the receptor, this could increase the level of nitric oxide synthase III (NOS III) in the tissue which in turn increases the level of NO in the tissue inducing renal vasodilatation (Fernandez-Patron et al., 1999). It has been documented that endothelin-1 is released in the fibrotic liver inducing contraction of the HSC and other structures which can exacerbate the injury and cause complications such as portal hypertension observed in the cirrhotic liver (Zhang et al., 1994;Pinzani et al., 1996).

1.7 Hypothesis, Rationale and Objectives

1.7.1 Hypothesis

Relaxin receptors are expressed in human liver and H2-relaxin can antagonise the profibrogenic phenotype in cultured HSC. H2-relaxin inhibits the contraction of HSC in collagen gels. The knockdown of RXFP-1 inhibits the antifibrotic and anticontractile effect of H2-relaxin.

1.7.2 Rationale

Since the discovery of the family of GPCRs that respond to relaxin and relaxin-like peptides in 2002 there has been resurgence in interest in research into relaxin in multiple disease states. There are publications describing the possible antifibrotic role of relaxin for review see (Samuel, 2005a). Many of the papers are based on data collected from *in vitro* and *in vivo* animal work. Recombinant relaxin was used in the liver group in Southampton to treat CCl_4 injured rats. The results revealed relaxin had antifibrotic properties in the rat liver (Williams et al., 2001). Human clinical trials have been carried out using H2-relaxin as a continuous subcutaneous treatment for scleroderma (a form of skin fibrosis). The patients receiving 25 μg/kg relaxin per day had reduced skin thickening,

improved mobility and function. This affect was seen in patients with moderate to severe diffuse scleroderma (Seibold et al., 2000). The earlier studys of relaxin carried out by Williams and colleagues were before the deorphanisation of the receptors. The previous observations justified a preliminary experiment too quantify the relaxin receptor expression in CCl_4 injured rat liver. The results confirmed that relaxin receptors were expressed in the liver and were up regulated during injury (appendix 1). There has only been limited work carried out in rat liver and very little work has been published investigating relaxin in human models of liver fibrosis. The relaxin field would benefit from studies carried out to investigate the antifibrotic properties in human liver fibrosis therefore these preliminary results supported the study of relaxin in human models of liver injury.

1.7.3 Objectives

- To assess the relaxin receptor expression profile in human liver and hepatic stellate cells.
- To investigate the effect of H2-relaxin on the expression of markers of fibrosis such as α–SMA, TIMP-1, procollagen-1, MMP-1, MMP-2.
- To test the effect of H2-relaxin on cell viability through MTS assays and the expression of PARP-1.
- To determine the effect of H2-relaxin on the contractile properties of HSC in gel contraction assays.
- To determine if the phenotypic effects observed for H2-relaxin in HSC are through the activation of RXFP-1.

Chapter 2

Methods and Materials

2.1 Extraction and culture models of human hepatic stellate cells and hepatic stellate cell lines

All methods were carried out by the author unless otherwise stated. All human tissue was obtained and stored in accordance with the Human Tissue Act 2004. Liver tissue was sourced from Southampton General Hospital through surgeons carrying out tumour resections (Mr Pierce and Professor Primrose). Normal margins around the tumour tissue (around 30-50 grams) were dissected by a pathologist (in the pathology unit at Southampton General Hospital). The tissue was then used to extract cells and some was kept for fixation for later staining procedures.

The isolation and culture of Kupffer cells, sinusoidal endothelial cells and HSC was first described by (Friedman and Roll, 1987). This enabled researchers to study the cells which were believed to be major contributors to hepatic fibrosis in more detail. Human HSC have since been extensively characterised and are accepted as good model to study fibrotic changes *in vitro*. If cultured on plastic or a collagen-1 type matrix, HSC undergo a phenotypic change from a quiescent vitamin A storing cell, to a proliferative myofibroblast like cell. This mimics what is believed to occur *in vivo* during liver injury. The isolation of HSC depends on a density gradient that isolates the vitamin A storing cells from red blood cells and hepatocytes.

2.1.1 Human hepatic stellate cell isolation, preparation of enzyme solutions

Enzymes were weighed out, 100 mg Pronase (Sigma), 20 mg Collagenase (Roche), 10 mg DNase-1 (Roche). Each enzyme was dissolved in 20ml Hanks Buffered Salt Solution (HBSS-) (Invitrogen) and filtered through a 0.2 micron sterile filter (Fisher). HBSS is supplied with or without calcium chloride, magnesium chloride and sodium bicarbonate. When HBSS is used it will be stated whether it was plus or minus the aforementioned supplements.

2.1.2 Preparation of the liver

The liver was washed in HBSS- the peripheral fibroblast rich area was removed and the remaining liver was then cut into the smallest pieces possible. 2 ml of diluted DNase-1 was added. The liver was then transferred to a 500 ml autoclaved bottle and the diluted pronase and collagenase B were added. HBSS- was added up to 150 ml and this was incubated at 37ºC for 30-45 minutes in an orbital shaker (until liver is pale in colour). The liver homogenate is then filtered through a small weave Nybolt mesh (John Stainer + Co) (this is to achieve complete homogenous suspension), 1 ml DNase is added to non-specifically cleave any DNA released from damaged cells without harming the intact cells. HBSS+ was used to wash the liver through the nybolt mesh to make up a final volume of 200 ml of homogenate, which was then split into four 50 ml polypropylene Falcon tubes (Becton Dickenson).

2.1.3 Density Gradient Centrifugation

The four 50 ml Falcon tubes were then centrifuged at 1800 rpm for 7 minutes with the brake on. The supernatant was discarded and the pellet was resuspended in 1 ml of diluted DNase-1, add then HBSS+ to 50 ml. The tubes were then centrifuged for a further 7 minutes at 1800 rpm with the brake on (optional wash spin). The supernatant was discarded and the pellets were resuspended in 1 ml diluted DNase-1. The pellets are all pooled into one Falcon tube and were then made up to a final volume of 44.4 ml with HBSS+. 14 ml of Optiprep (Axis Shield) and 15.6 ml of HBSS+ were added to an autoclaved 100ml bottle and mixed. The pooled pellets were added to the optiprep/HBSS mix (gradient mix) and mixed well and were then divided into two Falcon tubes, 35 ml in each. A layer of 3 ml HBSS+ was then added slowly against the wall of the tube, this remained a layer on top of the gradient mix. The tubes were then centrifuged at 3500 rpm for 17 minutes with the brake off. This spin produced layers. The top layer was HBSS+, the next layer was the stellate cells, and there was a clear

band of cells between the HBSS+ and the optiprep layers. The layer of stellate cells was removed carefully (around 10 ml per 50 ml Falcon tube) and pooled together in a new 50 ml Falcon tube. 1 ml of diluted DNase-1 was added and then made up to 50 ml with HBSS+. The Falcon tube was gently inverted to wash the cells and then centrifuged at 1800 rpm for 7 minutes with the brake on. The supernatant was discarded from the cell pellet. The optional wash step was carried out, so the cells were resuspended in 1 ml diluted DNase-1 to 50 ml with HBSS+. The stellate cells were re-pelleted by spinning for 7 minutes at 1800 rpm, and discarding the supernatant as before leaving a cell pellet.

2.1.4 Cell culture

The pellet is resuspended in 16% Dulbecco's Modified Eagles Medium (DMEM) (with phenol red) (Invitrogen). To make up the 16% DMEM, 100 ml of DMEM was removed from the 500 ml bottle, 80 ml of fetal bovine serum (FBS) (Invitrogen) , 5 ml of pen/strep (Invitrogen), 5 ml of L-glutamine (Invitrogen) and 5 ml of sodium pyruvate (Invitrogen) was then added to the DMEM. 10% FBS DMEM was used for all of the assays carried out and the cells were cultured in 10% DMEM for 24 hours prior to the assay taking place. The addition of antibiotic and pyruvate is assumed unless otherwise stated. Cells were counted on a heamocytometer and plated out at 1 million cells per T75 flasks (Greiner), the number of flasks depended on the size of the cell pellet. The next day the cells were checked for fluorescence (retinoid droplets inside the stellate cells shine under the light microscope). The cells were fed by changing the media on day one, then every 3-4 days until confluent. Cells are passaged using an enzymatic reaction using trypsin. 10 x Trypsin-EDTA (Autogen Bioclear) was diluted with HBSS- or 1 X phosphate buffered saline (PBS) (Invitrogen) to a 1 X solution by adding 1 ml of trypsin to 9 ml of HBSS or PBS. HBSS- is used as trypsin efficiency is reduced in the presence of calcium and FBS. 5 ml of 1x trypsin was added to a T75 flask. The flask was returned to the humid 37°C, 5% $C0_2$ incubator for 5 minutes or until the cells

had lifted from the plastic. Ensuring all the cells had been removed from the plastic 5 ml of 16% DMEM was added to the T75 flask. This was to inhibit the enzyme reaction before the cells were damaged. The 10 ml cell solution was then added to a 15 ml Falcon and the cells were centrifuged at 800 rpm for 5 minutes. The supernatant was removed and discarded. The remaining cell pellet was resuspended in 9 ml of 16% DMEM. 3 ml of cell solution was then added to three T75 flasks. 7 ml of 16% DMEM was then added to each flask and the cells were returned to the 37°C incubator for 24 hours. The media was then removed and discarded form each flask and 10 ml of 16% DMEM was added to each flask. The cells were then retuned to the incubator until confluent or required feeding. Any liquid waste including cell culture media that came into contact with human cells was treated with a bleach solution (diluted virkon) to ensure no microorganisms could survive before disposal of the liquid waste.

2.1.5 Culture of human HSC cell lines

LX-2 cells were sourced from Professor Friedman's lab (Xu et al., 2005). LX-2 cells were made from primary stellate cells extracted from a normal liver, allowed to activate after being cultured on plastic and then transformed with the SV40 promoter, large T-antigen. These cells were named LX-1 cells. LX-1 cells were then grown under low growth serum selection pressure (2% serum), the majority of the cells died but the cells that grew through were found to have lost the SV40, large T antigen. These cells were named LX-2 cells and were found to tolerate low growth serum conditions with no loss of replication capacity (Xu et al., 2005). LX-2 cells can be cultured up to 50 passages but for use in these experiments the cells were not used over passage 25. LX-2 cells were cultured in 10% DMEM with phenol red.

2.1.6 Cell culture on matrigel

Growth factor reduced (GFR) matrigel basement membrane (Becton Dickenson) was coated on 100 mm culture dishes (Greiner) using the thick coating method. GFR matrigel was thawed by keeping on ice for 24 hours. All serological pipettes (Greiner) and 100 mm culture dishes that were to be coated were cooled. The coating procedure was carried out using aseptic techniques in a tissue culture hood. The culture plates were kept on ice whilst 5 ml of GFR matrigel was pipetted using cooled pipettes. The solution was spread evenly across the surface of the dish and then placed at 37ºC to solidify for one hour. The coated dishes were then washed with culture media before cells were plated on the matrix. Primary HSC that had been part activated by two days culture on plastic were plated on the matrigel matrix alongside being plated on plastic tissue culture dishes. Cells from the same prep were used for comparison. The cells were extracted after 2 weeks of culture. A cell dissociation solution, matrisperse (Becton Dickenson) was added to the cells plated on matrigel. This was to release the cells from the matrigel as after a few days the cells do not remain on top of the matrix but become associated with it. RNA and protein extracted is extracted from the isolated cells. Cells plated on tissue culture plastic are harvested for either RNA or protein directly from the plate after washing any media from the cells. The RNA and protein was then screened for HSC activation markers and relaxin receptor expression.

2.1.7 H2-Relaxin treatment of hHSC

Activated primary HSC and LX-2 cells were harvested using trypsinisation. The cells were counted on a heamocytometer using trypan blue exclusion and plated in 6 well culture plates (Greiner) at a density of 100,000 cells per well. The cells were cultured in 10% DMEM for 24 hours. The H2-relaxin ligand (Phoenix Pharmaceuticals) was reconstituted with PBS (Invitrogen) containing 1% BSA (Promega). The ligand was supplied in 20 µg vials and a 1 mM stock solution

was made by adding 3.35 µl PBS-BSA. The volume required to make the stock solution was calculated using the molecular weight of H2-relaxin.

$$\text{Number of moles} = \frac{\text{mass}}{\text{Molecular weight (MW)}}$$

$$\text{Number of moles} = \frac{20 \times 10^{-6}}{5963} = 3.354 \times 10^{-9}$$

$$\text{Number of moles} = \frac{\text{volume}}{1000} \times \text{concentration}$$

$$3.354 \times 10^{-9} = \frac{\text{volume}}{1000} \times 1 \times 10^{-3}$$

$$3.354 \times 10^{-9} \times 1000 = \text{volume} \times 1 \times 10^{-3}$$

$$\frac{3.354 \times 10^{-6}}{1 \times 10^{-3}} = \text{volume}$$

Volume = 3.354×10^{-3} ml or 3.354 µl

A 1 in 100 dilution was made from the stock to give a concentration of 10 µM in PBS-BSA. The media was replaced in the 6 well culture plates with 1.5 ml of 10% DMEM directly before treatment. The primary HSC and LX-2 cells were then treated with 1.5 µl of stock, 1.5 µl of the 10 µM dilution or 1.5 µl of PBS-BSA (the control well). This made the final concentration in the well 1 µM and 10 nM. The cells were then incubated at 37ºC for a further 24 hours before the same treatments are added. The cells were incubated for a further 24 hours before a third treatment is added. The cells were then incubated until the next morning before a final treatment is added. The cells were then incubated for a further 6 hours before the conditioned media was removed and placed in 2 ml Eppendorfs (Greiner). The media was stored at -20°C for future use. The cells were washed with two changes of PBS and then protein and RNA was extracted from the cells directly off the plate. If the assay was to asses the degree of apoptosis the culture media (10% DMEM) was replaced 24 hours before the

cells were lysed for protein extraction with SFM. The cells were incubated in SFM to induce apoptosis. The effect of relaxin could then be assessed in the presence or absence of serum. The assay was carried out after transfection with RXFP-1 siRNA. The affect of relaxin could then be assessed without the presence of its main functional receptor. The cells were also plated in 96 well plates (5000 cells per well) and treated with the same concentrations of relaxin and control vehicle as before for the use in the MTS assays. The assay was carried out with or without RXFP-1 siRNA in 6 well plates for use in the LDH cytotoxicity assay. The media used in this assay had no added pyruvate or antibiotics. The media was retained in 2 ml Eppendorfs before the cells were lysed in 1.5 ml of DMEM with 1% Triton X. The cells were incubated in the triton x solution for 5 minutes at room temperature. If the cells were fully lysed the cell culture supernatant was removed and stored at -20ºC in 2 ml Eppendorf tubes.

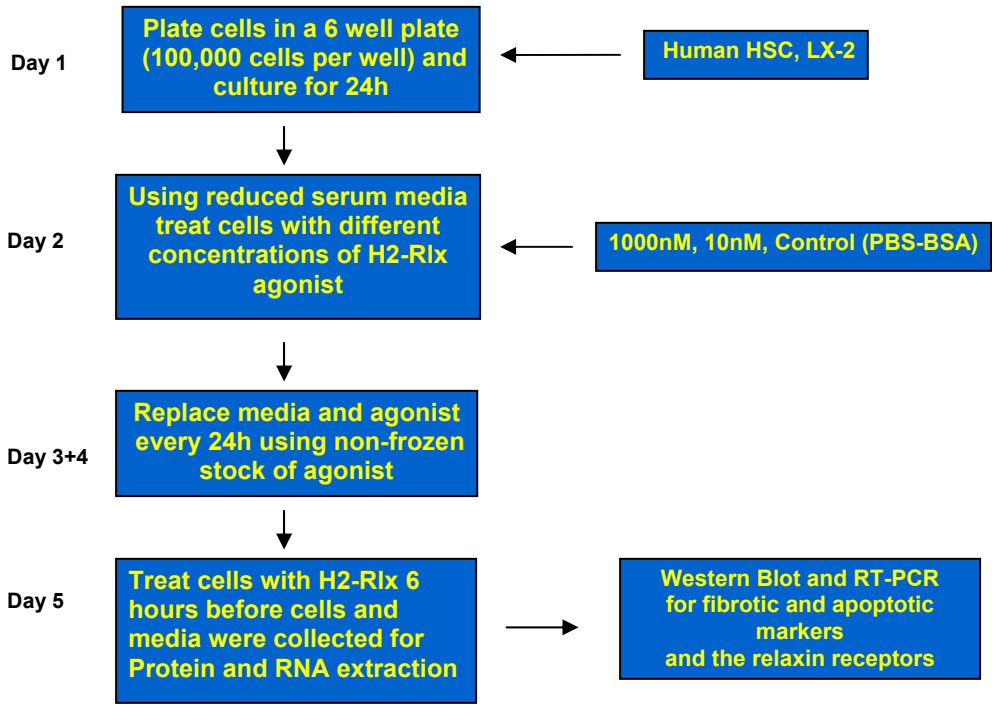

Figure 2.1. General protocol used to treat human stellate cells with a RXFP-1 agonist, H2-relaxin.

2.2 Phenotypic analysis of cells through RNA isolation and PCR amplification

The relaxin receptor expression was established and cell culture models were analysed for any phenotypic changes by looking at any up or down-regulation in gene transcription of mRNA. To enable us to detect any changes, the total RNA was isolated from the cells and then transcribed to cDNA. The cDNA was then used as the template in PCR amplification reactions using primers designed to amplify regions of the DNA specific to genes such as TIMP-1, MMP-2, GAPDH and the relaxin receptors. Extraction of RNA was carried out using Qiagen spin columns. The columns have been designed to purify RNA from small amounts of starting material through the selective binding of RNA to a silica based membrane. High salt buffer systems allow up to 100 μg of RNA longer then 200 bases to bind to the silica membrane using the high speed microspin technology. Samples are lysed and homogenised using a highly denaturing guanidine thiocyanate containing buffer which inactivates RNases (buffer RLT). This ensures purification of intact RNA. Ethanol is added to the buffering systems ensuring appropriate binding conditions. Total RNA binds to the membrane and the contaminates are washed away, this systems enriches mRNA binding as rRNAs, tRNAs and are excluded based on size (rRNA and tRNA are usually smaller then 200 bases). The RNA was then used for creating cDNA templates for use in PCR amplification reactions.

The amplification reaction can be carried out using a standard reverse transcription PCR (RT-PCR) reaction where the end point product is analysed. All PCR reactions are based on a three stage cycle that critically depends on temperature and time for efficient amplification of the PCR product (figure 2.2). This method allows semi quantitative analysis if housekeeping genes are also amplified from the same samples. The amount of PCR product is measured through agarose gel analysis and normalised to the housekeeping genes such as

GAPDH or β-actin amplified from the same sample. The amount of product is detected on the gel through software analysis that enables the intensity and size of the band on a gel to be quantified. The quantified end product is normalised relative to the housekeeping gene and this value for each sample relates to the amount of mRNA for that particular gene in the original sample. The disadvantage of standard PCR is the end product may be anywhere in the amplification stage (figure 2.3). If the reaction has reached a plateau for all of the samples it may be very difficult to detect any difference in the amount of product. To reduce any error in standard PCR the cycle numbers for amplification where kept below 28 cycles for both housekeeping genes and genes of interest, which will increase the chance of the reaction being stopped in the linear phase of the amplification cycle. The Reverse Transcription (RT) system provides lot-tested reagents to efficiently reverse transcribe poly (A) + mRNA or total RNA to cDNA within 15 minutes. cDNA synthesised with the Reverse Transcription System can be used directly in PCR. KOD hot start DNA polymerase (Promega) is a premixed complex of KOD HiFi DNA polymerase and two monoclonal antibodies that inhibit the DNA polymerase and 3'-5' exonuclease activities during PCR reaction assembly at ambient temperatures (Mizuguchi et al., 1999). KOD polymerase is named after the bacteria that it is isolated from Thermococcus Kodakaraensis. KOD hot start couples the high fidelity, fast extension speed and processivity of KOD HiFi with the high specificity of an antibody mediated hot start. Non-specific amplification is reduced since the mispriming events during set up and initial temperature increases are avoided. This enzyme efficiently amplifies genomic and phage/plasmid DNA targets up to 12 to 20 kbp, respectively. Guanine-Cytosine (GC)-rich targets are also efficiently amplified although the maximum GC content for primers was kept below 50% where possible.

Quantitative reverse transcription PCR (qRT-PCR) uses fluorescent dyes to detect the amount of product at each cycle in the amplification reaction. There are two common methods for qRT-PCR, one uses a fluorescent dye such as

SYBR green that intercalates with double stranded DNA and one that uses a an oligo sequence labelled with a fluorescent dye such as FAM (called a fluorescent probe) that will only bind to a specific sequence of DNA, the PCR target sequence. Continuous data retrieval, i.e. the amount of fluorescence detected after each cycle, throughout the amplification reaction (up to 45 cycles), enables sensitive and accurate detection of the amount of dsDNA for a specific gene. The fluorescence can be compared to a standard curve created for each gene that you which to amplify by amplifying from a known starting mRNA concentration, using 6-8 points on a logarithmic scale which allows you to give an absolute value, copies/µl for each gene of interest. The fluorescence can also more simply be compared to a set of housekeeping genes for each sample giving a relative amount but will also control for presence of primer dimmers. Threshold values are used to detect in which cycle of the reaction the fluorescence crossed the baseline and amplification becomes exponential. The reaction is continued until the fluorescence reaches a plateau. The cycle number at which the fluorescence detected crosses the baseline is called the CT value (figure 2.3). The CT value is used in a calculation to give you a final value, allowing comparison of fold changes in amount of product. The relative gene expression is calculated assuming 100% efficiency of the PCR (Stahlberg et al., 2005).

$$\frac{\text{Sample 1}}{\text{Sample 2}} = \frac{2^{(CT_{B1} - CT_{B2})}}{2^{(CT_{A1} - CT_{A2})}} = 2^{(CT_{B1} - CT_{B2})} - 2^{(CT_{A1} - CT_{A2})} = 2^{\wedge\wedge CT}$$

Taq polymerase (Primer Design) was used in all of the qRT-PCR reactions. Taq was also named after the bacteria that it was isolated from, thermus aquaticus (Chien et al., 1976). Taq polymerase is a hot start enzyme with an optimum operating temperature of 75-80˚C. It has a half life of 9 minutes at 97˚C and similar to KOD polymerase can amplify 1000 base pairs in 30-60 seconds at 72˚C. Taq has a low replication fidelity due to the lack of 3'-5' exonuclease proof reading activity, it has an error rate of 1 in 9000 nucleotides (Lawyer et al., 1993). RNA and DNA methods were carried out using aseptic techniques. The

plastic ware and water used were DNase and RNase free and also UV illuminated before use. UV illumination ensures crosslinking of any contaminating DNA which ensures the DNA cannot be amplified.

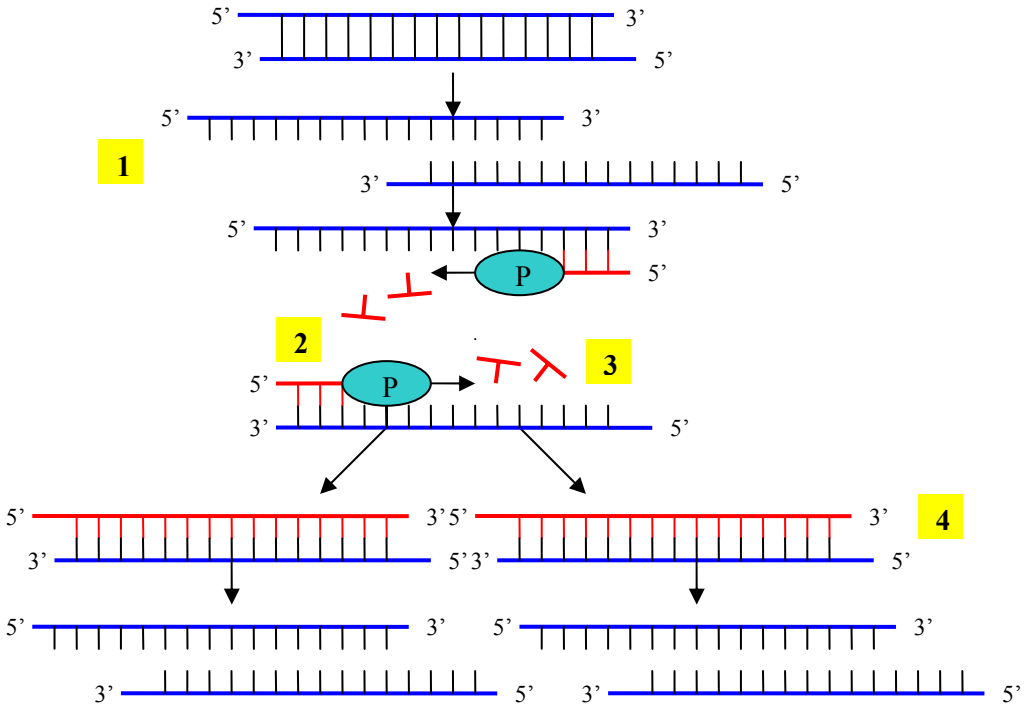

Figure 2.2. PCR amplification cycle. 1. cDNA is denatured at 95°C. 2. The temperature is then rapidly cooled to the melting temperature of the primers (usually between 50-60°C) to allow primers to anneal to the specific sites in the genome to which they were designed. 3. The temperature is then rapidly ramped to the extension temperature (68°C for KOD polymerase) where your chosen polymerase will continue adding dNTPs along the region of the gene which is to be amplified. Each polymerase can add base pairs at different rates (KOD polymerase requires 1 minute to add 1000 base pairs). The polymerase will discontinue adding dNTPS when the reverse primer stop codon is reached, KOD polymerase is a hot start, proof reading enzyme that enables accurate amplification of long sequences. 4. The newly amplified DNA goes back into the cycle which is repeated up to 25-35 times, increasing the number of copies of DNA exponentially. qRT-PCR undergoes the same reaction but a dye such as SYBR green will bind to any dsDNA products formed and the reaction is continued to 45-50 cycles.

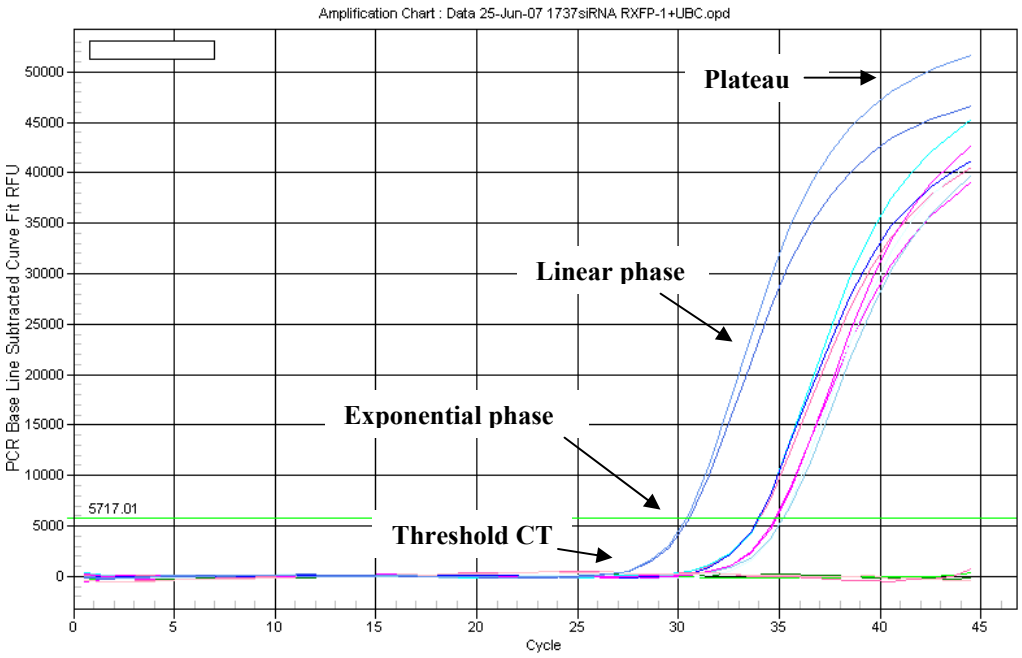

Figure 2.3. PCR cycle. The graph is a read out from a qRT-PCR but both qRT-PCR and standard PCR follow the same cycle. To be able to accurately semi quantitate a standard PCR, the reaction should be stopped within the linear phase.

2.2.1 RNA isolation

All centrifugation steps were performed at 20–25°C in a standard microcentrifuge at room temperature. Cells were either disrupted by adding buffer RLT directly to the cell culture vessel after several washes with PBS, method continues below, or cells were harvested from the cell culture vessel by trypsinisation. The cells were pelleted and the supernatant was removed by gentle aspiration. Complete removal of the cell-culture medium was essential as any carry through would inhibit lysis of the cells and dilute the lysate. This would affect the conditions for binding of RNA to the RNeasy silica-gel membrane, which would reduce RNA yield. Cells were grown in a monolayer and no more then 1 x 10^7 cells were used per column.

Cell lysis

The cells were disrupted by addition of Buffer RLT (Qiagen). The pelleted cells were loosened by thoroughly by flicking the tube. The appropriate volume of Buffer RLT (<$5x10^6$ cells= 350 µl, $5x10^6$ – $1x10^7$ cells = 600 µl) was added depending on the number of cells pelleted. Complete resuspension of the pellet was achieved by vortexing or pipetting up and down. Incomplete loosening of the cell pellet would lead to inefficient lysis and reduced yields. β - Mecaptoethanol (Sigma-Aldrich) was added to Buffer RLT before use (10 µl/ml).

Homogenisation

Incomplete homogenization would lead to significantly reduced yields and can cause clogging of the RNeasy mini spin columns (Qiagen). Homogenization with rotor–stator or QIAshredder homogenisers generally resulted in higher RNA yields than with a syringe and needle. The lysate was pipetted directly onto a QIAshredder spin column (Qiagen) placed in a 2 ml collection tube, and was centrifuged for 2 min at maximum speed.

RNA extraction

1 volume (usually 350 µl or 600 µl) of 70% ethanol (Fisher) was added to the homogenized lysate, and mixed well by pipetting. The lysate at this point was not centrifuged. Some volume of lysate is lost during homogenization, so the volume of ethanol was adjusted accordingly. Visible precipitates formed after the addition of ethanol when preparing RNA from certain cell lines, but this did not affect the RNeasy procedure. 700 µl of the lysate, including any precipitate that may have formed, was added to an RNeasy mini column placed in a 2 ml collection tube (Qiagen). The tube was closed gently and centrifuged for 15 s at 8000 x *g* (10,000 rpm). The flow-through was discarded and the collection tube reused. When the volume of the lysate exceeded 700 µl, aliquots were loaded successively onto the RNeasy column, and centrifuged as above. Again the flow-through was discarded after each centrifugation step. 700 µl Buffer RW1

(Qiagen) was loaded on to the RNeasy column and the tube gently closed before being centrifuged for 15 s at 8000 x *g* (10,000 rpm). This step was to wash the column. The flow-through was discarded and a new 2 ml collection tube was used for the next step (provided in the Qiagen kit). 500 µl of Buffer RPE (Qiagen) was added onto the RNeasy column. The tube was gently closed and centrifuged for 15 s at 8000 x *g* (10,000 rpm). The flow through was discarded. Buffer RPE is supplied as a concentrate. 220 ml of 100% absolute ethanol was added to Buffer RPE before use. 500 µl of Buffer RPE was again added to the RNeasy column and centrifuged for 2 min at 8000 x *g* (10,000 rpm) to dry the RNeasy silica-gel membrane. It was important to dry the RNeasy silica-gel membrane since residual ethanol may interfere with downstream reactions. The extra centrifugation step ensured that no ethanol was carried over during elution. Following the centrifugation the RNeasy mini column was removed from the collection tube carefully so the column did not contact the flow-through as this will result in carryover of ethanol. The RNeasy column was placed in a new 1.5 ml elution tube and 30–50 µl RNase-free water (Qiagen) was pipetted directly onto the RNeasy silica-gel membrane, the tube was closed gently and centrifuged for 1 min at 8000 x *g* (10,000 rpm). If the expected RNA yield was <30 µg, the elution step was repeated as described above with a second volume of RNase-free water and eluted into the same collection tube. To obtain a higher total RNA concentration, this second elution step was performed by using the first eluate. The yield was 15–30% less than the yield obtained using a second volume of RNase-free water, but the final concentration was higher.

2.2.2 Concentration and cleanup of RNA

The volume of the sample was adjusted to 100 µl or 200 µl with RNase-free water. 350 µl or 700 µl of Buffer RLT was added and mixed thoroughly. If started with an RNA pellet, the pellet had to be dissolved in RNase-free water before Buffer RLT was added. 250 µl or 500 µl of 96–100% ethanol was added to the diluted RNA, and mixed thoroughly by pipetting. 700 µl of the sample

was added to an RNeasy MinElute Spin Column in a 2 ml collection tube. The tube closed gently, and centrifuged for 15 s at 8000 x *g* (10,000 rpm) the flow-through was discarded. For samples >700 µl the remaining sample was applied (up to 700 µl) and the centrifugation was repeated. The flow-through and collection tube were discarded at this point. The spin column was transferred into a new 2 ml collection tube (Qiagen). 500 µl of Buffer RPE was added to the spin column. The tube was gently closed, and centrifuged for 15 s at 8000 x *g* (10,000 rpm) to wash the column. The flow-through was discarded. 500 µl of 80% ethanol was added to the RNeasy MinElute Spin Column. The tube was gently closed, and centrifuged for 2 min at 8000 x *g* (10,000 rpm) to dry the silica-gel membrane. The flow-through was discarded. Following the centrifugation, the RNeasy MinElute Spin Column was removed from the collection tube carefully so the column does not come into contact with the flow-through as this will result in carryover of ethanol. The spin column was then placed into a 1.5 ml elute tube and 30-50 µl of nuclease free water was added to the column before being centrifuged for 1 minute at full speed. The RNA was stored at -80°C.

2.2.3 RNA quantification

Preparing the gel-dye mix (RNA 6000)

550 µl of RNA 6000 gel matrix (Ambion) was pipetted into a spin filter (Ambion). The gel matrix was then centrifuged at 1000 rpm for ten minutes. 65 µl of filtered gel was aliquoted into 0.2 ml RNase-free microfuge tubes. The filter was discarded and the filtered gel was kept in 4°C and used within 4 weeks. The dye concentrate was equilibrated to room temperature for 30 min. The dye concentrate was vortexed for ten seconds, and spun down. 1 µl of dye was added to a 65 µl aliquot of filtered gel. The solution was mixed well by vortex and then spun at 10,000 rpm for ten minutes at room temperature. During the preparation of the gel-dye mix all of the reagents were protected from the light. All reagents were allowed to equilibrate to room temperature before

use and aseptic techniques, minimalising contamination from RNA, DNA and RNase, were strictly adhered to throughout the procedure.

Running the RNA 6000 assay

The bioanalyser was cleaned before the start of every assay using a cleaning chip (Ambion) containing deionised water followed by a chip containing RNA zap (Ambion) to clean the electrodes. 9 µl of the gel preparation was pipetted into the first well marked G on the quantification chip (Ambion). The chip was placed in the pressurizer (Ambion) and the plunger pushed down for 30 seconds. The pressure was released and the plunger was allowed to rise for 5 seconds before the plunger was retuned to the 1 ml mark. 9 µl of gel preparation was pipetted into the two other wells marked G. 5 µl of marker (Ambion) was pipetted into all the sample wells including the well marked for the ladder (Ambion). 2µl of each RNA sample and ladder were denatured at 70°C for 2 minutes in a heated lid thermocycler before loading on the chip. 1 µl of ladder was pipetted into the ladder well and 1 µl of each RNA sample into each of the sample wells. If there were any sample wells unused 1 µl of marker was added to ensure the chip was loaded correctly. The chip was vortexed for 60 seconds and immediately place in the bioanalyser. The software enabled each well to be labeled and the quantification of each well could be followed on screen. The bioanalyser could detect the quantity and quality of RNA in the sample, preventing use of denatured or contaminated RNA.

2.2.4 cDNA synthesis for RT-PCR

A master mix containing Nuclease-Free Water (Promega), Reverse Transcription (RT) 10x Buffer (Promega), deoxyribonucleotide triphosphate (dNTP) mixture (Promega), Magnesium Chloride ($MgCl_2$) (Promega), Recombinant RNasin® Ribonuclease Inhibitor (Promega), avian myeloblastosis virus (AMV) Reverse Transcriptase (Promega), and Random Primers (Promega) was made up using the amounts listed in table 2.1. The reaction master mix was scaled up depending

on the number of RNA samples. 10% extra master mix was made to cover pipetting error. The use of a master mix not only reduced the time taken to set up the reaction but also the number of pipetting steps reducing error and the chance of contamination.

Component	Amount
$MgCl_2$	4 µl
Reverse Transcription 10x Buffer	2 µl
DNTP Mixture	2 µl
Recombinant RNasin Ribonuclease Inhibitor	0.5 µl
AMV Reverse Transcriptase	0.75 µl
Oligo (dT) 15 Primer OR Random Primers	2 µl
Total volume	**11.25 µl**

Table 2. Contents of master mix used for reverse transcription reaction

1µg of total RNA was placed in 0.2 ml microcentrifuge tubes and incubated at 70ºC for 10 minutes. No more then 8.75 µl of RNA could be added to the final volume. If 1 µg of RNA exceeded 8.75 µl, the concentration was reduced to 0.5 or 0.25 µg. If 1 µg of RNA was under 8.75 µl then the volume would be made up with nuclease free water. The tubes were spun briefly in a microcentrifuge, and then placed on ice. A 20 µl reaction mix was prepared by adding 11.25 µl of master mix to each 8.75 µl sample of denatured RNA. Random primers were used (random hexamers), so the samples were incubated at room temperature for ten minutes before placing the tubes in a thermocycler for 15 minutes at 42ºC. Random hexamers are a mix of short oligomers, usually six base pairs long that should be able to anneal to all of the sequences found. Random hexamers will transcribe rRNA, tRNA and mRNA (Kubista et al., 2006). The additional incubation at room temperature allowed extension of the primers so they remain hybridised when the temperature was raised to 42ºC. The samples were then ramped to 95ºC for 5 minutes, and then ramped back down to 4ºC for 5 minutes. This inactivated the AMV reverse transcriptase and prevented it from binding to

the cDNA. The first strand cDNA template was stored at -20ºC. The reaction was performed in a thermocycler due to the quick ramping times and heated lid which prevents recoiling of the RNA and evaporation of the reaction mix.

2.2.5 RT-PCR

In many cases the standard reactions will provide satisfactory amplification. A negative control reaction should be included lacking only the template. The inclusion of a positive control reaction using a template known to amplify with the primers may also be helpful. The concentration of enzyme, $MgCl_2$, template and primers can be varied to optimise the reaction. For each 25 µl reaction, the following assembly was prepared in a 0.2 ml PCR tube on ice (Table. 3).

Component	Amount
PCR grade Water (Novagen)	14.5 µl
10X PCR Buffer for KOD Hot Start DNA polymerase (Novagen)	2.5 µl
dNTPs (final concentration 0.2 mM) (Novagen)	2.5µl
DMSO (1% in final reaction)	1 µl
$MgSO_4$ (final concentration 1 mM) (Novagen)	1 µl
5' primer (final concentration 0.3 µM) (Sigma Genosys)	1 µl
3' primer (final concentration 0.3 µM) (Sigma Genosys)	1 µl
KOD Hot Start DNA polymerase (Novagen)	0.5 µl
Total Volume	**24 µl**

Table 3. Contents of master mix for RT-PCR.

The master mix was then mixed gently and centrifuged briefly to bring reaction components to the bottom of the tube. 1 µl of cDNA template from RT reaction was added to each tube. The thermocyclers used all had heated lids and therefore no oil droplets to prevent evaporation were required. The samples were placed in a thermocycler where the PCR reaction can take place. The KOD polymerase was activated by heating for 2 minutes at 95˚C followed by 15 seconds at 94˚C, which was required to denature the DNA, allowing access of the polymerase and

primer sequences to the exposed nucleotides (step 1). The reaction was then ramped to 60˚C for 30 seconds. This allowed the primers to anneal to the correct sequence in DNA ready for the extension step (step 2). The extension step was carried out at 68˚C for 30 seconds. The KOD polymerase requires a temperature of 68˚C to be able to carry out the extension step with the greatest efficiency. The polymerase will move along the single stranded cDNA from the position at which the primers have annealed at the 5' end. The polymerase adds dNTPs, which are free in the buffered reaction mixture, to the single stranded cDNA. The primer annealed at the 3' end contains a stop codon so the polymerase will drop off the DNA after the sequence between the forward and reverse primers has been completed (step 3). The double stranded DNA is now ready to under go another round of amplification. Steps 1-3 are repeated for 28 cycles. The amplification reaction is depicted in figure 2.1. The annealing temperature in step 2 can vary depending on the melting temperature of the primers. The extension time in step 3 can vary depending on the size of the product. KOD polymerase can add 1000 nucleotides every minute and therefore a DNA product expected at 500 base pairs will require a 30 second extension. The annealing temperature and extension times stated above were used for all of the primers designed for standard PCR reactions in this thesis. The primers all had similar melting temperature and the product sizes were also similar. The cycle number was reduced for GAPDH and β-actin as these are more abundant proteins. Conditions were optimised for all primer pairs.

Primer design is important for successful PCR amplification. The primers should be complementary to the template, especially the 3' end. It is important to determine the proper annealing temperature for any pair of primers. Long extension times may cause smearing. For all RT-PCR and qRT-PCR primer sequences see Appendix 2.

2.2.6 RT-PCR product analysis by agarose gel

To analyse the reaction products, 10 µl of sample was removed and added to a loading dye (Promega). A 1.5 % agarose gel containing 0.5 µg/ml ethidium bromide was used to load and run the reaction products. To prepare the agarose gel 0.75 grams of agarose is weighed out and added to 50 ml of 1x Tris Borate ethylene diamine tetra-acetic acid (EDTA) or TBE buffer (Sigma) containing 5 µl of 0.5 µg/ml ethidium bromide (Sigma). The gel is pored into a gel tank and the appropriate lane comb placed in the gel. The gel is left to solidify before the DNA plus loading dye is carefully loaded onto the gel. A DNA molecular weight ladder (Promega) is also loaded onto the gel. There were two ladders available, a lower molecular weight marker that went up to 2000 base pairs and a high molecular weight marker that could accurately separate bands up to 10,000 base pairs. The bands were visualized under UV illumination using the SynGene System (Syngene Ltd UK, 2002) and camera or the transilluminator. Pictures could then be analysed using phoretix software to quantify the density and area of the bands. The products on the gel were often sequenced to ensure the correct DNA product was amplified. The bands on the gel were cut out and the DNA extracted.

2.2.7 DNA isolation from an agarose gel

300 µl of SpinPrep GelMelt Solution (A) (Novagen) was added per 100mg of gel slice for DNA run on a gel of up to 2% agarose. For DNA run on gels greater than 2% agarose, 600µl of GelMelt solution was added. The tube was vortexed briefly and transfered to a 50°C water bath or heat block. The gel slice was then incubated for ten minutes or until the gel slice had fully melted. A SpinPrep Filter (Novagen) was placed into a SpinPrep eluate 2 ml receiver tube (Novagen). 700µl (maximum capacity) of the dissolved gel solution was transferred to the SpinPrep filter and centrifuged at top speed for 30 seconds. The flow-through in the receiver tube was discarded. 400µl of fresh SpinPrep

Gel Melt Solution (A) was added to the spin filter and was centrifuged again at top speed for 30 seconds. The flow-through in the receiver tube was discarded before 650 µl of reconstituted SpinPrep Wash Buffer (B) (Novagen) was added and centrifuged at top speed for 30 seconds. The flow-through in the receiver tube was discarded and the empty spin filter was centrifuged for an additional 2 min to remove residual SpinPrep Wash Buffer (B) (this was important as any transfer of residual buffer can result in reduced yield of DNA). The SpinPrep Filter was then transferred to the provided 1.5 ml Eluate Receiver Tubes (Novagen). Between 30 and 50 µl of pre-warmed (50°C) SpinPrep Elute Buffer (C) (Novagen), (or DNase free/distilled water) was added to the SpinPrep Filter membrane. The cap of the receiver tube was closed before being incubated for 3 min at 50°C in a heat block. The Spinprep unit was then centrifuged for 1 min to elute the DNA into the 1.5ml receiver tube and the DNA was stored at -20°C or sent off for sequencing. DNA for sequencing was sent to GATC.

2.2.8 DNA-free treatment of RNA

All tubes and water is UV irradiated to ensure any contaminating DNA was crosslinked. The RNA was then cleaned of any genomic DNA contamination by undergoing a DNAase-free reaction. 0.1 volume of 10X DNase 1 buffer (Ambion) was added to the RNA and mixed gently. For routine DNase treatment 1 µl of recombinant DNase 1 (Ambion) was added to up to 10 µg of RNA in a 50 µl reaction and was incubated at 37°C for 20-30 minutes. The reaction conditions removed up to 2 µg of genomic DNA from the total RNA in a 50 µl reaction. If the reaction requires more rigorous DNase treatment, then various methods such as diluting the RNA or increasing the concentration of enzyme can be adopted. 0.1 volume of DNase Inactivation reagent (Ambion) was added to each reaction and mixed well. Each reaction was incubated for 2 minutes at room temperature, mixing occasionally. Each reaction was then centrifuged at 10 x g for 1.5 mins and RNA transferred to a fresh tube. RNA is stored at -80ºC.

2.2.9 cDNA synthesis for quantitative RT-PCR (qRT-PCR)

The DNase treated RNA was then used to carry out a reverse transcription reaction to create cDNA for use as the template in the PCR reaction. Master mix was prepared in a microcentrifuge tube containing 4 µl of moloney murine leukemia virus (MMLV) 5 X buffer (Primer Design), 5.2 µl of RNase/DNase free water (Primer Design), 0.8 µl of MMLV enzyme (Primer Design). The volumes were scaled up for the number of reaction to be carried out plus an extra 10% for pipetting error. 8 µl of RNA was added to 2 µl of OligodTprimer/dNTP mix (primer design) in a sterile 1.5ml Eppendorf. The advantage of using oligodT primers is they will only create cDNA from mRNA due to hybridizing to the poly A tail of the mRNA molecule. The primers hybridise to the RNA at the 3' end and transcription of the RNA molecule proceeds, as long as there are no breaks before the PCR target sequence reverse transcription using OligodT primers is more efficient and less dependent on temperature. The possibility of amplifying non-specific products in the PCR reaction is reduced (Kubista et al., 2006). Tubes were incubated at 65°C to denature for 5 minutes in a heating block. Tubes were placed directly on ice and 10 µl of ice cold master mix was added to each denatured sample before incubating for 1 hour at 42°C. cDNA was then stored at -20°C or used in a PCR reaction.

2.2.10 SYBR Green qRT-PCR in 96 well format

Master mix was prepared for each final 20 µl reaction. 10 µl of SYBR green master mix (primer design), 1 µl of primer mix (pre-validated for each primer set, including house keeping genes UBC and pLA_2 from primer design) and 4 µl of DNase free water were added to a microcentrifuge tube. The volumes are scaled up for the number of reactions to be carried out, including an extra 10% for pipetting error.

15 µl of master mix was aliquoted into each well and each cDNA sample was diluted 1/10 into DNase free water, before adding 5 µl per reaction. Each sample is run in duplicate for each primer set and negative control. Negative controls were a PCR control without cDNA and an RT control without RNA. The 96 well plate was sealed with 96 well plate adhesive covers (biorad), the plate was then spun down at 4°C for 30 secoonds at 1000 x g. The reaction was carried out on a Icycler using a SYBRGreen filter, 45 cycles with melt curve analysis Data was analysed using biorad IQ5 software and the CT values were normalised to the house keeping genes and fold changes were calculated using $2^{\Delta\Delta ct}$. All primers used in SYBR green qRT-PCR were from primer design and all sequences are listed in Appendix 2.

2.3 Protein analysis of cell culture models

Western blotting was used to analyse the phenotype of the cells used in the *in vitro* cell culture models described above. Any changes in protein expression of fibrotic and apoptotic markers such as α-SMA and PARP-1 cleavage products were detected using this method. The protein of interest must be obtained in soluble form before separation by SDS-PAGE. This is carried out by using buffer containing a detergent and also peptidase inhibitors to inhibit intracellular proteases released during the solubilisation process from denaturing the proteins of interest. Dissociation of proteins into polypeptide subunits is achieved using strongly anionic detergent, SDS, a reducing agent e.g. mercaptoethanol), and heat. This denatures the proteins before being loaded on the polyacrylamide gel for analytical electrophoresis. The gel itself is composed of cross-linked chains of polymerized acrylamide, N, N, N', N'-tretramethylethylenediamine (TEMED) and ammonium persulfate are added to accelerate the polymerization. The denatured proteins bind to SDS and become negatively charged. The proteins of larger molecular weight migrate through the polyacrylamide gel more slowly because they bind more SDS. When an electric current is passed through the gel, the proteins can then be separated by molecular weight. An

electric current is used for transfer of the proteins from the polyacrylamide gel to a nitrocellulose sheet. The western blot is first exposed to specific primary antibody and thereafter, extensive washing before the secondary alkaline phosphatase conjugated antibody is applied. Again the blot undergoes extensive washing before the substrate for alkaline phosphatase is applied (Laemmli, 1970).

Cytokines play an important role in innate immunity, apoptosis, angiogenesis, cell growth and differentiation. They are involved in most disease processes such as cancer and fibrosis. Cytokines interact with the cellular immune system, this is a dynamic process that involves positive and negative stimuli as well as positive and negative feed back loops. These processes often involve multiple cytokines therefore the ability to detect multiple cytokines in the same sample could lead to an increase in understanding of how cytokines interact in cellular and disease processes (Rameshwar et al., 2003). Currently two dimensional polyacrylamide SDS page coupled with mass spectrometry is the main stream approach to analyzing multiple protein expression levels. The applications require sophisticated devices and lack quantitative measurements that limit there broad application. Cytokine arrays offer a simple format that is a highly sensitive approach that can simultaneously detect multiple cytokine expression levels from conditioned media, cell lysates, patient's sera and other sources (Zhou et al., 2005;Turtinen et al., 2004). Cytokine arrays were used to detect any changes in the conditioned media after H2-relaxin treatment of HSC. Cytokines are traditionally detected by elisa but the array format allows the simultaneous detection of many cytokines. Cytokine arrays can detect as little as 4 pg/ml of protein. Therefore the sensitivity as well as the detection range is greater then an elisa and there is also less variation between samples. The array format utilizes antibodies to detect active cytokines that would be secreted from the cell, reflecting a snap shot of the activity of the cell when the sample was taken.

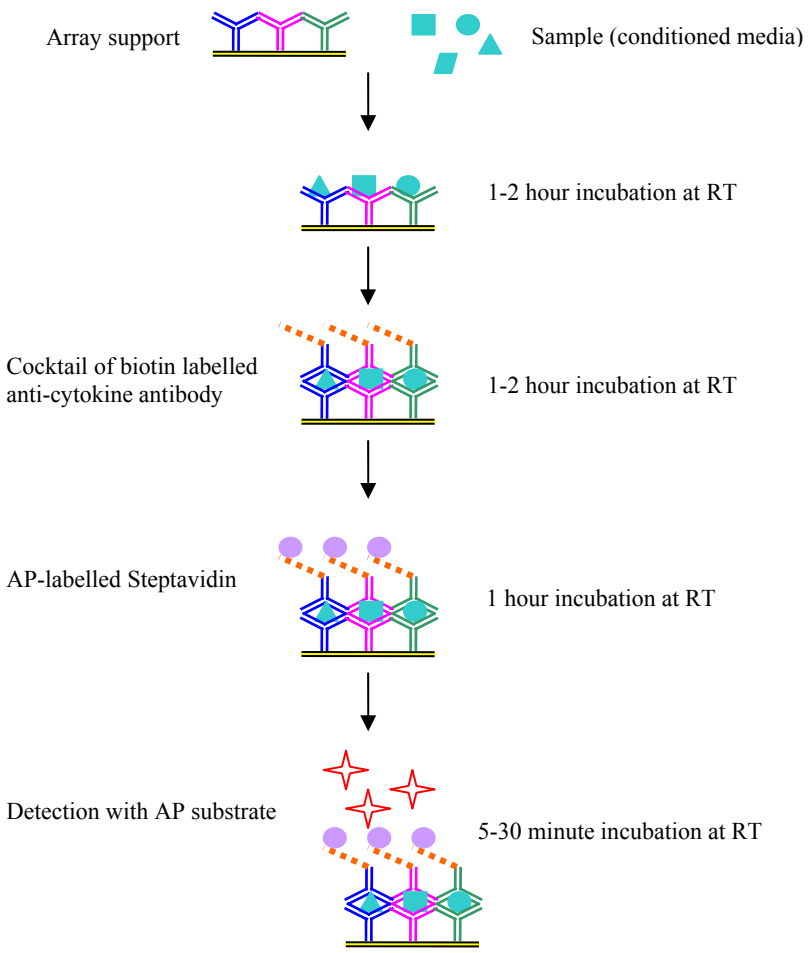

Figure 2.4. Principle of human cytokine antibody membrane array

The cytokine array procedure is similar to the technology developed for immunhistochemical staining and elisa assays (figure 2.4). The antibody detection system uses an indirect two stage system to amplify the signal. The array membranes are spotted with antibodies for many different cytokines. The samples are incubated with the membranes to allow the antigens in the conditioned media to bind to the antibodies on the membrane. Once the cytokines have bound to the membrane a cocktail of biotinylated primary antibody, designed to bind to different epitopes then the antibody spotted on the membrane, is then applied. The biotinylated primary antibodies bind to the various antigens of the cytokines bound to the membrane. The alkaline

phosphatase -labelled streptavidin is then applied and binds with high affinity to the biotin labelled primary antibody. The activity of the alkaline phospahtase now bound to the specific antigens can be detected using an alkaline phosphatase substrate, the colour develops as a purple precipitate.

2.3.1 Total protein extraction

Total protein extraction from mammalian cells was achieved by incubating the adherent cells with an appropriate amount of mammalian protein extraction reagent (M-PER) (Pierce) including halt protease inhibitor cocktail (Pierce) at 10 µl/ml concentration. Adherent cells in a 100mm dish or 6-well plate were washed with PBS, M-PER was then added directly to the cells (300 µl per well for a 6 well plate or 1 ml in a 100mm dish). The cells were gently agitated for 5 minutes at room temperature (until the cells were fully lysed). The cells may require scraping if they do not appear fully lysed. Cell lysate is then added to microcentrifuge tubes to be spun at 10,000 rpm for 5 minutes. All the cell debris should remain at the bottom of the tube and the supernate can be added to a new microcentrifuge tube. The protein is then quantified using the BCA

2.3.2 Protein quantification

A fresh set of protein standards were prepared by diluting the 2.0 mg/ml BSA stock standard, in the same diluent as the samples (the dilutions are given in table.4). A 1 ml ampoule of the 2.0 mg/ml BSA standard was sufficient to prepare a set of diluted standards.

Volume of BSA stock	Volume of diluent to add	Final BSA concentration
0.5 ml of Stock	4.5 ml	200 µg/ml (A)
2.0 ml of A	8.0 ml	40 µg/ml (B)
4.0 ml of B	4.0 ml	20 µg/ml (C)
4.0 ml of C	4.0 ml	10 µg/ml (D)
4.0 ml of D	4.0 ml	5 µg/ml (E)
4.0 ml of E	4.0 ml	2.5 µg/ml (F)
3.2 ml of F	4.8 ml	1.0 µg/ml (G)
4.0 ml of G	4.0 ml	0.5 µg/ml

Table 4. Serial Dilution of BSA stock solution

The Working Reagent (WR) was prepared by mixing 25 parts of Micro BCA Reagent MA (Pierce) and 24 parts of Micro BCA Reagent MB (Perbio/pierce) with 1 part of Micro BCA Reagent MC (Pierce). When Micro BCA Reagent MC was initially added to the solution, turbidity was observed that quickly disappeared upon mixing to yield a clear green WR. A sufficient amount of WR was prepared to enable each test to be done. Each test tube assay to be done required 150 µl of WR. The WR was stable for at least 1 day when stored in a closed container at room temperature (it is sensitive to light).

150 µl of each standard or unknown sample were pipetted into the appropriate plate wells. 150 µl of the diluent was used for the blank wells. 150 µl of the working reagent was added to each well, the plate was then mixed on a plate shaker for 30 seconds. The plate was covered and then incubated at 37ºC for 2 hours. After incubation, the plate was cooled to room temperature. The absorbance was measured at or near 562 nm on a plate reader. The average 562 nm reading for the blanks was subtracted from the 562 nm reading for each standard or unknown sample. A standard curve was prepared using Graph Prism (Graph Pad Software, Inc San Diego USA); by plotting the average blank corrected 562 nm reading for each BSA standard verses its concentration in µg/ml. The protein concentration for each unknown sample was determined using the standard curve.

2.3.3 Gel Electrophoresis

The correct volume of protein was calculated from the concentration (in the protein bank) to load 5 µg of protein for α-SMA detection and 25 µg for PARP-1 detection. The protein samples were then added to a micro-centrifuge tube and the volume made up to 20 µl with ultra pure water. 10 µl Sample Buffer LDS (Invitrogen) and 5 µl NuPage 10x reducing agent (Invitrogen) was then added making the total volume 35 µl. Reducing agent was added to the sample immediately before heat denaturing. The final sample solution was heated at 90ºC for ten minutes. Samples were mixed and 20 µl was loaded on to the gel. A short centrifugation was used to remove bubbles before loading if necessary. 20 µl of each sample was loaded on to a NuPAGE-pre cast bis-tris 10% 12 well gel cassette (Invitrogen), and using the X-cell Surelock Mini-cell (Invitrogen) and NuPAGE running buffer (Appendix 2), the samples were run at 200 volts (constant) for fifty minutes or until the front had reached 5 mm from the bottom of the gel.

2.3.4 Western transfer to nitrocellulose membrane

During the following procedures, gloves were worn at all times to prevent contamination of gels and membranes and exposure to irritants commonly used in electrophoresis and electro-transfer. The gels were removed from the Cassettes and placed in the correct orientation for transfer using Novex pre-cut membrane/filter paper sandwiches and blotting pads (Invitrogen) ensuring no bubbles remained within the blotting pads or between the gel and the nitrocellulose membrane (this was important as any air bubbles may compromise the quality of the transfer). The blot module was then placed into an X-cell Surelock Mini-cell and the transfer buffer (Appendix 2), was placed into the blotting chamber, only to just above the level of the sandwich, to ensure the quality of the transfer, as the current will run more efficiently if the buffer is

at this level. Deionised water was placed in the outer chamber to keep the set up cool. 30 volts constant current was then run through the blotting module for 90 minutes. Preparing Tris-Buffered Saline (TBS) (Sigma), Tris-Buffered Saline-Tween (TBS-T) and blocking reagent solutions TBS was diluted 1 in 10 in deionized water 100ml TBS in 900 ml deionised water. This was then used in preparation of TBS-T where 500 µl of 0.05% Tween 20 (Sigma) were added to the 1000 ml of TBS. 200ml of TBS-T were then removed to be used for the blocking reagent. 2.5 grams of 1% blot qualified Bovine serum Albumin (BSA) (promega) were weighed out and dissolved into the 200 ml of TBS-T (blocking reagent).

2.3.5 Antibody probe of nitrocellulose membranes

Stored nitrocellulose membranes were rewetted with TBS-T, before being incubated for 30 minutes at room temperature in blocking reagent as described above. Primary antibodies were diluted 1:500-1:5000 with TBS-T (table.5). The membranes were then incubated in this solution for two hours using a rotating table. The membranes were washed three times for five minutes each in TBS-T. The secondary antibody (anti-mouse IgG-AP conjugate from Promega) was also diluted using TBS-T to a 1:5000 concentration. The membranes were then incubated in the secondary antibody for 45 minutes. After washing the membranes three times using TBS-T and once in TBS to remove any unbound antibody, Western Blue Stabilised Alkaline Phosphatase (Promega) was used to start the colour reaction. Colour development usually took between 1 and 15 minutes. Once sufficient colour had developed the membranes were washed in distilled water.

A picture was taken of each blot using a CCD camera. The image was analysed using the Phoretix software. The Phoretix software package allowed the molecular weight of the bands to be calculated compared to a molecular weight standard ladder (e.g. SeeBlue Plus2). The program would also measure the

volume and intensity of the band allowing a quantity to be assigned to the target band which could then be normalised to a GAPDH or β-actin band in the same sample.

Antibody	Concentration	Molecular weight
Monoclonal TIMP-1 (Sigma)	1/500	28 kD
Monoclonal α-SMA (Sigma)	1/1000	42 kD
Monoclonal MMP-1 (Sigma)	1/500	53 kD and 51 kD
Monoclonal MMP-2 (Sigma)	1/500	72 kD and 68 kD
Monoclonal PARP-1 (Serotec)	1/500	116 kD, 89 kD, 24 kD
Monoclonal GAPDH (Abcam)	1/3750	36 kD
Monoclonal β-actin (Abcam)	1/3750	42 kD

Table 5. Antibodies used in western blotting, concentrations and molecular weights of target bands.

2.3.6 Safestain of electrophoresis gels

After electrophoresis the gel can be stained directly before transferring the proteins to a nitrocellulose membrane. The stain used will bind to all the proteins on the gel. This enables detection of over expressed proteins and can also be used to ensure even loading of protein across the gel. The stain can also be used on the electrophoresis gel after transfer to a nitrocellulose membrane to detect if the transfer was complete. The mini-gel was rinsed 3 times for 5 minutes with 100 ml deionized water to remove SDS and buffer salts, which interfere with binding of the dye to the protein. The mini-gel was stained with enough Simplyblue Safestain (~20 ml) to cover the gel. Staining took around 1 hour at RT with gentle shaking. Bands began to develop within minutes. After incubation the stain was discarded and was not reused (gel can be stained for up to three hours, but after that, sensitivity will decrease). After staining the mini-gel was washed with 100ml of water for 1 to 3 hours. The gel can be left in the

water for several days without loss of sensitivity. (There is a small amount of dye in the water that is in equilibrium with the dye bound to the protein, so proteins will remain blue.) To obtain the clearest background for photography, a second 1-hour wash with 100 ml water was performed. An alternative method is to heat the gel with Simplyblue Safestain (Invitrogen). This enhances the staining process, allowing faster detection. After electrophoresis the gel was placed in 100 ml of ultrapure water in a loosely covered container and microwaved on High (950 to 1100 watts) for 1 minute until the solution almost boiled. The gel was shaken on an orbital shaker or rocker for 1 minute the water was then discarded. Steps 1 and 2 were repeated two more times. After the last wash 20 ml of SimplyBlue Safestain was added and the gel and microwaved on high for 45 seconds to 1 minute until the solution almost boiled. The gel was shaken on an orbital shaker or rocker for 5 minutes. The gel was washed in 100 ml of ultrapure water for 10 minutes on a shaker. A picture was taken of the gel directly and if the gel is to be kept it was dryed using gel drying solution (Invitrogen).

2.3.7 Cytokine membrane array

Blocking solution is diluted one in two with deionised water. Enough blocking solution was made up to use four ml per membrane. Blocking solution was applied to the membranes and they were incubated at room temperature on a rocker for thirty minutes. Media samples were thawed on ice and centrifuged at 10,000 rpm for two minutes. 600 µl of sample was then added to each membrane including a media control sample that has not been incubated with cells but contains the same percentage FBS, P/S and glutamine/pyruvate that was applied to the cells to obtain the conditioned media. Samples were incubated for 2 hours at room temperature.

Wash buffer one and two were made up whilst the samples were incubating. Both wash buffers were diluted one in twenty using deionised water. Enough

wash buffer was made to use 2 ml per wash for each membrane. Samples were removed from the membranes and 2 ml of wash buffer one was applied to each membrane for 5 minutes at room temperature. This was repeated twice more before wash buffer two was applied to the membranes, again for 5 minutes. Wash buffer two was repeated and then the biotin conjugated anti-cytokine antibody was applied to the membranes for 1 hour 30 minutes. The biotin conjugated anti-cytokine antibody was supplied with the kit and each vial supplied was diluted into two ml of blocking solution. 1 ml of antibody was applied to each membrane.

The membranes were washed as previously described with wash buffer one and two. The protocol was then altered from the manufactures protocol. The detection system was changed to enable and AP-substrate to detect the spots. Therefore an AP-conjugated Strepavidin (DAKO) was diluted 1:1000 in 1x blocking solution and incubated at room temperature for 1 hour. Membranes were then washed as described previously and then two additional washes with TBS for five minutes at room temperature were carried out before 1 ml of AP-substrate (promega) was applied to each membrane. The substrate was left on the membranes for as long as was required for the spots to become visible. Each membrane was left for the same period of time before they were washed in distilled water and then tap water before a picture was taken in the syngene. All of the membranes were pictured together to ensure the exposure time of the CCD camera was the same for each membrane. Spots were quantified using phoretix array software.

2.4 Histological staining of human tissue sections and fixed cells

Sirius red was discovered as a connective tissue stain in the 1960s (Sweat et al., 1964). Sirius red is a strong anionic dye that stains collagen via its sulphonic acids groups that interact with the basic groups present in collagen. The elongated dye molecules are attached to the collagen fibres in such a way that

their long axes are in parallel. The parallel relationship between dye and collagen results in enhanced birefringency. When examined through polarised light the larger collagen-1 fibres are yellow, orange or red depending on the tissue and the thinner collagen III fibres appear green. Collagen II fibres are of variable colours according to tissue and species (Junqueira et al., 1978;Junqueira et al., 1979). Birefringence was found to be highly specific for collagen and the use of circularly polarised light enabled simple detection (Whittaker et al., 1994). Sirius red is a well characterised histological method of staining collagen in tissue sections and can be used to help grade the level of scarring and damage in fibrotic tissue.

Immunohistochemistry/immunocytochemistry is the in situ detection of antigens in tissue sections and cells by labeled reagents such as lectins, monoclonal and polyclonal antibodies. The antibody:antigen reaction is exploited, the antigen can display one or more specific binding sites or epitopes which are identified by using labeled antibodies. Antigen-antibody interactions are visualised through markers such as fluorescent dyes, enzymes or radioactive elements. Albert H Coons and colleagues were the first to label antibodies with fluorescent dyes and use them to identify antigens in tissue sections (COONS and KAPLAN, 1950). With the advancement of the immunhistochemistry technique enzyme labels such as peroxidase and alkaline phosphatase were developed (Nakane and Pierce, Jr., 1966;Avrameas and Uriel, 1966;Mason and Sammons, 1978). The detection system used was the avidin-biotin complex (ABC) method. Avidin is a large glycoprotein that is labeled with peroxidase. It has a very high affinity for biotin which is a low molecular weight vitamin which can be conjugated to a variety of biological markers such as secondary antibodies. The ABC system is a 3 layer indirect method of visulising the antigens that allows signal amplification. An unlabeled primary antibody will bind to the antigen allowing several different reactions with the biotinylated secondary antibody with different antigenic sites on the primary antibody. A complex of avidin bound to biotin peroxidase is then applied which can bind to the multiple biotin labeled

secondary antibodies. The colour development is then dependent on peroxidase activity. The 3, 3'-diaminobenzidine (DAB) chromgen is the final stage which reacts with the peroxidase enzyme to form a coloured end product at the specific antigen sites (figure 2.5).

The tissue sections used were paraffin embedded and required processing before antibody staining could commence. Kidney and liver tissue has a high level of endogenous biotin. To prevent unwanted avidin binding the sections had to be pretreated with unconjugated avidin which is then saturated with biotin. Many tissues have a level endogenous peroxidase activity and this was blocked before introduction of the primary antibody by saturating the tissue with hydrogen peroxide. An additional blocking step was carried out using media containing fetal bovine serum (FBS) and bovine serum albumin (BSA). This was to reduce the primary antibody from binding to nonspecific antigen sites.

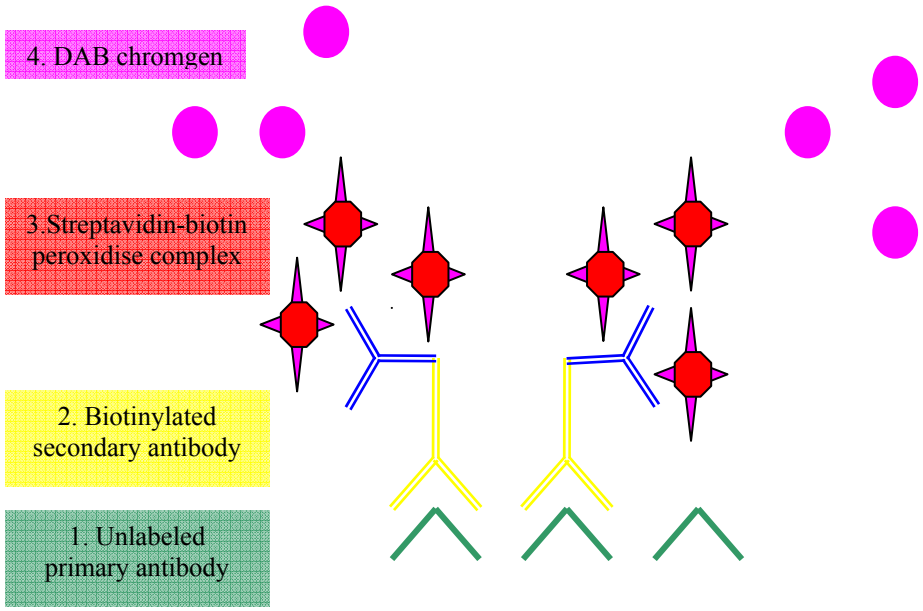

Figure 2.5. ABC method of immunhistochemistry. Paraffin-embedded sections were hydrated with water and treated with protein blocking agents to reduce non-specific binding of antibodies. The tissues were then sequentially incubated with 1) primary antibody, which binds to specific tissue antigens, 2) secondary biotinylated antibody,

which binds to the primary antibody and 3) Streptavidin-biotin peroxidase complexes bind to the biotinylated secondary antibody. 4. Addition of the DAB chromagen mixture results in a coloured precipitate at the sites of the where the primary antibody has bound to the specific tissue antigen. Visualization is aided by counterstaining with haematoxylin.

2.4.1 Sirius red stain

Before Sirius red staining could be carried out the following solutions were prepared. 0.5 grams of Sirius red F3B (BDH VWR international Ltd) was added to 500ml of saturated Picric Acid solution 1.3% (Sigma Aldrich), (ensuring the picric acid solution is saturated, this was achieved by adding a little solid picric acid). This is solution A. 5 ml glacial acetic acid (Sigma Aldrich) was added to 1 litre of distilled water, this is solution B.

To de-wax and rehydrate the paraffin sections they were placed in xylene substitute (sigma-aldrich) and different concentrations of ethanol (Sigma-Aldrich). Sections were dewaxed in three changes of xylene substitute. The sections wee left in the xylene substitute for ten minutes at a time. The sections were then rehydrated with graded alcohol solutions. Sections were placed in 100% ethanol, 95% ethanol, 70% ethanol and filtered distilled water, each for 5 minutes.

Optional staining of the nuclei was carried out using Weigert's haematoxylin. The slides were then washed for ten minutes in running tap water (this develops the blue colour of the haematoxylin stain). The slides were stained in the Picro-Sirius red solution (Solution A) for one hour, this gave optimal levels of staining as the equilibrium was reached, and staining for longer times did not increase the intensity. Sections were then washed twice in acidified water (Solution B). The majority of the water was physically removed by either vigorously shaking or with damp filter paper. The sections were then dehydrated in three changes of

100% ethanol. The sections were then cleared in xylene substitute before being mounted in a resinous medium (DPX). In bright-field microscopy collagen is red on a pale yellow background (Nuclei are ideally stained black but may be grey or brown). The crosslinked collagen fibers can be seen using polarized light.

2.4.2 Immunohistochemistry

All liver tissue was fixed in 4% paraformaldehyde for at least 48 hours before embedding in paraffin wax and cutting tissue sections can commence. Pre-fixed tissue was given to a histology unit technician to embed in paraffin wax and cut sections, who also carried out H+E staining on every ten serial sections Kidney sections were cut from normal or fibrotic kidney held in the tissue store that had already been embedded in paraffin wax. Each staining run began by using a positive control tissue section that is known to display a specific positive reaction with the primary antibody and that has been prepared in identical manner to the test tissue. Failure of the positive control tissue to stain appropriately invalidates the results with the test specimens for the antibody. Each staining run included a negative control antibody or non-immune serum in place of the primary antibody, to permit identification of non-specific staining. Evaluation of specific staining on the test slide was made in comparison to any nonspecific staining seen on the negative control slides.

Dewaxing, rehydrating and blocking of endogenous peroxidase

All stages were carried out at room temperature unless otherwise stated. Sections were allowed to warm to room temperature before the protocol was started. Sections were deparaffinised in xylene substitute and rehydrated through graded alcohols to 100%-70%. The sections were not allowed to dry out after this point. The endogenous peroxidase activity was blocked for ten minutes with 0.5% hydrogen peroxide (Calbiochem) in methanol (Romil) (0.1ml in 5.9ml respectively). The sections were then washed well in running tap water

for at least 5 minutes. The antigen retrieval technique was then carried out that was appropriate for the antibody used. The technique used for the relaxin receptor family of antibodies was microwave pre-treatment in citrate buffer pH 6.0 (appendix 2).

Antigen retrieval

Three plastic staining racks were filled with slides (some that are to be stained and some that are blanks to fill the racks) and then placed in polythene boxes of the same size. The load was maintained by always using 3 polythene boxes, together with 72 slides. The temperature will hopefully be constant throughout all of the sections. Each box was then filled with 330 ml of citrate buffer and the perforated lids placed firmly on the boxes. The three boxes were then placed in the microwave on medium power for 25 minutes. The slides were then placed under cold running water for 2-3 minutes.

IHC antibody staining

Slides were placed in staining racks and washed three times for five minutes in TBS (Sigma). The slides were drained and the avidin solution (vector laboratories) was applied for twenty minutes. Slides were rinsed three times for two minutes with TBS. Slides were then drained and the biotin solution (vector laboratories) was applied for twenty minutes. The slides were drained and washed three times for two minutes in TBS, drained and the blocking culture media (appendix 2) was applied for twenty minutes. The slides were then drained (not rinsed) and the primary antibody is applied at this point in the appropriate dilution (table.6) and the slides were incubated overnight at 4˚C in the humid staining rack to prevent evaporation.

The slides were removed from the fridge 30 minutes before the resumption of the protocol. The slides were drained and washed three times for five minutes before the addition of the biotinylated secondary antibody at appropriate dilution (table.6) for thirty minutes. Slides were drained and washed three times for five

minutes and then the strepavidin biotin-peroxidase complexes (Dako cytomation) were applied for thirty minutes. The slides were drained and washed three times for five minutes and then the DAB substrate (Biogenex) (appendix 2) was added for between three and five minutes. The working chromogen solution was prepared immediately prior to use, and was used within 24 hours. Slides were rinsed in distilled water and washed in running tap water for five minutes before being counterstained with Mayer's Haematoxylin (sigma). The sections were then blued in running tap water. The sections were then dehydrated through graded alcohol, cleared in xylene substitute and mounted in DPX. Sections were allowed to dry for 24 hours before taking pictures with the axioskop camera, microscope and software.

Antibody	Concentration	Tissue
Polyclonal RXFP-1 (12715) (Abcam)	1/400	Liver
Polyclonal RXFP-1 (12714) (Abcam)	1/600	Kidney
Polyclonal RXFP-3 (Abcam)	1/200-1/400	Liver and Kidney
Polyclonal RXFP-4 (Abcam)	1/50	Liver and Kidney
Monoclonal α-SMA (Sigma)	1/40,000	Liver and Kidney
Monoclonal VEGF C1 (Santa Cruz)	1/200	Kidney
Monoclonal Synaptopodin (Progen)	1/20	Kidney
Monoclonal EMA (Vector)	1/300	Kidney
Lectin LTA (Vector)	1/3000	Kidney
Secondary Swine anti-rabbit (Dako)	1/200	Liver and Kidney
Secondary Rabbit anti-mouse (Dako)	1/200	Liver and Kidney

Table.6. Antibody concentrations used for IHC (EMA-epithelial membrane antigen, LTA- lotus teragonolobus antigen).

2.4.3 Immunocytochemistry

Primary HSC were cultured on cover slips in 6 well plates. 50,000 cells were plated per well and grown to confluence. Tissue culture media was then removed and cells were washed with several changes of PBS. The cells were then fixed by applying ice cold methanol and incubating at 4ºC for 10 minutes. The cell were then washed with ice cold PBS. Cells could be stored at this stage at -20°C for later use or used directly in the staining protocol. The immunodetection of α-SMA and RXFP-1 could now take place. The assay was carried out following the immunhistochemistry protocol. The only change was the concentration of primary antibodies, α-SMA was applied at 1/5000 and RXFP-1 was applied at 1/400.

2.5 Functional/mechanistic cell based assays

cAMP assays were used to detect functional relaxin receptors in LX-2 and primary HSC and to establish if the siRNA knockdown of RXFP-1 could abolish the cAMP response to H2-Relaxin. A new generation of cAMP assay has been developed for high throughput screening that allows fast and accurate results. Enzyme fragment complementation (EFC) technology is a homogeneous, non-radioactive technology based on splitting the E. coli β-galactosidase into two genetically engineered fragments, a large protein fragment (enzyme acceptor, EA) and a small peptide fragment (enzyme donor, ED). These fragments are inactive separately but in solution they rapidly recombine to form an active enzyme that hydrolyse substrate to produce an easily detectable luminescent signal. cAMP from cell lysates compete for antibody binding against labeled cAMP (ED-cAMP). Unbound ED-cAMP is free to complement EA to form active enzyme by EFC, which subsequently produces the luminescent signal.

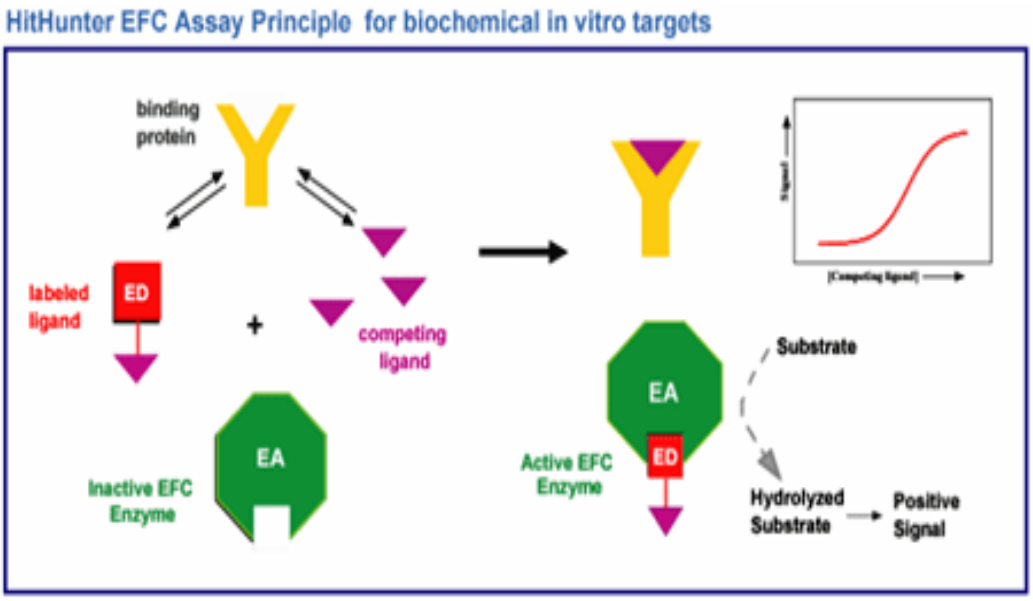

Figure 2.6. cAMP assay principle

A mechanistic assay was carried out to test the vasoregulatory properties of relaxin in activated HSC, to determine if relaxin receptors may be a potential target in the treatment portal hypertension. The contraction of collagen lattices by human fibroblasts was first described in 1979 by Bell and collegues (Bell et al., 1979). The contractility of HSCs was found to be activation dependent and could be manipulated by vasoactive mediators. Hepatocytes did not possess the same contractile properties as activated HSC (Rockey et al., 1993). The principle of the assay is to determine the contractility of cells cultured on a collagen-1 lattice. Collagen lattice contraction assays provide a model for tissue contraction that takes advantage of the finding that cell populated hydrogels contract over time in a predictable consistant manner (Ngo et al., 2006). The collagen lattice will shrink as the cells contract, the traditional method to quantify the shrinkage is to measure the diameter of the gel. HSC have been found to contract in the presence of serum in the tissue culture media as well as ET-1 and other vasoactive substances. The assay conditions for all of the cells was kept consistent, the only change for each well was the treatment of either ET-1 or H2-relaxin.

The principle of the nitric oxide (NO) assay was to determine the nitric oxide concentration in culture media supernatant, based on the enzymatic conversion of nitrate to nitrite by nitrate reductase. The reaction was followed by the colorimetric detection of nitrite as an azo dye product of the Greiss reaction. The Greiss reaction was based on the two step diazotization reaction in which acidified NO_2 produced a nitrosating agent reacts with sulfanillic acid to produce the diazonium ion. This ion was then coupled to N-(1-naphthyl) ethylenediamine to form the chromophoric azo-derivative which absorbs light at 540-570 nM.

2.5.1 cAMP assay (Amersham)

All reagents were supplied by amersham as part of the discoverX kit unless otherwise stated. Cells were harvested and counted either on a haemocytometer using trypan blue exclusion. Cells are resuspended in antibody solution supplied in the kit at the appropriate dilution for the required seeding density. 500 mM 3-Isobutyl-1-methylxanthine (IBMX) (sigma) suspended in 100% DMSO is diluted into the cell solution 1/1000. IBMX is a potent non-specific inhibitor of cAMP and cGMP phosphodiesterases. As a result of this inhibition the levels of cAMP in the cell will increase leading to activation of Protein Kinase A (PKA), which can lead to decreased proliferation, increased differentiation and induction of apoptosis. IBMX can also act as an adenosine receptor antagonist. IBMX is added to prevent the breakdown of any cAMP that accumulates in the cell in response to the ligand. LX-2 cells were then plated into a 384 well plate at a density of 10,000 cells per well. Primary HSC were plated at a density of 12,000 cells per well. Each well contained 10 µl of cell solution or wells that were required for the cAMP standard curve in duplicate contained 10 µl of antibody solution alone. The plate was returned to the 37˚C incubator whilst the serial dilutions of cAMP standard (supplied in the kit already reconstituted), relaxin receptor agonist (H2-relaxin, INSL3, H3-relaxin or INSL5) (phoenix pharmaceuticals) or forskolin (sigma) were reconstituted

with 1% PBS-BSA or 100% DMSO respectively. Forskolin was reconstituted with 100% DMSO to make a stock solution of 10 mM. Relaxin agonists were reconstituted with PBS-BSA to a stock concentration that depended on the top concentration used in the assay. An example of the reconstitution volume required is given below.

100 µM stock solution = 33.54 µl PBS-BSA to reconstitute 20 µg of H2-relaxin (MW: 5963.06)

20 µl of stock is added to 190µl of PBS-BSA, this gives a top concentration of 3.5 µM in the assay plate. Half log serial dilutions are then carried out by adding 63 µl of the top concentration to 137 µl of PBS-BSA, this is then repeated to give a 12 point curve.

cAMP standard was diluted from stock, 1/3 in PBS. 50 µl of stock solution was added to 100 µl of PBS, this was used as the top concentration in the assay and then a further 11 descending serial dilutions in PBS were made. The serial dilutions ranges used in the assay for all of the ligands are stated as final concentrations in the plate in table 7, the dilution factor is 1 in 3 in the plate. The assays were optimized using a half log 12 point curves for each of the ligands, ranging from the highest to the lowest concentration stated.

Molar	E	LOG
	9.48e-6	-5
3.16 µM	3.16e-6	-5.5
	9.97e-7	-6
316 nM	3.14e-7	-6.5
	9.92e-8	-7
31.6 nM	3.13e-8	-7.5
	9.87e-9	-8
3.16 nM	3.11e-9	-8.5
	9.82e-10	-9
316 pM	3.10e-10	-9.5
	9.78e-11	-10
31.6 pM	3.08e-11	-10.5
	9.73e-12	-11
3.16 pM	3.07e-12	-11.5
	9.68e-13	-12
316 fM	3.05e-13	-12.5

Table 7. Serial dilutions of relaxin ligands or forskolin using half log increments were made by adding 63 µl of the top concentration to 137 µl of PBS-BSA or DMSO. Molar concentrations are the final concentrations in the plate.

5 µl of relaxin agonist, cAMP standard or forskolin were then added. Each dose response to the relaxin agonist was repeated in triplicate for each cell extraction, the cAMP standard and forskolin dose responses were repeated in duplicate for each plate. Plate was returned to the 37˚C incubator for 90 mins. 20 µl of ED/subtrate lysis mix was then added to all of the wells. ED/substrate lysis mix contained 7.6 ml of lysis buffer, 400 µl of galacton star, 2 ml of emerald II and 10 ml of ED reagent (all reagents supplied in the kit). Plate was covered with foil to protect the reagents from light and incubated at room temperature for 60 mins. 20 µl of EA-reagent was added to all of the wells and the plate is then sealed with Packard Topseal film, covered in foil and left to develop in the dark at room temperature for 6-16 hours. The plate seal was removed and the luminescence was then measured on the analyst AD, all wells read as counts per second. Raw data is captured to windows XP excel file for further data processing and evaluation on graphpad prism. If the assay required the cells to be pre-stimulated with forskolin, all the cells were exposed to one concentration

of 5 µl forskolin (chosen to be 80% of the maximal response concentration in each cell type) for 5 mins. 5 µl of relaxin ligands were then added to the cells and the assay was continued as described previously.

2.5.2 Gel contraction assay

500 µl of Bovine Collagen-1 (Cultrex) was added to each well of a 24 well culture plate under culture sterile conditions. The acidified collagen is neutralized with ammonia. An ammonia (sigma) soaked tissue is taped to the inside of the lid of the 24 well plate. The plate was incubated at 37°C for two hours and was then removed from the 37°C incubator and the ammonia soaked tissue removed. The plate was then left with the lid off in a tissue culture hood for 2-4 hours. The collagen gel would remain solidified, therefore 500 µl of PBS (Invitrogen) is then added to each well for 10 minutes at room temperature. PBS is removed and another 500 µl is added to the wells and the plate is incubated at 37°C overnight.

Activated human stellate cells that had been cultured on plastic non-transfected or LGR7 and –ve control siRNA (ambion) transfected were enzymatically removed from the culture plastic and plated onto the prepared collagen-1 gels in a 24 well plate. The cells were plated at a density of 100,000 cells per well and were cultured overnight at 37°C, 5% CO_2 in DMEM (Invitrogen) containing 10% FBS (Invitrogen). DMEM was replaced before treatments were added. Single concentrations of H2-Relaxin (Phoenix Pharmaceuticals Inc), Endothelin-1 (Phoenix Pharmaceuticals Inc), (table 2.7). The plate is incubated for a further 2 hours at 37°C, 5% CO_2 and then another dose of the treatments are applied before the gels are released (ringed) from the well using a small pipette tip. Images are taken of the gels at 24, 48 and 72 hours post ringing. These images are imported into Imagej where gel contraction can be measured as the area of the gel.

Pre-treatment	Treatment at T=0
Serum free DMEM	10% DMEM
10% DMEM + Vehicle (PBS-BSA)	10% DMEM + Vehicle (PBS-BSA)
10% DMEM + 1 μM H2-Rlx	10% DMEM + 1 μM H2-Rlx
10% DMEM + 200 nM ET-1	10% DMEM + 200 nM ET-1
10% DMEM + 1 μM H2-Rlx	10% DMEM+ 200 nM ET-1
10% DMEM + 200 nM ET-1	10% DMEM+ 1 μM H2-Rlx

Table 8. Treatment of HSC in gel contraction assays.

2.5.3 Total NO/Nitrite/Nitrate detection (R+D systems)

Test samples were collected from gel contraction assay wells. The cell culture supernatant was collected after 72-96 hours of cell culture. Cell culture supernates were centrifuged at 13000xg for 2 mins to remove particulates. 500 μl of each sample was then filtered using 10,000 molecular weight (MW) cut-off filters (Millipore). 500 μl of each test sample was centrifuged through the 10,000 MW filters at 10,000 rpm for two minutes. Supernatant that was able to pass through the filter was collected and stored in 2 ml Eppendorf tubes. Samples were stored at -20°C until ready to assay.

Reagent Preparation

All reagents were brought to room temperature before use. 10x reaction diluent (30ml of a 10 fold concentrated buffer containing detergent) was diluted using distilled water, 30 ml into 300 ml. Nitrate reductase enzyme was reconstituted with 1.0 ml nitrate reductase storage diluent (1.2ml of buffer containing glycerol) and vortexed vigorously, allowed to sit for 15 mins at room temperature and vortexed again, allowed to sit for an additional 15 mins at room temperature, vortexed again. Nitrate reductase was then diluted immediately

before use, determining the number of samples and standards in duplicate, the following equation was used:

A. Nitrate Reductase (µl) = no. of wells x 5 µl
B. Reaction Diluent (1 x) (µl) = volume from step A x4
C. Volumes from steps A and B were added to a clean test tube and vortexed
D. Reaction was placed on ice and used within 15 mins of dilution

NADH Reagent (lyophilized reduced ß-Nicotiamide adenine dinucleotide- must be stored in the dark)

NADH was reconstituted with 5 ml deionized water and allowed to sit for 3 minutes with gentle agitation. NADH was used within 15 minutes or placed on ice.

Nitrite/Nitrate standard (0.5ml of sodium nitrate/nitrite solution 2000 µmol/L in buffer)

500 µl of 1x reaction diluent was then added to eight sterile 2 ml Eppendorfs. 500 µl of the 2000 µmol/L standard (nitrate or nitrite) stock was added to the first 2ml Eppendorf in the dilution series, the tube was mixed thoroughly and the serial dilution was continued, changing pipette tips between each transfer. This resulted in an eight point standard curve, top of curve high standard was 500 µmol/L and 1x reaction diluent was the blank.

Nitrite assay procedure - The assay procedure was used to measure the concentration of endogenous nitrite present in the sample

All reagents were brought to room temperature before use and all samples and standards are assayed in duplicate. All reagents, standards and samples were prepared as above. The microplate was removed from the sterile bag and any unwanted wells were returned to the storage bag. 50 µl of 1x reaction diluent was added to the blank wells. 50 µl of nitrite standard or sample was added to the remaining wells. 50 µl of 1x reaction diluent was added to all the wells. 50

µl of Griess Reagent 1 (12 ml Sulfanilamide in 2N Hydrochloric acid, was added to all the wells before 50 µl of Griess Reagent II (12ml of N-(1-Naphthyl) Ethylenediamine in 2 N Hydrochloric acid) was added to all the wells. The plate was then mixed well by tapping the plate gently and incubated at room temperature for 10 minutes. The optical density was determined for each well of the microplate using a plate reader set to read at 540 nm with a wavelength correction of 620 nm.

Nitrate reduction assay procedure – The assay procedure was used to measure total nitrite by converting nitrate to nitrite.

To determine the nitrate concentration in the sample, the endogenous nitrite concentration measured from the Nitrite Assay procedure must be subtracted from the converted nitrite concentration measured in this procedure. All reagents were brought to room temperature before use and all samples and standards are assayed in duplicate. All reagents, standards and samples were prepared as above. The microplate was removed from the sterile bag and any unwanted wells were returned to the storage bag. 50 µl of 1x reaction diluent was added to the blank wells. 50 µl of nitrate standard or sample was added to the remaining wells. 25 µl of NADH, diluted as above was added to all the wells. 25 µl of diluted nitrate reductase was added to all the wells. Plate was mixed and covered with the adhesive strip provided. Plate was then incubated at 37˚C for thirty minutes. 50 µl of Griess reagent I and 50 µl of Griess reagent II were added to all the wells, plate was mixed and incubated for 10 minutes at room temperature. Optical density was determined in a microplate reader set at 540 nm with wavelength correction at 620 nm.

Calculation of results

All duplicate readings were averaged and a standard curve plotted on a log scale to linearise the data. Concentration of samples read form the standard curve are multiplied by the dilution factor (samples were read undiluted in this case). Endogenous and total nitrite concentrations are now known. To calculate the

total nitrate concentration the endogenous nitrite concentration is subtracted from the total nitrite concentration.

Nitrate concentration = (Y-X) μmol/L.
The results from the test samples were averaged from the three wells before entering them into the calculation. The results from the three experiments were averaged and plotted on a histogram, including the standard deviation. A t-test was used to determine if the differences observed were significant.

2.6 siRNA studies

RNA interference (RNAi) is an evolutionary conserved phenomenon observed in nearly every eukaryote ever studied. In nature RNAi is a recognised pathway in the cellular defence against viral invasion and represents a unique form of post transcriptional gene silencing (PTGS). RNAi can be initiated when the host cell encounters long dsRNA transcribed from an invading virus, an endogenous inappropriately transcribed sequence or by the newly identified class of regulatory non-coding micro RNAs (miRNAs). The RNAi pathway was recognised as a biological pathway that could be utilised to develop valuable tools for systematic gene function analysis. Functional intermediates, short interfering RNAs (siRNA) can be synthesised by a variety of methods and can be introduced to the cell or organism to effect changes in gene function. SiRNA has become a potent and specific method of gene silencing which exploits a naturally occurring pathway.

The original observations were explained over a decade ago. Fire and Mello described injection of a double stranded RNA that lead to the efficient loss of target mRNA. There was little or no silencing by injecting single stranded sense or antisense RNA. The silencing observed was specific for the homologs of the dsRNA sequence. The dsRNA had to correspond to the mature mRNA, neither intron nor promoter sequences triggered a silencing response. It was

hypothesised that the dsRNA was acting post transcriptionally utilising a cytoplasmic mechanism. The targeted mRNA disappeared suggesting it was degraded. It was observed that only a few molecules of dsRNA were required per cell for effective silencing, it was suggested that the dsRNA is amplified or is acting catalytically (Fire et al., 1998). Since the discovery of effective silencing through the injection of dsRNA, great advances have been made. The RNAi interference pathway has been elucidated (figure 2.7)

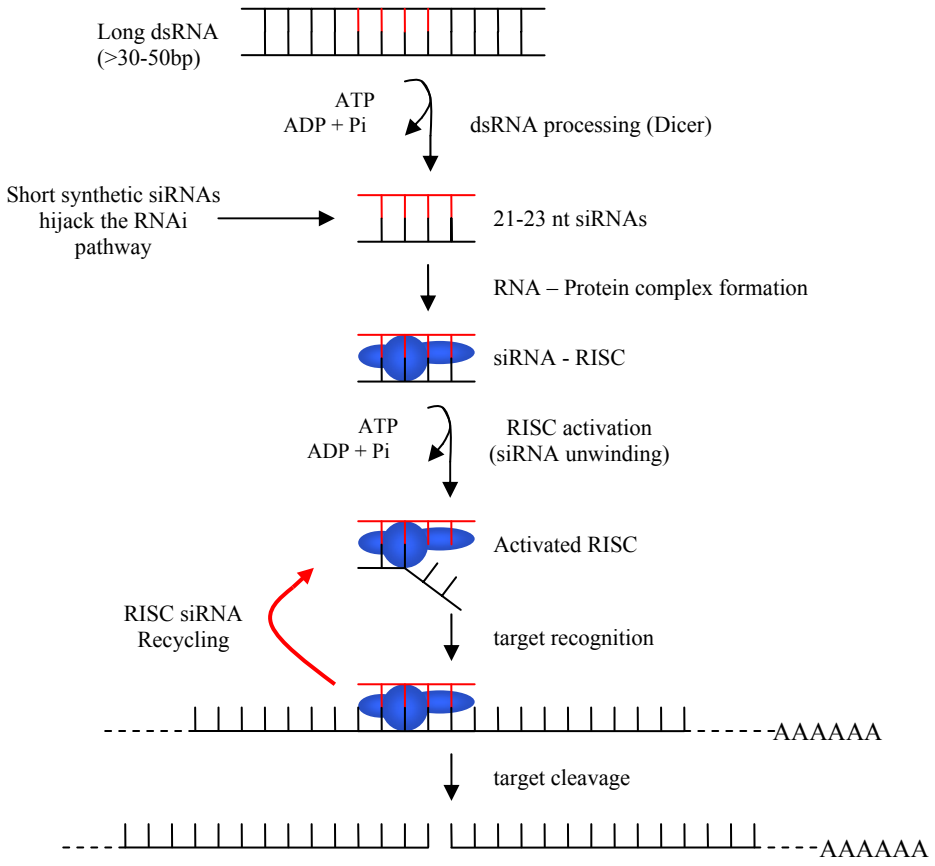

Figure 2.7. The RNA interference pathway

The appearance of dsRNA induces a cascade of events that involves a cytoplasmic RNase III like protein known as a dicer and the multi-protein RNA induced silencing complex (RISC). In the cytoplasm Dicer is responsible for cleaving double stranded molecules, endogenously expressed miRNAs, replicating viruses or siRNAs, which are 19-25 base pairs long and have

characteristic 3' overhangs. siRNA is incorporated into RISC and the RISC associated ATP dependent helicase activity unwinds the duplex. This enables either two strands to independently guide target mRNA recognition. Complimentarity between the guide strand and the target mRNA determines whether silencing is achieved via site specific cleavage of the message in the region of the siRNA-mRNA duplex or through a miRNA like mechanism of translational repression. SiRNA silencing releases the cleavage products which are degraded leaving the siRNA programmed RISC to survey and further deplete the available pool of target mRNA (Fire et al., 1998). Synthetic siRNAs function catalytically at nanomolar concentrations. They are capable of cleaving up to 95% of the target mRNA in the cell. Highly potent siRNAs have been found to effectively silence the gene through several cell divisions, persisting up to 10 days in mammalian culture. Researchers are using siRNA to assess the contribution of genes to cellular processes such as apoptosis, differentiation and signalling. The ability to produce knockout animals that stably suppress gene expression through a version of siRNA called short hairpin RNA (shRNA) has advanced the field not only through increased accessibility but through the capacity to produce multigene knockouts (Leung and Whittaker, 2005). ShRNA are siRNA sequences that have been ligated into a vector to create a plasmid that is incorporated into the cell or organisms genetic machinery. SiRNA has also become a screening tool to elucidate the function of genes or to identify which genes are important in a particular biological process. The siRNA field has advanced in recent years, developing rational design and pooled siRNA which not only increases successful knockdown of the gene but reduces the off target affects. There are many different delivery methods such as lipid based transfection reagents or electroporation, none of which have been found to universally suit all cell types. Cell lines are more robust and can be transfected using higher concentrations of siRNA and transfection reagent compared to primary cells. This usually increases the efficiency of delivery and the level of knockdown achieved. Lipid based transfection reagents and even siRNA alone can be toxic to both cell lines and

primary cells. This has to be controlled for by using cell viability and cytotoxicity assays to assess the cell viability after each different experimental condition to ensure the decrease in gene expression is not due to cellular necrosis (Fire et al., 1998;Leung and Whittaker, 2005).

3(4,5-dimethylthiazol-2-yl)-5-(3-carboxymethoxyphenyl)-2-(4-sulfophenyl)-2H-tetrazolium, inner salt (MTS) is used as an indicator of cell viability. The MTS assay used has combined MTS with an electron coupling agent, phenazine ethosulfate (PES) that has enhanced stability allowing it to combine with MTS to form a stable solution. MTS is bioreduced by cells to form a coloured formazan product that is soluble in tissue culture medium (figure 2.8) (Cory et al., 1991). The coloured formazan product is produced through the break down of NADPH or NADH to NADP or NAD^+ respectively. The process requires dehydrogenase enzymes from metabolically active cells (Berridge and Tan, 1993).

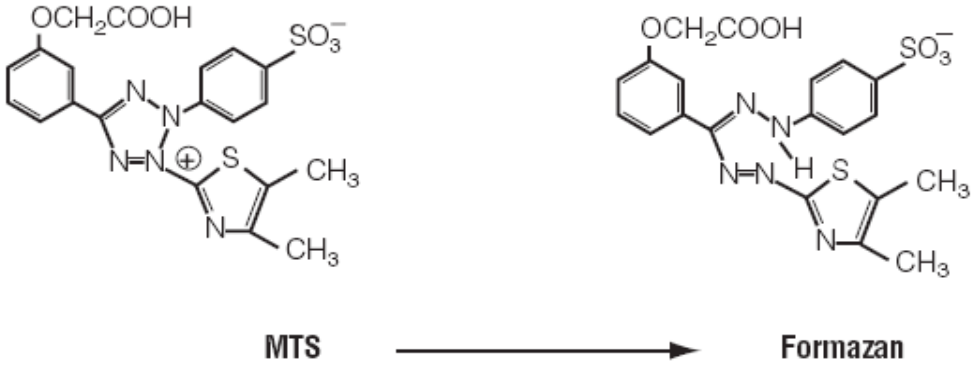

Figure 2.8. Conversion of MTS to Formazan (Promega)

The colour change produced by the formation of formazan can be measured by reading the absorbance wavelength at 490 nM on a spectrophotometer. The colour change is directly proportional to the number of viable cells in the well (figure 2.9.). The assay can be used to detect the number of viable cells after manipulation by siRNA or cytotoxic substances. It can be used in conjunction

with other assays such as apoptosis and LDH cytotoxicity assays to ascertain the method by which cells may be reducing or increasing their viability and number.

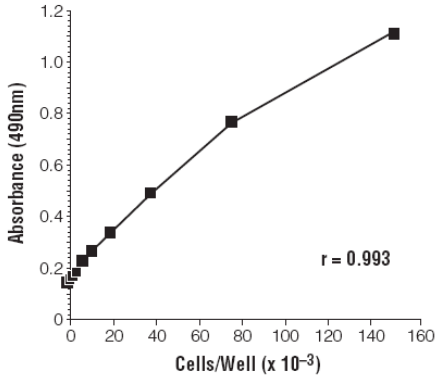

Figure 2.9. Absorbance plotted against cell number to show linearity (Promega)

The advantage of using MTS over traditional MTT or INT assays is that the coloured product is soluble in tissue culture media and the PES electron coupling reagent is stable when combined with MTS. Also there are no radioactive or volatile organic solvent compounds to handle unlike similar assays. This not only allows for fewer steps in the assay, reducing the time and any possible error but also increases the flexibility of the assay. The plate can be returned to the incubator for further colour development if required.

The lactate dehydrogenase (LDH) assay is a colorimetric assay used to quantify cell death and cell lysis. Cell death has been classically evaluated by quantification of plasma membrane damage. Many different standard methods including the uptake or exclusion of vital dyes or the release of radioactive isotopes are used to quantify cell death (Yuhas et al., 1974;Oldham et al., 1977). The disadvantage of these techniques is the quantification can be easily under or over estimated. The measurement of cytoplasmic enzyme activity released from damaged cells is a robust method that directly relates to the proportion of lysed cells. LDH is released into the supernatant from the cytosol of damaged cells.

LDH is a stable cytoplasmic enzyme present in all cells that is rapidly released upon damage to the plasma membrane. The colour reaction required for quantification undergoes two steps. Firstly NAD^+ is reduced to $NADH/H^+$ by the LDH catalysed conversion of lactate to pyruvate. The second step is catalysed by diaphorase which transfers the hydrogen ions from $NADH/H^+$ to the tetrazolium salt INT, which reduces it to form the coloured product formazan (figure 2.10) (Korzeniewski and Callewaert, 1983).

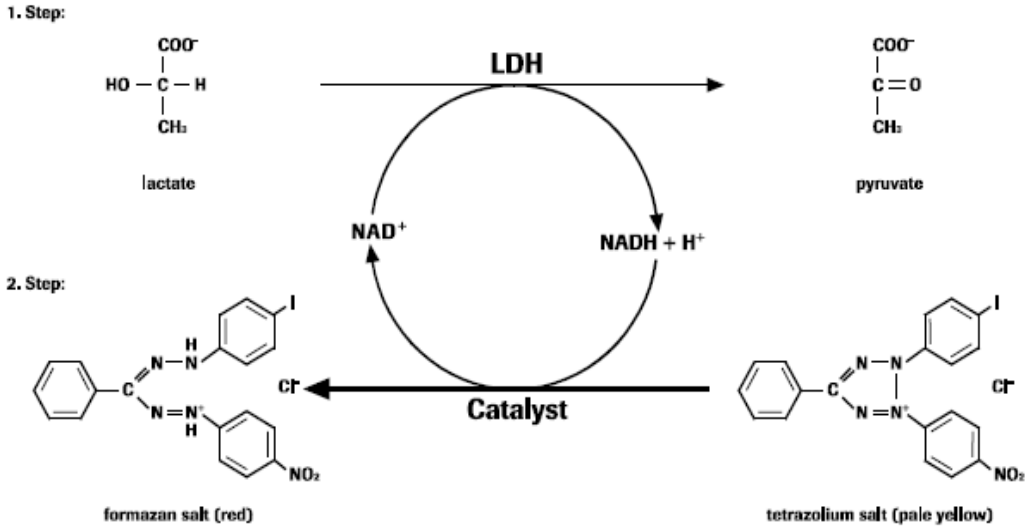

Figure 2.10. Colorimetric LDH cytotoxicity assay reaction (Roche)

If there is an increase in dead/lysed cells then there will be an increase in LDH enzyme activity in the cell culture supernatant. The enzyme activity directly correlates to the amount of formazan formed which is soluble in water or cell culture media. The absorbance wavelength of formazan can be detected at 490 nM on a standard spectrophotometer or elisa plate reader. A reference absorbance can be measured above 600 nM. The reference absorbance is subtracted from the actual reading and is used to eliminate any interference from colours absorbed at different wavelengths. Pyruvate can inhibit step 1 of the reaction through a feedback mechanism. Pyruvate is present in some

formulations of cell culture media and serum and therefore care must be taken to ensure the concentration is as low as possible in this assay.

2.6.1 SiRNA transient transfection

Human HSC or LX-2 cells were plated at a density of 100,000 cells per well in a 10 cm dish or 50,000 cells per well in a 6 well plate. Cells were cultured for 24 hours in antibiotic free 10% DMEM. Media was then replaced with 4.8 ml or 800 µl of serum free media and cells returned to the 37°C incubator whilst the siRNA/lipid complexes were formed. All serum free media (SFM) used was DMEM with phenol red, without serum, antibiotics or sodium pyruvate. Concentration of siRNA was determined by transfecting several different concentration of siRNA into HSC or LX-2 cells. The lowest possible concentration which gave the maximum knockdown and the least cytotoxicity for each cell type was used. LX-2 cells could be transfected with a higher concentration of siRNA due to the minimal toxicity observed in these cells.

Preparation and transfection of complexes in LX-2 cells

LX-2 cells were transfected with 100nM of siRNA whilst primary HSC were transfected with 25 nM siRNA. LX-2 cell transfection in a 6 well plate was carried out entirely in a tissue culture hood using aseptic techniques. 2 µl of RXFP-1 or –ve control siRNA (ambion) were added to 183 µl of serum free media (SFM) in a DNAase/RNAase free 1.5ml Eppendorf tube. 4 µl of oligofectamine transfection reagent (Invitrogen) was added to 11 µl of SFM in a separate sterile Eppendorf. Each tube was incubated at room temperature for 5 minutes. The siRNA and oligofectamine was then combined and incubated at room temperature for 20 minutes. The 200 µl siRNA/lipid complexes were then added directly to the cells that contain SFM. The cells are then returned to the 37°C incubator for 4 hours before 0.5 ml of 30% DMEM w/o antibitotics or pyruvate was added to the cells. The cells remained in antibiotic and pyruvate free media throughout the transfection process and during any subsequent

assays that the cells were used in. All amounts were multiplied by 6 for transfections in a 100 mm dish.

Preparation and transfection of complexes in primary HSC

Primary HSC transfection in a 6 well plate was carried out entirely in a tissue culture hood using aseptic techniques. 0.5 µl of RXFP-1 or –ve control siRNA (ambion) were added to 184.5 µl of serum free media (SFM) in a DNAase/RNAase free 1.5ml Eppendorf tube. 4 µl of oligofectamine transfection reagent (invitrogen) was added to 11 µl of SFM in a separate sterile Eppendorf. Each tube was incubated at room temperature for 5 minutes. The siRNA and oligofectamine was then combined and incubated at room temperature for 20 minutes. The 200 µl siRNA/lipid complexes were then added directly to the cells that contain SFM. The cells are then returned to the 37°C incubator for 4 hours before 0.5 ml of 30% DMEM w/o antibiotics or pyruvate was added to the cells. The cells remained in antibiotic free media throughout the transfection process and during any subsequent assays that the cells are used in. All amounts were multiplied by 6 for transfections in a 100 mm dish.

2.6.2 MTS cell viability assay (Promega)

MTS assays were used to determine the cell viability after transfection with siRNA and after relaxin treatment in HSC. Suitable controls were carried out for each assay and the optimal cell density was determined before experimental conditions were tested. The optimal cell density for HSC was found to be 5000 cells per well of a 96 well plate. Each condition was plated in triplicate and the background was read and subtracted each time using wells containing cell culture media DMEM containing 10% serum and phenol red but no cells. MTS reagent (Promega) was thawed before each use and returned to -20ºC thereafter.

The cells were then transfected with RXFP-1 and –ve control siRNA in a 6 well plate as described previously. The cells were also exposed to transfection reagent and the siRNA alone. This was to ensure neither the transfection reagent nor the siRNA could individually effect the viability of the cells. The cells were trypsinised and counted using a haemocytometer after 5 hours exposure to the siRNA. A flat bottom 96 well clear cell culture plate was used to seed each condition in triplicate at a density of 5000 cells per well in 100 µl of 10% FBS DMEM with phenol red. The cells were placed back in the 37ºC incubator overnight. After 24 hours 20 µl of MTS reagent was added to the wells which were to be read 24 hours after transfection. The plate was protected from the light and replaced in the 37ºC incubator for 1 hour. The absorbance was then read at 490 nM on a spectrophotometer. The plate was returned to the 37ºC incubator for a further 24 hours. The wells which were to be read 48 hours after transfection now had 20 µl of MTS reagent added. The absorbance was again read after 1 hour in the dark at 37 ºC at 490 nM on a spectrophotometer and returned to the incubator. The procedure was carried out again 72 hours after transfection.

The MTS assay was also used to detect the cell viability after 72 hours of relaxin treatment. Cells were plated at a density of 5000 cells per well in a flat bottomed 96 well cell culture plate. Cells were retuned to the incubator overnight before culture media was replaced, ensuring each well had 100 µl of 10% FBS DMEM. Cells were then treated with 1 µM of relaxin or vehicle (PBS/BSA) and returned to the incubator for 72 hours (cells were treated with relaxin every 24 hours). 20 µl of MTS reagent was added to each well including control well and the plate was returned to the incubator protected from the light for 1 hour. The absorbance was then read at 490 nM on a spectrophotometer.

Both assays were carried out with three different preps of HSC. The average results were calculated after subtracting the background. The results were used

to compare between treatment groups and therefore absolute values of cell viability were not required.

2.6.3 LDH cytotoxicity assay

Colorimetric LDH cytotoxicity assays were used in conjunction with MTS assays to determine if siRNA transfection and treatment with relaxin is cytotoxic to HSC. The assay required 3 different controls to be carried out to enable a percentage cytotoxicity to be calculated. The background LDH activity was controlled for by adding 10% FBS DMEM that had not been exposed to cells. The high control was the maximal LDH released from the cells. This was achieved by adding 1% triton X diluted in 10% FBS DMEM to the cells after the culture supernatant had been removed. Triton X is a detergent that lyses the cells but does not interfere with the colour reaction. The final control was an internal experimental control such as –ve control siRNA and non-transfected cells being used to compare RXFP-1 siRNA transfected cells. Also within the relaxin treatment experiment the internal control was cells treated with PBS containing 1% BSA. This was the vehicle used to deliver relaxin to the cells in culture. Assay samples were collected directly from the 6 well plates in which the cells were either transfected or exposed to relaxin in. The high control was collected for each individual sample by adding 1% triton X to the adherent cells in the 6 well plate. Each sample % cytotoxicity was calculated using its own high control. This controlled for any changes in cell number.

Directly before the experiment could be carried out the reaction mixture was prepared. The catalyst diaphorase/NAD+ mixture (Roche) had to be reconstituted with 1 ml of deionised water. This was left to stand at room temperature for ten minutes before 250 µl was added to 11.25 µl of dye solution (iodotetrazolium chloride (INT) and sodium lactate) (Roche). The reaction mixture was sufficient to carry out 100 reactions in a 96 well plate. The supernatant was removed from the cells cultured in the 6 well plates and placed

in 2 ml Eppendorf tubes. The samples were spun at 10,000 rpm for 2 minutes and the supernatant was removed and stored in a new 2 ml Eppendorf. The samples were stored at -20ºC or used directly in the assay. 100 µl of supernatant was added in triplicate for each sample to a flat bottomed 96 well culture plate. 100 µl of reaction mix was added to each sample which was incubated at room temperature in the dark for 30 minutes. The absorbance was then measured at wavelength 490 nM on a spectrophotometer. The reference wavelength was above 600 nM. The cells used in the assay were cultured in 10% FBS DMEM with phenol red. Although the assay conditions suggest using serum concentrations of below 5%, the experimental conditions had to correspond with the experimental conditions for all of the siRNA studies. There were no antibiotics in the media used for the siRNA transfected cells and the percentage pyruvate was kept as low as possible, i.e. there was no extra pyruvate added to the media and the DMEM used did not have a high percentage pyruvate content. Percentage cytotoxicity was calculated using averaged experimental and control values from each experiment that used triplicate wells and from the three different cell preps, see below.

$$\% \text{ Cytotoxicity} = \frac{\text{(Experimental value-background control)}}{\text{(Experimental value+ high control)-background}} \times 100$$

All of the samples were calculated using this formula**.** The experimental values such as relaxin treated cells were then compared to the control wells such as PBS-BSA treated cells and were plotted on a graph plus or minus standard of the mean and a t-test was used to calculate any significant differences. Absolute LDH activity could be calculated using a spiked standard curve but this was not deemed necessary as only the percentage cytotoxicity was required to be able to compare samples.

2.7 Statistical analysis

Results are all normalized to appropriate controls and standard deviations are applied as error bars on all control and experimental values. A two tailed, paired T-Test was then carried out to compare each result to the control. Results are shown as significant ** ($p<0.01$) = 99% confidence, * ($p<0.05$) = 95% confidence. One results has been shown as * ($p<0.1$) = 90% confidence. Cytokine array data in chapter 4 was analysed using Graphpad Prism4. A repeated measures one way ANOVA was carried out using a suitable post hoc test, in this case a Bonferroni correction analysis. This enabled each column of values for each respective cytokine to be compared to each other, allowing for comparisons between each cytokine and its respective control value, between each cytokine within the control and treatment groups and each cytokine between these two groups.

Chapter 3

In vitro characterisation of relaxin receptors in human models of fibrotic liver disease

3.1 Introduction

3.1.1 Introduction

Relaxin knockout mice develop age related fibrosis (Samuel et al., 2005b) and consequently there has been a resurgence of interest in relaxin by academic labs and pharmaceutical companies alike in the idea of using relaxin as an antifibrotic therapeutic agent. Two receptors that respond to H2-relaxin and INSL3 were identified in 2002 (Hsu et al., 2002) and more recently the receptors that respond to H3-relaxin (RXFP-3) (Liu et al., 2003) and INSL5 (RXFP-4) (Liu et al., 2005b). Therefore the relaxin receptor family are a relatively new area of research and the discovery of the relaxin receptors has enabled more detailed pharmacological approaches to help reveal the true therapeutic potential of this hormone. Previous studies have revealed relaxin receptors to be expressed in rat HSC and localised in rat and human cirrhotic liver sections (Bennett et al., 2005;Bennett et al., 2007). The characterisation of these receptors in hepatic stellate cells (HSC), which are the main effector cells in fibrotic liver disease (Friedman et al., 1985;Friedman et al., 1985), will allow the evaluation of the key issues to be addressed in the thesis. Relaxin receptor expression and localisation in liver tissue will be studied using several different techniques including RT-PCR and immunohistochemistry in *in vitro* models of fibrotic liver disease including growth of HSC on Matrigel. In the normal liver HSC reside on basement membrane and grow long projections that link the endothelial and hepatocyte layer in the Space of Disse (Imai et al., 2000). Culture of HSC on Matrigel can deactivate HSC, allowing the study of HSC in a less fibrotic phenotype (Gaca et al., 2003). The activity of the relaxin receptors in response to their respective ligands will be determined by cAMP assay.

3.1.2 Hypothesis, Aims and Objectives

Hypothesis

Relaxin receptors are expressed in LX-2 and primary HSC and the expression may be dependent upon activation.

Aims

Determine the expression and localisation patterns of the relaxin receptors in HSC and human liver sections, whilst confirming the presence of active receptors that respond to their respective ligands.

Objectives

- Determine the expression pattern of relaxin receptors in LX-2 and primary HSC using RT-PCR and immunocytochemistry.
- Assess RXFP-1 and RXFP-2 expression in activated HSC, hepatocytes and hepatocellular carcinoma (HCC) by RT-PCR.
- Establish the receptor localisation in human liver sections by immunhistochemistry.
- Verify the loss of RXFP-1 expression in deactivated HSC using cells cultured on Matrigel.
- Confirm the presence of active receptors in LX-2 and primary HSC in cAMP assays and assess the *in vitro* pharmacological ligand concentrations required for a maximal response required for later studies.

3.2 Results-Relaxin receptor expression profile in different liver cell types

3.2.1 Expression patterns of the relaxin receptors and their ligands in activated HSC

RNA extracted from LX-2 cells and passage 1 (p1) hHSC and was used to assess the expression profile of RXFP-1, 2, 3 and 4. RXFP-1, 3 and 4 were all expressed in primary HSC and LX-2 cells (figure 3.1a). RXFP-1 had the highest expression and no band was detected for RXFP-2 in either LX-2 or p1 hHSC. H2-relaxin, H3-relaxin and INSL5 were found to have local expression in p1 HSC (figure 3.1b).

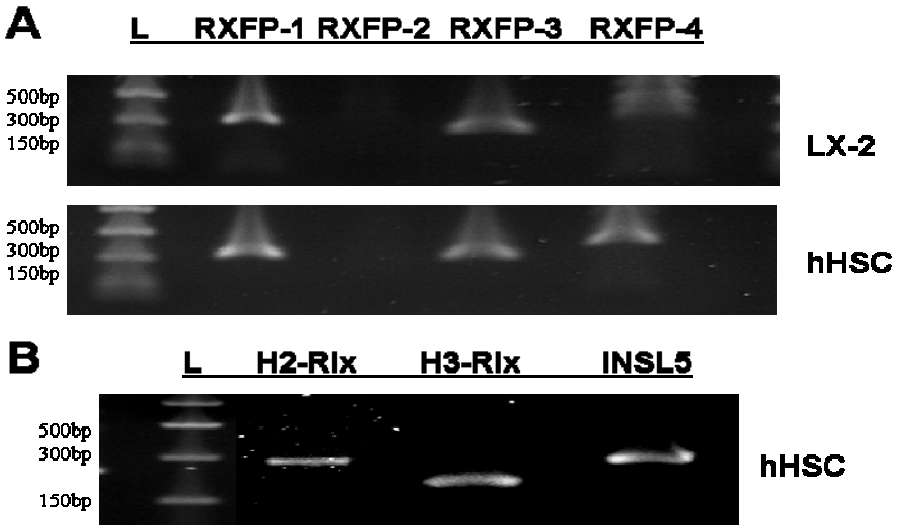

Figure 3.1 (A) Expression of RXFP 1-4 in primary HSC and LX-2 cells assessed by RT-PCR. RXFP-2 was not expressed in p1 priamry HSC or LX-2 cells. RXFP 1 (314bp), 3 (288bp) and 4 (356bp) were all expressed in both primary HSC and LX-2 cells (n=3) **(B)** expression of H2, H3-relaxin and INSL5 in primary HSC assessed by RT-PCR. All three relaxin ligands are expressed by primary HSC (n=3).

3.2.2 RXFP-1 and RXFP-2 expression in activated HSC, hepatocytes (HEP) and a hepatocellular carcinoma (HCC) cell line HepG2

RXFP-1 and 2 expression was assessed in HSC of different passage number, hepatocytes and HepG2 cells (hepatocellular carcinoma (HCC) cell line). RXFP-1 was expressed in p1, p3 and p4 HSC (figure 3.1a). RXFP-1 expression peaked in p3 HSC which coincides with the highest level of α-SMA protein expression, a marker of activation, assessed by immunoblotting (figure 3.2b). RXFP-1 was also expressed in hepatocytes (HEP) and had a very weak expression in HCC (HepG2 cells) (figure 3.1a). RXFP-2 expression was assessed in all of the cell types (figure 3.1a). RXFP-2 was expressed in p4 HSC but the expression was very weak and required a higher cycle number compared to RXFP-1 to be able to see this low level of expression.

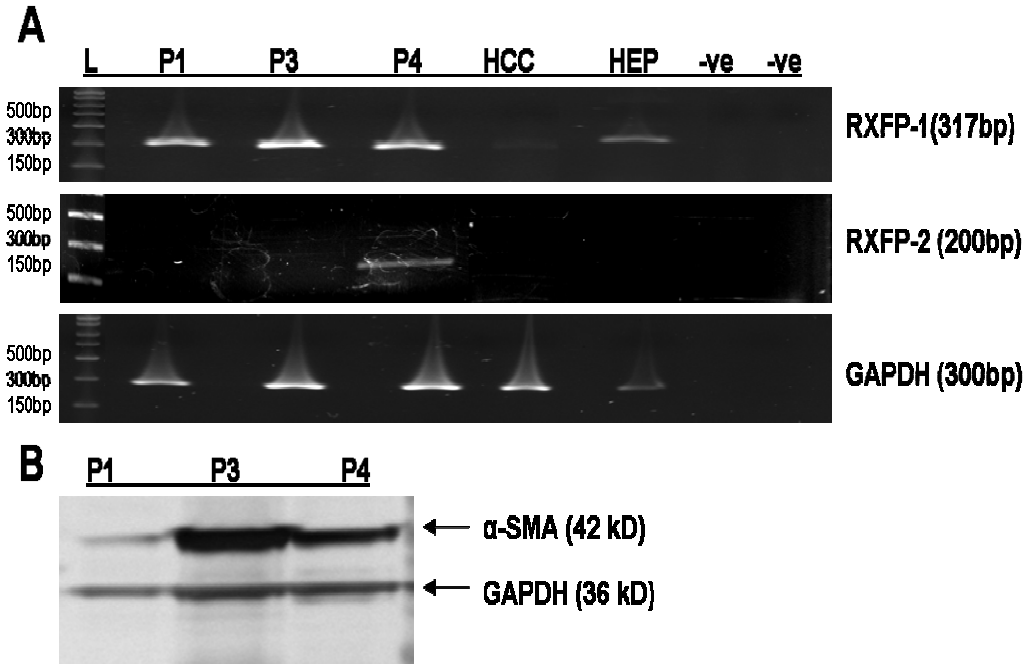

Figure 3.2 (A) Expression of RXFP-1(317bp), RXFP-2(200bp) and GAPDH in p1, p3, and p4 primary HSC, human HepG2 (hepatocellular carcinoma cell line) and human hepatocytes assessed using RT-PCR. RXFP-1 is expressed in p1, p3 and p4 HSC, hepG2 cells and hepatocytes. The greatest level of expression was found in p3 HSC

and the lowest level of expression was found in HCC (hepG2 cells) (n=3). **(B)** Expression of α-SMA and GAPDH in P1, P3 and P4 HSC assessed by immunoblotting (n=3). α–SMA expression was greatest in p3 HSC which confirms RXFP-1 expression increases in parallel with levels of activation.

3.2.3 RXFP-1 and α-SMA cellular localisation in activated HSC

To confirm the protein expression of RXFP-1 in activated primary HSC, immunocytochemistry was used. This also tested the purity of the preparations of HSC. Activated HSC are α-SMA positive in culture unlike possible contaminates such as macrophages and endothelial cells. Immunocytochemistry was carried out on p1 cells that had been cultured on cover slips. Immunocytochemistry revealed activated HSC extracted from human liver were a single population of cells that expressed both α-SMA (figure 3.3.a and b) and RXFP-1 protein (figure 3.3.c and d).

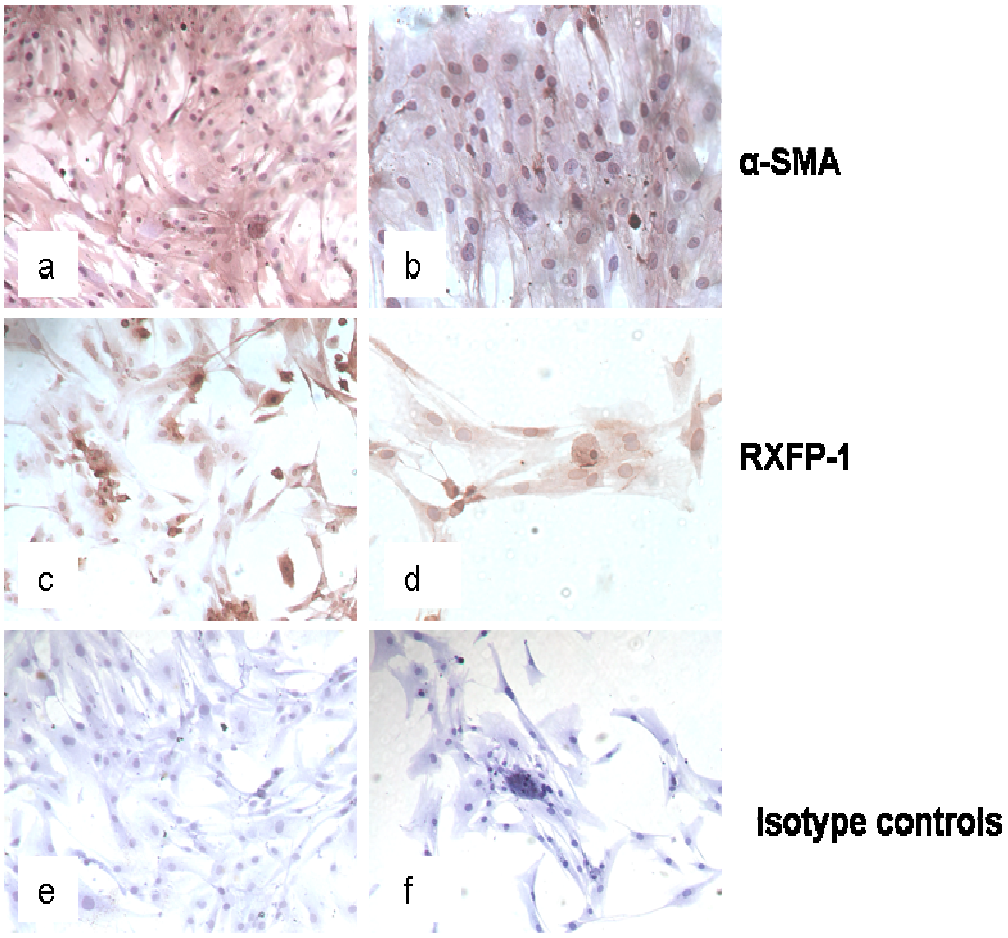

Figure 3.3. (a) α–SMA (1/1000) antibody staining of p2 human HSC 10 x objective **(b)** α–SMA (1/1000) antibody staining of p2 human HSC 20 x objective **(c)** RXFP-1 antibody staining of p2 human HSC (antibody dilution 1/200) **(d)** RXFP-1 antibody staining of p2 human HSC (antibody dilution 1/200) **(e)** rabbit (1/200) 10 x objective and **(f)** mouse (1/200) 20 x objective, IgG negative control staining of p2 human HSC. All images were taken using Zeiss Axioskop camera and software. An n=3 was obtained for each antibody stain.

3.3 Localisation of relaxin receptors in paraffin embedded liver sections

3.3.1 Identification of liver structures by H+E and the comparison of RXFP 1-4 localisation

Liver tissue that been removed from the normal margin of patients undergoing liver resection for hepatocellular carcinoma were fixed in 10% formalin and embedded in paraffin wax. The fixed tissue was used to study the localisation of relaxin receptors. Serial sections were cut and every tenth slide was stained with haematoxylin and eosin (H+E). This was carried out by a technician in the histology unit (figure 3.4a). The specimens characteristically had areas of scarring and areas of normal morphology within the section. The sections were stained using α-SMA antibody to be able to asses the level of fibrosis, and localise the activated stellate cells in the sections. The α-SMA staining of the liver reveals the activated hepatic stellate cells to be within the scar region around the artery and blood vessels as well as in the Space of Disse between the hepatic sinusoid and the hepatocytes (figure 3.4.b v-red arrows). Relaxin receptor localisation was determined by antibody staining. RXFP-1, RXFP-3 and RXFP-4 were localised in human liver sections (figure 3.4b). RXFP-1 was found to have a relatively high expression in areas of scarring in the human liver sections around the arteries and blood vessels in the portal triad (black arrow). RXFP-1 is also localised in the hepatocytes but the expression is low compared to the areas of scarring (figure 3.4.b i and ii). RXFP-3 had a similar pattern of expression but was not as highly expressed as RXFP-1 (figure 3.4.b iii). RXFP-4 was localised in areas of bile duct proliferation and around the areas of scarring but again compared to RXFP-1 the expression was low (figure 3.4.b iv).

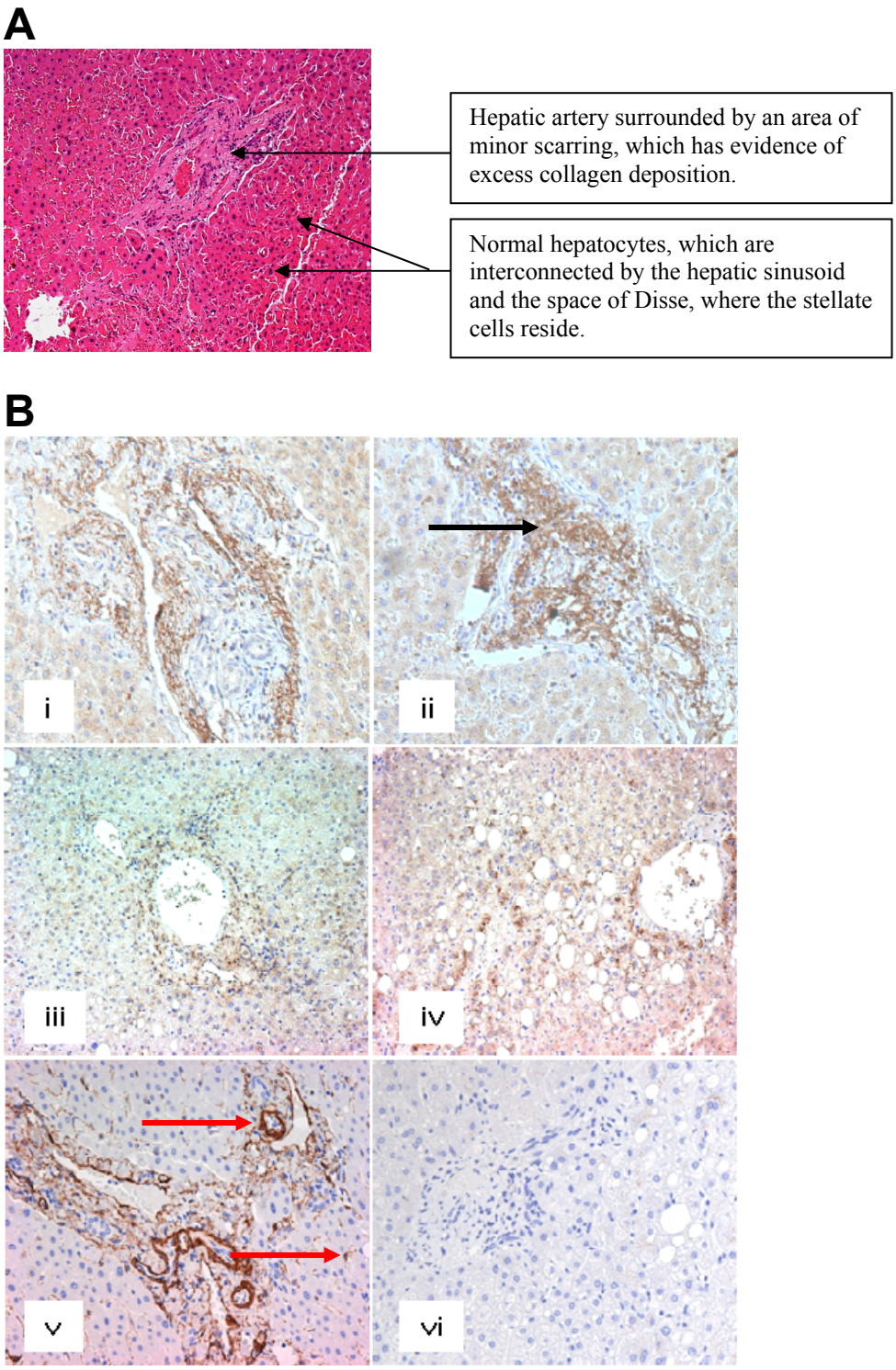

Figure 3.4. (A) Representative image of H+E staining of human liver sections. Structures such as the hepatic artery, hepatocytes and the hepatic sinusoid can be identified (n=3) **(B)** Representative images of immunohistochemical staining of paraffin embedded human liver sections. Antibodies for (i and ii) RXFP-1 (1/200 dilution), (iii)

RXFP-3 (1/200 dilution), (iv) RXFP-4 (1/50 dilution), (v) α–SMA (1/40,000) and (vi) IgG isotype control (1/200), were used to localise human relaxin receptors in liver tissue. RXFP-1 is strongly positive in areas of scarring (black arrow) and weakly positive in the hepatocytes (confirmed using RT-PCR), RXFP-3 is weakly positive around areas of scarring and RXFP-4 is positive in areas surrounding bile duct proliferation and areas of localised scarring. All images were taken using 20x objective on the Zeiss Axioskop camera and software. An n=3 was obtained for each antibody stain.

3.3.2 Serial section staining comparing RXFP-1 with sirius red and α-SMA

The cellular localisation of RXFP-1 was confirmed by using serial sections stained using H+E, Sirius red, α-SMA, RXFP-1 and a negative control. RXFP-1 is localised in areas of α-SMA positive staining, suggesting RXFP-1 is up regulated in areas of injury where HSC have become activated (figure 3.5. iii). Sirius red staining revealed fibril collagen formation in areas that were also stained for RXFP-1 (figure 3.5. iv).

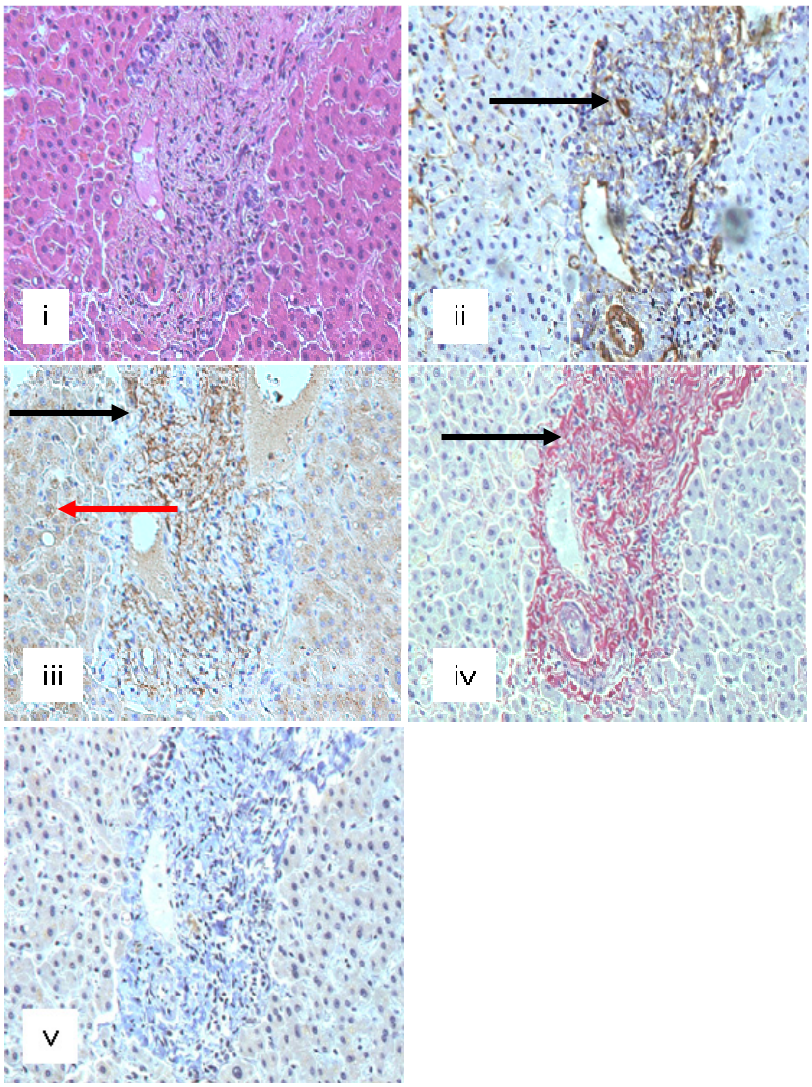

Figure 3.5. Representative images of paraffin embedded serial sections of human liver stained with (i) H+E, (ii) α-SMA (1/40,000 dilution), (iii) RXFP-1 (1/200 dilution), (iv) Sirius Red (fibrous collagen marker) and (v) IgG isotype control (1/200). RXFP-1 is clearly colocalised in an area of scarring that is also positive for α-SMA and Sirius red (black arrows). RXFP-1 is also localised in hepatocytes (red arrow). Images were taken with Zeiss Axioskop camera and software using 20 x objective. An n=3 was obtained for each antibody stain.

3.4 cAMP response to H2-Relaxin and relaxin-like ligands in HSC and LX-2 cells

The measurement of cAMP is a reproducible and reliable method of detecting activation of a cAMP linked receptor. cAMP is produced in cells in response to H2-relaxin (Halls et al., 2005a;Halls et al., 2006). The cAMP produced in response to H2-relaxin, H3-relaxin, INSL3 and INSL5, in LX-2 and primary HSC was measured. LX-2 cells were used to optimise the assay for the range of cAMP produced in response to H2-relaxin, due to difficulty in reproducibility in primary HSC. A standard curve is performed each time the assay is run (figure 3.6.a). The cAMP assay carried out in LX-2 cells revealed a dose dependent increase in cAMP accumulation in response to H2-relaxin, the ligand for RXFP-1 (figure 3.6.b). The Log EC_{50} value was -9.4 and the assay gave a 1.7 fold window. The log EC_{50} value is the point on the curve that gives 50% maximal response. The concentration of H2-relaxin that gave 50% maximal response in LX-2 cells was therefore $3.6x10^{-10}$ M. A plateau or Vmax is reached between Log concentration -8 and -7 (which corresponds to 10 – 100 nM). There was no dose dependent increase in cAMP in response to INSL3 the ligand for RXFP-2 although at the highest dose (10 μM) there was a small increase in signal. H3-Relaxin and INSL5 did not increase the amount of cAMP in the cell and the only response observed in the initial assay was a small decrease at the highest dose (10 μM) of H3-relaxin (figure 3.6.c). Activated RXFP-3 and RXFP-4 receptors decrease the amount of cAMP in the cell, therefore the LX-2 cells were pre-stimulated with forskolin to induce an accumulation of cAMP before the ligands, H3-relaxin and INSL5 are added. H3-relaxin and INSL5 both induced a dose dependent decrease in cAMP accumulation in LX-2 cells. The activity at the RXFP-3 receptor was more potent then that of RXFP-4 with a Log EC_{50} of -8.2 ($6.016x10^{-9}$ M) the curve was shifted to the left. The fold window for H3-relaxin was 1.27 and the Vmax was reached between Log concentration -6 and -5 (1 μM- 10 μM). RXFP-4 was stimulated with two INSL5 ligands, a long chain and a short chain ligand. The different ligands were developed to determine the

essential binding domains. Both ligands elicited a similar response, the long chain Log EC_{50} was -6.017 ($9.6x10^{-7}$ M) with a fold window of 1.21 whereas the short chain had a Log EC_{50} of 6.211 ($6.156 x10^{-6}$ M) with a fold window of 1.39. Vmax for both ligands is reached at Log concentration -5 (10 μM) (figure 3.6.c).

The cAMP response to relaxin ligands was then tested in primary HSC. The top concentration in the dose response curve was increased by two half log concentrations to -6.5 due to the top of the curve not being reached in the first assay. Once the assay had been optimised in primary HSC, it was found to be reproducible and a dose dependent response to H2-relaxin in primary HSC was observed. The ligand was not as potent as in LX-2 cells as the curve shifted to the right with a Log EC_{50} of -8.7 ($1.6x10^{-9}$ M) but the fold window was greater at 2.6. The Vmax was reached between Log concentration -7 and -6 (100 nM- 1 μM) (figure 3.6.d).

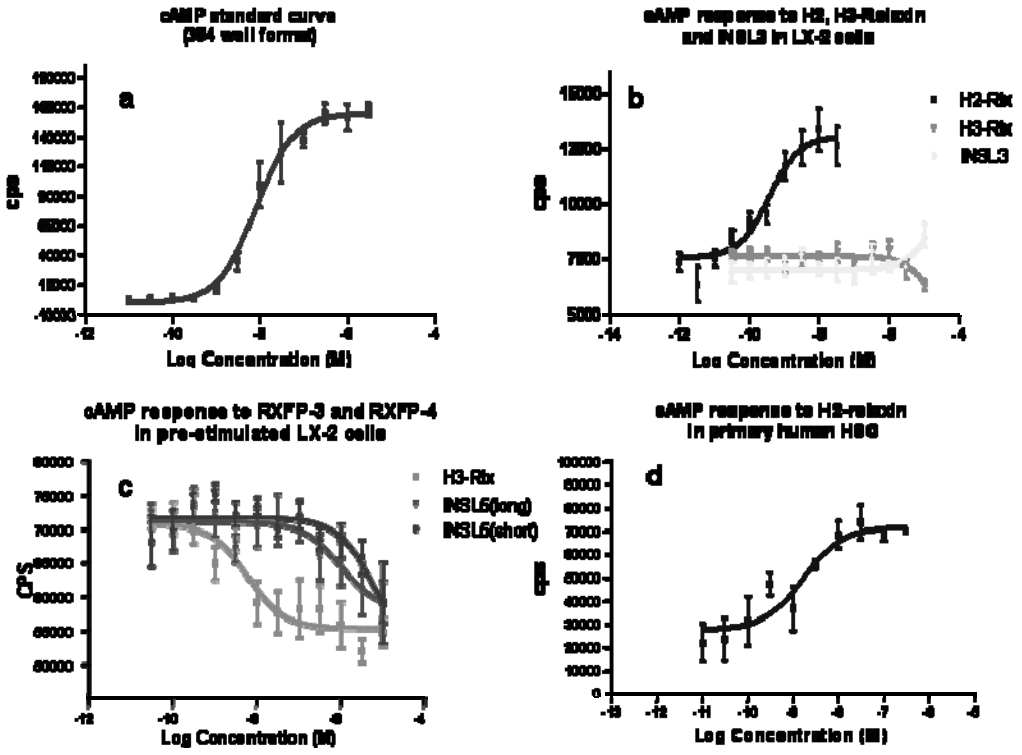

Figure 3.6. (a) cAMP standard curve in a 384-well plate format (n=4), all assays were designed around a 384-well plate format **(b)** Change in cAMP production in LX-2 cells

in response to stimulation with H2-rlx (n=11), H3-rlx (n=8) and INSL3 (n=8) for 90 minutes. LX-2 cells increase the intracellular production of cAMP in a dose dependent manner in response to H2-rlx with an EC_{50} of 363 pM. LX-2 cells do not increase their intracellular cAMP in response to H3-rlx and only respond to INSL3 at very high doses, which could represent cross reactivity at the RXFP-1 receptor **(c)** cAMP response of LX-2 cells when stimulated with H3-rlx (n=3), INSL5 (short chain) (n=3) and INSL5 (long chain) (n=3) for 90 minutes after a 10 minute pre-stimulation with forskolin. H3-rlx decreased the intracellular production of cAMP in a dose dependent manner in LX-2 with an EC_{50} of 6.016 nM. The long and short chain of INSL5 reduced the production of cAMP in a dose dependent manner in LX-2 cells with an EC_{50} of 961.5 nM and 6.16 μM respectively, revealing the full length chain of INSL5 is required for normal signalling at the RXFP-4 receptor **(d)** Change in cAMP production in hHSC in response to stimulation with H2-rlx (n=6) for 90 minutes. hHSC increase the intracellular production of cAMP in a dose dependent manner in response to H2-rlx with an EC_{50} of 1.67 nM.

3.5 *In vitro* model comparing expression of RXFP-1 and several fibrotic markers in activated *vs* quiescent HSC

Human HSC were isolated and plated, 1 million cells per 75 cm flask. The cells were grown on plastic for seven days before they were trypsinised and re-plated at the same density on plastic or a Matrigel 3D matrix (1 million cells per 100 mm culture dish). Cells were then cultured for 14 days and morphology was observed. The cells grown on the 3D Matrigel matrix did not appear to become confluent whilst in the same time scale the cells grown on plastic continued to proliferate and became confluent (figure 3.7a). There were also morphological differences clearly evident between the two populations of cells. The HSC plated on plastic remained proliferative and myofibroblast in appearance. The cells plated on Matrigel remained as individual cells that did not appear to proliferate and grew spindle like projections to neighbouring cells (figure 3.7a). The cells were analysed for expression of fibrotic markers after 14 days of culture. Procollagen-1 and TIMP-1 mRNA were both reduced in cells grown on

Matrigel although the procollagen-1 mRNA was reduced by a greater extent (figure 3.7b). Interestingly RXFP-1 mRNA expression was considerably reduced in cells grown on Matrigel (figure 3.7b). MMP-1 mRNA expression increases in cells grown on Matrigel but not to the extent that MMP-2 expression was up regulated (figure 3.7c). TIMP-1 and α-SMA protein expression were both appreciably reduced (figure 3.6c) whilst pro-MMP-2 (72 kDa band) protein expression was to some extent upregulated in the cells grown on Matrigel, the cleaved/active form of the protein (68 kDa band) had been substantially up regulated and could now be detected on the blot (figure 3.7c). Pro-MMP-1 (53 kDa band) protein expression and the cleaved/active form (51 kd band) were both up regulated in cells grown on Matrigel (figure 3.7c).

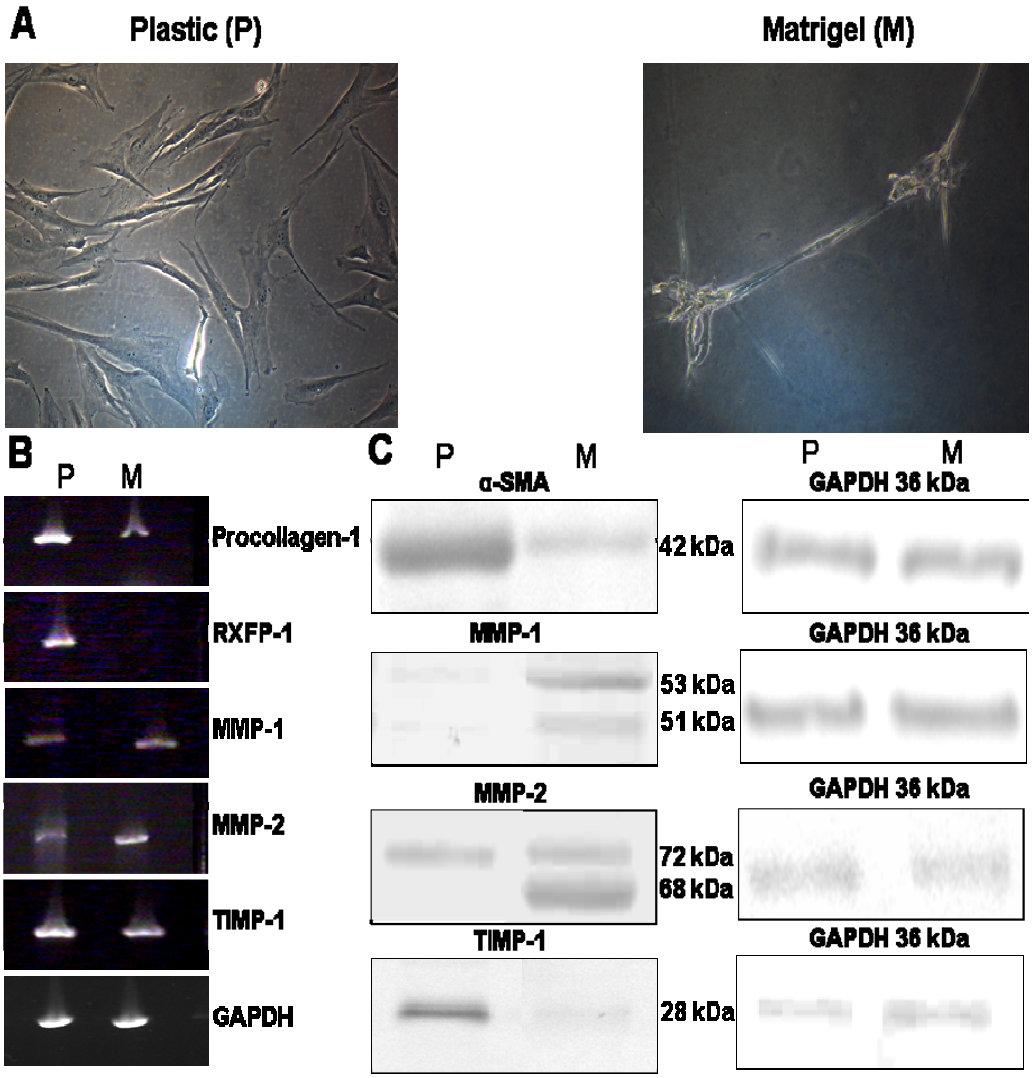

Figure 3.7. (A) Representative phase contrast images of p1 hHSC after 14 days culture on plastic (P) or growth factor reduced Matrigel basement membrane (M). Primary HSC cultured on plastic are activated myofibroblasts compared to cells cultured on Matrigel which lose their ability to proliferate and appear to revert to a more quiescent phenotype (n=3). **(B)** Expression of fibrotic markers and RXFP-1, assessed by RT-PCR, in p1 hHSC after 14 days culture on plastic or Matrigel. Fibrotic markers such as procollagen-1 and TIMP-1 are reduced after culture on Matrigel whereas MMP-1 and MMP-2 expression is increased. The most significant finding was the almost complete loss of RXFP-1 expression in HSC cultured on Matrigel, suggesting non-activated HSC do not express RXFP-1 (n=3). **(C)** Expression of fibrotic markers, assessed by western blotting, in p1 hHSC after 14 days culture on plastic or Matrigel. Fibrotic markers a-

SMA and TIMP-1 expression where reduced in HSC after culture on Matrigel whereas the expression of immature (53 kDa) and mature (51 kDa) forms of MMP-1 was increased as well as the expression of the mature form (68 kDa) of MMP-2.

3.6 Summary of key findings

- RXFP-1,3 and 4 were expressed by activated primary human HSC and LX-2 cells, assessed by RT-PCR.
- RXFP-1 was localised in cultured HSC by immuncytochemistry.
- RXFP-1 is localised to areas of scarring in the human liver.
- LX-2 and HSC respond to H2-relaxin by activating the accumulation of cAMP in a dose dependent manner. Pre-stimulated LX-2 cells can respond to H3-relaxin and INSL5 by inhibiting the accumulation of cAMP in the cell in a dose dependent manner.
- HSC grown on Matrigel lose expression of RXFP-1 mRNA concomitant with decreased detection of mRNA for procollagen-1 and reduction in mRNA and protein for TIMP-1, whilst showing increased amounts of MMP-1 and 2 mRNA and protein.

3.7 Discussion

Relaxin receptor expression in activated human HSC and LX-2 cells has been confirmed. Receptors RXFP-1, 3 and 4 are expressed in both LX-2 and primary HSC and the ligands H2-relaxin, H3-relaxin and INSL5 also have a low level of expression in HSC, potentially facilitating autocrine activation of the receptors. RXFP-1 is localised in areas of scarring in the human liver but is also expressed in hepatocytes. Relaxin has various signalling mechanisms that are cell and tissue dependent (Bathgate et al., 2005). Relaxin may activate different signalling pathways which can up or down regulate various genes such as TIMP-1 and MMP-1 which are critical not only in HSC survival but also fibrotic mechanisms (Murphy et al., 2002;Iredale et al., 1992). Relaxin has been found

to up regulate metastatic invasiveness of some forms of cancers, particularly breast and prostate cancer. This may be due to the up regulation of MMPs (Binder et al., 2002;Feng et al., 2007). Cells extracted from hepatocellular carcinoma (HCC) tissue did not express RXFP-1, therefore suggesting relaxin would not act directly on HCCs. RXFP-1 expression in HSC appears to be activation dependent. The expression of RXFP-1 correlated with the level of activation evaluated through α-SMA protein expression. This suggests that relaxin receptors may have an important role in activated HSC. This role may be speculated upon but H2-relaxin may contribute to the regulation of stellate cells in an anti-fibrotic, negative feedback capacity by activating RXFP-1. The phenotype of HSC in response to H2-relaxin will be investigated in chapter 4. HSC become activated and lay down extracellular matrix in the normal course of repair in the liver. This process only becomes pathogenic when the injury and inflammation becomes chronic (Iredale et al., 1998). Therefore the HSC in a normal liver will need to become activated whilst repair is taking place and then either revert to a quiescent phenotype or undergo apoptosis once the injury has ceased and the normal liver architecture has been restored. The process of recovery has been described by (Iredale et al., 1998) in an *in vivo* model of liver fibrosis. It has been described that vasoactive mediators such as relaxin, vasopressin, angiotensin II and endothelin-1 can contribute to HSC regulation (Rockey and Weisiger, 1996;Reynaert et al., 2002;Wilson and Summerlee, 1994;Morales et al., 2003). Vasoconstrictor substances such as vasopressin and angiotensin II have a mitogenic affect on HSC promoting activation and proliferation through G-protein coupled signalling (Lo et al., 2008). Vasodilator substances such as prostaglandin E2 and nitric oxide have been reported to act as anti-mitogenic factors reducing the proliferation of HSC (Goss et al., 1992b;Goss et al., 1992a). Growth factors that promote HSC proliferation such as PDGF require Ca^{2+} influx to exert their effects. Relaxin is a vasodilator substance that has been purported to not only inhibit uterine muscle contraction but inhibit the release of vasopressin and oxytocin (both vasoconstrictor substances), therefore inhibiting the release of intracellular calcium and increase

nitric oxide release through G-protein coupled signalling mechanisms (Dayanithi et al., 1987;Nistri and Bani, 2003). As a potential regulator of fibrosis relaxin may promote the reversion of activated HSC to a quiescent phenotype or advance the cell into apoptosis. H2-relaxin is also expressed by activated HSC which may suggest an autocrine negative feedback regulation of activated HSC. Regultation of HSC may also be through a paracrine mechanism if H2-relaxin was expressed by hepatocytes or by an endocrine mechanism through activation of RXFP-1 by circulating H2-relaxin. It is also reported that marcophages typically THP-1 cells express relaxin receptors. H2-relaxin induces an anti-inflammatory and antifibrotic gene expression profile in THP-1 cells (Dschietzig et al., 2004;Ho et al., 2007).

The Matrigel *in vitro* model used to compare activated with deactivated stellate cells had been previously described by Benyon and colleagues (Gaca et al., 2003). In the previous study Matrigel was used as a matrix to grow rat hepatic stellate cells that had been grown on plastic to activate directly after isolation and then re-plated on either plastic, Matrigel or collagen-1 coated plastic. Matrigel is a basement membrane like substance that contains laminin, collagen-IV, entacin and heparin sulphate proteglycan and can be used as an *in vitro* 3-dimensional matrix for cell attachment that is more similar to a normal liver basement membrane *in vivo* (Gaca et al., 2003). The expression of fibrotic markers such as α-SMA, procollagen-1 and TIMP-1 were compared for all three types of matrix. The results from Benyon and colleagues showed that cells grown on Matrigel, even though they were fully activated at the time of plating were able to revert to a more quiescent phenotype, losing their expression of α-SMA, procollagen-1 and TIMP-1, reducing their proliferation and also becoming fluorescent under UV light, suggesting the cells have regained their vitamin A storage capacity (Gaca et al., 2003;Friedman et al., 1993). In this study the same model was used, plating activated human HSC on a growth factor reduced Matrigel (GFR Matrigel) matrix or plastic (the collagen-1 matrix was not used in this study). The results obtained were very similar to the previous study (Gaca

et al., 2003). Culturing HSC on Matrigel induced a reduction or loss of profibrogenic markers including procollagen-1, α-SMA and TIMP-1, whilst MMP-1 and MMP-2 expression was increased. Interestingly this correlated with loss of RXFP-1, suggesting the balance was shifted to a less fibrogenic phenotype as the activity of the main interstitial collagenase (MMP-1) was up regulated and its inhibitor TIMP-1 expression was reduced and this would favour fibril collagen degradation (Iredale et al., 1996;Iredale et al., 1998). MMP-2 expression and activation was also increased, this could be due to the nature of the cells grown on a surface that consists of large amounts of collagen IV as MMP-2 is a type IV collagenase but can also degrade collagen V, VII, X, fibronectin, laminin and elastin and denatured collagen 1 (Hemmann et al., 2007). Certain cell types are dependent upon contact with one another for survival (Jung et al., 2005), HSC grown on different matrix have been shown to have various phenotypes (Priya and Sudhakaran, 2008) and certain studies have shown activated HSC to have invasive/migratory properties (Wang et al., 2005). HSC activation and survival is dependent upon autocrine and paracrine factors released such as TGF-β, which have a greater effect when in contact with one another (Gressner and Bachem, 1990). Therefore I propose HSC grown on matrigel may up regulate MMP-2 to be able to migrate through the gel to be able to come into contact with one another. HSC would have to degrade the collagen IV matrix and therefore might increase their expression of MMP-2 to facilitate this process. RXFP-1 expression was increased in activated HSC and was localised in areas of scarring. The cells grown on Matrigel display a less fibrogenic phenotype and lose their expression of RXFP-1. This model taken together with the expression of RXFP-1 increasing in parallel with the level of activation of HSC provides further evidence that relaxin signalling through RXFP-1 could have a vital role in regulating the fibrogenic phenotype and activation of HSC. The question is, does H2-relaxin increase the fibrotic phenotype and activation or does it reduce the expression of these parameters?

To be able to determine the properties of H2-relaxin in HSC the confirmation of active signalling needed to be established. HSC and LX-2 cells exhibited a dose dependent increase in cAMP in the presence of H2-relaxin. The concentration of H2-relaxin required to reach the EC_{50} (50% maximal response) and maximal response (Vmax) was higher in HSC then LX-2 cells. The relative expression of RXFP-1 at the membrane in LX-2 cells may have been higher as LX-2 cells are an engineered HSC cell line that exists in the activated state (Xu et al., 2005). cAMP assays showed LX-2 cells also expressed active receptors for H3-relaxin (RXFP-3) (Liu et al., 2003) and INSL5 (RXFP-4) (Liu et al., 2005b). RXFP-3 and RXFP-4 are negatively coupled to cAMP and treatment with H3-relaxin and INSL5, their respective ligands, in pre-stimulated LX-2 revealed a dose dependent inhibition of cAMP accumulation. H3-relaxin was also applied to non stimulated LX-2 cells to test for cross reactivity at the RXFP-1 receptor. There was no reaction until the highest dose when the cAMP signal decreased. This would not have been due to cross-reactivity with RXFP-1, as activation of this receptor should induce an increase in cAMP (Bathgate et al., 2005). The decrease in cAMP observed may have been due to the activation of the RXFP-3 receptor and even though the cells were not pre-stimulated with forskolin the inhibition of adenylate cyclase was enough to reduce the concentration of cAMP below the baseline. H3-relaxin was more potent then INSL5 in pre-stimulated LX-2 cells. This may be due to less RXFP-4 receptors being expressed in LX-2 cells or just the normal pharmacodynamics of each receptor in response to their respective ligands. An INSL3 dose curve was performed in LX-2 cells. There was no response to the ligand until the highest dose. PCR had shown that activated HSC expressed a very low level of RXFP-2, which could explain the small response at the highest dose was due to the activation of the RXFP-2 receptor (Sudo et al., 2003). The concentration of ligand to induce a maximal response at the RXFP-1 receptor in both HSC and LX-2 cells has now been quantified. H2-relaxin can now be applied to the cells to determine any phenotypic changes in HSC that may indicate relaxin can regulate activated HSC.

Chapter 4

H2-relaxin reduces the expression of pro-fibrotic markers and the cellular contractility of human hepatic stellate cells

4.1 Introduction

4.1.1 Introduction

Human hepatic stellate cells (hHSC) plated on plastic differentiate into a myofibroblast like cell. The process under which the cells change their phenotype is called activation and will occur spontaneously if the cells are plated on either a plastic or collagen-1 matrix (Friedman et al., 1992). The process of activation has been documented in rat hepatic stellate cells. These cells were found to be the major source of collagen, α-SMA, TIMPs and MMPs in the injured liver (Friedman et al., 1985;Rockey et al., 1992;Arthur et al., 1989). This process requires the presence of growth factors and cytokines such as PDGF and TGF-β, which HSC express and utilize in an autocrine manner (Pinzani et al., 1989). The cells up regulate their expression of TIMPs, proinflammatory and profibrogenic cytokines and growth factors such as IL-1, TGF-β and begin to express α-SMA. LX-2 cells are a human stellate cell line that express TIMPs, MMPs and α-SMA (Xu et al., 2005). They have already undergone the activation process and can be passaged up to 50 times. TIMP-1 expression is lower in LX-2 cells than in freshly isolated activated primary hHSC but LX-2 cells are still considered to be a good model to study possible antifibrotic therapies. LX-2 cells were used to optimise the experiment before using primary hHSC in the cell based *in vitro* assays described in this chapter. The expression of fibrotic markers such as TIMP-1, α-SMA, MMP-1, MMP-2 and TGF-β were used to evaluate any phenotypic changes in response to H2-relaxin and PARP-1 cleavage was used to detect any increase or decrease in apoptosis. Cytokine arrays were carried out to detect any regulation of inflammatory or fibrotic cytokines by H2-relaxin in HSC. Previous studies in rat HSC have shown relaxin to have antifibrotic properties (Bennett et al., 2003).

A gel contraction assay was designed to study the contractile properties of hHSC. The mechanisms of contraction in HSC have been investigated through

the use of vasoactive substances such as endothelin-1 and vasopressin (Housset et al., 1995;Housset et al., 1993;Bataller et al., 1997). Endothelin-1 is a potent vasoconstrictor when acting through the endothelin A receptor (ET_A). Endothelin B receptors (ET_B) have been found to induce an up-regulation of nitric oxide (NO) and therefore relaxation of the cell/tissue in which the receptors are found. It has been documented that endothelin-1 is released in the fibrotic liver inducing contraction of the stellate cell and other structures which can exacerbate the injury and cause complications such as portal hypertension observed in the cirrhotic liver (Zhang et al., 1994;Pinzani et al., 1996). It is possible that RXFP-1 not only activates NO synthesis through its own second messenger systems but may also induce an up-regulation in ET_B expression, favouring relaxation over contraction in HSC.

4.1.2 Hypothesis, Aims and Objectives

Hypothesis

H2-relaxin promotes an antifibrotic phenotype in cultured LX-2 and primary HSC *in vitro.*

Aims

To treat LX-2 and primary HSC with H2-relaxin and test the effect on the expression of markers of fibrosis, expression of inflammatory cytokines and the ability to contract collagen gels.

Objectives

- Assess changes in gene expression of markers of fibrosis in hHSC after H2-relaxin treatment.
- Determine the change in protein expression of markers of fibrosis and apoptosis in hHSC after H2-relaxin treatment.
- Observe any changes in cytokine profile in hHSC after H2-relaxin treatment, particularly fibrosis and inflammatory related cytokines.

- Identify a change in hHSC contractility after H2-relaxin treatment in gel contraction assays.

4.2 Results - Evaluation of the phenotypic changes in LX-2 cells and primary HSC induced by treatment with H2-Relaxin

4.2.1 H2-relaxin treatment of LX-2 cells, phenotypic changes observed in gene expression

Primary HSC and LX-2 cells are both able to respond to H2-Relaxin by increasing the level of cAMP in the cell, as described in chapter 3. The response to H2-relaxin is believed to be through the RXFP-1 receptor. The downstream phenotypic effects of activating RXFP-1 in human HSC were unknown. A simple assay was devised, allowing endpoint measurements using immunoblotting and PCR to evaluate the expression of fibrotic markers. LX-2 cells were used in the initial assays to determine the effective dose of H2-relaxin and the time point at which a significant phenotypic change may be observed. A time course study was set up using LX-2 cells to detect gene expression changes after 1, 2, 4, 6, 24, 48 and 72 hours H2-relaxin treatment. No significant changes were detected throughout the time course until the 48 and 72 hour time point, when the greatest changes in gene expression were detected, which was confirmed by observing protein expression changes at 48 and 72 hours (figure 4.2). LX-2 cells respond to H2-relaxin after 72 hours continuous exposure, by reducing the gene expression of MMP-2, RXFP-1, TIMP-1 and procollagen-1 (figure 4.1). MMP-2 is decreased by 20% in response to 1 μM H2-relaxin. RXFP-1 expression is reduced by 40% in response to 10 nM H2-relaxin but expression does not change from control levels of expression after treatment with 1 μM H2-relaxin. Procollagen-1 expression is reduced by 10% by 1 μM H2-relaxin but is unchanged in cells treated with 10 nM H2-relaxin. TIMP-1 expression decreased by 20% in the 10 nM treated cells but only by 10% in the 1 μM H2-relaxin treated cells. None of the gene expression changes observed in

LX-2 cells were significant and the changes observed were not dose dependent. Similar results regarding dosing had been observed in a clinical trial using H2-relaxin to treat scleroderma. The response rates were more significant in patients not receiving the maximum dose, therefore giving bell shaped response curves (Seibold et al., 2000).

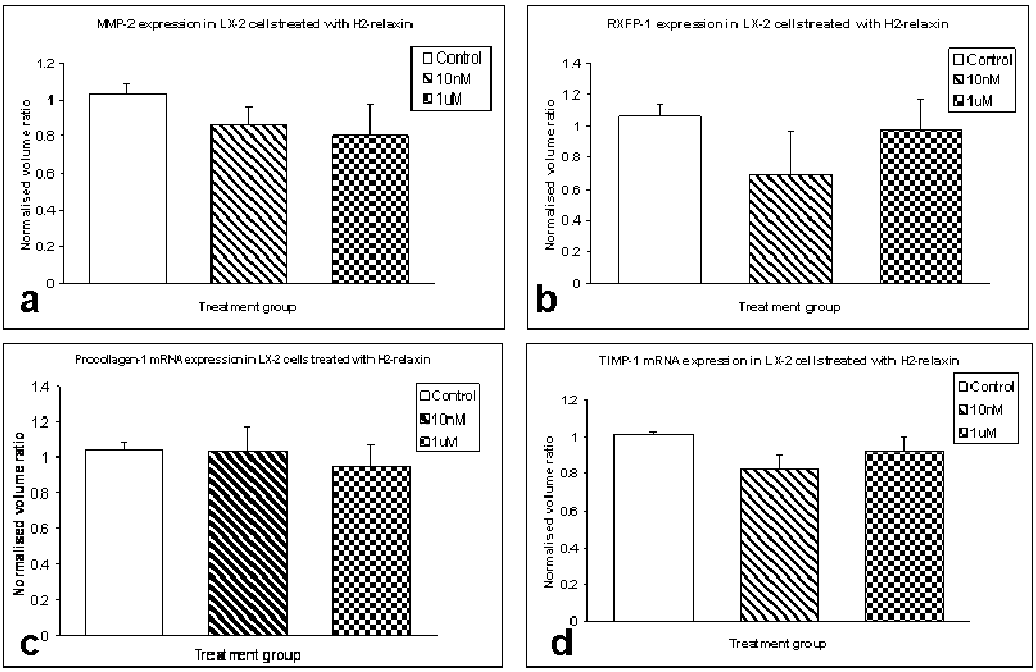

Figure 4.1. (a) MMP-2, (b) RXFP-1, (c) procollagen-1 and (d) TIMP-1 mRNA expression in LX-2 cells that had been treated with 10 nM and 1 μM of H2-Rlx for 72 hours (n=3), assessed by RT-PCR. 10nM H2-rlx reduces the expression of RXFP-1 after 72 hours but the trend is not continued with the 1 μM dose. Results are not significant ($p>0.1$).

4.2.2 H2-relaxin treatment of LX-2 cells, phenotypic changes observed in protein expression levels

α-SMA and PARP-1 protein expression in LX-2 cells were semi-quantified using immunoblotting. α-SMA protein expression appeared unchanged after 48 hours of H2-relaxin treatment but was significantly reduced by 40% after 72

hours of 1 μM H2-relaxin treatment (figure 4.2a). Therefore H2-relaxin requires 72 hours before gene and protein expression changes can be observed. Both doses will be used to repeat the experiment in HSC but the experiment will be carried out over 72 hours rather then 48 hours. The protein expression of PARP-1 was determined after 72 hours H2-relaxin treatment (figure 4.2b). The antibody used detected both cleaved and uncleaved PARP-1. Cleaved PARP-1 is a marker of apoptosis and therefore the ratio of cleaved to uncleaved PARP-1 can indicate an increase in apoptosis. Uncleaved PARP-1 protein expression can increase in cells that are under stress conditions, this is a mechanism to prevent cell death through apoptosis. LX-2 cells had increased expression of cleaved PARP-1 but uncleaved PARP-1 was also increased and therefore the ratio of cleaved to uncleaved did not indicate an increase in apoptosis.

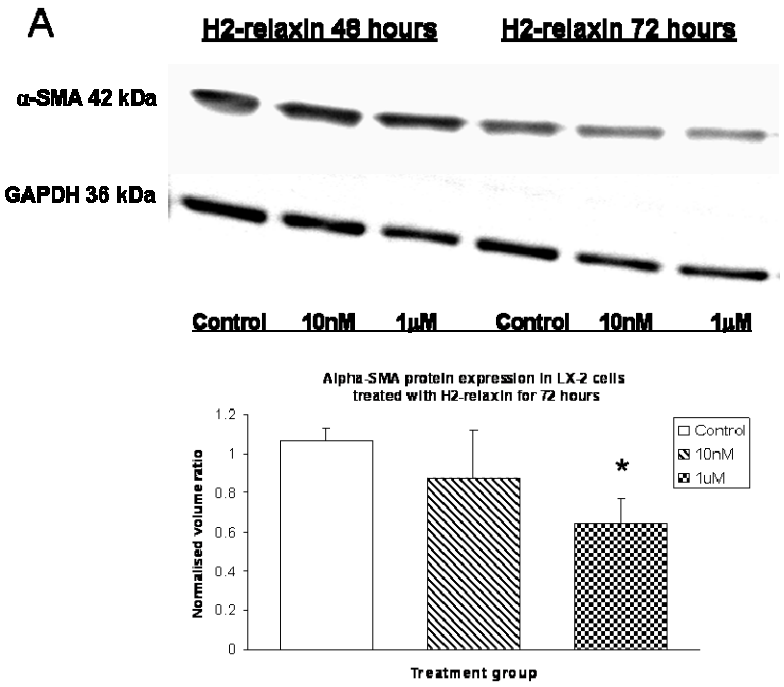

Figure 4.2. (A) α-SMA protein expression in LX-2 cells that had been treated with 10 nM and 1 μM H2-Rlx for 48 and 72 hours (n=3), assessed by western blotting. α-SMA protein is unchanged after 48 hours but is significantly reduced after 72 hours 1 μM H2-relaxin treatment ($p<0.05$).

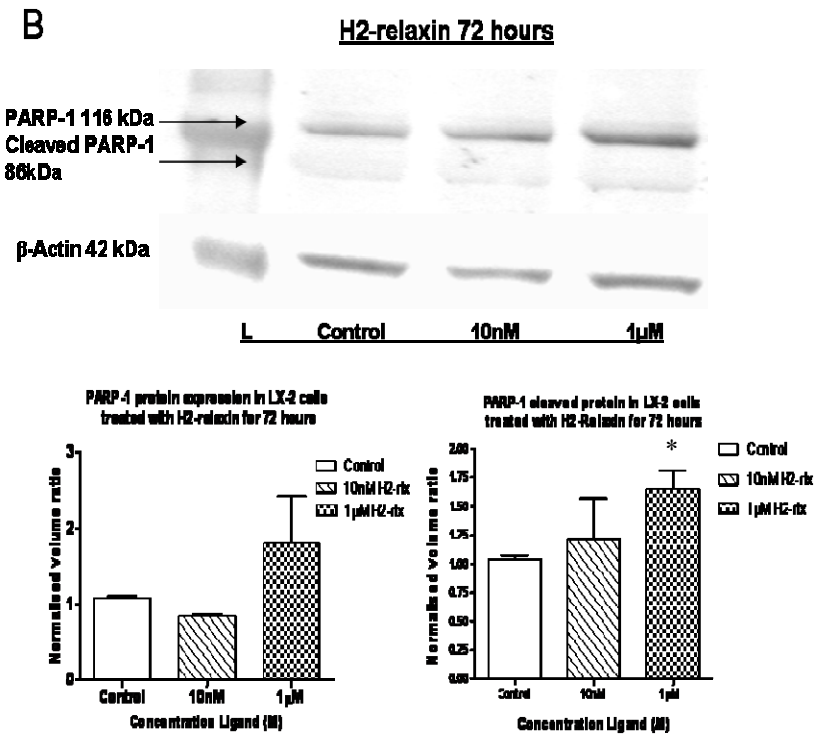

Figure 4.2. (B) PARP-1 and PARP-1 cleavage protein expression in LX-2 cells that had been treated with 10 nM and 1 μM H2-Rlx for 72 hours (n=3). PARP-1 expression increased in a similar ratio to the cleaved PARP-1 band, which had been significantly induced by 1 μM H2-relaxin ($p<0.05$) and therefore there was no evidence of increased apoptosis.

4.2.3 H2-relaxin treatment of HSC, phenotypic changes observed in mRNA expression levels

Primary human HSC were used to continue the study as these may be a more representative model, RT-PCR and qRT-PCR were used to quantify gene expression changes. The same dosing schedule was repeated in primary HSC as the responses did not appear to be dose dependent in LX-2 cells, although RNA and protein was extracted only at the 72 hour time point. Primary HSC responded to H2-relaxin with significant changes in MMP-1 and RXFP-1 expression, quantified by RT-PCR (figure 4.3). MMP-1 expression was significantly increased by over 2 fold after 72 hours H2-relaxin treatment (figure

4.3ii) and RXFP-1 expression was significantly decreased by 72 hours 10 nM and 1 μM H2-relaxin treatment (figure 4.3v). Other changes observed such as a decrease in TIMP-1 and procollagen-1 and an increase in MMP-2 expression were not significant when quantified by RT-PCR. The increase in MMP-2 expression was different from the results observed in LX-2 cells, where a small decrease in MMP-2 expression was observed. Li90 cells, another HSC cell line, also responded to H2-relaxin showing a dose dependent decrease in TIMP-1 expression and a dose dependent increase in MMP-2 (appendix 1). The results are an n=1 and are therefore used to reinforce the similar observations in primary HSC, which are contradictory regarding MMP-2 in the LX-2 cell line. A more sensitive technique was required to detect any subtle changes after H2-relaxin treatment and therefore qRT-PCR was used to confirm the results in primary HSC.

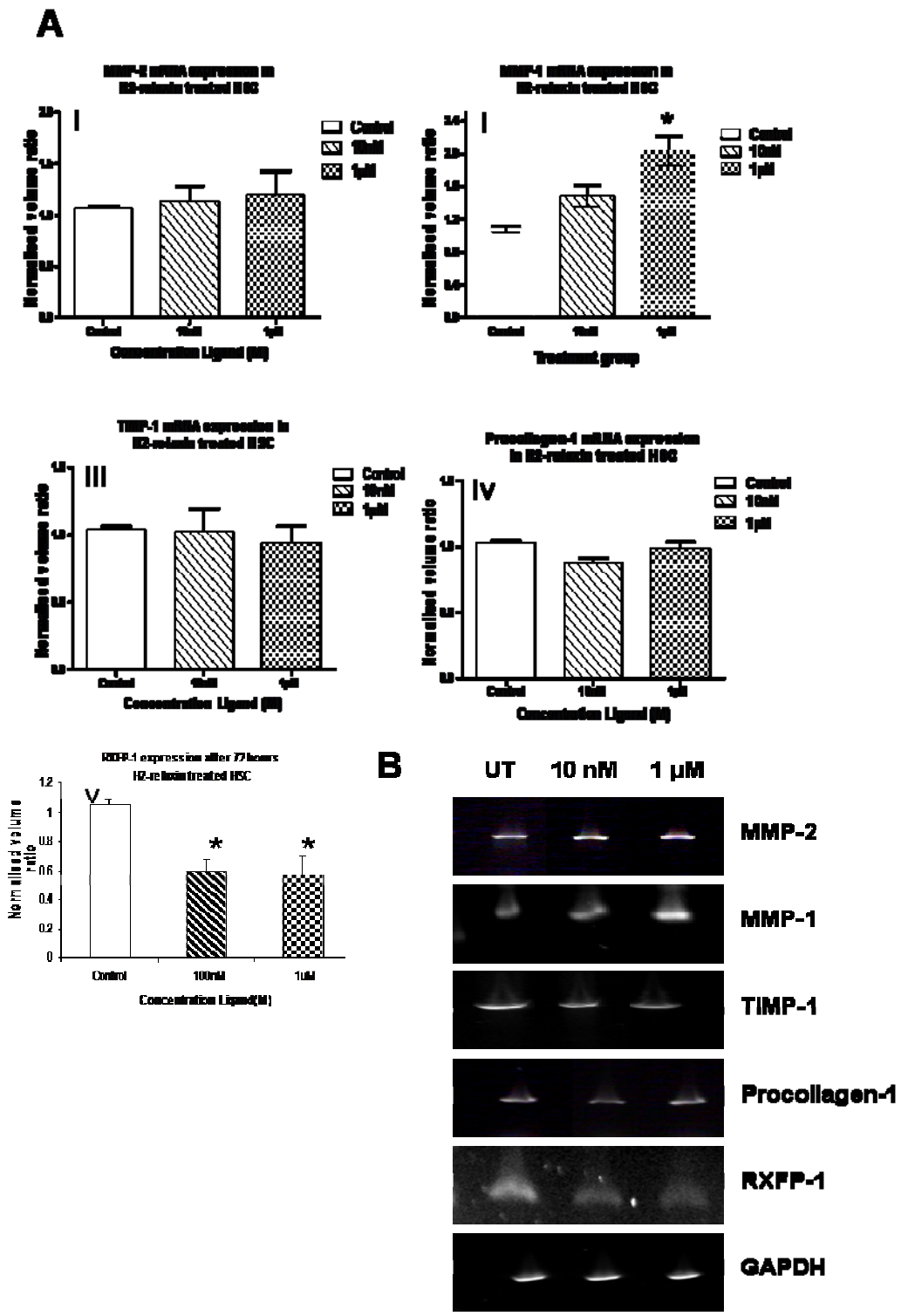

Figure 4.3. (A) Expression of fibrotic markers (i) MMP-2, (ii) MMP-1, (iii) TIMP-1, (iv) procollagen-1 and (v) RXFP-1 after 72 hours H2-relaxin treatment of primary human HSC, assessed by RT-PCR (n=3). MMP-1 expression was significantly

increased by 1 μM H2-relaxin $p<0.05$. RXFP-1 expression was significantly reduced by both 10 nM and 1 μM H2-relaxin $p<0.05$. MMP-2, TIMP-1 and procollagen-1 were not significantly different although TIMP-1 and procllagen-1 both showed a trend to decrease after 1 μM H2-relaxin treatment and MMP-2 expression showed a trend to increase. **(B)** Representative images of RT-PCR products used to semi-quantify the expression changes (n=3).

Quantitative PCR was used to confirm the mRNA changes observed in primary HSC after 72 hours H2-relaxin treatment. Several additional genes were quantified including α–SMA, TGF-β, and CTGF, which are all markers of HSC activation and fibrogenesis. The initial experiment confirmed the differential expression of the fibrotic markers in primary HSC activated by culture on plastic (figure 4.4a). Procollagen-1 had the greatest expression in activated HSC, which was over 3 fold greater then TIMP-1 and α-SMA. TIMP-1 was also nearly 3 fold greater then α-SMA expression. Procollagen-1, TIMP-1 and α-SMA are all profibrotic genes which are up-regulated in activated HSC. Surprisingly CTGF expression, although not significantly, was greater then TGF-β expression which are both up-regulated in activated HSC. MMP-2 expression was greater then MMP-1 and TGF-β. MMP-1 and TGF-β had the lowest levels of expression but all of these genes were expressed to a greater extent compared to RXFP-1. After establishing the normal level of gene expression in activated HSC the expression levels were measured after 72 hours 1 μM H2-relaxin treatment (figure 4.4c). Results are expressed as fold changes compared to untreated activated HSC. H2-relaxin induces a significant decrease in gene expression of α-SMA (30%), TGF-β (38%), CTGF (28%) and TIMP-1 (28%) in activated HSC. Procollagen-1 expression decreased by over 10% but the result was not significant. The greatest change was the reduction in TGF- β expression, which was reduced by 38%. MMP-1 expression was significantly increased by 79% compared to untreated HSC, whilst MMP-2 expression increased by 35% but this increase was not significant due to different responses observed in different primary cell cultures.

A

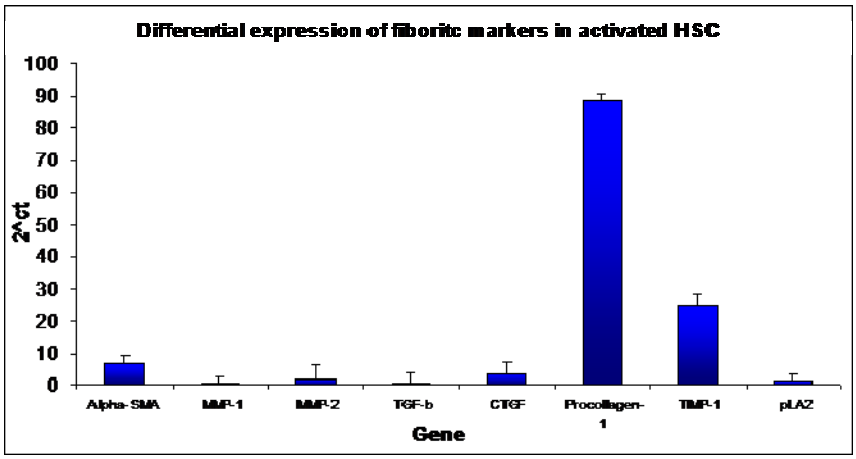

B

1	2	3
α-SMA	Unknown 1 15.4	Unknown 1 15.1
TGF-β	Unknown 2 20.3	Unknown 2 20.1
CTGF	Unknown 3 13.9	Unknown 3 14.2
MMP-1	Unknown 4 17.9	Unknown 4 17.8
MMP-2	Unknown 5 16.2	Unknown 5 16.1
Procollagen-1	Unknown 6 11.7	Unknown 6 11.8
TIMP-1	Unknown 7 12.0	Unknown 7 12.4
pLA_2	Unknown 8 18.4	Unknown 8 17.0

C

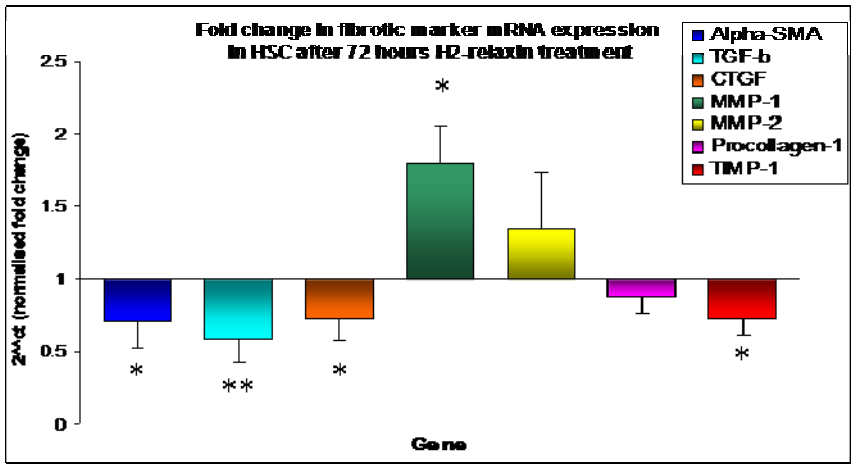

Figure 4.4. (A) Differential expression of fibrotic markers in human HSC, assessed by qRT-PCR (n=3), **(B)** including an example of raw data ct values (n=3). **(C)** Expression of fibrotic markers including TGF-β1 and CTGF after 72 hours 1 μM H2-relaxin treatment of primary HSC, assessed by qRT-PCR (n=3). α-SMA, CTGF, and TIMP-1 were significantly reduced after H2-relaxin treatment $p<0.05$ but the most significant

reduction was TGF-β1 $p<0.01$, which is a key profibrotic cytokine. MMP-1 was significantly increased after 72 hours H2-relaxin treatment ($p<0.05$) and MMP-2 was increased but not in all patients tested.

4.2.4 H2-relaxin treatment of HSC, phenotypic changes observed in protein expression

α-SMA and PARP-1 protein expression was assessed in H2-relaxin treated HSC compared to untreated controls. α-SMA protein expression was significantly reduced by over 50% after 72 hours in HSC treated with both 10 nM and 1 μM H2-relaxin (figure 4.5a). PARP-1 cleavage was assessed using immunoblotting as a measure of apoptosis (figure 4.5b). The ratio of PARP-1 to PARP-1 cleaved protein expression was significantly increased by over 30% in HSC treated with 1 μM H2-relaxin, suggesting H2-relaxin can induce apoptosis in primary HSC. To confirm these observations a cell viability assay was carried out (figure 4.5c). A significant decrease in cell viability was detected after 72 hours 1 μM H2-relaxin treatment in primary HSC. The assay used to detect cell viability was a measure of the number of live cells remaining. The results were normalised to untreated controls.

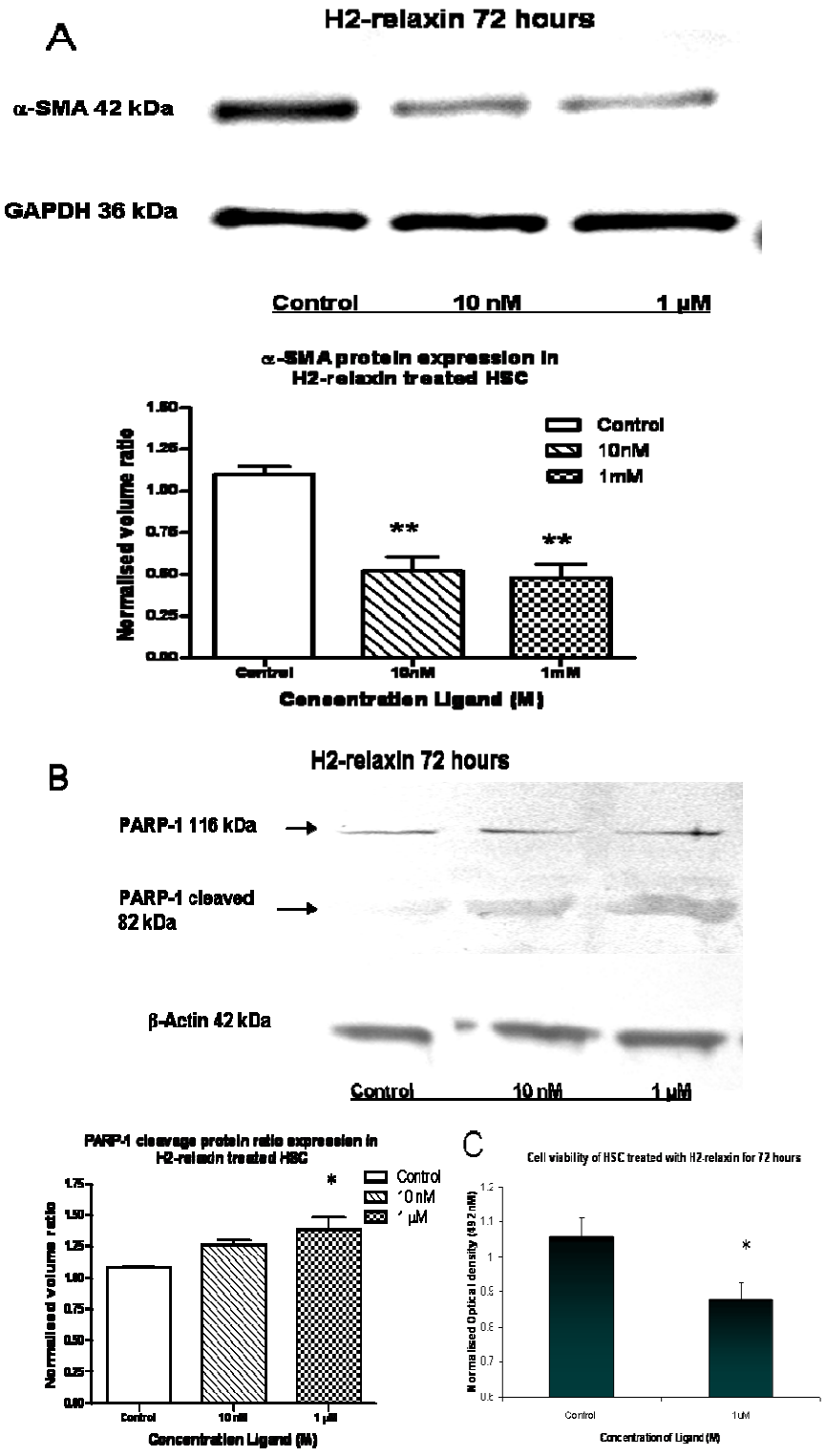

Figure 4.5. (A) α-SMA protein expression in primary human HSC treated for 72 hours with H2-relaxin, assessed by western blotting (n=3). Both 10 nM and 1 μM significantly reduced the expression of α-SMA by over 50% ($p<0.01$ confidence).

(B) PARP-1 and cleaved PARP-1 protein expression in primary human HSC treated for 72 hours with H2-relaxin, assessed by western blotting (n=3). The ratio of cleaved PARP-1 to PARP-1 expression was significantly increased by over 30% by 1 μM H2-relaxin ($p<0.05$). The increase in cleaved PARP-1 suggests that H2-relaxin increases the apoptosis of primary HSC. **(C)** Cell viability of primary human HSC after treatment with 1 μM H2-relaxin for 72 hours was assessed by MTS cell viability assay (n=3). There was a 20% decrease in the number of viable cells after H2-relaxin treatment ($p<0.1$ confidence).

4.3 Cytokine array profile of hHSC comparing H2-Relaxin treated with untreated control cells using cytokine antibody spotted membranes

4.3.1 Overview of all cytokines spotted on the membranes

Cytokine array membranes were used to evaluate the change in secreted cytokine level in H2-relaxin treated primary HSC (figure 4.6a). A single concentration of 100nM H2-relaxin was used to treat the cells and the conditioned media from 6 different primary cell cultures was used to run the cytokine array experiments. Two different membranes were used with many cytokines that are known to be secreted by HSC and several that have not been previously quantified in human HSC. The results are presented as fold changes compared to untreated controls, and each of the cytokines on individual membrane arrays were plotted on a single graph (figure 4.6b). The results are not significant due to variation between the primary cell cultures responses to H2-relaxin and the variability in cytokine levels in untreated controls. Therefore the results suggest a trend for H2-relaxin to down regulate many profibrotic cytokines such as TGF-β1, TIMP-1,2 and 4, PDGF, and FGF in primary HSC. There was also a trend for H2-relaxin to down regulate several pro-inflammatory cytokines such as IL-1 α, IL-2, IL-4, IL-6 and IL-13. H2-relaxin up regulated

several cytokines including Fas ligand, NT-4, VE-cadherin, and MMP-9 (figure 4.6b).

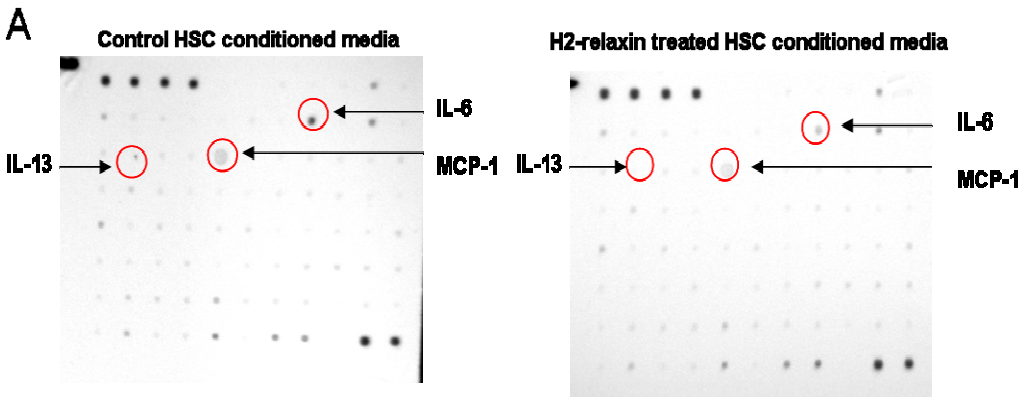

Figure 4.6. (A) Example of cytokine array membranes, including examples of spots that are down regulated in H2-relaxin treated HSC

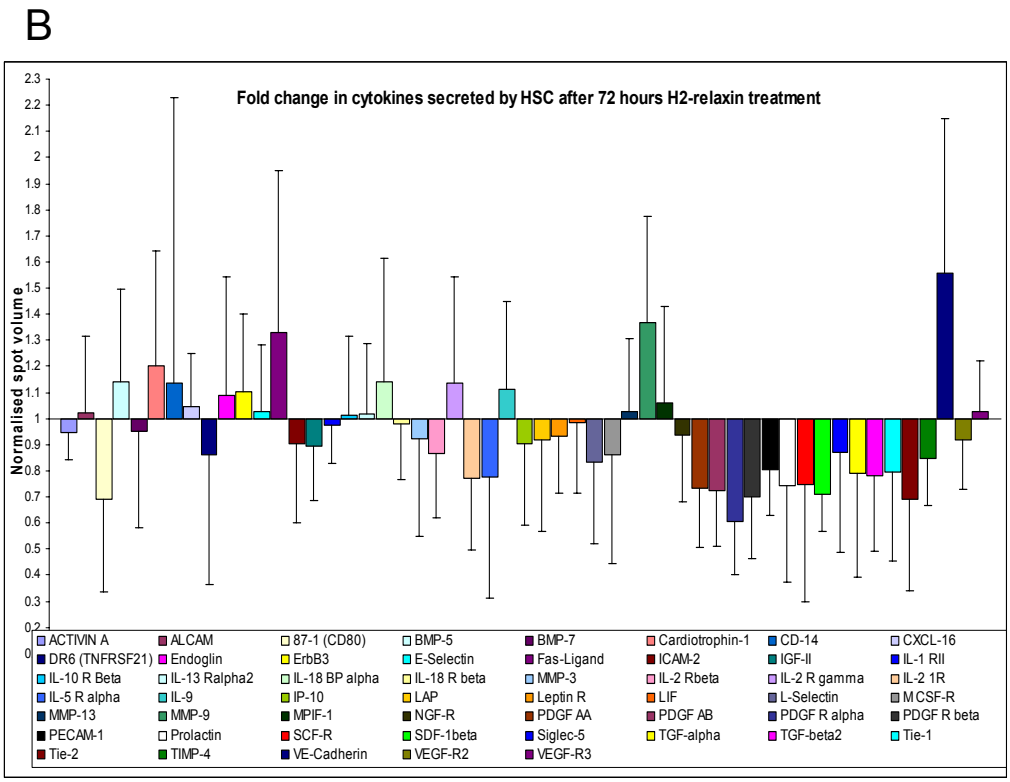

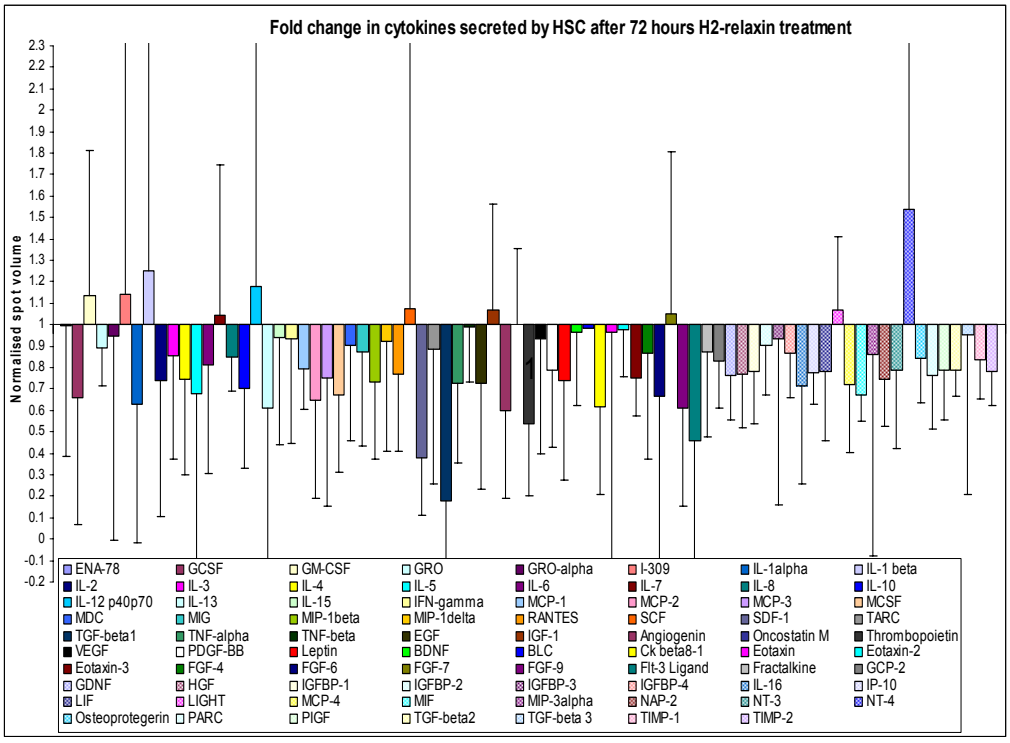

Figure 4.6. (B) Fold changes in cytokine secretion after 72 hours 100nM H2-relaxin treatment, compared to untreated HSC, (n=6). Cytokine array analysis of conditioned media reveals H2-relaxin could potentially regulate many different cytokines in primary HSC. The results obtained are not significant due to large inter-patient variability, but show a trend in the H2-relaxin treated cells to a less fibrogenic/inflammatory but pro-apoptotic phenotype.

4.3.2 Cytokines down regulated by H2-relaxin treatment

The membrane arrays contained several closely related cytokines. Fold changes in cytokines that were down regulated by more then 30%, or are a close member of the family of a down regulated cytokine, have been plotted on individual graphs (figure 4.7.a). TGF-β1 was down regulated by over 80% in H2-relaxin treated HSC, although the change was not significant due to the large variation in the level of TGF-β1 between different primary cell cultures (figure 4.7.a i). TGF-β2, TGF-α, Tie-1 and Tie-2 were also down regulated by H2-relaxin, the greatest change observed was Tie-2, with a 30% decrease (figure 4.7.a ii). SDF-

1 was down regulated by over 70% in H2-relaxin treated cells (figure 4.7.a iii) and SDF-1 beta was down regulated by over 30% (figure 4.7.a iv). FGF-4, FGF-6, FGF-9 and Flt-3 ligand are all down regulated by H2-relaxin, the greatest change was in Flt-3 ligand which was down regulated by over 50%. There was a small increase in FGF-7 in H2-relaxin treated HSC (figure 4.7.a v). TIMP-1, TIMP-2 and TIMP-4 were all down regulated by over 15% in H2-relaxin treated HSC (figure 4.7.a vi). The decrease in TIMP-1 secretion is similar to the decrease in mRNA expression observed in figure 4.4.b. PDGF AA, PDGF AB, PDGF R alpha, and PDGF R beta were all down regulated by H2-relaxin, the greatest change was PDGF R alpha which was down regulated by over 40% (figure 4.7.a vii). Overall the greatest change in cytokine secretion was the decrease in TGF-β1, therefore the level of TGF-β1 was quantified by ELISA assay. The same media samples were used to detect the changes in total and active TGF-β1 secreted from H2-relaxin treated HSC. The total TGF-β1 was reduced by over 10% whilst the active TGF-β1 was reduced by nearly 20% in H2-relaxin treated HSC (figure 4.7.b). The results had to be normalised to control values as the starting concentration of TGF-β1 in each sample was extremely varied (standard deviation was not shown), results are not significant. The decrease of TGF-β1 quantified by ELISA assay was not as great as the decrease observed in the cytokine array assay. This may have been due to freeze thawing of the media samples as TGF-β1 is susceptible to degradation, the results shown are from three experiments as not all of the conditioned media samples had detectable levels of TGF-β1.

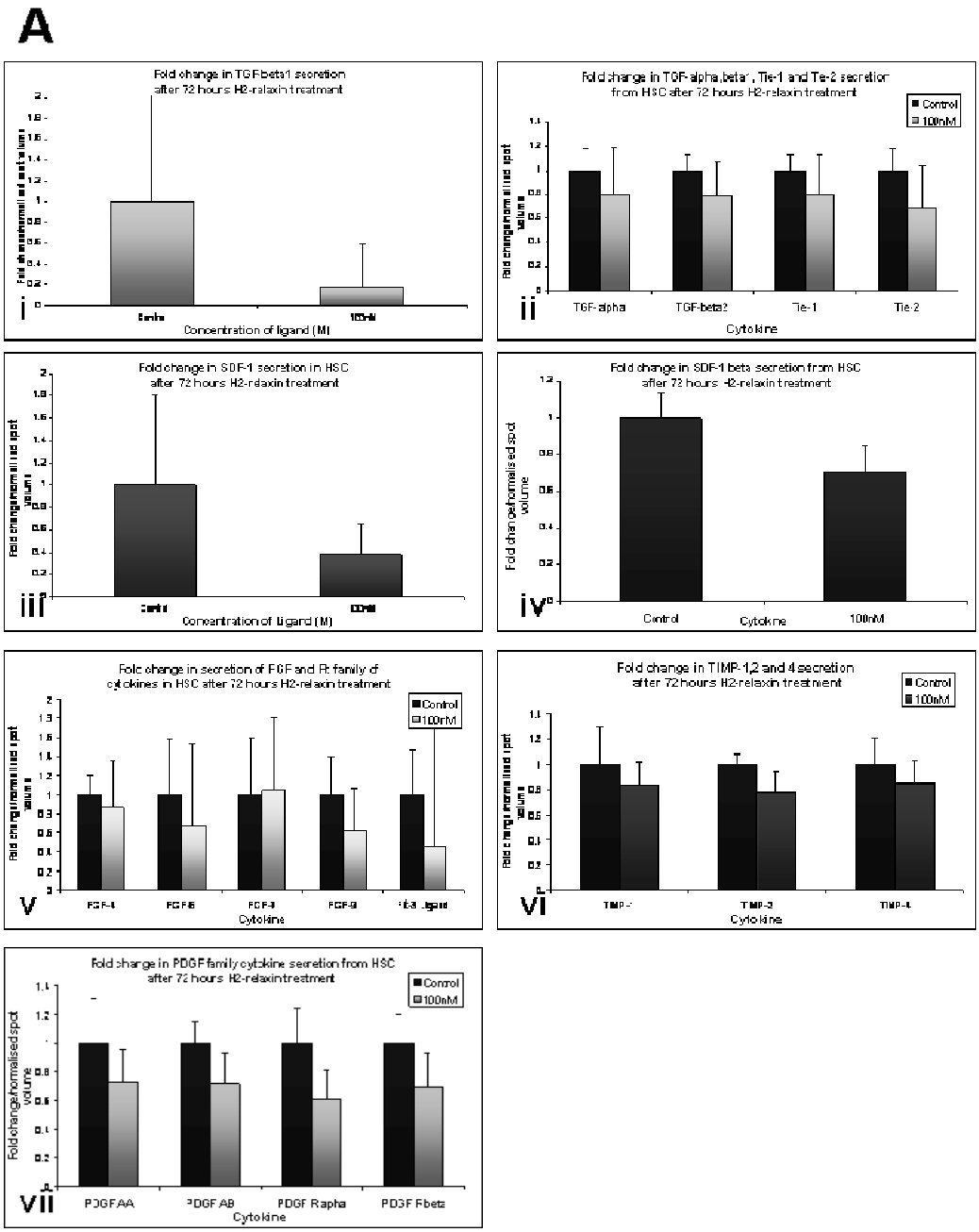

Figure 4.7. (A) Fold changes in cytokines that were down regulated, over 50% or were interesting fibrosis related cytokines, by 100 nM H2-relaxin after 72 hours (n=6). The interesting families of secreted proteins include **(i)** TGF-β, **(ii)** TGF-α, Tie-1, Tie-2, **(iii)** SDF-1, **(iv)** SDF-1 beta, **(v)** FGF family and Flt-3 ligand, **(vi)** TIMP-1,2 and 4, and **(vii)** PDGF family.

B

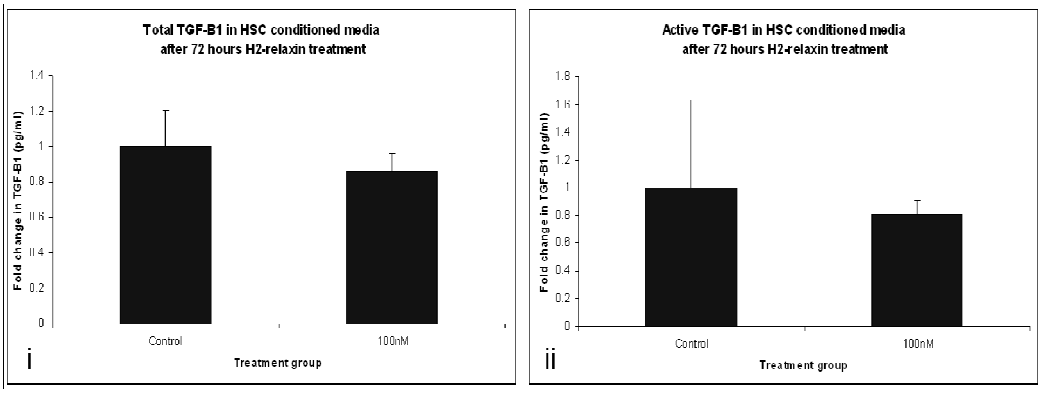

Figure 4.7. (B) The regulation of **(i)** total and **(ii)** active TGF-β1 by H2-relaxin was further investigated by ELISA analysis (n=3), using the same media samples as the cytokine array. H2-relaxin down regulated active TGF-β1 by 20%. Results were normalized to the control samples, error bars were added to the controls and due to the varied concentration of TGF-β1 in the conditioned media between different patients the error bars are large, which is similar to the result in the cytokine arrays.

4.3.3 Cytokines up-regulated by H2-relaxin treatment

The secretion of several cytokines was up regulated by 100 nM H2-relaxin in primary HSC (figure 4.8.), NT-4 (i), VE-Cadherin (ii) and Fas-ligand (iii) were all up regulated by over 30%. MMP-9 was also up regulated by over 30%, whilst MMP-3 and MMP-13 were unchanged (figure 4.8. iv). Changes observed were not significant.

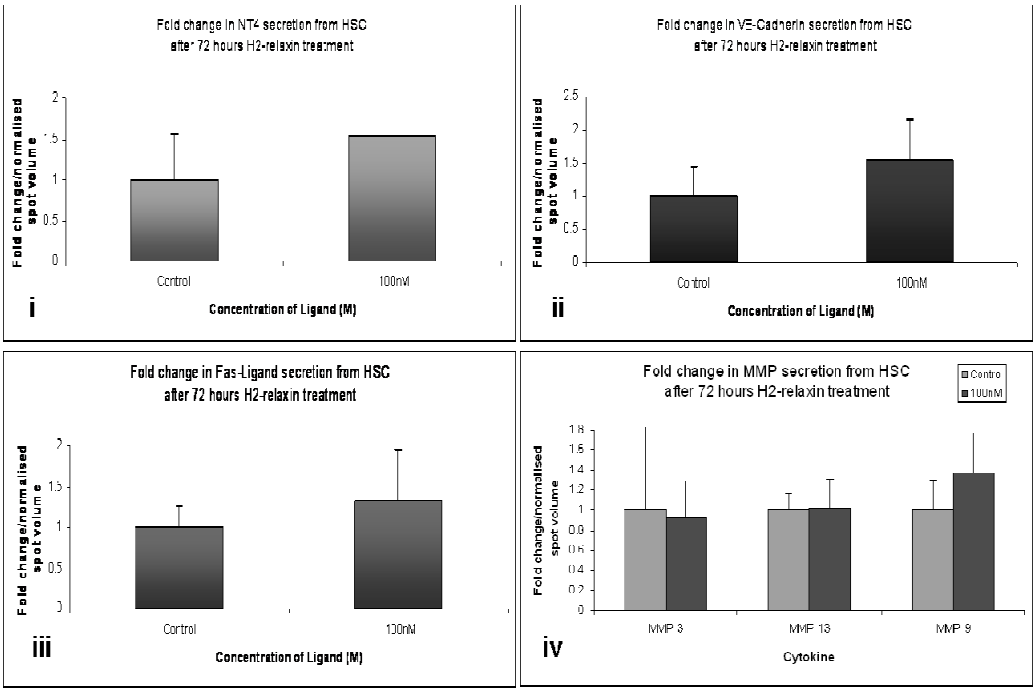

Figure 4.8. (i) NT4, **(ii)** VE cadherin and **(iii)** Fas ligand were all up regulated by more then 30% (n=6). Secretion of MMP-9 was also up regulated in the H2-relaxin treated cells, although MMP-3 and MMP-13 were not.

4.4 Investigation into the contractile properties of HSC in the presence of H2-Relaxin

4.4.1 Endothelin-1 receptor expression in H2-relaxin treated HSC

Endothelin-1 is a potent vasoconstrictor when acting through the endothelin A receptor (ET_A) whereas endothelin B receptors (ET_B) have been found to induce an up regulation in nitric oxide and therefore relaxation of the cell or tissue in which the receptors are found. Previous studies in other cell types have reported H2-relaxin to increase ET_B expression but this was not observed in these cells (Dschietzig et al., 2003). Endothelin-1 has been shown previously to cause contraction of HSC (Rockey and Weisiger, 1996). ET_B has been found to increase the level of nitric oxide, therefore decreasing the contraction of the surrounding tissue. The endothelin receptor expression was investigated in

activated HSC in order to see whether any contractility changes could be explained by changes in endothelin receptor expression in response to H2-relaxin. It was observed that ET_A expression was greater then ET_B expression in activated primary HSC, assessed by RT-PCR (figure 4.9.a). After 72 hours 1 μM H2-relaxin treatment the expression of ET_A was reduced whereas ET_B expression remained unchanged (figure 4.9.b). ET_B receptors have previously been shown to be up regulated by H2-relaxin, although this was not detected after 72 hours, although ET_A expression is down regulated.

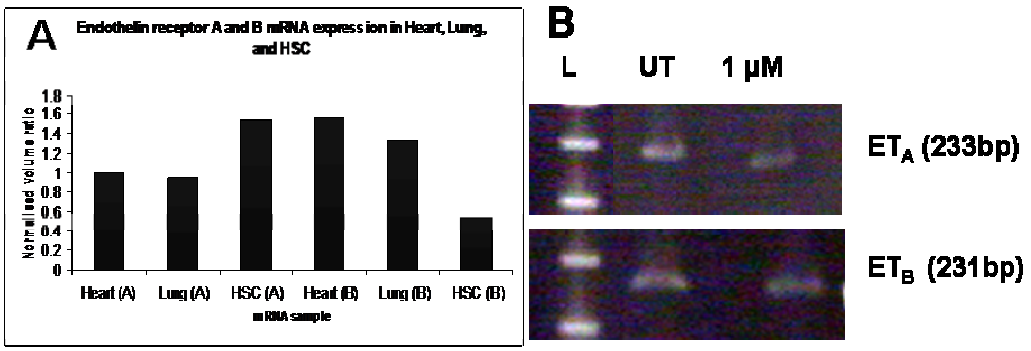

Figure 4.9. (A) Endothelin receptor A and B expression in human heart, lung and activated HSC, assessed by RT-PCR and normalised to GAPDH. ET_B expression is 50% lower in activated primary HSC compared to ET_A expression (n=1). **(B)** ET_A and ET_B expression in HSC treated with 1 μM H2-relaxin for 72 hours, assessed by RT-PCR. ET_A is down regulated whilst ET_B remains unchanged (n=2).

4.4.2 H2-relaxin regulation of HSC contraction using gel contraction assays

Activated primary HSC have contractile properties *in vivo* and *in vitro* culture conditions. Activated HSC plated on a collagen-1 matrix will induce contraction of the matrix which allows us to measure the extent of cellular contraction (figure 4.10. a). Gel contraction assays were carried out as described in chapter 2. It was observed that LX-2 cells did not induce gel contraction to the same extent as activated primary HSC. Activated HSC will contract with no external stimuli other then 10% FBS in the media (serum), all wells contain

serum and serum alone was used as the control which all fold changes in gel area were normalised to. Contraction of the gel was monitored by measuring the area of the gel at 24 and 72 hours. Endothelin-1 and serum have a synergistic contractile effect, causing HSC to contract by over 10% more then in the presence of serum or H2-relaxin. The increased contraction observed after endothelin-1 treatment was not significant but was greatest at 24 hours rather then the 72 hour time point (figure 4.10.b i). HSC in the presence of H2-relaxin exhibited the least contraction, gel area was significantly increased by over 40% after 72 hours compared to serum alone. Gel area was increased after 24 hours H2-relaxin treatment although at this time point the increase was not significant (figure 4.10.b i). Interestingly HSC treated with H2-relaxin and then after 2 hours treated with endothelin-1 (at the time of gel release), still exhibited similar contractile properties after 72 hours compared to HSC treated with just endothelin-1, but if HSC were treated with endothelin-1 for two hours before treatment with H2-relaxin (at the time of gel release) then HSC exhibited less contractile properties, similar to when treated with H2-relaxin alone (figure 4.10.b ii).

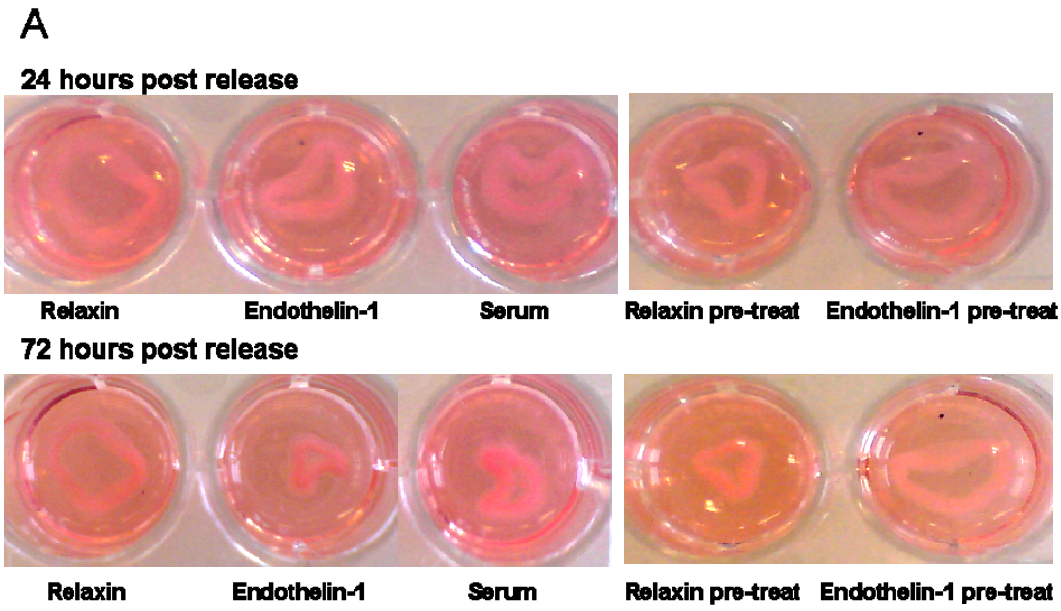

Figure 4.10. (A) Representative example of a gel contraction assay, 24 hours and 72 hours post gel release (n=4).

B

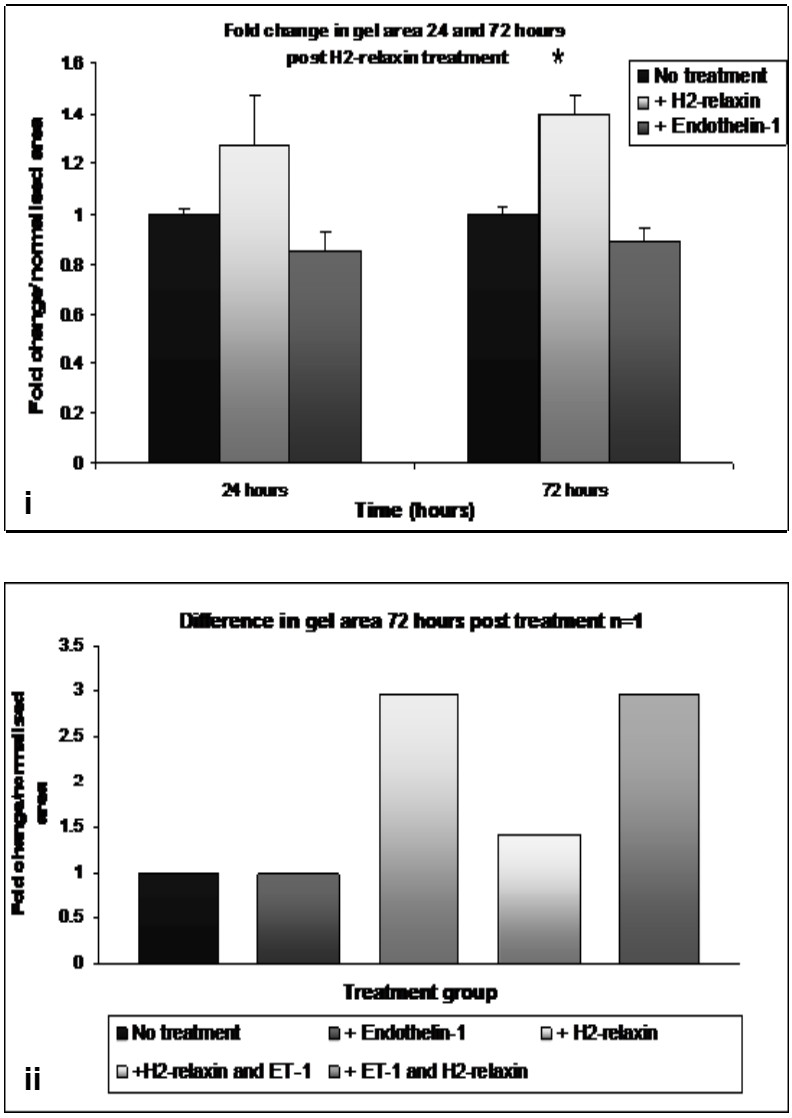

Figure 4.10. (B) (i) Gel area was calculated using ImageJ software. H2-relaxin decreased the contraction significantly after 72 hours compared to untreated (serum), and endothelin-1 treated cells ($p<0.05$) (n=4). Endothelin-1 caused a small increase in contraction compared to the untreated cells but this was not significant. **(ii)** Pre-treatment with relaxin before treating with endothelin-1 did not inhibit the contraction compared to endothelin-1 treated cells alone. Pre-treatment with endothelin-1 before treating with H2-relaxin did not inhibit the relaxation compared to H2-relaxin treated cells alone (n=1).

4.4.3 Secreted nitric oxide quantification in gel contraction assays

Nitric oxide release from HSC during the gel contraction assays was quantified as described in chapter 2. The fold change in nitrite (the stable metabolite of nitric oxide) after 72 hours H2-relaxin treatment was normalised to HSC in the presence of 10% FCS (figure 4.11). H2-relaxin increases nitric oxide release from HSC by over 20%. The changes observed were not significant but the mechanism of cellular relaxation in the presence of H2-relaxin may be explained by a combination of factors including the reduction of α–SMA, reduction in ET_A expression, the increase in nitric oxide and the regulation of intracellular calcium.

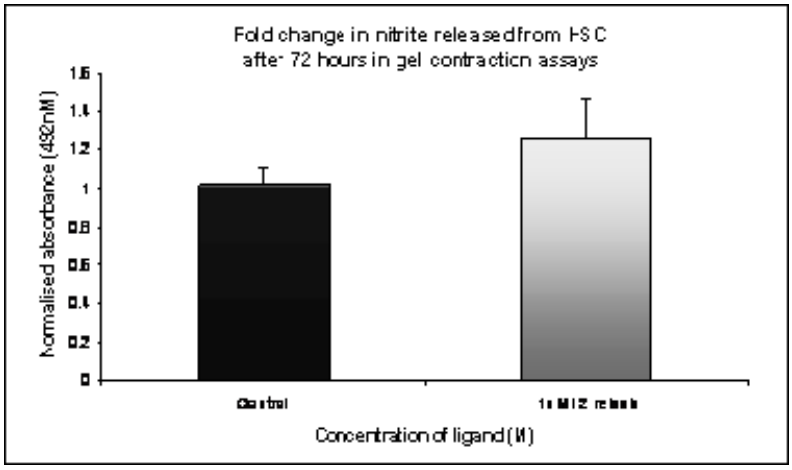

Figure 4.11. The level of nitric oxide secreted into the media over the 72 hour gel contraction experiment was determined. H2-relaxin treated cells increased the level of nitric oxide by 20% compared to untreated cells (n=3).

4.5 Summary of key findings

- H2-Relaxin induced a down regulation of the pro-fibrotic factors such as α-SMA, procollagen-1, TIMP-1, CTGF and TGF-β in human HSC.
- HSC up regulated MMP-1 and MMP-2 in the presence of H2-Relaxin.

- H2-Relaxin increased PARP-1 cleavage in HSC suggesting an up regulation of apoptosis which was supported by a down regulation in the number of viable cells in culture.
- H2-Relaxin inhibited the contraction of HSC

4.6 Discussion

4.6.1 H2-relaxin and specific markers of fibrosis

LX-2 cells were used to initially study the effect of H2-relaxin due to their availability and reported similarity to primary human stellate cells (HSC). Before the cells were used each batch was tested for expression of α-SMA and TIMP-1 the two main fibrotic markers expressed by activated HSC *in vitro*. LX-2 cells have a lower expression of TIMP-1 compared to primary HSC but the level is still easily detectable with RT-PCR methods. LX-2 cells were used in experiments between p8 and p25, after which the cells were discarded and a new batch grown up. To look at gene expression changes a time course experiment was set up. The mRNA was extracted from LX-2 cells treated with 1 μM H2-relaxin after 1 hour, 2 hours, 4 hours and 6 hours. The gene expression profile for TIMP-1, MMP-2 and pro-collagen-1 and RXFP-1 were assessed using RT-PCR. LX-2 cells revealed only small changes in mRNA expression for these genes over the 6 hour period and even after 48 or 72 hours of exposure to H2-relaxin the cells did not significantly alter their gene expression pattern. The results for the time course are not shown as the greatest gene expression changes were after 72 hours. The detection method was either not sensitive enough to pick up small changes in gene expression or it was possible that LX-2 cells did not significantly alter their gene expression patterns in response to H2-relaxin. This may be due to LX-2 cells being a permanently activated cell line, which after plating on Matrigel could not respond by reverting to an inactive phenotype, unlike primary HSC (Gaca et al., 2003) and therefore could resist changes in their gene expression profile. There is evidence that LX-2 cells are

more resistant to apoptosis then primary HSC, due to their differential expression of p21 and p53 related genes (Xu et al., 2005). LX-2 cells were initially treated for 48 and 72 hours with H2-relaxin, replenishing the ligand every 24 hours to look at protein expression changes. After 48 hours of H2-relaxin treatment LX-2 cells revealed a small decrease in α-SMA protein expression but after 72 hours of H2-relaxin treatment the decrease in α-SMA protein expression was significant. The amount of PARP-1 cleavage protein present in LX-2 cells after 72 hours of H2-relaxin treatment was compared to non treated controls. The PARP-1 cleavage product increased in the H2-relaxin treated LX-2 cells but the ratio between cleavage product and total protein did not increase significantly due to total PARP-1 protein expression increasing. Although the increase in uncleaved PARP-1 can be an indication the cells were trying to prevent apoptosis at this time point. An increase in total PARP-1 protein expression can be a sign of cellular stress. The cells would be expected to increase the expression of PARP-1 to maintain genomic integrity due to the role of PARP-1 in genome repair, DNA replication and regulation of transcription (Aikin et al., 2004). Over expression of PARP-1 can deplete the cell of vital energy stores which can cause energy failure and cell death through necrosis. When PARP-1 is cleaved by caspase 3 the activity is lost, which prevents the survival of damaged DNA and releases energy which the cell can then use to undergo apoptosis (Aikin et al., 2004). Therefore LX-2 cells treated with H2-relaxin may have increased the expression of PARP-1 because the cells were under stress and although cleaved PARP-1 protein expression increased as well, H2-relaxin alone did not increase the level of apoptosis but could induce cell death through necrosis of LX-2 cells. If the assay had been continued there may have been an increase in apoptosis at later time points. It was thought that primary HSC would be more dynamic in their response to H2-relaxin revealing greater gene and protein expression changes compared to the LX-2 cell line.

The gene and protein expression profile of primary HSC was studied after 72 hours H2-relaxin treatment. The cells were treated every 24 hours with 10 nM

and 1 μM H2-relaxin, and the RNA and protein was extracted 4-6 hours after the final treatment to ensure the ligand was still active. The gene expression profile was studied using RT-PCR and qRT-PCR due to the small changes observed in LX-2 cells, a more sensitive method was used to confirm the results. Procollagen-1 and TIMP-1 had the highest expression, α-SMA was detectable in the same range but TGF-β1 and MMP-1 were expressed the least, although they were still present in activated HSC. TGF-β has been studied in great detail in several fibrotic diseases and it is believed that the expression of TGF-β promotes fibrogenesis by enhancing the activation and proliferation of quiescent HSC. The expression of TGF-β promotes the sustained and possibly autocrine activation of HSC (Dooley et al., 2000;Dooley et al., 2003;Gressner and Weiskirchen, 2006). Primary HSC treated with H2-relaxin significantly decreased their expression of α-SMA, TIMP-1, TGF-β, and CTGF after 72 hours. MMP-1 expression was significantly increased by 2 and 1.75 fold in both RT-PCR and qRT-PCR assays respectively. Gene expression changes were detected for procollagen-1 (over 10% decrease) and MMP-2 (over 20% increase) but these changes were not significant in either RT-PCR assay. Both PCR assays show good correlation but quantitative PCR was able to detect more significant changes in gene expression. The changes in gene expression observed after 72 hours H2-relaxin treatment suggest a shift to a less fibrotic and increased fibrolytic phenotype in primary HSC.

Primary HSC responded to H2-relaxin by significantly reducing α-SMA protein expression by over 50% in both 10 nM and 1 μM treatments and by significantly increasing the cleaved PARP-1 protein expression by 25% in the 1 μM treatment. The increase in PARP-1 cleavage is indicative of increased apoptosis but an additional technique had to be used to confirm the result. MTS proliferation assays were used to detect the cell viability after H2-relaxin treatment. MTS assays utilise the cells mitochondrial machinery to induce a colour change and therefore the greater the colour change the greater number of viable cells are present. The assay revealed 30% decease in cell viability in H2-

relaxin treated HSC, which was consistent with the PARP-1 cleavage assay. Therefore the data would indicate H2-relaxin induced a 20-25% increase in apoptosis in primary HSC after 72 hours. Li90 cells, a human tumourgenic source of hepatic stellate cells, were treated with a dose response 0.1 nM – 1 μM of H2-relaxin for 72 hours. There was a dose dependent reduction in TIMP-1 and a dose dependent increase in MMP-2 expression assessed by RT-PCR. The data supports the findings in primary HSC (appendix 1). These results add to the evidence that H2-relaxin has antifibrotic properties in primary HSC by causing a decrease in activation and number of HSC and also a decrease in TIMP-1, TGF-β and CTGF, which are all profibrotic factors. The increase in MMP-1 expression coupled with the decrease in TIMP-1 expression will enable the breakdown of scar forming collagen-1 in the liver. The primary HSC response is more significant and dynamic compared to LX-2 cells in this study. Although LX-2 cells are a good tool for developing new assays, primary HSC are the gold standard, especially concerning responses to potential antifibrotic agents that will be safe and effective for use in humans.

4.6.2 Effect of H2-relaxin on expression of cytokines and associated inflammatory and fibrotic markers

Cytokine arrays were carried out to show any protein changes that occur in primary HSC after 72 hours of H2-relaxin treatment. Many of the proteins on the arrays were present in the mRNA analysis, which allowed the comparison between mRNA and protein expression. Many cytokines were regulated by H2-relaxin although the changes were not significant due to cell variation extracted from different patients, but the overall trend showed a reduction pro-inflammatory and pro-fibrogenic cytokines. The cytokines up or down regulated over 30% or interesting related cytokines were looked at in closer detail.

H2-relaxin down regulated cytokines

H2-relaxin was shown to inhibit the protein expression and/or secretion of several cytokines expressed by activated HSC. Several pro-inflammatory and pro-fibrotic factors were reduced including stromal derived factor 1 (SDF-1), members of the PDGF family, members of the FGF family, several members of the TIMP family, TGF-β, and TNF-α. Transforming growth factor beta (TGF-β) is a one member of the transforming growth factor superfamily that consists of inhibins, activins, bone morphogenic proteins and other TGF proteins such as TGF-α. TGF-β protein has three isoforms, TGF-β1, TGF- β2 and TGF-β3. These proteins are present in most cell types and have several functions including controlling cellular proliferation and differentiation. TGF-β1 can act synergistically with TGF-α to induce cellular transformation. TGF-β1 is translated as a large precursor protein which has an N-terminal signal peptide that is required for secretion from the cell. This form of TGF-β1 is known as the latent form which requires removal of the latency-associated protein and latent TGF-β1 binding protein to release an active TGF-β1 protein. The protein then undergoes acidification which disrupts the non covalent interactions or proteolytic cleavage, typically by plasmin, to become an active protein (Sato et al., 1990). The mature TGF-β1 protein forms a 25 kDa homer dimer that can bind type II receptors. Binding to the type II receptor initiates the recruitment and phosphorylation of the type I receptor. A signal cascade then follows which requires the phosphorylation of small mothers against decapentaplegics (SMADs) which can then form a complex that translocates to the nucleus. Once in the nucleus the complexed SMAD proteins can act as transcription factors altering the gene expression of the target cell. There have been several SMADs identified, some of which are pathway specific and some that may inhibit the pathway specific SMADs (Heldin et al., 1997;Massaous and Hata, 1997). TGF proteins and particularly TGF-β1 has been found to have a critical role in liver fibrogenesis. Liver damage of any eitiology rapidly induces TGF-β1 signal transduction. TGF-β1 down stream signalling pathways lead to the migration of neutrophils, macrophages and fibroblasts to the site of injury. These cells in turn

can release more proinflammaotry and profibrogenic cytokines. TGF-β1 is required for the activation and transdifferentiation of hepatic stellate cells, which has implicated TGF-β1 as a major player in liver fibrogenesis (Gressner et al., 1996;Gressner et al., 2002;Gressner and Weiskirchen, 2006). The greatest irrefutable evidence to support TGF-β1 as a profibrogenic factor comes from the transgenic mouse model which over expresses active TGF-β1 and will develop spontaneous liver fibrosis (Sanderson et al., 1995). Hepatocytes respond to TGF-β1 by undergoing apoptosis, although more recently it has been discovered that hepatocytes can also differentiate into a fibroblast like phenotype in the presence of TGF-β1. This process is known as epithelial mesenchymal transistion (EMT). This process is relevant when considering the formation of cancer cells but will also contribute to the progression of fibrosis. Microarray analysis revealed up regulation of genes expressed in hepatocytes that had been stimulated with TGF-β that were involved in EMT and fibrosis such as Snail and CTGF respectively (Meindl-Beinker and Dooley, 2008;Dooley et al., 2000;Sheahan et al., 2008). H2-relaxin down regulated TGF-β1 and TGF-β2 in activated HSC in this study. A previous study has shown relaxin can inhibit TGF-β1 signalling by blocking SMAD 2 phosphorylation and its subsequent translocation to the nucleus. TGF- β binding to the receptor was not affected by relaxin. Inhibition of TGF-β1 signalling together with an up regulation of MMP-2 and MMP-9 expression was suggestive of a less fibrotic phenotype in renal fibroblasts and prevented TGF-β mediated fibroblast activation and function in cardiac fibroblasts (Heeg et al., 2005;Mookerjee et al., 2005b). H2-relaxin has been reported to increase the levels of nitric oxide, which may also reduce the level of TGF-β1 in the cell. Therefore H2-relaxin may inhibit the activation of HSC and prevent apoptosis and EMT occurring in hepatocytes, which may also be a major source of activated myofibroblasts in the injured liver (Dooley et al., 2008). There are hazards related to the inhibition of TGF-β1 including increased malignancy, atherosclerosis and the deregulation of the immune system, although due to the importance of TGF-β1 in initiating the activation of HSC and potentiating the fibrotic reponse thereafter it is still an

ideal target for future therapies (Khan et al., 2005). TNF-α is a pro-inflammatory cytokine that is a key factor in liver diseases such as cachexia and cholestasis. TNF-α induction is one of the earliest events in hepatic inflammation and can trigger a cascade of different cytokines that can kill hepatocytes, recruit inflammatory cells and initiate a would healing response (Tilg, 2001;Diehl, 2000). Activation of TNF-α receptors leads to aggregation and recruitment of various adaptor proteins that activate downstream kinases and proteases. Adaptation in the healthy liver allows hepatocytes to protect themselves against TNF-α and even use it to proliferate in the regenerating liver, but in the pre-injured liver this adaptation cannot occur. Anti-TNF agents such as infliximab have been shown to reduce injury in CCl_4 models. Anti-TNF therapy reduces TGF-β1 levels in the liver and could be beneficial as a therapeutic antifibrotic (Bahcecioglu et al., 2008). H2-relaxin down regulated TGF-β1 by 80% which was the greatest change observed in the cytokine array. The down regulation observed in the cytokine array was quantified using an ELISA assay to measure total and active TGF-β1. The levels of total TGF-β1 were not decreased as much as the active TGF-β1. The difference in total and active was not significant although it does suggest H2-relaxin could have multiple, perhaps indirect effects, not just on gene expression but on the processing of growth factors and cytokines, which may be equally important as the total level of expression of many proteins that require proteolytic cleavage before secretion and/or activation/maturation is enabled. Others have shown that reduction in active TGF-β1 can prevent rat hepatic fibrosis (Okuno et al., 2001).

SDF-1α and SDF-1β are small cytokines that belong to the intercrine family (Bleul et al., 1996). SDF-1 is also known as chemokine ligand 12 (CXCL-12). SDF-1α and SDF-1β are encoded by a single gene found on chromosome 10, and arise through alternative splicing. The intercrine family was first described in 1991 to distinguish a family chemokines through their chromosomal location and unique structural features (Oppenheim et al., 1991). The chemokines have 20-50% sequence homology and are mainly located on chromosome 4 and 17.

They are basic, heparin binding polypeptides. Many chemokines in the family can be induced by proinflammatory stimuli such as lipopolysacharide (LPS), TNF and IL-1. The chemokines in the intercrine family have proinflammatory or reparative activities (Oppenheim et al., 1991). Members of the intercrine family include IL-8, IP-10, GRO, I-309 and RANTES. SDF-1 activates leukocytes and is strongly chemotactic for lymphocytes, acting in the emigration pathway of lymphocytes from the blood to sites of inflammation (Bleul et al., 1996). SDF-1 induces T-cell migration and actin polymerisation in leukocytes. Actin polymerisation is thought to be essential for migration of neutrophils, known to depend on the formation and redistribution of filamentous actin. The rearrangement of the actin cytoskeleton regulates intergrin mediated adhesion, as well as the migration and mechanical properties of activated neutrophils (Horuk and Peiper, 1996;Sheikh et al., 1997). Many leukocytes express high levels of CXCR4, the receptor for SDF-1. SDF-1 knockout is lethal and thought to be due to its second function, which establishes hematopoieses in bone marrow during development. It is thought there is a major role for SDF-1 in murine stem cells homing from fetal liver into the bone marrow and its repopulation during development (Lapidot, 2001). Therefore if relaxin down regulates SDF-1α and SDF-1β, there will be a decrease in activation and migration of leukocytes from the blood stream into the tissue. The liver's resident leukocyte, the kupffer cell, is believed to be at least partly responsible for the initial activation of HSC. If H2-relaxin can down regulate the level of SDF-1 it may reduce the activation and migration of kupffer cells in the liver and therefore reduce the initial and sustained activation of HSC.

There are several forms of PDGF that make up the family of growth factors secreted from several different cells types to regulate cell growth and division, also having important functions in angiogenesis. The PDGF ligand is a dimeric glycoprotein composed of two α or two β chains. There are five different isoforms, including A, B, C, D, AB and two receptors PDGFRα and PDGFRβ. The receptors have been classified as tyrosine kinase receptors. Upon activation

by their respective ligands the receptors dimerise and are switched on by auto-phosphorylation of several sites on the cytosolic domain (Matsui et al., 1989b;Matsui et al., 1989a;Heidaran et al., 1991;Yu et al., 1995). PDGF is a profibrogenic growth factor, liver fibrosis has been induced in transgenic mice which overexpress PDGF-B. It was shown that PDGF-B did not up regulate TGF-β but did cause the activation of hepatic stellate cells marked by the increase in expression of α-SMA and PDGFR-β. Collagen-1 deposition, shown through histological staining of liver sections, was increased in the transgenic mice (Czochra et al., 2006). Other studies have found all forms of PDGF to be up regulated in models of liver fibrosis, and PDGFR-B is accepted as a marker of hepatic stellate cell activation. PDGF-BB induces the migration of HSC, which is rapidly up regulated in the first two days of primary cell culture and is then constantly expressed. PDGF-B expression was actually found to be rapidly down regulated in primary HSC undergoing activation but the other more recently discovered forms PDGF-C and D were strongly induced, 5 and 8 fold respectively. It was postulated that PDGF-C and D may compensate for the loss of PDGF in hepatic fibrosis. There were small changes in PDGF-A, but the changes observed were not significant in comparison to the other isoforms (Breitkopf et al., 2005). H2-relaxin was shown to down regulate PDGF-AA and PDGF-AB, as well as both forms of the receptor. Therefore relaxin may have an antifibrotic effect in human primary HSC due to the decrease in PDGF released from HSC, which may act in an autocrine manner. The other forms of PDGF were not present on the membrane, but it would be interesting to investigate the effect H2-relaxin has on all of the members of the PDGF growth factor family.

Fibroblast growth factors (FGFs) are a family of growth factors involved in angiogenesis, wound healing and embryonic development. FGFs are heparin binding proteins that are key players in proliferation and differentiation of cells. There are 23 members of the family in humans. FGF was first isolated and purified from bovine pituitaries by Gospodarowicz in 1974. The growth factor was shown to promote the growth and differentiation of human and murine

fibroblasts in vitro. Growth of human fibroblasts was increased two fold in the presence of FGF, compared to cells cultured in fetal calf serum alone. FGF was shown to increase DNA synthesis in 3T3 cells (Gospodarowicz et al., 1977;Gospodarowicz and Moran, 1975). More recently the effect of FGF on embryonic development has been studied. FGF-7 has been shown to stimulate the growth of oocytes in vitro (Cho et al., 2008), FGF-7 can also induce the differentiation of hepatoblasts into biliary epipthelial cells (BEC's) (Yanai et al., 2008). H2-relaxin reduces the expression of FGF-4, FGF-6 and FGF-9. FGF-7 expression is slightly increased in the presence of H2-relaxin. The implication of a reduction in FGF's after H2-relaxin treatment is a reduction in a fibroblast-like cells ability to proliferate and differentiate. Therefore the ability for quiescent HSC to differentiate into activated myofibroblasts and then proliferate after activation would be reduced in the presence of H2-relaxin.

FLT-3 is a receptor tyrosine kinase that is expressed by immature hematopoietic progenitor cells and is structurally related to the receptors for PDGF and colony stimulating factor (CSF). FLT-3 ligand is membrane bound or can be proteolytically cleaved to generate a biologically active soluble ligand that is expressed by a variety of cells including hematopoietic and bone marrow stromal cells. The activation of the FLT-3 receptor leads to tyrosine phosphorylation of various key adaptor proteins that are known to be involved in various signal transduction pathways. FLT-3 ligand is thought to be important in controlling proliferation, differentiation and survival of progenitor cells but cannot stimulate proliferation alone (Drexler and Quentmeier, 2004). FLT-3 ligand synergises with CSFs and interleukins to induce growth and differentiation of progenitor cells that develop various cell types including natural killer (NK), pre-B, pre-T, monocytes and macrophages. FLT-3 ligand is important in the development of lymphocytes and is therefore effective in promoting immunity against intracellular viral and non viral pathogens. The immune response is increased in the presence of FLT-3 ligand and there is evidence of increased inflammatory cell infiltrate in the liver in mice that over

express FLT-3 ligand (Juan et al., 1997). Relaxin reduces the expression of FLT-3 ligand, which would reduce the inflammatory infiltrate in the injured liver. A reduction in the infiltration of activated B and T-cells as well as macrophages in the liver would reduce the activation of HSC. The immune response is vital in patients with Hepatitis C and an effective clearance of viral particles from the liver can rescue the patient from chronic damage that can lead to permanent fibrotic scarring and cirrhosis but in patients where damage to the liver is caused by other factors including alcohol and obesity the reduction of inflammatory mediators may reduce the fibrotic response.

Tissue inhibitors of matrix metalloproteinases (TIMPs) are the cells natural regulators of MMP activity. There are four known TIMPs and all known MMPs are inhibited by at least one of the four. The mechanism of TIMP inhibition has been elucidated through studying the crystal structures of TIMP-MMP complexes (Gomis-Ruth et al., 1997). TIMP-1 is believed to play a pivotal role in fibrosis and in particular liver fibrosis. TIMP-1 inhibits the activity of MMP-1, the main interstitial collagenase, therefore protecting newly formed scar forming collagen from MMP degradation. TIMP-1 and TIMP-2 are expressed by activated HSC. The expression of TIMP-1 correlates to the severity of liver disease in animal models. TIMP-1 has also been shown to protect liver cells but particularly activated HSC from apoptosis (Iredale et al., 1998;Murphy et al., 2002) and therefore the reduction of TIMPs by H2-relaxin would increase the degradation of scar forming collagen-1 by preventing the inhibition of MMPs and increase the apoptosis of HSC.

Tie-1 and Tie-2 are cell surface tyrosine kinase receptors. They possess unique multiple extra-cellular domains and can bind angiopoietins (Ang) which are protein growth factors that promote angiogenesis. Tyrosine kinase receptors posses a hormone binding domain, a carboxyl terminal segment and multiple tyrosines for autophosphorylation. Binding of Ang-1 to Tie-2 is believed to activate the receptor, initiating a signal cascade that ultimately leads to changes

in gene transcription. Tie-2 and Ang-1 knockout models have similar phenotypes (Maisonpierre et al., 1997). Ang-2 is thought to inhibit Tie-2. Until recently Tie-1 was an orphan receptor mainly found on endothelial cells. The ability to purify Tie-1 and Tie-2 together lead researchers to believe the receptors formed a heterodimer. The role for Tie-1 has finally been elucidated and it is believed that Tie-1 can modulate Tie-2 driven signalling, modulating blood vessel morphogenesis but they do not form a dimer. Ang-1 induces Tie-1 phosphorylation in endothelial cells but this is Tie-2 dependent. Tie-2 can induce cell survival as well as angiogenesis. These receptors have been implicated in the survival of cancer cells (Yuan et al., 2007). H2-relaxin down regulates the expression of Tie-1 and Tie-2, Tie-2 is down regulated to a greater extent then Tie-1. Down regulation of Tie-2 could reduce the survival of the cells that express the receptor, therefore in this case increasing HSC susceptibility to be driven into apoptosis.

H2-relaxin up regulated cytokines

H2-relaxin up regulated cytokines include, Fas ligand, VE-cadherin, Neurotrophin-4 (NT-4) and MMP-9, whilst MMP-3 and MMP-13 remain unchanged. NT-4 belongs to a family of neurotrophins including nerve growth factor (NGF), brain derived nerve growth factor (BDNF), neutrophin-3 (NT-3), and neurotrophin-5 (NT-5). NT-4 is less conserved compared to the other members of the family due to a truncated pro-region and a 7 amino acid insertion in the mature region (Ip et al., 1992). Neurotrophins act through signalling via membrane bound receptors. There are two types of receptor that NT-4 will signal through, the high affinity tyrosine kinase (Trk) receptors, which there are three TrkA, TrkB and TrkC, and the low affinity nerve growth factor p75 (NTR) receptor (Samah et al., 2008). Neurotrophins are known to promote neuronal survival, they are involved in brain development, nerve regeneration and can modulate gene expression in the nervous system. Neurotrophins were traditionally thought of as mediators of the nervous system (Ip et al., 1992) but more recently expression of these factors and their receptors have been found in

peripheral tissues and cells related to the immune system such as T-cells, B-cells and macrophages (Samah et al., 2008). Neurotrophins may have a role in modulating the critical functions of macrophages such as chemotaxis. It has also been reported that NGF can enhance phagocytosis, and increase the production of TNF-α and nitric oxide. Neurotrophins NGF, BDNF, NT-3, NT-4 and NT-5 are expressed by hepatic stellate cells and their expression can be induced by pro and anti inflammatory agents such as TGF-β, LPS and dexamethasone although NT-4 was not as inducible compared to NGF and NT-3 (Cassiman et al., 2001). NT-4 is the least well described neurotrophin and its role in peripheral tissue is largely unknown but it may have a role in tissue healing mechanism by acting on cells involved in inflammation and the immune response (Samah et al., 2008). HSC are the main effector cells in liver injury but macrophages also have an important role in activation of HSC to a myofibroblast type cell. Neurotrophins may act on kupffer cells (the livers resident macrophages) but they may also have a role in the regulation of HSC in the injured liver. Previous work has shown NGF to be expressed by rat hepatocytes during liver injury. Peak levels of hepatocyte NGF expression occurs 48 hours post CCl_4 injury which coincides with peak HSC apoptosis and when recombinant NGF is added to rat HSC *in vitro* it causes a dose dependent increase in apoptosis (Oakley et al., 2003). H2-relaxin induces the expression of NT-4 in primary HSC and although the expression of NGF is unchanged the increase in NT-4, which will signal through the same receptors as NGF may induce apoptosis in an autocrine manner. To confirm if NT-4 has a role in HSC apoptosis *in vitro* a recombinant form of NT-4 would be added to the cultured primary HSC.

Fas ligand (FasL) is a type II transmembrane protein that belongs to the TNF family. Soluble FasL (sFasL) is generated by MMP-7 cleaving membrane bound FasL at a conserved cleavage site. Binding to the Fas receptor, also known as APO-1 or CD95, induces apoptosis but there is suggestion in recent years that binding of the soluble form can inhibit apoptosis by blocking the binding of full length FasL to its receptor (O'Connell et al., 2001). Binding of

FasL to the FAS receptor initiates the recruitment of several other proteins to the intracellular death domain of Fas to form a death-inducing signalling complex, or DISC (Medema et al., 1997). Of the proteins recruited the Fas-associated death domain (FADD) proteins acts as an adaptor that links procaspase-8 to stimulated Fas (Chinnaiyan et al., 1995). Pro-caspase-8 is then activated by proteolytic cleavage, active caspase 8, also known as Fas linked interleukin-1β-converting enzyme-like protease (FLICE) instigates a caspase cascade leading to proteolysis of protein targets that are essential for the apoptotic process (Martin and Green, 1995). Apoptosis is regulated in some cell types by the expression of proteins such as Bcl-2, Bcl-x_L, PARP-1 (inhibit apoptosis) Bax, Bak, and p53 (promote apoptosis) (Kroemer, 1997). Other functions of FasL include regulation of the immune system (O'Connell., 2001) and regulating the progression of cancer as described in hepatoma cells (Natoli et al., 1995). Fas receptors are expressed by primary HSC and these cells have been shown to become susceptible to apoptosis by soluble FasL (sFasL) after activation into a myofibroblast like cell. The increased sensitivity to sFasL driven apoptosis was believed to be at least in part due to the decrease in expression of Bcl2 and Bcl-x_L by HSC (Gong et al., 1998). H2-relaxin increases the expression of FasL in primary HSC, indicating H2-relaxin is pro-apoptotic in these cells. An increase in FasL could also indicate an increase in sFasL which is processed by MMP-7. Although there are indications that sFasL is pro-apoptotic in HSC (Gong et al., 1998) further investigations are needed to completely understand the role of FasL and sFasL in liver disease.

Vascular endothelial (VE)-Cadherin is a recently characterised member of the cadherin family (Lampugnani et al., 1992). VE-cadherin is also known as cadherin-5 (Suzuki et al., 1991). VE-cadherin is located at intercellular adheren junctions and has important functions in cohesion and organisation of the junction as well as regulating the permeability properties of the vascular endothelium (Bazzoni and Dejana, 2004). VE-cadherin also has properties related to angiogenesis in normal and tumourogenic tissue. VE-cadherin is

barely detectable in sinusoidal endothelial cells in the normal liver (Scoazec et al., 1994;Scoazec and Feldmann, 1994) but in diseased liver, including hepatitis infection, cirrhosis and HCC both the mRNA and protein expression increases (Kato et al., 2007). H2-relaxin induces the expression of VE-cadherin in primary HSC. H2-relaxin is known as a vasoactive substance that could be important in maintaining the blood flow through the sinusoid of the liver and therefore transport of vital nutrients to the hepatocytes through the space of disse, especially during liver injury, particularly fibrosis, when the space of disse may become blocked with excess extra cellular matrix and the fenestrae of the endothelium are lost. Inducing the expression of proteins such as VE-cadherin could implicate a role for H2-relaxin in maintaining the permeability of the vascular endothelium and maintaining intercellular adheren junctions that are important for sustaining the structure of the space of disse and the contact between the hepatocytes and the hepatic sinusoid through the HSC.

Matrix metalloproteinase 9 (MMP-9) is a member of a family of zinc dependent proteolytic enzymes. In a healthy liver the homeostasis of extracellular matrix is regulated by the balance of MMPs and their inhibitors TIMPs. In chronic liver damage activation of HSC induces the expression of TIMPs, particularly TIMP-1, which causes the inhibition of MMPs ultimately leading to the accumulation of extra-cellular matrix and fibrosis (Schuppan et al., 2001;Iredale, 1996;Iredale, 1997). MMPs are divided based on their main substrate for example, collagenases, gelatinases, and metalloelastases. MMPs are secreted as zymogens and are activated by cleavage of their propeptide (Somerville et al., 2003). MMP-9 a 92 kDa protein is activated by the proteolytic cleavage by MMP-3 to an 86 kDa protein. MMP-3 is activated by plasmin before it can activate MMP-9. MMP-9, also known as gelatinase B, has similar targets to MMP-2, also known as gelatinase A, such as gelatins, collagen 1, IV, V, VII, X, fibronectin, laminin and elastin. MMP-9 is produced by Kupffer cells in primary culture (Knittel et al., 1999). During liver disease HSC, inflammatory cells and mononuclear cells are also a source of MMP-9 (Knittel et al., 2000;Han

et al., 2007). MMP-9 expression increases during the activation of HSC, however MMP-9 activity is not associated with the degree of fibrosis but is linked to tissue inflammation, consistent with earlier findings linking MMP-9 expression to the presence of HCV infection (Lichtinghagen et al., 2001). There have been inconsistent results as regards to the expression of MMP-9 in several different models of acute and chronic liver injury in rats. Up regulation of MMP-9 at the beginning of recovery in mouse models has been observed at the mRNA and protein level (Knittel et al., 2000;Ueberham et al., 2003). Disruption of the $\alpha_v\beta_3$ integrin and type 1 collagen interactions has been shown to induce apoptosis of HSC and increase the expression of MMP-9. Active recombinant MMP-9 protein can promote apoptosis of HSC (Zhou et al., 2004). It has also been shown that over expression of MMP-9 can reduce type 1 collagen and hydroxyproline content in the liver, thus MMP-9 may indirectly contribute to fibrolysis by accelerating HSC apoptosis (Roderfeld et al., 2006). Antagonism of inflammatory cytokines through addition of IL-1 and TNF antagonists anakinra and etanercept, has been shown to reduce TIMP-1 mRNA levels in experimental toxic liver injury. In addition to the reduction of TIMP-1 mRNA, MMP-9 mRNA levels increased (Roderfeld et al., 2006). H2-relaxin increases the expression of active MMP-9 in HSC, which has been previously documented in renal fibroblasts (Heeg et al., 2005). After reviewing the literature, an increase in MMP-9 could induce apoptosis of HSC and reduce their fibrotic phenotype, reducing the expression of TIMP-1 and ultimately the accumulation of type 1 collagen. The induction of MMP-9 at the onset of fibrosis could have implications in allowing fibrosis to develop but due to the complexity of MMPs and their inhibitors in fibrosis the best model to test the affect of relaxin would be an in vivo model of fibrosis, where all of the cell types are present allowing the interactions between cell types through the levels of secreted cytokines to show the true response.

4.6.3 H2-relaxin effects on contractile properties of HSC

Gel contraction assays were carried out to discover if the contractile properties of activated human HSC were affected by H2-relaxin treatment. Several pro-fibrotic agents such as endothelin-1 and vasopressin have been reported to increase the contraction of HSC compared to unstimulated cells. Therefore the hypothesis was H2-relaxin, as an antifibrotic agent with known vasodilatory properties, would reduce the contraction of activated HSC. Endothelin-1 was used as a positive control, although activated HSC will contract in the presence of serum alone. Gel contraction assays were originally carried out using LX-2 cells, but they did not display the same contractile properties as primary HSC. H2-relaxin significantly reduced the contraction of HSC compared to both serum and endothelin-1, which is a novel observation. The contraction of HSC was measured indirectly by calculating the area of the gel after 24 and 72 hours of exposure to either H2-relaxin or endothelin-1, therefore the larger the gel the greater the relaxation. At 24 hours HSC treated with H2-relaxin had a 20% increased gel area compared with untreated HSC, although the increase in gel area at this time point was not significant, by 72 hours the gel area had significantly increased to 50% above the untreated HSC and 60% above endothelin-1 treated HSC. Endothelin-1 only modestly increased the contraction of HSC compared to untreated HSC and at no time point was the increase in contraction significant. In contrast to H2-relaxin the greatest increase in HSC contraction by endothelin-1 was observed at 24 hours. The results from a single experiment suggest that when HSC are pre-treated with H2-relaxin for 2 hours before applying endothelin-1 the relaxation observed in H2-relaxin alone treated HSC was significantly reduced. HSC pre-treated with endothelin-1 before treatment with H2-relaxin retained the increase in gel area and therefore relaxation observed for H2-relaxin treatment alone. If taken into account the earlier time course conducted in LX-2 cells and the delay in significant relaxation of HSC in the gel contraction assay, the antifibrotic effects

of H2-relaxin appear to have a slow onset of action, possibly due to changes in gene and protein expression required for relaxation of HSC to take place.

The mechanism of relaxation in HSC by H2-relaxin was investigated by measuring the amount of nitric oxide released into the media during the gel contraction assay. Nitric oxide cannot be measured directly and therefore the stable metabolites nitrite and nitrate are used to compare the levels of conversion in treated and untreated HSC. H2-relaxin increased the level of nitric oxide in the media by 20% compared to untreated HSC after 72 hours. Therefore a possible mechanism of relaxation of HSC after treatment with H2-relaxin may be through the induction of nitric oxide and several previous studies have proposed that H2-relaxin can induce nitric oxide through several mechanisms (Nistri and Bani, 2003;Sherwood, 2004b) (figure 4.12). Activation of the RXFP-1 activates second messenger systems inside the cell, activating G protein Gs can increase the cAMP levels in the cells and induce phosphorylation of AKT by PI3-kinase. Increasing cAMP initiates the activation of PKA, which then goes on to phosphorylate transcription factors such as NF-κB, an important transcription factor in the regulation of fibrosis (Oakley et al., 2005;Watson et al., 2008), which can induce the transcription of NOS II and therefore increase production of NO (Nistri and Bani, 2003;Sherwood, 2004b). The phosphorylation of AKT can induce the activation of NOS III, and therefore NO. H2-relaxin treated HSC do not change their expression ET_B, which is required for vasodilation in endothelial cells and signals through the induction of nitric oxide. Although the expression of ET_A is decreased and ET_B remains unchanged, which confers a more vasdilatory phenotype. Some groups have reported ET_B expression up regulation by H2-relaxin (Dschietzig et al., 2003) whereas others have reported regulation of ET_B protein has no role in H2-relaxin regulation of ET_B/nitric oxide pathway (Kerchner et al., 2005).

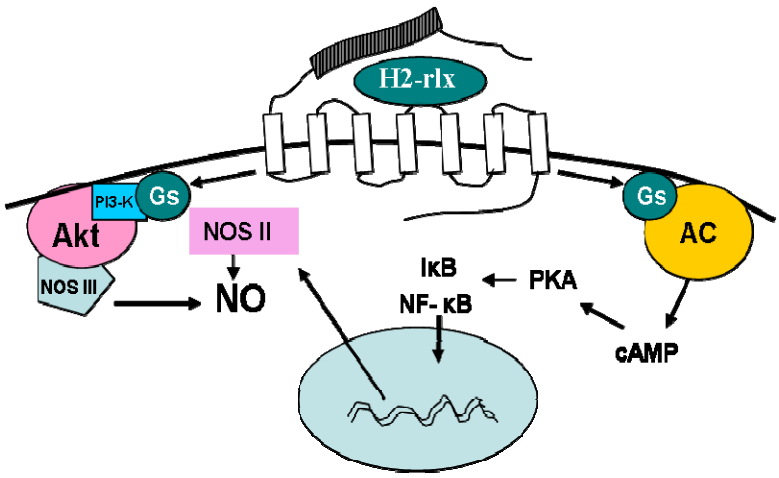

Figure 4.12. Adapted from (Nistri and Bani., 2003). Potential nitric oxide induction pathways used by H2-relaxin.

H2-relaxin may also regulate HSC contractility through regulating intracellular calcium release. It has been shown that relaxin modulates myometrial contractility, the mechanisms are complex and only partially understood (Downing and Hollingsworth, 1993;Sherwood, 2004b;Sanborn, 2001). The myometrium is the middle layer of the uterine wall, consisting largely of smooth muscle cells but also supporting stromal and vascular tissue. The myometrium allow expansion and contraction of the uterine wall during pregnancy (Schofield and WOOD, 1964;Schofield, 1957). It has been described that relaxin can regulate the contractility of vascular smooth muscle not only of the reproductive organs but of several different organs including the heart, kidneys and liver through the regulation of intracellular free calcium and/or nitric oxide levels in the cells (Failli et al., 2002;Bani et al., 1999). Calcium binds to calmodulin which forms a complex that binds to and activates the myosin light chain kinase (MLCK). Activated MLCK can phosphorylate the regulatory chain of myosin which will ultimately enhance its interaction with actin and actin activated myosin ATPase which will bring about contraction. Phosphorylation of MLCK can inhibit the formation of calmodulin complexes and therefore contraction (Sherwood, 2004b;Sanborn, 2001).

There are several different mechanisms described by which relaxin may regulate this cascade of events (figure 4.13) but one is through the increase in intracellular levels of cAMP and its subsequent activation of PKA, which causes the phosphoylation of MLCK, reducing its affinity for myosin and therefore blocking the cascade (Sherwood., 2004). It has been suggested that relaxin can bind to Ca^{2+} making it unavailable to the contractile elements (Fields, 2005). Activation of PKA may also inhibit DAG + IP_3 mediated release of calcium from intracellular stores thus reducing the available calcium (figure 4.13). H2-relaxin can blunt the calcium response in normotensive but not hypertensive rats. The levels of protein kinase G are reduced in hypertensive rats which could explain the difference in sensitivity to relaxin treatment (Failli et al., 2002). Protein kinase G (PKG) is a serine threonine specific protein kinase signalling molecule that is activated by increases in cGMP. PKG has been found to play a pivitol role in the nitric oxide-cGMP signalling pathway, contributing to the regulation of not only smooth muscle relaxation but also in the pulmonary venous system (Lincoln et al., 1993;Walsh et al., 1995;Gao et al., 1999). These studies indicate the vasorelaxant effects of H2-relaxin may be dependent upon the levels of protein kinase G and therefore nitric oxide levels in the cell.

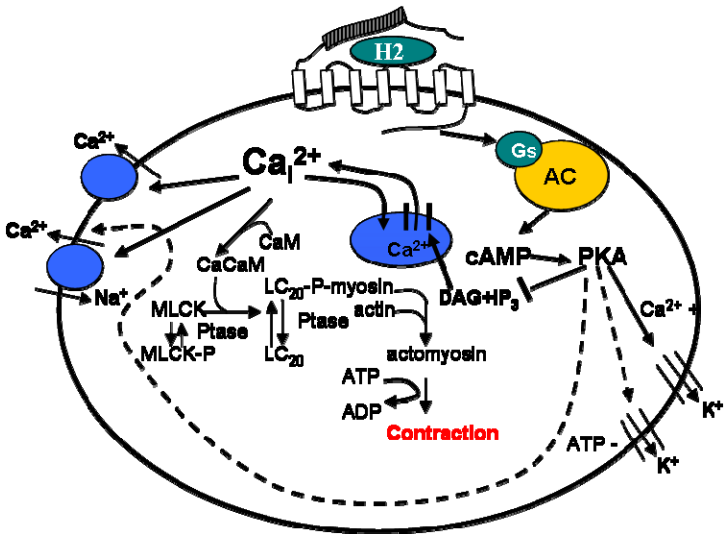

Figure 4.13. Adapted from (Sherwood., 2004) Mechanisms by which, H2-relaxin could modulate intracellular calcium levels. The bold arrows indicate known mechanisms, whereas the dashed arrows indicate potential mechanisms of action.

Others have shown that contractility of HSC correlates with levels of activation and expression of α-SMA (Rockey et al., 1993). Actin is required for cell migration, maintenance of morphology and contraction (Machesky and Hall, 1997;Hinz and Gabbiani, 2003). There are several different isoforms that are expressed by different cells types, but myofibroblasts (activated HSC) predominantly express the vascular isoform, α smooth muscle actin (α-SMA). Therefore a decrease in α-SMA may reduce the available actin in the cell, which is required for contraction (Hinz et al., 2002). H2-relaxin decreases the expression of α-SMA and seems to reverse the activated phenotype, therefore perhaps decreasing contractility by this mechanism. TGF-β has also been shown to up regulate α-SMA contraction of myofibroblasts (Meyer-ter-Vehn et al., 2008), therefore the decrease in α-SMA expression coupled with the decrease in TGF-β expression by H2-relaxin may further reduce contraction of activated HSC. HSC adhesion and migration is important in ECM remodelling and fibrosis and is dependent upon the expression of α-SMA. An increase HSC adhesion and migration is profibrotic in LX-2 cells (Wang et al., 2005). Therefore a decrease in α-SMA expression by H2-relaxin could also decrease

HSC adhesion and migration, another mechanism by which H2-relaxin could exert antifibrotic effects (Hinz et al., 2003). A decrease in adhesion to collagen-1 could affect the gel contraction assay results. If a fewer number of HSC are attached to the gel, a decrease in contraction will be observed.

Addition of a nitric oxide inhibitor, L-NAME, was added to the cells in the gel contraction assay. The concentration of inhibitor may have been too high as no contraction was observed, indicating possible cell death in those wells. Unfortunately these experiments were not repeated and therefore mechanism of gel contraction by H2-relaxin remains to be fully elucidated. The inhibition of contraction by H2-relaxin may be a complex sequence of events that includes several different mechanisms. We now know that H2-relaxin decreases α-SMA and TGF-β expression, increases MMP expression, and increases nitric oxide levels in primary HSC. H2-relaxin may use a combination of these factors and other mechanisms that we have not studied such as the inhibition of intracellular free calcium to inhibit contraction in activated HSC. To determine if the effects of H2-relaxin observed in this chapter were through the activation of the receptor RXFP-1, siRNA studies were carried out. These studies assisted in understanding the mechanisms by which H2-relaxin has antifibrotic and anticontractile effects in HSC.

Chapter 5

H2-relaxin induced reduction of pro-fibrotic markers and cellular contractility in human hepatic stellate cells is dependent upon the expression of functional RXFP-1

5.1 Introduction to siRNA studies

5.1.1 Introduction

RXFP-1 activation is the major signalling pathway utilised by H2-relaxin. Studies using siRNA targeted to RXFP-1 were designed to determine whether the phenotypic effects described in chapter 4, after H2-relaxin treatment are dependent upon activation of RXFP-1. Many of the assays carried out in chapter 4 were repeated after siRNA transfection and confirmation of RXFP-1 knockdown in primary HSC. SiRNA transfection conditions had to be optimised for both LX-2 and primary HSC. The percentage knockdown was assessed using qRT-PCR and all the results are compared to percentage of expression after negative control siRNA transfection. The toxicity of the siRNA oligonucleotides were assessed by MTS cell viability and LDH assays, which determine the number of live cells compared to the control or the number of dead cells compared to the total population in that well respectively. Transfection efficiency was determined using cAMP assays to quantify the knockdown of active receptor in response to H2-relaxin. Off-target effects were evaluated by monitoring the expression of RXFP-3, a closely related member of the relaxin receptor family. Transfection with a negative control siRNA or scrambeled sequence also controlled for specificity and negative off-target effects.

5.1.2 Hypothesis, Aims and Objectives

Hypothesis

H2-relaxin exerts its phenotypic effects on HSC through the activation of relaxin receptor RXFP-1.

Aims

To treat primary HSC with H2-relaxin and test the effect on expression of markers of fibrosis and the ability to contract collagen gels after knocking down RXFP-1.

Objectives

- Knockdown RXFP-1 in LX-2 and primary HSC using siRNA
- Verify cell viability and transfection efficiency using MTS, LDH and cAMP assays
- Check the phenotype of HSC lacking RXFP-1 receptor in the presence of H2-relaxin.

5.2 Results-Validation of siRNA oligonucleotide knockdown of RXFP-1 receptor in primary HSC and LX-2 cells

Transient siRNA transfection was used to knockdown RXFP-1 in both LX-2 cells and primary HSC. Three siRNA oligonucleotide sequences were tested in LX-2 cells. LX-2 cells were transfected with 50, 100 and 200 nM of all three RXFP-1 siRNA. The lowest concentration with the most effective knockdown was RXFP-1 siRNA 1 at 100 nM (figure 5.1). At 200 nM the negative control siRNA effected RXFP-1 expression suggesting toxic effects, and at 50 nM the knockdown was not as significant. One sequence was found to knock down the receptor more efficiently and therefore RXFP-1 siRNA 1 sequence (RXFP-1 siRNA) was used in all further studies. Negative control siRNA was a predesigned sequence used for all LX-2 cell transfections. Knockdown of RXFP-1 in LX-2 cells was also quantified by qRT-PCR (figure 5.2c i).

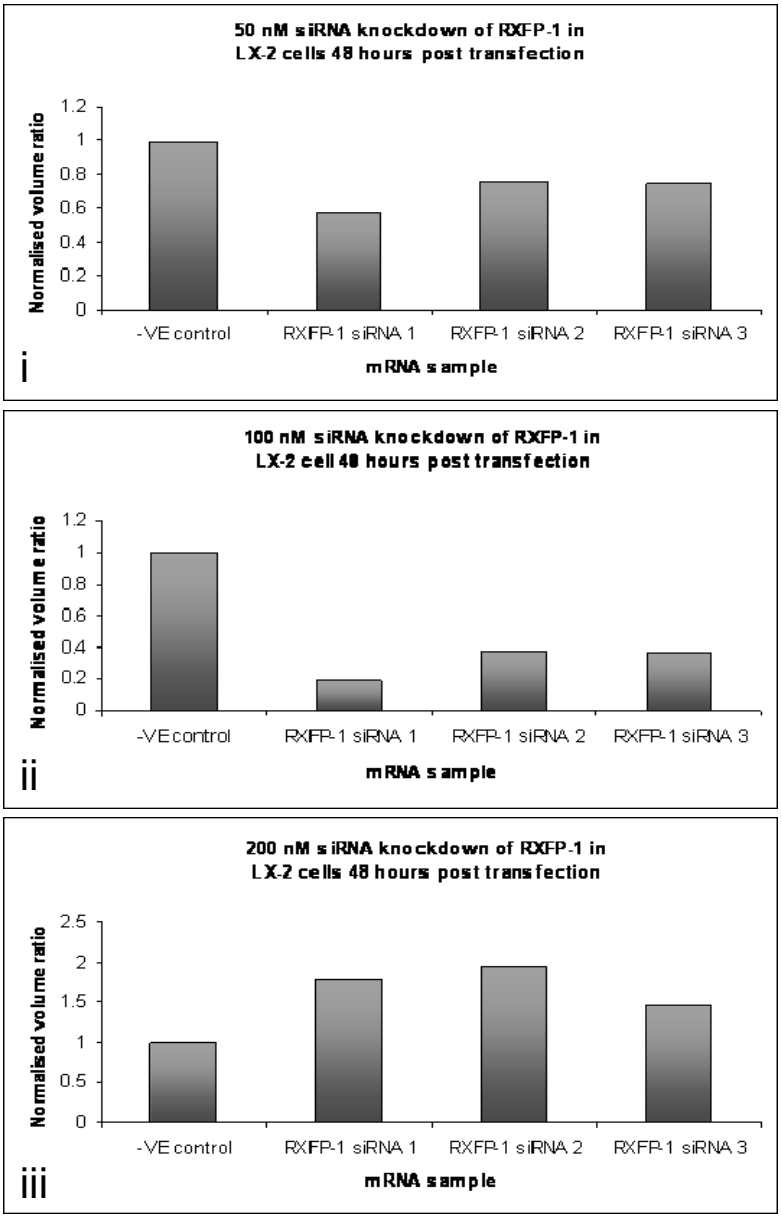

Figure 5.1. RXFP-1 siRNA test knockdown in LX-2 cells. RXFP-1 expression 48 hours post transfection assessed by RT-PCR (n=1). RXFP-1 expression was normalised to GAPDH and the knockdown of the receptor was normalised to the negative control siRNA. (i) 50 nM, (ii) 100 nM and (iii) 200 nM siRNA concentrations were tested, 100 nM RXFP-1 siRNA #1 efficiently knocked down the receptor by over 80%.

Primary HSC were initially transfected with 100 nM RXFP-1 siRNA, but this concentration was found to be toxic to the cells. Therefore lower concentrations

of 50 and 25 nM were tested alongside pooling all three RXFP-1 siRNA sequences at all three concentrations. RXFP-1 expression was detected by RT-PCR. 25 nM RXFP-1 siRNA was found to be effective at knocking down RXFP-1 expression normalised to GAPDH. Pooling the sequences was not found to be more effective then the single sequence used in LX-2 cells (figure 5.2a). Both predesigned negative control siRNA and RXFP-1 scrambled siRNA were transfected at the same concentrations and neither sequences significantly affected RXFP-1 expression, assessed by RT-PCR (figure 5.2a). Oligofectamine was the transfection reagent used in both LX-2 cells and primary HSC. Oligofectamine and the RXFP-1 siRNA oligo (100 nM) were added to HSC individually and their effect on RXFP-1 expression was also assessed by RT-PCR (figure 5.2a). Oligofectamine did not alter RXFP-1 expression but RXFP-1 siRNA, despite not having any transfection reagent present, induced a small reduction in RXFP-1 expression. Expression of RXFP-3 was assessed to ensure siRNA specifically down-regulated RXFP-1 whilst not effecting a close member in the relaxin family of receptors. RXFP-3 expression was not affected by 25 nM RXFP-1 siRNA transfection (figure 5.2b). All the results in this study are normalised to negative control siRNA transfected or non-transfected cells depending on the appropriate control. The negative control used in LX-2 cells was the predesigned sequence. RXFP-1 scrambled sequence was found to have the least effect on RXFP-1 expression in primary HSC and therefore all results in these cells are normalised to this negative control. RXFP-1 receptor was significantly knocked down by up to 90% in LX-2 cells (figure 5.2c i) and up to 70% in primary HSC (figure 5.2c ii) when quantified by qRT-PCR. LDH and MTS assays were carried out to determine the cell viability after siRNA transfection of primary HSC. There was a significant difference in LDH released comparing each condition to triton x treated (permeablised) cells, 24, 48 and 72 hours post transfection (figure 5.2c iii and iv). Therefore there was no significant release of LDH into the media from transfected cells indicating the cells were still viable. No significant change was observed in MTS cell viability for each condition tested in LX-2 cells (figure 5.2.c v) and primary HSC (figure

5.2.c vi), 48 hours post transfection. Once the knockdown had been confirmed and the off target effects and toxicity of the siRNA were controlled, siRNA transfected HSC were used to evaluate the phenotype of cells with a reduced expression of RXFP-1.

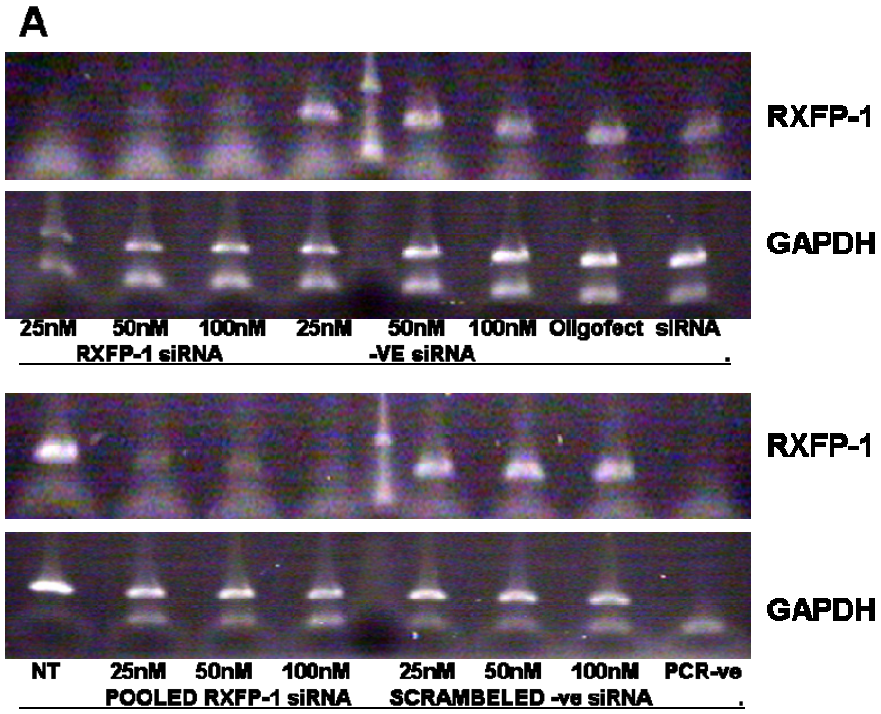

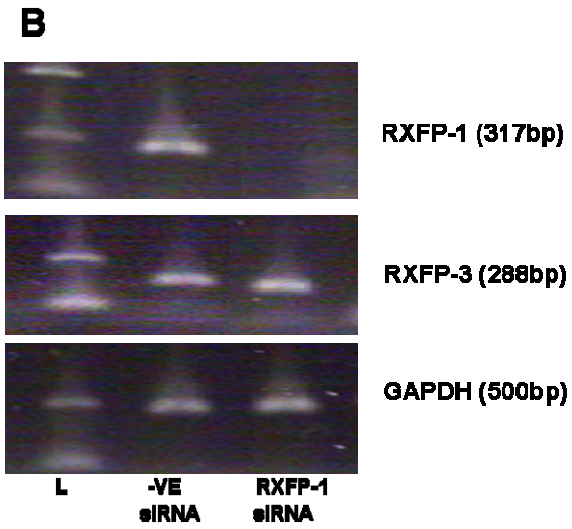

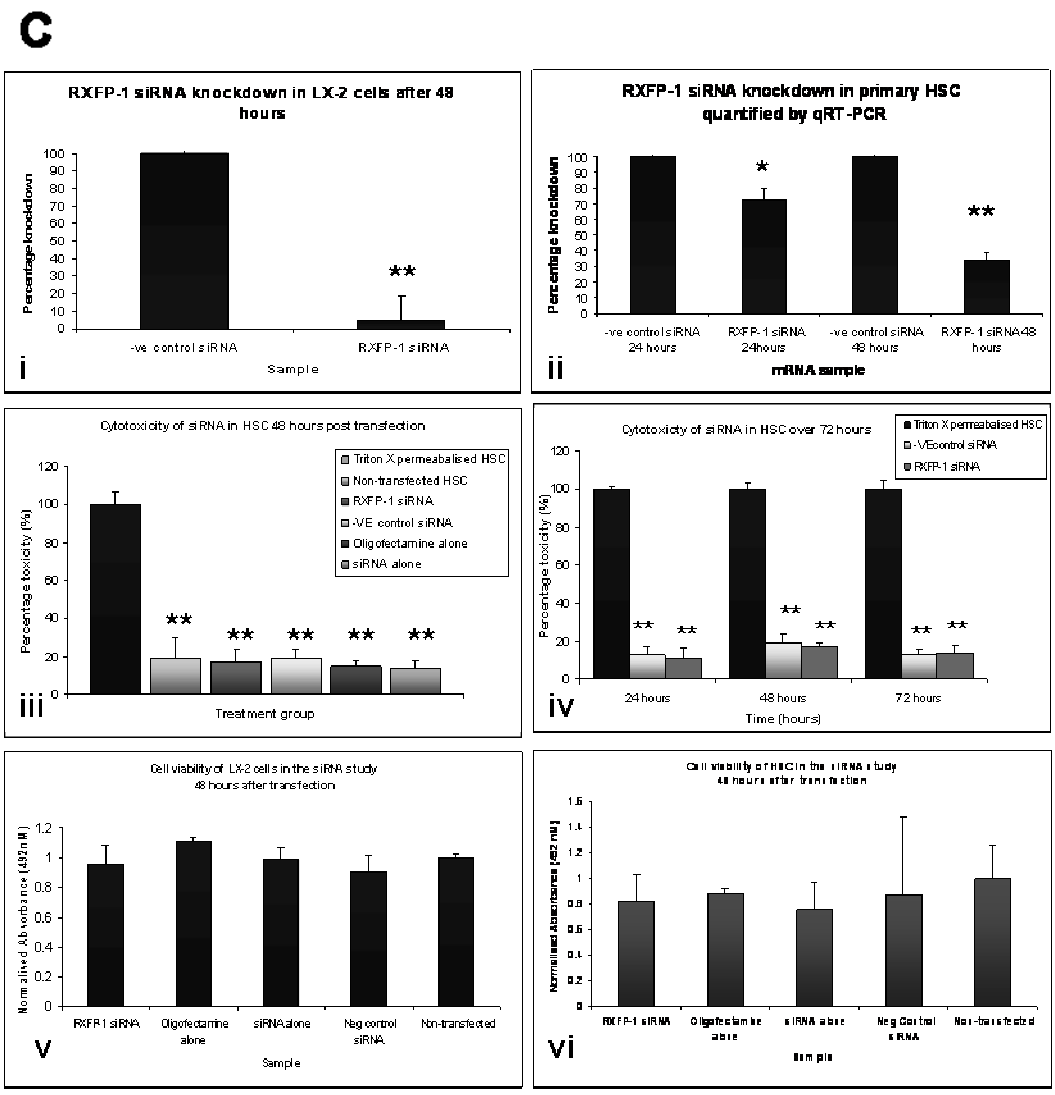

Figure 5.2. (A) Expression of RXFP-1 in primary HSC, 48 hours after different siRNA transfection conditions, assessed by RT-PCR and normalised to GAPDH expression (n=1). **(B)** Expression of RXFP-1 and RXFP-3 in primary HSC, 48 hours post 25 nM siRNA transfection, assessed by RT-PCR (n=3). **(C) (i)** Expression of RXFP-1 in LX-2 cells is significantly knocked down by 90% 48 hours post siRNA transfection ($p<0.01$), assessed by qRT-PCR (n=3). **(ii)** Expression of RXFP-1 in primary HSC is significantly knocked down by over 25% after 24 hours ($p<0.05$) and by 70% 48 hours ($p<0.01$) post siRNA transfection, assessed by qRT-PCR (n=3). **(iii)** LDH assay at 48 hours post transfection of primary HSC. The toxicity of RXFP-1 siRNA, negative control siRNA, oligofectamine without siRNA, and siRNA without oligofectamine were not significantly different compared to non-transfected cells but were significantly different

compared to triton x permeablised cells ($p<0.01$) (n=3). **(iv)** LDH cytotoxicity assays were carried out on primary HSC 24, 48 and 72 hours post transfection. Neither negative control siRNA or RXFP-1 siRNA exhibited over 20% cytotoxicity which was significantly different from triton x permeablised cells for each time point ($p<0.01$) (n=3). **(v)** MTS cell viability of LX-2 cells 48 hours post tranfection. Various conditions were compared including non-transfected, negative control siRNA, RXFP-1 siRNA, siRNA without oligofectamine and oligofectamine without siRNA. None of the conditions significantly reduced the cell viability of LX-2 cells (n=3). **(vi)** MTS cell viability of primary HSC 48 hours post transfection. None of the conditions significantly reduced viability of primary HSC (n=3).

5.3 cAMP assay using siRNA transfected primary HSC and LX-2 cells, evaluation of transfection efficiency

The cAMP response to H2-relaxin was abolished in LX-2 cells transfected with RXFP-1 siRNA (figure 5.3.a), indicating the amount of active receptor produced by the cells is reduced and the cells can no longer respond to H2-relaxin through the cAMP pathway. This suggests that the transfection efficiency was high since to the amount of active receptor at the membrane must have been reduced in the majority of the population transfected, otherwise there would still be a cAMP response in the cells that remained untransfected. The EC_{50} values for non-transfected (0.12 nM) and negative control siRNA (0.41 nM) are similar (figure 5.3.d), although the predesigned negative control used in LX-2 cells did reduce the Vmax or maximal cAMP response to H2-relaxin compared to non-transfected cells (figure 5.3.a). The cAMP response to H2-relaxin was also reduced in primary HSC transfected with RXFP-1 siRNA (figure 5.3.b), indicating the amount of active receptor produced by the cells is reduced and the cells therefore have a reduced response to H2-relaxin through the cAMP pathway. The EC_{50} values for RXFP-1 siRNA (1.7 nM), RXFP-1 scrambled siRNA negative control (4.7 nM) and non-transfected cells (7.6 nM) are comparable (figure 5.3.d) but the Vmax or maximal response is significantly reduced in the RXFP-1 siRNA transfected cells (figure 5.3.b). This result

indicates the transfection was not as efficent as in LX-2 cells, as there is some active receptor present in the transfected population. This may be due to poorer transfection efficiency as well as a reduced percentage knockdown compared to LX-2 cells (figure 5.2.c ii). Primary HSC transfected with RXFP-1 siRNA and negative control siRNA were still able to respond to forskolin (Forsk) by increasing the intracellular accumulation of cAMP compared to non-transfected cells (figure 5.3.c) and EC_{50} values were comparable (figure 5.3.d).

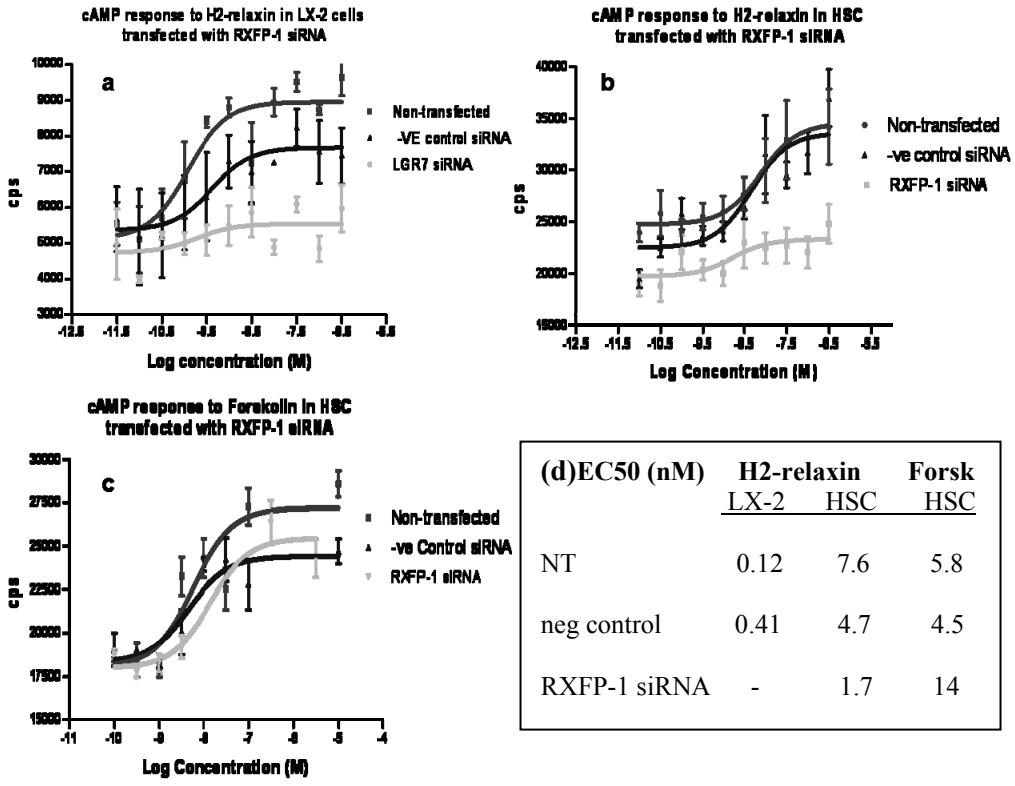

(d)EC50 (nM)	H2-relaxin		Forsk
	LX-2	HSC	HSC
NT	0.12	7.6	5.8
neg control	0.41	4.7	4.5
RXFP-1 siRNA	-	1.7	14

Figure 5.3. Examining the siRNA transfected cells response to H2-relaxin in the cAMP accumulation assay. **(a)** cAMP response to H2-relaxin in LX-2 cells transfected with RXFP-1 siRNA compared to non transfected and –ve control siRNA transfected cells. RXFP-1 siRNA transfected LX-2 cells had no response to H2-relaxin, suggesting a very high proportion of the cells were transfected. The predesigned negative control used in LX-2 cells caused a reduced Vmax cAMP response to H2-relaxin but this did not effect its EC_{50}. **(b)** RXFP-1 siRNA transfected primary HSC have a reduced cAMP response to H2-relaxin compared to –VE control siRNA transfected and non transfected cells.

The EC_{50} in RXFP-1 siRNA transfected cells was similar to the control cells but the Vmax was reduced by over 5-fold compared to either control suggesting a high proportion of the cells were transfected bearing in mind RXFP-1 was only knocked down by 70% at the mRNA level. The negative control siRNA used in this experiment was the scrambeled sequence of the RXFP-1 siRNA used to induce knockdown. Cells transfected with the new negative control siRNA sequence have no reduction in response to H2-relaxin compared to non-transfected cells, therefore this sequence was used for the remaining experiments carried out in primary HSC. **(c)** Confirmation through stimulation with forskolin that cells transfected with either RXFP-1 siRNA or the negative control siRNA do not lose their ability to accumulate intracellular cAMP in response to adenylate cyclase activation. **(d)** Table of EC_{50} values for the three conditions in both primary HSC and LX-2 cells.

5.4 Evaluation of the phenotypic changes observed in human HSC transfected with RXFP-1 siRNA after 72 hours H2-relaxin treatment

In chapter 4 gene expression changes were observed after 72 hours H2-relaxin treatment of primary HSC, the experiment was repeated comparing the expression of various fibrosis related genes in RXFP-1 siRNA transfected cells. Gene expression of pro-fibrotic genes such as α-SMA, TGF-β, CTGF, and TIMP-1 were all increased in RXFP-1 siRNA transfected cells after 72 hours H2-relaxin treatment, compared with negative controls. Results are expressed as fold changes compared to negative control siRNA transfected cells. The change in gene expression was significantly increased above 3-fold for α-SMA and CTGF, and above 2-fold for TGF-β, procollagen-1 and TIMP-1. MMP-2 was also significantly increased 2 fold when RXFP-1 expression was knocked down, whilst MMP-1 expression was significantly decreased by over 50%. These results are in contrast to H2-relaxin treated primary HSC in chapter 4, when α-SMA, TGF-β, CTGF, TIMP-1 and procollagen-1 were all down regulated, whilst MMP-1 was up regulated suggesting transcriptional regulation of these genes by H2-relaxin is dependent upon signalling through RXFP-1. MMP-2

was up regulated by H2-relaxin treatment but was also still up regulated in RXFP-1 siRNA transfected HSC in the presence of H2-relaxin. This result suggests the regulation of MMP-2 by H2-relaxin is not dependent on signalling through RXFP-1.

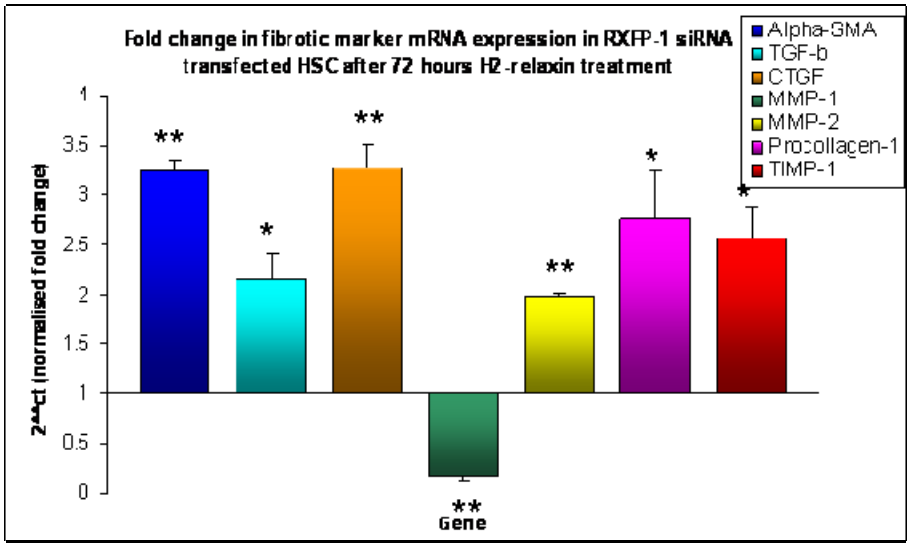

Figure 5.4. Gene expression profile of primary HSC transfected with RXFP-1 siRNA compared to negative control siRNA transfected primary HSC after 72 hours H2-relaxin treatment. α-SMA and CTGF were significantly up regulated by over 3 fold ($p<0.01$), TGF-β, procollagen-1 and TIMP-1 were significantly up regulated by over 2 fold ($p<0.05$), and MMP-2 was significantly up regulated by 2 fold ($p<0.01$). MMP-1 was the only gene that was down regulated by over 50% ($p<0.01$).

5.5 Investigation into the contractile properties of hHSC after transfection with RXFP-1 siRNA in the presence of H2-relaxin

5.5.1 Gel contraction assay with RXFP-1 siRNA transfected HSC

RXFP-1 siRNA transfected primary HSC were used in gel contraction assays to investigate the contractile properties of primary HSC with reduced signal transduction in response to H2-relaxin. Previously we have shown that H2-

relaxin reduces the contraction of HSC when cultured on collagen-1 gel. HSC contraction was measured indirectly as gel area and therefore H2-relaxin increases the area of the gel compared to untreated and endothelin-1 treated cells. RXFP-1 siRNA transfected cells in the presence of H2-relaxin did not significantly reduce the contraction of HSC, in fact the increase in gel area was completely abolished compared to non transfected and negative control siRNA transfected HSC after 24 or 72 hours (figure 5.5b). All results are normalised to untreated primary HSC and are expressed as fold changes. A significant 40% increase in gel area was still present in non-transfected and negative control siRNA transfected primary HSC after 72 hours H2-relaxin treatment. The siRNA knockdown of RXFP-1 was confirmed in the cells extracted from the gel after the completion of the contraction experiment. Significant 70% knockdown was still present in primary HSC extracted from the collagen gels after 72 hours assessed by qRT-PCR (figure 5.5c). H2-relaxin inhibits the contraction of primary HSC and the inhibition is abolished when the main receptor for H2-relaxin is knocked down. Therefore the anti-contractile properties of H2-relaxin appear to be dependent on the activation of RXFP-1.

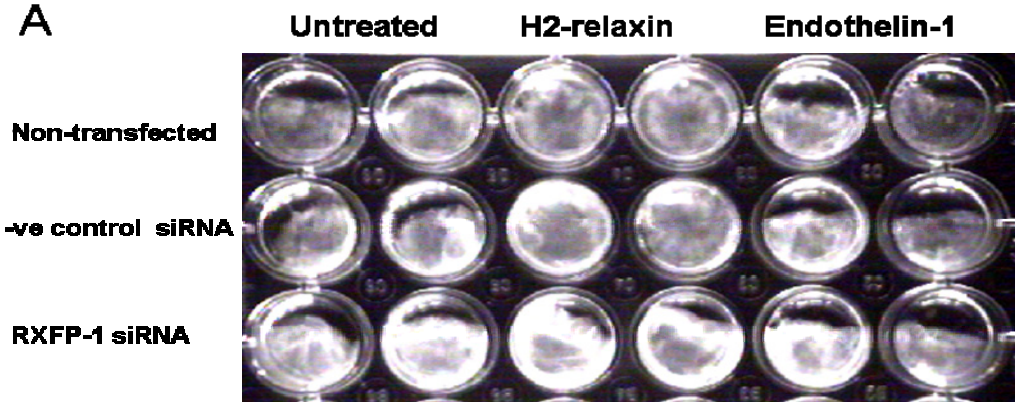

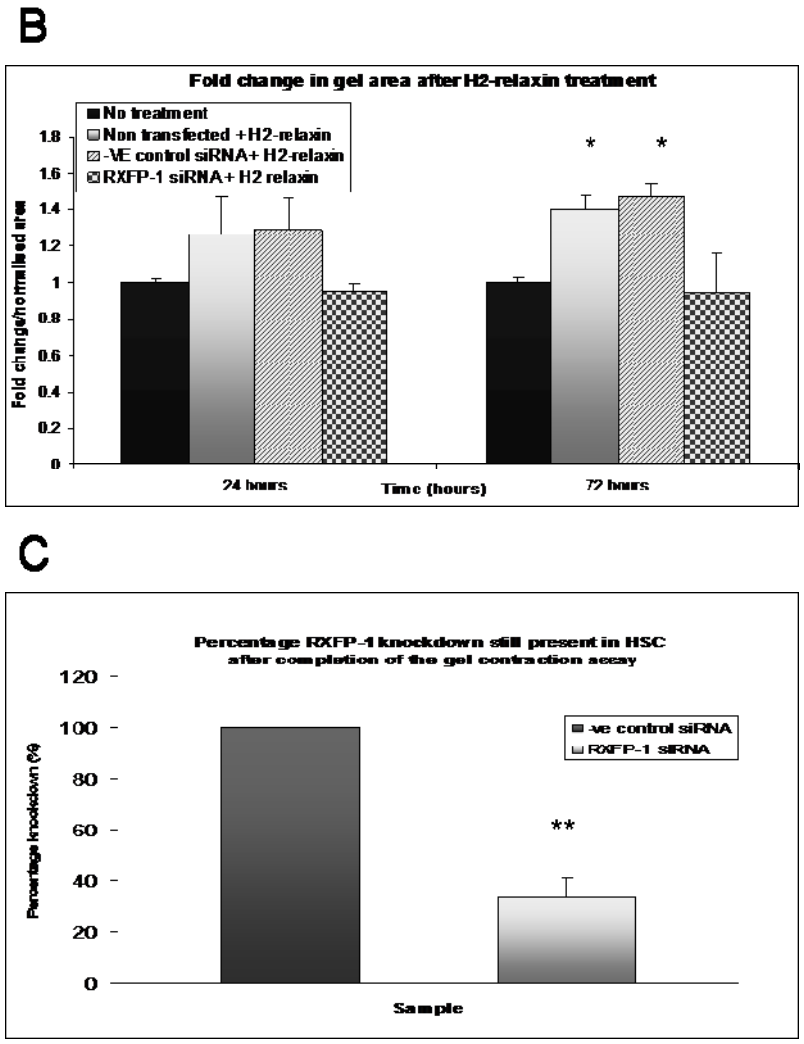

Figure 5.5. Gel contraction assays carried out with siRNA transfected HSC **(a)** Representative image of collagen gels in a 24 well plate after 72 hours, comparing RXFP-1 siRNA transfected, negative control transfected and non transfected cells that have been treated with H2-relaxin with untreated cells **(b)** Gel area was calculated using ImageJ software 24 hours and 72 hours after the gel release and fold changes in gel area are plotted on the histogram. H2-relaxin treatment significantly increases the gel area of both non-transfected and negative control siRNA transfected cells ($p<0.05$), but there is no increase in gel area of RXFP-1 siRNA transfected cells compared to untreated cells after 72 hours. **(c)** SiRNA knockdown of RXFP-1 in primary HSC that have been used in the gel contraction assay. To ensure the knockdown was present in cells after 72 hours culture on collagen-1 matrix, RNA was extracted from cells after isolation from

the collagen-1 gels. Over 60% knockdown of RXFP-1 was still present in the cells after the gel contraction assay was completed ($p<0.01$).

5.5.2 Secreted nitric oxide determination in RXFP-1 siRNA transfected primary HSC

The treatment of HSC with H2-relaxin had previously shown a 20% increase in the release of nitric oxide. Media samples removed from RXFP-1 siRNA transfected primary HSC in gel contraction assays were used to measure the level of nitric oxide release after 72 hours H2-relaxin treatment. Fold changes in nitric oxide release are normalised to non-transfected cells and compared to non-treated RXFP-1 siRNA transfected cells. Knockdown of RXFP-1 in primary HSC has abolished the increase in nitric oxide seen in H2-relaxin treated non-transfected cells (figure 5.6).

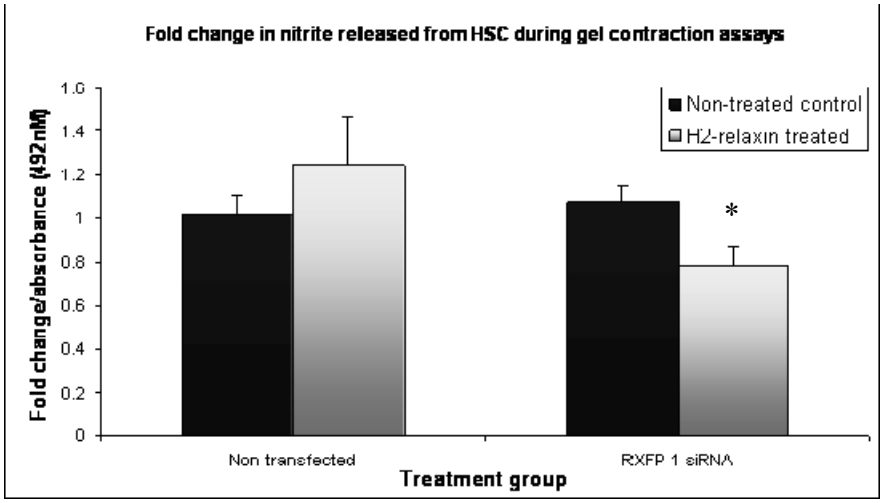

Figure 5.6. Nitric oxide level determination in gel contraction assays. Media was removed from the cells after completion of the gel contraction assay and the nitrite released into the media (stable metabolite of nitric oxide) over the course of the experiment was measured in a 96 well plate based assay. Nitric oxide release was increased 20 % in H2-relaxin treated cells but RXFP-1 siRNA transfected cells did not increase the nitric oxide released, which was conversely significantly reduced by over 20% compared to non-treated controls ($p<0.05$).

5.6 Summary of key findings

- RXFP-1 siRNA significantly reduces the expression of RXFP-1 by 90% in LX-2 cells and 70% in primary HSC. siRNA transfection did not reduce the viability of the cells but substantially reduced the cAMP response to H2-relaxin in both primary HSC and LX-2 cells.
- The down regulation of pro-fibrotic factors such as α-SMA, pro-collagen-1, TIMP-1, CTGF and TGF-β by H2-relaxin in human hepatic stellate cells is inhibited in RXFP-1 siRNA transfected cells.
- Primary HSC up regulate MMP-1 and MMP-2 in the presence of H2-relaxin. The up regulation of MMP-1 is inhibited by RXFP-1 siRNA transfection but MMP-2 continues to be up regulated to a similar extent suggesting MMP-2 is not regulated by signalling through RXFP-1.
- H2-relaxin inhibition of HSC contractility is reversed in cells transfected with RXFP-1 siRNA.
- The increase in nitric oxide in H2-relaxin treated HSC is reversed when RXFP-1 is knocked down.

5.7 Discussion

SiRNA experiments were designed to verify the effects of H2-relaxin in primary HSC were through RXFP-1 signalling. SiRNA knockdown of the receptor was achieved by transfecting with a transfection reagent specifically designed for introduction of siRNA. Three different RXFP-1 siRNA sequences were tested in LX-2 cells. Only one siRNA sequence was found to significantly knockdown the mRNA expression of RXFP-1. This siRNA sequence was then used to determine the most effective concentration. The most desirable concentration is the lowest concentration that gives the maximum knockdown, whilst having low toxicity. LX-2 cells were transfected with 100nM siRNA to achieve 90% knockdown measured by RT-PCR and qRT-PCR. Cell viability was unaffected

at this concentration. cAMP assays were used to assess transfection efficiency. RXFP-1 siRNA transfected LX-2 cells do not respond to H2-relaxin, there was no increase in cAMP detected whilst negative control siRNA transfected cells had a comparable EC_{50} to non-transfected cells. Negative control siRNA transfected LX-2 cells had a reduced Vmax response to H2-relaxin, showing the negative control siRNA sequence used in LX-2 cells was affecting the protein expression of RXFP-1. A different negative control siRNA sequence was used in primary HSC (a scrambled sequence of the RXFP-1 siRNA sequence). Primary HSC were transfected using the same conditions used in LX-2 cells. This initial experiment showed that although there was good knockdown in primary cells the cell viability was greatly reduced at 100 nM. Therefore the concentration of siRNA used to transfect primary HSC was optimised. Again the lowest concentration that gave the best knockdown and the least toxicity was chosen for the siRNA study in primary HSC. The same siRNA sequence that gave 90% knockdown in LX-2 cells was used to achieve significant 70% knockdown in primary HSC. The concentration of siRNA was reduced to 25 nM and this concentration was not toxic in primary HSC when compared to negative control siRNA and non-transfected cells. Therefore before experiments began in primary HSC a scrambled sequence of the RXFP-1 siRNA was designed. The new negative control siRNA was used in all of the primary HSC experiments and was shown to have very little effect on cell viability and off target effects. The off target effects were tested by determining the expression RXFP-3 assessed by RT-PCR. RXFP-3 is a closely related member of the relaxin receptor family and both the RXFP-1 siRNA and the negative control siRNA did not effect its level of expression. It is difficult to say that RXFP-1 and negative control siRNA sequences do not cause off target effects, to be able to make this statement a microarray analysis on as many genes as possible in transfected primary HSC would have to be carried out. These sequences do not reduce the cells viability and do not effect the expression of RXFP-3. Other closely related relaxin receptors in the family may have been up regulated in response to the knockdown of RXFP-1 to compensate. cAMP

assays were used to assess the transfection efficiency in primary HSC. The cAMP response to H2-relaxin in primary HSC was reduced in RXFP-1 transfected HSC.

cAMP assays showed that in both LX-2 cells and primary HSC the knockdown in expression of RXFP-1 reduced the accumulation of cAMP after H2-relaxin treatment. The experiment shows that a siRNA that can reduce the gene expression of RXFP-1 also reduces the functional protein expression and shows that H2-relaxin can increase the cAMP in primary HSC, specifically through the RXFP-1 receptor. The original Ambion negative control was used in the LX-2 cells and this showed a reduction in cAMP in response to H2-relaxin compared to non-transfected HSC. This is why the scrambled siRNA sequence was used for the primary HSC experiments and in the cAMP there was little reduction in response compared to non-transfected cells. To verify the reduction in cAMP was specific to the RXFP-1 receptor, the response to forskolin was recorded. Forskolin is a natural bicyclic hydrocarbon or labdane diterpene that is produced by the Indian coleus plant, coleus forskolin. It is commonly used to increase the intracellular levels of cAMP through its activation of adenylate cyclase in intact cell membranes and is a known hypotensive agent (Seamon et al., 1981). cAMP is important for the proper signal transduction/ biological response of many hormones. In these experiments forskolin was introduced to the primary HSC which had been transfected with RXFP-1 siRNA to establish if the cells could still increase the levels of cAMP in a dose dependent manner through a mechanism independent upon the activation of RXFP-1. If HSC could still respond to forskolin it would verify RXFP-1 siRNA transfected cells reduced the level of cAMP in response to H2-relaxin because of the decrease in active RXFP-1 at the cell membrane and not because of a loss of viability or cell membrane integrity.

RXFP-1 siRNA transfected HSC treated with H2-relaxin for 72 hours were used to investigate the expression of fibrotic markers compared to negative control

siRNA transfected HSC. The expression of αSMA, TGF-β, CTGF, procollagen-1, and TIMP-1 were all significantly increased by more then 2-fold when relaxin receptor RXFP-1 expression was decreased. The up regulation of the pro-fibrotic genes when H2-relaxin is unable to signal through RXFP-1 demonstrates H2-relaxin could have an important regulatory role in progression of fibrosis in the liver and other tissues that is dependent on the expression of RXFP-1. Gel contraction assays showed that RXFP-1 siRNA transfected primary HSC lost their ability to inhibit contraction after 72 hours H2-relaxin treatment. The increase in nitric oxide release was also inhibited by the knockdown of RXFP-1. RXFP-1 signalling appears to be important in inhibition of cell contraction in primary HSC, which may be through the increase in nitric oxide secretion. Therefore the suggested mechanisms of NO induction described in chapter 4 that were dependent upon the activation of RXFP-1, i.e. the increase in cAMP leading to transcriptional up regulation of NOS II and the phosphoylation of AKT by PI3-kinase leading to the activation of NOS III may be the mechanisms by which H2-relaxin induces nitric oxide secretion (Nistri and Bani et al., 2003; Sherwood., 2004). The phenotype described for HSC lacking RXFP-1 is a novel observation. Previous studies using RXFP-1 siRNA in different cancer cell types have shown that short term treatment with H2-relaxin induces cell motility and invasiveness, possibly due to the increased elastinolytic and ECM degrading phenotype. Increases in MMP-2 and MMP-9 have been described and all these effects were RXFP-1 dependent. Longer term treatment with H2-relaxin decreased proliferation of cancer cells and even in short term studies the proliferation of these cells was not increased only their invasive phenotype (Kamat et al., 2006;Hombach-Klonisch et al., 2006;Radestock et al., 2008). Reducing the expression of RXFP-1 in primary HSC reduces their collagen degrading/fibrolytic phenotype. Non-transfected cells treated with H2-relaxin increase their expression of MMP-1 and MMP-2 which is a similar to the findings in endometrial cancer cells (Kamat et al., 2006).

Many of the observations in chapter 4 revealing a less fibrotic phenotype in primary HSC after H2-relaxin treatment appear to be dependent upon the activation of RXFP-1. Primary HSC have a more fibrotic phenotype after RXFP-1 is knocked down, even in the presence of H2-relaxin. These studies suggest H2-relaxin has a role in regulating the fibrosis through down regulating activation of hepatic stellate cells, possibly through the down regulation of TGF-β and α-SMA (Heeg et al., 2005;Kharbanda et al., 2004). H2-relaxin can decrease fibrotic markers in pre-activated HSC suggesting H2-relaxin treatment of patients with pre-existing liver fibrosis could benefit due to the possible reversion HSC to a less fibrotic/activated phenotype. H2-relaxin also regulates HSC contraction, which could be through the deactivation of the cells as contraction seems to be dependent upon activation and expression of α-SMA (Rockey et al., 1993;Kharbanda et al., 2004) but also through the up regulation of nitric oxide (Bani et al., 2001). H2-relaxin may have a role in the treatment of portal hypertension as a vasorelaxant compound able to reduce the contraction of HSC, and reduce the build up of scar forming collagen, which will reduce the pressure on the portal vein that can become constricted in the fibrotic liver due to distorted architecture. Distorted architecture of the liver is due to excess collagen deposition originally in the space of disse, also reducing hepatic blood flow through the liver sinusoid which can be attributed to an increase in the number of activated HSC. Further studies need to be carried out to confirm the down stream signalling mechanisms involved in gene expression changes and regulation of cellular contraction by H2-relaxin through activation of RXFP-1.

Chapter 6

Localisation of the relaxin receptors in normal and fibrotic human kidney

6.1 Introduction

6.1.1 Introduction

In addition to potential roles in liver disease H2-relaxin may have a vasoactive role in the normal kidney and potential renal antifibrotic properties (Sherwood., 2004). Therefore H2-relaxin may ameliorate renal damage that has already occurred and help prevent any future damage occurring by decreasing renal vascular tone, increasing GFR and clearing any fibrosis/interstitial matrix build up that could be a consequence or cause of poor GFR. Its antifibrotic properties were initially tested in a model of scleroderma (Samuel et al., 2005c) and latterly using H2-relaxin knockout mice (Samuel et al., 2005b). Interestingly the knockout mice develop age related fibrosis of the kidney, heart, lung and reproductive tract (Samuel et al.,2005). Although there has been an interest in relaxin in the kidney for several years the receptor localisation profile has never been documented. The rationale behind the study was to map the receptor profile to try to gain a greater understanding and to be able to further hypothesise the role of relaxin and its receptors in kidney diseases. This could shed light on whether relaxin receptors would be a good therapeutic target in chronic kidney disease (CKD).

6.1.2 Hypothesis, Aims and Objectives

Hypothesis

Relaxin receptors are localised in different areas of the kidney and this expression pattern may change in fibrotic disease.

Aims

To establish relaxin receptor localisation in normal and fibrotic kidney

Objectives

- Localise relaxin receptors in normal and fibrotic kidney sections using immunohistochemistry
- Compare relaxin receptor localisation to markers of the specific structures using serial sections wherever possible.

6.2 Introduction to the kidney

6.2.1 Structure and function of the kidney

The kidneys are located in the retroperitoneum, weighing around 140 grams each they are vital for the excretion of the by products of metabolism. The kidneys convert over 1700 litres of blood into around 1 litre of urine everyday, this process is called ultrafiltration (Kumar et al., 2005; Chandrasoma and Taylor., 1998). The kidneys have developed a high degree of structural complexity to enable them to filter out the waste products of metabolism from the blood, to precisely regulate the body's concentration of salt and water, also maintaining the acid balance of plasma and secreting hormones such as renin and prostaglandins that are essential for the kidneys function. The human kidney is made up of cortex and medulla (Kumar et al., 2005). The kidneys have a rich supply of blood when considering they make up only 0.5% of the total body they receive 25% of total cardiac output. The cortex is highly vascularised receiving around 90% of the total renal blood supply. The main renal artery divides the anterior and posterior sections at the hilum. The arteries in the kidney are usually end arteries and occlusion of any branch may cause infarction of the area it supplies. The anatomical unit of the kidney is the nephron, composed of the glomerulus, proximal convoluted tubule, loop of henle, distal convoluted tubule and collecting tubule with each kidney containing around 1 million nephrons. These structures can be visualised in kidney sections when stained with H+E (figure 6.1). If considering the kidney from the perspective of diseases it can be subdivided into four components, blood vessels,

glomeruli, tubules and interstitum (Kumar et al., 2005, Chandrasoma & Taylor., 1998).

The glomerulus is composed of afferent and efferent arterioles, intervening capillaries that are lined by fenestrated endothelial cells (the glomerular tuft), the outer surface of the capillaries are lined by epithelial cells called podocytes which are continuous in the Bowmans Space and proximal tubule, the mesangium which consists of mesangial cells (the kidneys resident myofibroblasts), matrix and basement membrane (Chandrasoma and Taylor., 1998). Ultrafilatration of plasma occurs in the glomerular capillaries by the glomerular basement membrane (GBM). The GBM has a thick electron dense central layer called the lamina densa. The peripheral layers, called the lamina rara interna and the lamina rara externa are thinner electron lucent layers. The GBM consists of collagen (mostly type IV), laminin, polyanionic proteoglycans (mostly heparin sulphate), fibronectin, entactin and several other glycoproteins. Collagen IV forms a suprastructure framework to which the other glycoproteins such as laminn and entactin attach (Timpl and Brown, 1996;Timpl, 1996). The process is driven by hydrostatic pressure and the normal glomerular filtration membrane forms a barrier to molecules in the plasma based largely on molecular weight and charge of the particles. The acidic porous nature of the GBM determines its permeability characteristics and the charge dependent restriction of the GBM is extremely important in the exclusion of molecules, such as albumin, due to its anionic nature (Miner, 1999). Glomerular filtration rate (GFR) is around 120 ml/min, up to 80% of the ultrafiltrate is actively absorbed in the proximal tubule and molecules such as potassium, glucose and amino acids are completely reabsorbed. The proximal tubule is particularly vulnerable to ischemic damage as well as being susceptible to chemical damage due to the toxins that it frequently has to reabsorb (Dajak et al., 2008).

The tubules vary considerably at different levels in the nephron, to a certain extent correlating with function. The distal and collecting tubules are largely

concerned with water and sodium reabsorption under the control of an antidiruetic hormone called ADH or Vasopressin, as it is sometimes referred, which is under the control of the renin-angiotensin system (Madsen et al., 1988b). The filtrate that passes into the loop of henle is concentrated by the counter current multiplier, which increases the concentration gradient allowing more water to passively diffuse from the Loop of Henle which then encourages active reabsorption of sodium ions. Of the 120 ml/min of filtered blood only 1-2 mls is lost as urine. Urine is acidified and although the kidneys only excrete 1% of the acid excreted via the lungs as carbon dioxide and carbon monoxide everyday, if this mechanism fails metabolic acidosis can occur (Madsen et al., 1988b;Madsen et al., 1988a).

The entire glomerular tuft is supported by mesangial cells lying between capillaries. The mesangial matrix is a meshwork where the mesangial mesenchymal cells are centred. Mesangial cells are contractile, phagocytic and capable of proliferation, and are able to excrete ECM, including fibrilar collagens and biologically active mediators. The mesangial cells are quiescent in the normal kidney and will become activated under pathogenic or tissue remodelling conditions (Sterzel et al., 1993). They are important mediators in conditions such as glomerular nephritis. Mesangial cells can be compared to the HSC in the liver and although they do not store vitamin A when quiescent they have a similar role in the life cycle of the tissue. The interstitum is an important component of the normal cortex. The interstitium space is normally compact and occupied by fenestrated capillaries and a small number of fibroblast like cells (Kaissling and Le Hir., 2008). If there is any obvious macro or microscopic expansion of the interstitum this usually indicates abnormality. Expansion of the interstitium can be caused by oedema, inflammation and accumulation of chronic inflammation leading to fibrous matrix and tissue deposition (Kaissling and Le Hir., 2008). Presence of proteoglycans in the interstitial tissue of the medulla increases with age and in the presence of ischemia (Sterzel et al., 1993;Sterzel et al., 1992).

6.2.2 Chronic kidney disease (CKD)

Chronic kidney disease (CKD) is characterised by severely reduced glomerular filtration rate. It has many different aetiologies and an increasing worldwide prevalence. Currently worldwide over 1.2 million individuals are undergoing dialysis treatment for end stage kidney failure, with reported annual growth rates of between 5-8%. The statistics get worse when you also consider the population diagnosed with CKD but not undergoing dialysis. The prevalence in the US is an estimated 11% of the adult population, with similar results in the UK and Australia. The prevalence is much less in China with only a reported incidence of 2.53%. There are obvious differences in cohort, ethnicity and methods of data collections but it is evident that CKD is a worldwide health problem with significant repercussions (Eknoyan et al., 2004).

Nephrotic syndrome and renal fibrogenesis are two of the conditions that are included in CKD and both can be induced by several mechanisms. Nephrotic syndrome is characterised by proteinuria, hypoalbuminemia, hyperlipidemia, oedema and in a small number of cases hypertension. In adults the most common causes are membranous glomerulonephritis (MGN), focal segmental glomerularsclerosis (FSGS) and minimal change disease (MCD) (or lipoid nephrosis). All of these diseases affect the glomeruli of the kidneys and more specifically the podocyte (Mathieson, 2007;Saha and Singh, 2006;Daskalakis and Winn, 2006;Cattran, 2003). Podocytes (or visceral epithelial cells) form a crucial component of the glomerular filtration barrier, located on the outer epithelial membrane of the glomerular basement membrane. They contribute to size selectivity and maintenance of the filtration surface (Asanuma et al., 2007). Adjacent podocytes interdigitate to cover the basal lamina which is intimately associated with the glomerular capillaries, but also leaves thin filtration slits. The slits formed by the podocytes are covered by a slit diaphragm, which is composed of many different cell surface proteins including nephrin, p-cadherin and podocalyxin. This ensures that large macro-molecules such as albumin

remain in the blood stream. Small molecules such as water, glucose and ionic salts are able to pass through, forming an ultrafiltrate that is then processed as urine. Disruption of the slit diaphragm and/or disruption of the podocyte can lead to massive proteinuria as observed in MCD (Faul et al., 2007). Podocytes have several features that indicate a high rate of vesicular traffic, many coated vesicles and coated pits can be observed along the basolateral domain of the podocytes. Podocytes possess a well developed endoplasmic reticulum and a large golgi, which is indicative of a high capacity for protein synthesis and post translational modifications. There is also evidence that the podocytes have endocytic activity due to the large number of multivesicular bodies and other lysosomal components seen in the cells. Podocytes have an interesting morphology including pedicels or "foot processes" which extend to increase the surface area of the cells and can be seen using electron microscopy. Podocytes are therefore critical for the maintenance of size selective diffusions barriers and can synthesise GBM components (Asanuma et al., 2007;Faul et al., 2007). There are diseases that can cause destruction of the podocyte or diseases that can drive them into proliferation causing them to lose their normal function.

6.3 Results-Relaxin receptor localisation in normal and fibrotic kidney

As mentioned above relaxin receptors have not been mapped in human kidney and therefore, antibodies to all four relaxin receptors were used to immunohistochemically stain normal and fibrotic kidney sections described below. Lectins and antibodies that have been previously recorded to specifically stain structures such as the proximal tubules (lotus tetregonolobus antigen (LTA), distal tubules (epithelial membrane antigen (EMA)), podocytes (VEGF and synaptopodin) and activated fibroblasts (α-SMA) were used in series with the relaxin receptor antibodies to enable us to localise the staining to a particular structure or cell type.

6.3.1 H+E and Sirius red staining of normal and fibrotic kidney

To carry out the study serial sections were cut from paraffin embedded specimens that had been graded as normal and mildly fibrotic by a consultant pathologist. Tissue was collected in accordance with the human tissue act 2004. The sections were stained with H+E and Sirius red to ensure the different structures could be identified and a difference between the normal and fibrotic sections could be observed.

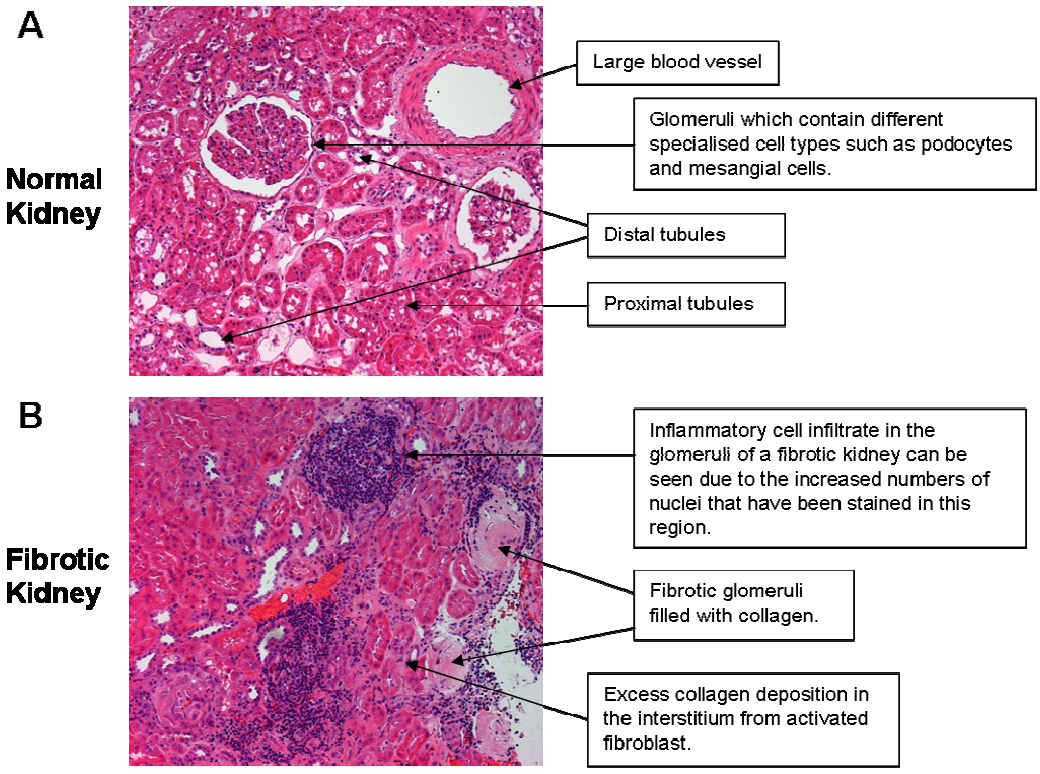

Figure 6.1. (A) H+E stain of a paraffin embedded normal human kidney section detailing different parts of the nephron. **(B)** H+E stain of a paraffin embedded fibrotic human kidney section detailing inflammation and areas of scarring.

6.3.2 Sirius red staining of normal and fibrotic kidney sections

Normal and fibrotic kidney sections were stained with sirius red to determine the level of collagen build up in the fibrotic sections (figure 6.2.). Sirius red stains collagen and under polarised light specifically collagen-1 and collagen-III fibres can be detected. The Sirius red stain detected more collagen build up in the fibrotic section.

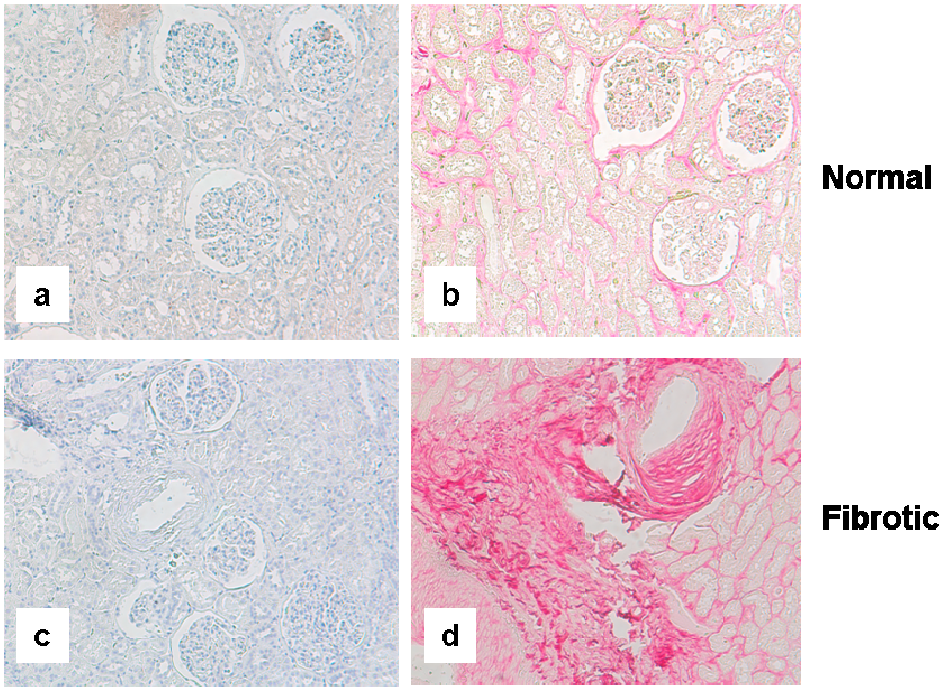

Figure 6.2. (a) Representative normal kidney –ve control section (b) representative sirius red stain of a normal kidney section (c) representative fibrotic –ve control section (d) representative Sirius red stain of fibrotic kidney section. Sirius red dye will stain collagen and the fibrous collagen-1 and collagen-III can be detected under polarised light. It is apparent that the level of fibrous collagen being laid down in the fibrotic kidney is increased compared to the normal kidney section (n=3). All images were taken with an Zeiss 10x objective using Zeiss Axioskop software.

6.3.3 RXFP-1 localisation in normal and fibrotic kidney

In the normal kidney RXFP-1 was localised most strikingly to the podocytes in the glomerular basement membrane (figure 6.1.). The staining pattern was confirmed by a pathologist and with serial staining with VEGF-C1 and synaptopodin, which are both podocyte markers. The proximal and distal tubules also appear to be positively stained but this was thought to be background staining as it was much weaker then the stain taken up in the podocytes.

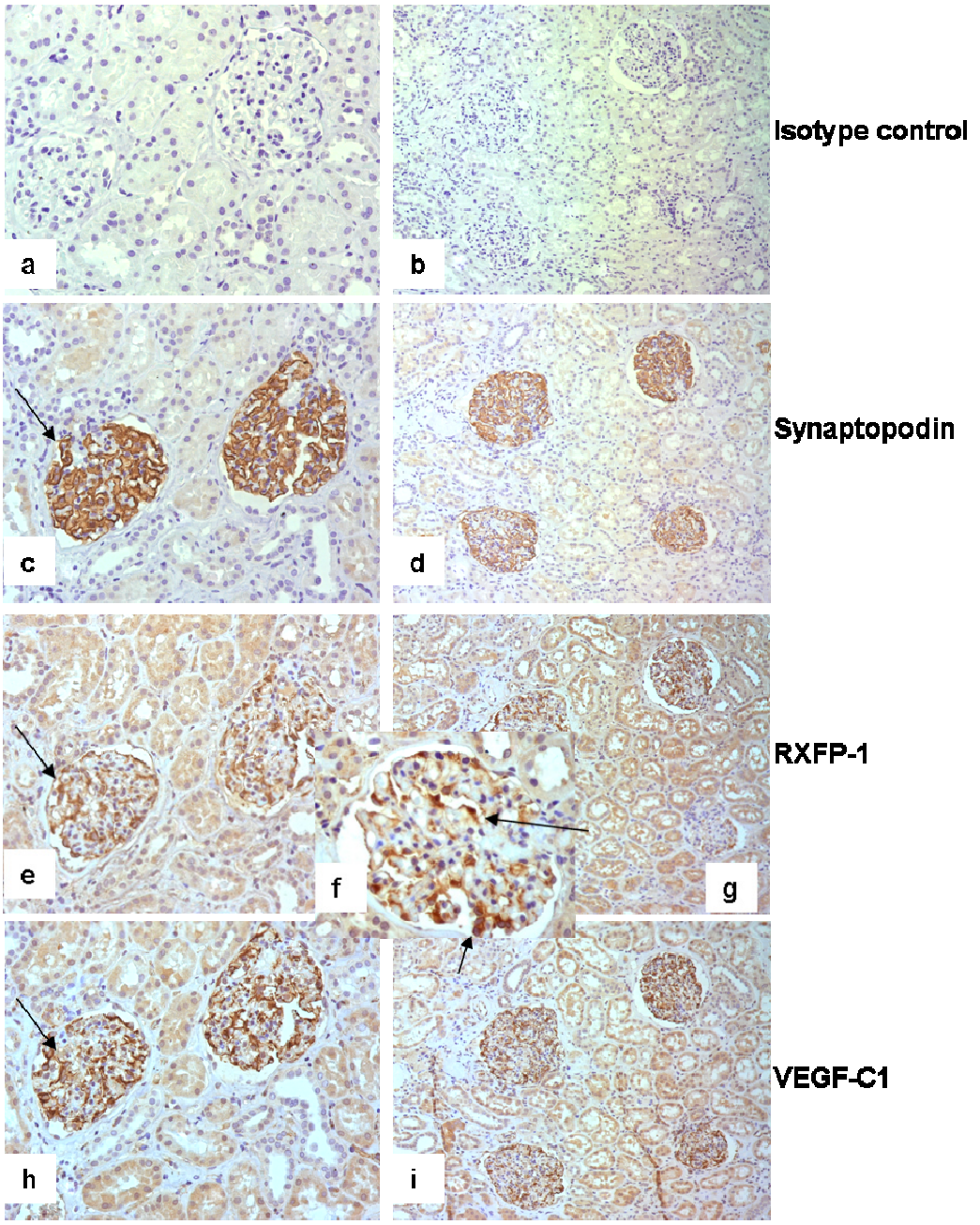

Figure 6.3. RXFP-1 localisation in normal kidney assessed by immunohistochemistry, in series with synaptopodin and VEGF-C1 which are both podocyte markers **(a)** rabbit isotype control of normal kidney at 20 x objective **(b)** rabbit isotype control of normal kidney at 10 x objective **(c)** synaptopodin (1/20) staining of normal kidney at 20 x objective. The arrow indicates positive staining of the podocytes in the glomerular basement membrane **(d)** synaptopodin staining of normal kidney at 10 x objective **(e)** RXFP-1 (1/600) staining of normal kidney at 20 x objective. The arrow indicates

positive staining of the podocytes **(f)** expanded image of glomeruli stained RXFP-1 (40 x objective), the arrow indicates positive staining of the podocytes in the glomerular basement membrane **(g)** RXFP-1 staining of normal kidney at 10 x objective **(h)** VEGF-C1 (1/200) staining of normal kidney at 20 x objective, the arrow indicates positive staining of podocytes in the glomerular basement membrane **(i)** VEGF-C1 staining of normal kidney at 10 x objective. All images were taken using Zeiss Axioskop software (n=4 different patients for all antibodies).

In the fibrotic kidney RXFP-1 was again localised in the podocyte but the staining of the distal tubules now appears to be positive compared to the background staining in the proximal tubules. Again staining was confirmed by a pathologist and by comparing the staining to a distal tubule (EMA) and podocyte (VEGF-C1) marker. Therefore comparing normal and fibrotic kidney, RXFP-1 is localised in the podocytes and the distal tubules begin to express more RXFP-1 in fibrosing kidney.

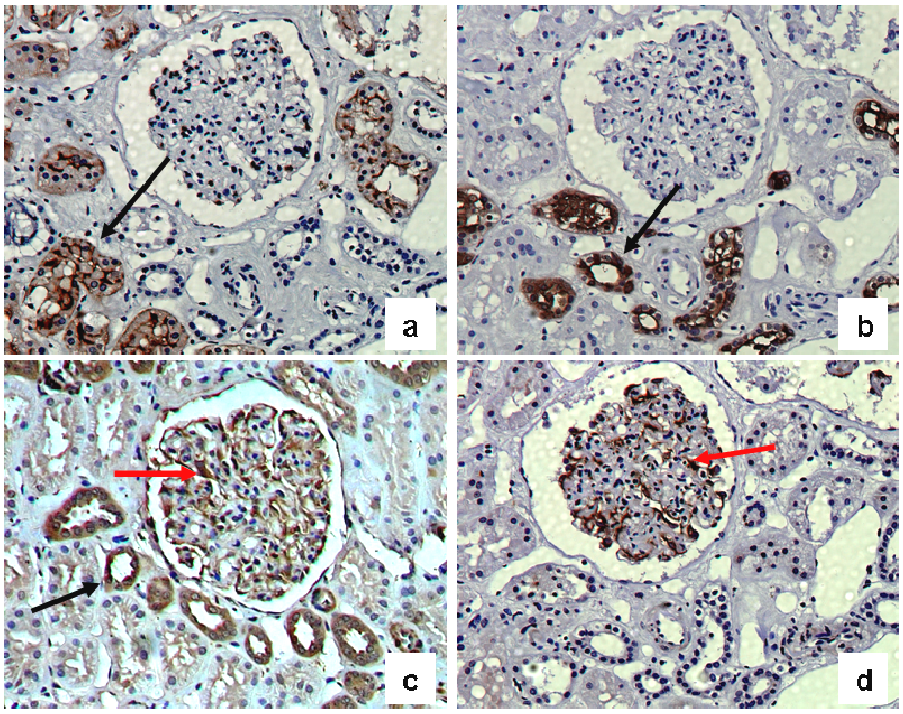

Figure 6.4. RXFP-1 localisation in fibrotic kidney, assessed by immunohistochemistry, comparing staining with a proximal tubule marker (LTA), a distal tubule marker (EMA)

and a podocyte marker (VEGF-C1) (a) LTA (1/3000) staining of fibrotic kidney, arrow indicates positive staining of a proximal tubule (b) EMA (1/300) staining of fibrotic kidney, arrow indicates positive staining of a distal tubule (c) RXFP-1 (1/600) staining of fibrotic kidney, red arrow indicates positive staining of podocytes and the black arrow indicates positive staining of a distal tubule (d) VEGF-C1 (1/200) staining of a fibrotic kidney, red arrow indicates positive staining of podocytes. All images were taken with a Zeiss 20 x objective using Zeiss Axioskop software (n=3 for all antibodies in the same patient).

6.3.4 RXFP-2 localisation in normal kidney

In the normal kidney RXFP-2 was localised in the proximal tubules, compared to proximal tubule marker LTA. The localisation did not change in fibrotic kidney.

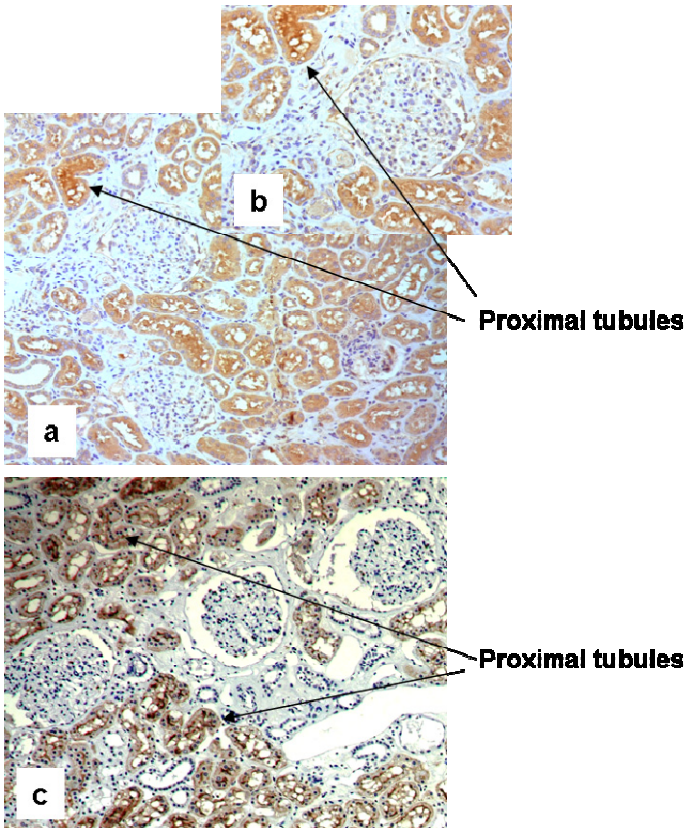

Figure 6.5. (a) RXFP-2 (1/200) localisation in normal human kidney, assessed by immunohistochemistry **(b)** expanded image of RXFP-2 localisation. RXFP-2 appears to

be localised in the proximal tubules when compared to LTA staining, a proximal tubule marker **(c)** LTA staining of normal human kidney section. Images were taken with Zeiss 10 x objective using Zeiss Axioskop software (n=3 for both antibodies in different patients).

6.3.5 RXFP-3 localisation in normal and fibrotic kidney

RXFP-3 was localised in the interstitium. Fibroblasts are the main cell type that occupy the intersitium which are important in maintaining the structure of the kidney through extracellular matrix turnover/remodelling. α-SMA is a fibroblast marker and positively stains the intersitium which is comparable to RXFP-3 staining.

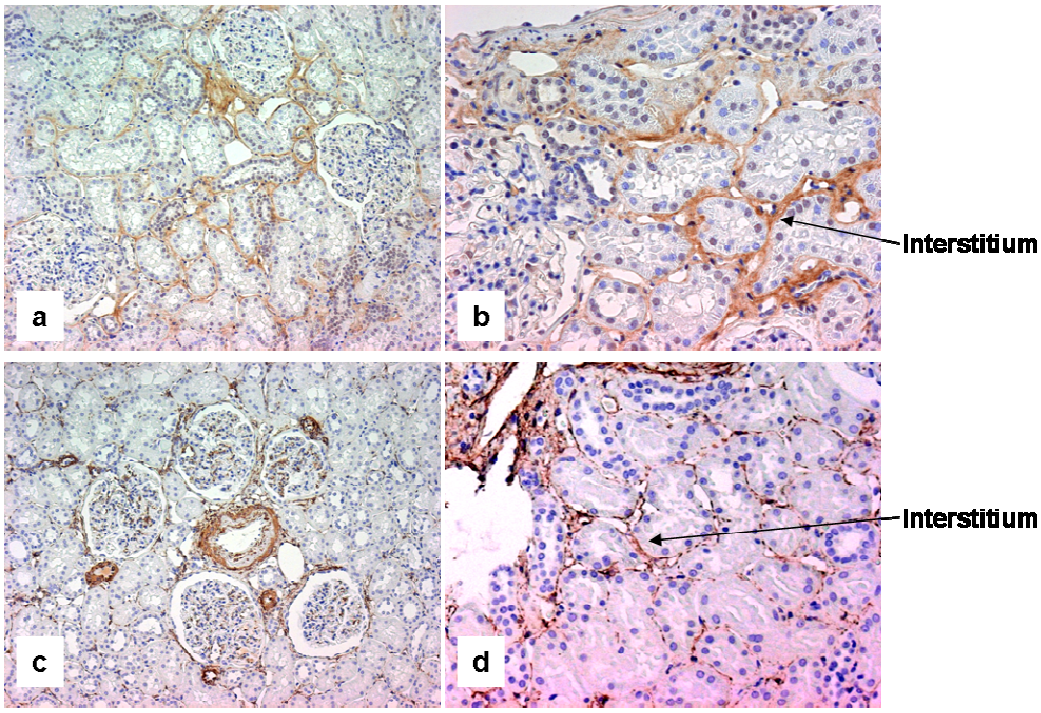

Figure 6.6. RXFP-3 localisation in normal kidney assessed by immunohistochemistry, comparing staining with a fibroblast marker α-SMA **(a)** RXFP-3 (1/400) staining of normal kidney at 10 x objective **(b)** RXFP-3 staining of normal kidney at 20 x objective. RXFP-3 positively stains the intersitium, which could be localised to fibroblasts **(c)** α-SMA (1/40,000) staining of normal kidney at 10 x objective **(d)** α-

SMA staining of normal kidney at 20 x objective. α-SMA positively stains the fibroblasts in the intersitium as well as areas of smooth muscle such as arteries. Images were taken using Zeiss Axioskop software (n=4 for both antibodies in different patients).

RXFP-3 was again localised in the interstitium in fibrotic kidney. The staining is comparable to α-SMA which appears to have an increased expression in fibrotic kidney. The increase in expression may be due to the increase in the number of fibroblasts which become activated in fibrosis, causing an increase in proliferation and therefore ECM deposition. α-SMA was also localised in the glomerli, which could be the mesangial cells which are the equivalent to stellate cells in the liver. Mesangial cells can also become activated in fibrosis to a myofibroblast-like cell, which is then positively stained by α-SMA (Sterzel et al., 1993).

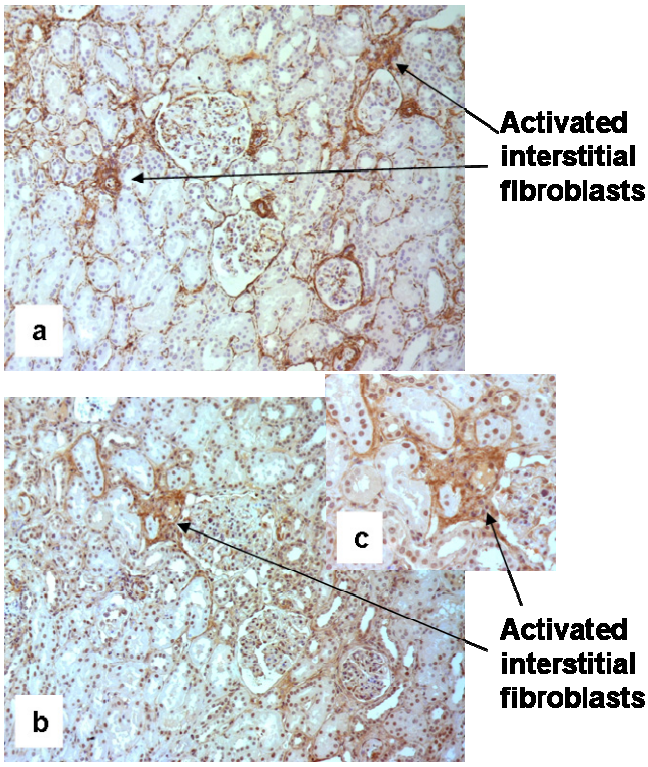

Figure 6.7. RXFP-3 localisation in fibrotic kidney serial sections, assessed by immunohistochemistry **(a)** α–SMA (1/40,000) staining of fibrotic kidney, arrows

indicate positive staining of interstitial fibroblasts which become activated in fibrosis **(b)** RXFP-3 (1/400) staining of fibrotic kidney, arrows indicate areas of positive staining which are comparable to α–SMA staining of activated interstitial fibroblasts **(c)** expanded image of RXFP-3 staining. Images were taken with a Zeiss 10 x objective using Zeiss Axioskop software (n=3 for both antibodies in the same patient).

6.3.6 RXFP-4 localisation in normal kidney

RXFP-4 was localised in the distal tubules in normal kidney. The staining was strongly and specifically positive in the distal tubules, which is confirmed by a pathologist and by comparing the expression to a distal tubule marker (EMA). The localisation did not change in fibrotic kidney.

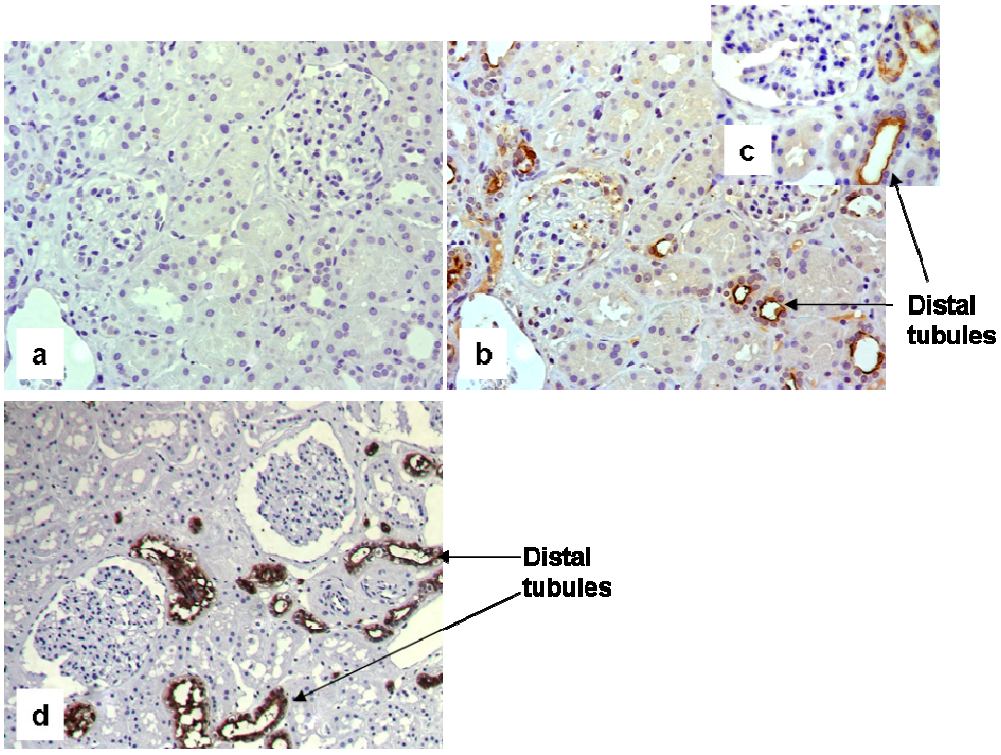

Figure 6.8. RXFP-4 localisation in normal kidney assessed by immunohistochemistry **(a)** rabbit isotype control **(b)** RXFP-4 (1/50) staining of normal kidney at 20 x objective. The arrows indicate RXFP-4 is localised in the distal tubules **(c)** expanded image of RXFP-4 staining (40 x objective) **(d)** EMA (1/300) staining of normal kidney at 20 x

objective, which is localised in the distal tubules. Images were taken using Zeiss Axioskop software (n=4 for both antibodies in different patients).

6.4 Summary of key findings

- RXFP-1 is localised in the podocytes of both normal and fibrotic kidney but is also localised in the distal tubules of fibrotic kidney.
- RXFP-2 is localised in the proximal tubules in both normal and fibrotic kidney.
- RXFP-3 localised to the interstitial fibroblasts in both normal and fibrotic kidney. The staining is more apparent in fibrotic kidney, which has activated fibroblasts in the interstitium.
- RXFP-4 is localised in the distal tubules of both normal and fibrotic kidney.

6.5 Discussion

Relaxin receptor localisation has been mapped in normal and fibrotic kidney using immunohistochemistry. The most definitive findings were that RXFP-1 localised in podocytes and RXFP-3 localisated in the interstitial fibroblasts. Podocytes are an important component of the glomerular filtration barrier and are therefore important in maintaining glomerular filtration rate (GFR). H2-relaxin the ligand for RXFP-1 has vasorelaxant properties. I have found these properties can regulate cellular contraction in HSC and therefore a possible role for RXFP-1 in the podocyte, may be the regulation of cellular contraction. This could alter the filtration rate through the glomerular basement membrane. I have also found H2-relaxin, through the activation of RXFP-1 can up regulate HSC apoptosis, therefore decreasing cell viability of activated myofibroblasts. In some diseases podocytes can begin to proliferate unchecked which causes the breakdown of the basement membrane and therefore modifies the GFR, causing protein loss and metabolic imbalance. H2-relaxin through the activation of

RXFP-1 may regulate the proliferation of podocytes, helping to regulate GFR and maintain homeostasis in the kidney. It would be interesting to examine relaxin receptor expression patterns in specific diseases that are known to display glomerular cellular changes such as minimal change disease (MCD), a disease that affects podocytes directly, focal segmental glomerular sclerosis (FSGS) and membranous glomerular nephritis (MGN) (Mathieson, 2007;Saha and Singh, 2006;Daskalakis and Winn, 2006;Cattran, 2003). RXFP-1 was also found in the distal tubules in fibrotic kidney, H2-relaxin may have a role in regulating fibrosis in the kidney through the activation of RXFP-1 (Samuel et al., 2005; Sherwood., 2004) and therefore up regulation of the receptor in fibrosis is an interesting finding that should be investigated further as it suggests that treatment with H2-relaxin could have potential as a therapeutic in the kidney.

RXFP-3 localisation in the interstitial fibroblasts suggests H3-relaxin may have a role in regulating fibrosis in the kidney. The role of H3-relaxin in fibrosis is undocumented and therefore we do not know if it will have a pro or anti-fibrotic effect. The receptor is negatively coupled to cAMP and therefore could have an opposing role to RXFP-1. An investigation into the phenotype of interstitial fibroblasts in culture after treatment with H3-relaxin could help to elucidate the role of RXFP-3 in kidney fibrosis. RXFP-2 is localised in the proximal tubules and RXFP-4 is localised in the distal tubules, which could suggest a role for these receptors in regulating filtration in the nephron but to fully elucidate the function of these receptors in the kidney further work needs to be carried out. Primary cultures of tubule epithelial cells could be examined in their responses to H2-relaxin, INSL3 (RXFP-2 ligand) and INSL5 (RXFP-4 ligand). The localisation of relaxin ligands could also be investigated to determine if the activation of the receptors is through autocrine, paracrine or endocrine sources.

Chapter 7

Final Discussion

7.1 Final Discussion

This study has shown that relaxin could have a role in the regulation of fibrotic liver disease in humans (figure 7.1). RXFP-1, 3 and 4 are expressed and functional in primary human HSC. RXFP-1 expression was confirmed using immunocytochemistry and the receptor was found to be expressed in activated primary HSC at the membrane. RXFP-2 gene expression is only detected in late passage HSC and the expression was very weak. Late passage HSC may have changed their phenotype significantly compared to freshly isolated cells. RXFP-1 and RXFP-2 have previously been shown to be expressed by rat HSC (Bennett et al., 2007) but the expression of RXFP-3 and RXFP-4 has not been reported in human HSC. The presence of functional receptors was established using cAMP assays and the EC_{50} values each relaxin ligand was determined. The concentration of H2-relaxin used in the functional experiments did not cross react with the other relaxin receptors present in HSC. RXFP-3 and RXFP-4 are negatively coupled to cAMP, unlike RXFP-1 and may have opposing effects when activated. RXFP-1 expression is up regulated in activated HSC, expression was assessed at different passage after extraction. The activation of the cells was evaluated by α-SMA protein expression. RXFP-1 gene expression correlated with the increase in α-SMA protein expression. RXFP-1 gene expression was also up regulated in CCl_4 injured rat liver (appendix 1). Expression of RXFP-1 decreases when HSCs are cultured on a basement membrane like substrate (Matrigel). Culture on Matrigel deactivated primary HSC, which was assessed by expression of fibrotic markers such α-SMA and TIMP-1. Deactivation of HSC cultured on Matrigel had been shown in a previous study (Gaca et al., 2003). This suggests that relaxin receptor expression increases in the injured liver when HSC become activated but expression remains undetectable in quiescent HSC. RXFP-1 was localised to areas of scarring in human liver sections, suggesting protein expression is also up regulated in activated HSC *in vivo*. Up regulation of RXFP-1 suggests a role for H2-relaxin in the regulation activated HSC. Activation of HSC is required

for the reversal of injury in the liver, this injury may be acute or sustained. Acute injury is common and only when the injury is sustained does the response become fibrotic. Therefore activated HSC require a signal, after activation in acute or sustained injury, to either revert back to quiescent cells or undergo apoptosis (Iredale et al., 1998). Activation of the RXFP-1 receptor through stimulation with H2-relaxin in activated HSC initiated a change to a less fibrotic phenotype in HSC. HSC express high amounts of TIMP-1, collagen-1 and α-SMA when cultured on plastic. Treating HSC with H2-relaxin for 72 hours caused a decrease in TIMP-1, collagen-1, α-SMA, TGF-β and CTGF, therefore reducing the fibrotic phenotype whilst also increasing the expression of MMP-1 and MMP-2. MMP-1 is the main interstitial collagenase and the increase in MMP-1 will facilitate the breakdown of collagen-1, the main fibril forming collagen in the fibrotic liver. MMP-9 was found to be up-regulated in the cytokine array analysis, although MMP-3 and MMP-13 were unchanged. MMP-2 and MMP-9 can have pro and anti-fibrotic roles depending on the level of expression and time of expression during the progression of liver fibrosis. Induction of MMPs by relaxin has been reported by many groups. Induction of MMP-1, MMP-2, MMP-3, MMP-9, MMP-12 and MMP-13 have been reported in various cell and animal models (Garber et al., 2001;Lekgabe et al., 2005;Williams et al., 2001;Mookerjee et al., 2005a). Cytokine array analysis identified many gene regulated by H2-relaxin in primary HSC. The changes in cytokine secretion were not significant in this assay but pro-apoptotic genes such as Fas Ligand and NT-4 were up regulated whilst pro-fibrotic cytokines such as TGF-β1, FGF and PDGF and various pro-inflammatory cytokines such as IL-1α, IL-2, IL-4, IL-6 and IL-13 were down regulated. Cytokine array analysis identified H2-relaxin as an inhibitor of TGF-β1 secretion. The mechanism of inhibition was not investigated although the production of active TGF-β1 was inhibited to a greater extent then total TGF-β1 production assessed by ELISA assay (the difference was not significant). Therefore H2-relaxin may inhibit the processing of TGF-β1 as well as significantly down regulating gene expression. We have also found that H2-relaxin can decrease the number of viable HSC and

increase the level of PARP-1 cleavage after 72 hours. This suggests the proliferation of HSC decreases in the presence of H2-relaxin and the cells begin to undergo apoptosis as PARP-1 cleavage by caspase 3 is an early marker of apoptosis. A reduction in the number of activated HSC producing collagen will over time decrease the amount of overall collagen-1/ liver weight *in vivo* (Williams et al., 2001). H2-relaxin through the activation of RXFP-1 may be an important regulator of HSC, driving the cells into a more quiescent phenotype. The senescence or reversion to quiescence of activated HSC has recently been documented as an important regulator of fibrosis, limiting the fibrogenic response to acute injury, as well as the apoptosis of HSC (Iredale et al., 1998;Krizhanovsky et al., 2008). H2-relaxin also reduces the expression of TIMP-1 and TGF-β both pro-survival factors (Murphy et al., 2002;Gressner and Bachem, 1990), and eventually initiates apoptosis.

The presence of relaxin receptors in activated HSC suggests a role in limiting the proliferation and fibrotic potential of these cells but we have also found the cells decrease their contractility in the presence of H2-relaxin. This is a novel finding that suggests a possible role for H2-relaxin in the treatment of portal hypertension which can be exacerbated by the contraction of HSC around the portal blood supply in the cirrhotic liver. It has been previously suggested that relaxin has vasoactive properties and these properties are controlled by the induction of nitric oxide. It has been proposed that relaxin can induce nitric oxide through several mechanisms (Nistri and Bani et al., 2003; Sherwood., 2004). In this study the inhibition of contraction of HSC was measured using a collagen-1 gel contraction assay. Relaxin was found to inhibit the contraction of HSC significantly after 72 hours. The level of nitric oxide was also determined and it was found that nitric oxide levels were increased after relaxin administration. The inhibition of contraction may be due to several actions of relaxin, the decrease in α-SMA levels, the increase in MMP levels, the increase in nitric oxide levels, the inhibition of intracellular free calcium or a combination of all of these. The decrease in α-SMA in the presence of H2-relaxin may affect

contraction in HSC. Actin fibres are important in cell contraction and inhibition of α-SMA expression has previously been reported to reduce cellular contraction in myofibroblasts (Hinz et al., 2002). As previously reported the down regulation of TGF-β may also contribute to the decrease in α-SMA induced contraction in H2-relaxin treated HSC (Meyer-ter-Vehn et al., 2008). In the late 1990's MMP-2 was found to increase the cleavage of big ET-1, producing ET_{1-32}, a novel ET-1 agonist. ET_{1-32} was found to have activity at both ET_A and ET_B receptors (Fernandez-Patron et al., 1999). The increase in MMP-2 by H2-relaxin in HSC may increase the production of ET_{1-32}, this coupled with the down regulation of ET_A receptors by H2-relaxin may increase the production of nitric oxide through ET_{1-32} activation of the ET_B receptor. The increase in MMP expression may also affect the collagen-1 gel that it used to measure HSC contraction. An increase in MMP secretion can enhance the breakdown of collagen and therefore reduce the area of the gel. An inhibitor of nitric oxide, L-NAME, was used in the gel contraction assay but there was not enough time to optimise the concentration. No contraction was seen in L-NAME treated HSC in either in H2-relaxin treated or controls. The concentration of inhibitor may have been too high and has subsequently killed the cells. The ability of relaxin to inhibit intracellular free calcium levels was not investigated but may have a significant role to play in the action of H2-relaxin in regulating HSC contractility.

Many of the phenotypic changes observed in H2-relaxin treated HSC, including the increase in cAMP, were found to be dependent upon the expression and activation of RXFP-1. A significant reduction in RXFP-1 gene expression by over 70% in primary HSC using siRNA, reversed the antifibrotic effects of H2-relaxin on HSC gene expression profile. Significant increases in TGF-β, TIMP-1, α-SMA, CTGF and procollagen-1 and a significant decrease in MMP-1 were observed in the presence of H2-relaxin in cells with reduced RXFP-1 expression, when compared to cells with a normal level of RXFP-1 in the presence of H2-relaxin. The expression of MMP-2 was significantly increased by 2-fold in

RXFP-1 siRNA transfected HSC, which is similar to the change in expression for H2-relaxin treated non-transfected cells. This result suggests the increase in MMP-2 by H2-relaxin is not through the activation of RXFP-1 but through an independent mechanism. It has been suggested that H2-relaxin can influence gene expression by activating glucocorticoid receptors (GR). To signal through GR, H2-relaxin must cross the cell membrane and activate GR at the nuclear membrane (Dschietzig et al., 2004;Bathgate et al., 2005). Investigations into the mechanisms of MMP-2 up regulation by H2-relaxin would further the understanding in H2-relaxin signalling. H2-relaxin inhibition of HSC contractility is also dependent upon RXFP-1 expression. The increase in nitric oxide released from H2-relaxin treated HSC was completely reversed in RXFP-1 siRNA transfected HSC. There was a significant 20% decrease in nitric oxide compared to non-transfected cells in the presence of H2-relaxin. This result suggests H2-relaxin signals through RXFP-1 mechanisms to increase nitric oxide in the cells. Activation of G protein Gs will not only increase cAMP, but can also increase the phosphorylation of AKT though PI3-kinase, both pathways have been suggested as possible mechanisms in H2-relaxin induction of nitric oxide (Nistri and Bani., 2003). Therefore HSC contractility may be dependent upon the expression of α-SMA and TGF-β as well as the regulation of nitric oxide secretion. Relaxin has a direct role in maintaining blood volume and circulation in the kidney (Sherwood., 2004) and I hypothesise from the findings in this thesis and from others that relaxin could also play an important role in circulation through the liver at the sinusoidal level (Bani et al., 2001), which is particularly important in the fibrotic liver.

H2-relaxin and RXFP-1 knockout mice demonstrate age related fibrosis of the kidney (Samuel et al., 2005b;Samuel et al., 2005a). The relaxin receptor localisation in normal and fibrotic kidney has now been established. An interesting pattern of expression was found, including RXFP-1 in the podocytes and RXFP-3 in the interstitial fibroblasts, which has implications for relaxin to be a regulator of glomerular filtration and interstitial fibrosis in the kidney. H2-

relaxin is a vasoactive hormone that is thought to regulate blood pressure during pregnancy through regulation of blood volume in the kidneys (Sherwood., 2004). Therefore expression of RXFP-1 in the podocytes indicates a role for regulation of GFR at the site of the epithelial glomerular basement membrane. The mechanism of GFR regulation could be through the regulation of podocyte contraction and/or proliferation.

7.2 Limitations

The limitation of the gel contraction assay is that it is not a direct measurement of cellular contraction and other factors such friction and adhesion of the gel to the culture vessel can result in incomplete contraction and distorted shaped gels (Vernon and Gooden, 2002). An assay designed to either directly measure HSC contraction or reduce the friction and adhesion of the gel would help confirm the results observed in the collagen-1 gel contraction assays. One group has monitored individual cell contraction using photomicrographs at different time points after addition of vasoactive compounds (Pang et al., 1993). This method would reduce the uncertainty of using an indirect measurement when using a compound such as H2-relaxin over a relatively long time period as it may alter the behaviour of the collagen-1 gel. The problem with using this method is that it requires more sophisticated equipment and therefore may not be possible to carry out in many labs. An alternative method which would reduce the friction of the gel in the culture vessel is an oil supported collagen retraction (OSCR) assay (Vernon and Gooden et al., 2002). This method still utilises collgen-1 lattices but in a low friction environment. The usual method of measurement for gel contraction assays is to measure the diameter of the gel and then calculate the gel area from this measurement. At the beginning of the study this method was used. It quickly became apparent that distorted gel shapes made measurement of contraction difficult to quantify and therefore pictures were taken and imagej analysis software was used to measure the whole area of the

gel rather then calculating the area from the diameter. This method improved the reproducibility of the results.

7.3 Suggestions for future Work

To continue this work the mechanism of HSC relaxation by H2-relaxin should be fully elucidated through the use of nitric oxide inhibitors, signalling mechanism inhibitors/inducers and intracellular calcium modifying agents. Chemical agents such as L-NAME, a nitric oxide inhibitor, could show that actions of H2-relaxin regulating cellular contraction are nitric oxide dependent. In this study we have shown that many of the actions of H2-relaxin in HSC are through the activation of RXFP-1 and therefore studying the down stream pathways of this receptor will help understanding of the mechanisms of action in these cells. Previous groups have shown that the increase in cAMP in response to H2-relaxin is biphasic and is linked initially to the Gs-adenylate cyclase pathway and the delayed response switches to a Gi linked PI3-kinase pathway (Bathgate et al., 2005;Halls et al., 2006). Possible downstream molecules include PKC, PKA, Erk 1/2 and transcription factors such as NF-κB (Bathgate et al., 2005). Inhibitors of PI3-kinase such as LY294002 and wortmannin have been shown to inhibit the second phase of response to H2-relaxin (Halls et al., 2006). These inhibitors could be used alongside PKC, PKA (PKA inhibitor 5-24 (calbiochem)) and Gi (pertussis toxin (PTX)) inhibitors to determine the pathways responsible for the phenotypic changes observed in HSC. Several PKC inhibitors are available that are designed to target specific isoforms such as PKCζ pseudosubstrate inhibitor myristoylated (calbiochem) or non-selective potent inhibitors such as protein kinase C inhibitor peptide 19-36 (calbiochem) can be used. H2-relaxin PKCζ activation and translocation to the membrane has been reported in a number of cell lines (Dessauer and Nguyen, 2005), therefore specifically targeting isoforms of PKC may identify the signalling pathway in HSC. Phosphoylation of proteins such as Erk1/2, AKT and JNK could be used determine the pathways that are activated by H2-relaxin and also to establish if

the inhibitors used are targeting the correct pathways. H2-relaxin activation of NF-κB can be studied through the electromobility shift assays (Takahra et al., 2004), and an inhibitor such as BAY 11-7082 (calbiochem) can confirm if NF-κB activation is essential for the phenotypic changes observed. Agents that target a potential relaxin pathway that regulates the intracellular calcium concentration such as an intracellular calcium chelator BAPTA-AM or calcium/calmodulin kinase II inhibitor KN62, could also be used to study the effect on cellular contraction in the presence of H2-relaxin. A CCl_4 rat model has already been used to study the effects of relaxin *in vivo* (Williams et al., 2001) but relaxin knockout mice have not been used to study liver fibrosis. H1-relaxin (the equivalent to H2-relaxin in humans) knockout animals could be given CCl_4 induced liver injury. The initial observation could establish if relaxin knockout mice develop liver fibrosis at an earlier stage or if the grade of fibrosis is more severe. A fibrosis recovery model could be set up to look at recovery rate after acute or sustained CCl_4 injury in the knockout model to determine if relaxin knockout animals recover more slowly from injury and finally the re-administration of relaxin to mice with fibrosis to establish if relaxin can hasten recovery.

Due to the vasorelaxant properties of H2-relaxin and our findings that H2-relaxin reduces the contraction of HSC, a model of portal hypertension could be set up using normal and relaxin knockout mice. There are several different models of portal hypertension, including portal vein ligation, bile duct ligation induced cirrhosis and CCl_4 induced cirrhosis (Geerts et al., 2008;Abraldes et al., 2006). Portal vein ligation induces portal hypertension independently from cirrhosis whereas the other models rely upon the development of cirrhosis to induce portal hypertension (Geerts et al., 2008;Abraldes et al., 2006). H1-relaxin knockout mice could be used in the portal vein ligation model to independently study the effects of relaxin on portal hypertension but a model that studies portal hypertension as a result of CCl_4 induced cirrhosis may be more relevant when considering a future possible therapy in cirrhotic induced

portal hypertension in humans. Therefore if H1-relaxin knockout mice were given sustained CCl_4 injury to induce cirrhosis, the development of portal hypertension could be monitored using hemodynamic studies comparing relaxin knockouts to controls. H1-relaxin knockouts could then be treated with H2-relaxin to monitor the effect on portal hypertension. Studies carried out on mice would be advantageous due to the amount H2-relaxin required to reach dosing concentrations would be reduced compared to studies in rats, and the H1-relaxin knockout mouse could be used.

The kidney is a complex structure with many different cell types, the localisation of the relaxin receptors in the kidney has highlighted possible roles for relaxin in normal and fibrotic kidney. An in depth study utilising podocytes and interstitial fibroblasts to elucidate the phenotype in the presence of relaxin would contribute to the understanding of the role of relaxin in the kidney.

7.4 Final comments

The recognition of H2-relaxin as a regulator of HSC activation and contractility has contributed to the understanding of relaxin as a regulator of fibrosis in the liver. RXFP-1 has been identified as a marker of HSC activation. A schematic representation of the findings has been constructed (figure 7.1). The finding that HSC contractility can be regulated by H2-relaxin has uncovered a new area of interest in relaxin as a potential therapy for portal hypertension. Additional studies using animal models will help to reveal the potential role for H2-relaxin as an antifibrotic therapy and possibly in the treatment of portal hypertension.

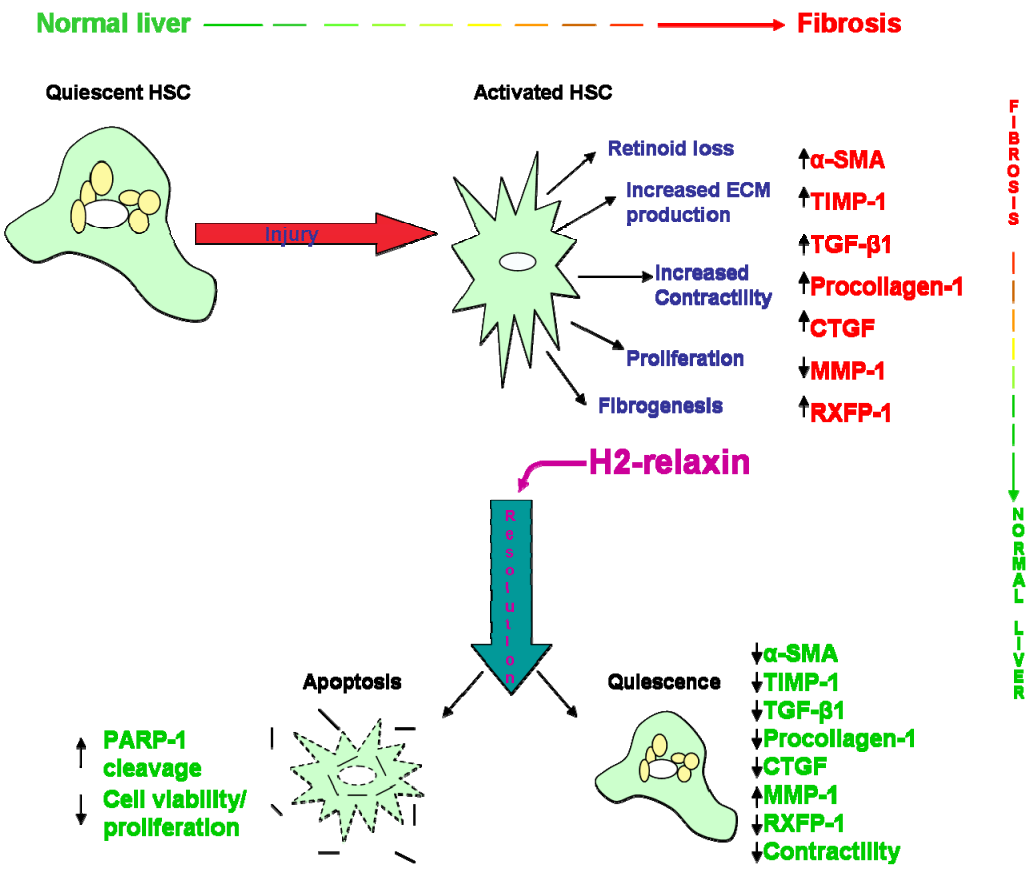

Figure 7.1. Schematic representation of the findings in this thesis. H2-relaxin drives HSC into a less fibrotic phenotype and after time a certain proportion will be driven into apoptosis.

Appendix 1

Supporting data

Appendix 1 - Supporting data

In vivo model of liver injury in rats

Liver injury is induced using CCl_4 as described previously (Iredale et al., 1998). Cohorts of 12 Sprague Dawley rats were given CCl_4 injury for 4 weeks to generate an early reversible fibrosis and another cohort of 12 were given injury for 12 weeks to be given advanced micronodular cirrhosis, which undergoes only partial resolution over one year of follow up. Three rats were sacrificed at 4 weeks and 12 weeks from the cohorts and three rats were in each group of follow up time points showing resolution in the rats given only 4 weeks fibrosis. The control rats were injected with olive oil twice a week. The rats were sacrificed and the liver was dissected. The whole liver from each rat was used for protein and RNA extraction. The RNA was then used to look at the mRNA expression of the RXFP-1 comparing whole liver from rats of the same age and species that were not given injury and at two different time points of injury (4 and 12 weeks).

RXFP-1 expression in CCl_4 model of liver injury

RXFP-1 mRNA expression was induced during CCl_4 rat liver injury in a whole liver extraction. A 4000-fold induction of RXFP-1 occurred after four weeks of injury compared to normal controls. 4 weeks CCl_4 induces mild fibrosis. The fold induction is so high due to the very low expression of RXFP-1 in normal rat liver. The peak induction of RXFP-1 to 5000-fold above controls was observed in the animals with twelve weeks CCl_4 injury, which have peak fibrosis and non reversible cirrhosis in some cases (figure 1.)

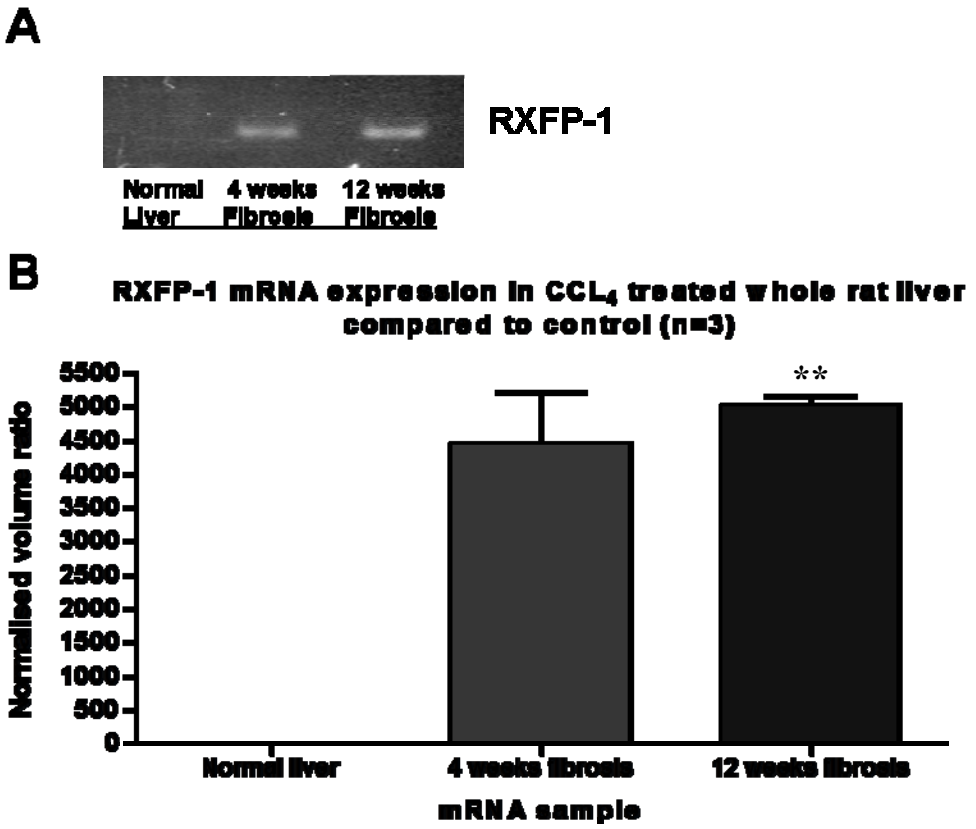

Figure 1. (A) Expression of RXFP-1 in CCL_4 injured rat whole liver, assessed by RT-PCR and normalised to GAPDH. **(B)** Fold change in RXFP-1 expression in normal whole rat liver compared to four weeks fibrosis and twelve weeks cirrhotic liver injury. RXFP-1 expression is induced after 4 and 12 weeks CCL_4 injury. A significant up regulation of RXFP-1 coincides with peak induction of injury after 12 weeks ($p<0.01$).

Li90 cells as a model of human fibrotic liver disease

Li90 cells are a tumourgenic hepatic stellate cell line (Murakami et al., 1995). They have not been immortalised but their lifespan in culture is up to twenty five passages. They have been isolated from the liver near a region of hepatocellular carcinoma and therefore these cells resist apoptosis and have longer life-span then primary cells isolated from normal areas of the liver (Murakami et al., 1995). Li90 cells appear very similar in morphology to primary hepatic stellate cells when cultured on plastic until later passage when a change in morphology

was observed, proliferation decreased and it was decided Li90 cells were not the best model to continue the studies.

It was decided that hHSC and LX-2 cells would be used for the rest of the experiments. LX-2 cells are a readily available HSC cell line which maintain their phenotype after many passages and are therefore useful for optimising assays and primary human HSC are still the gold standard for *in vitro* studies of human liver fibrosis.

H2-Relaxin treatment of Li90 cells

The treatment of Li90 cells (passage 15) with a dose response for H2-relaxin for 72 hours caused a dose dependent reduction in TIMP-1 and an increase in MMP-2 expression. The most significant reduction in TIMP-1 was after 1 nM treatment which reduced the expression by over 30%. MMP-2 expression was increased by nearly 2-fold at the lowest dose of 0.1 nM H2-relaxin. The greatest increase was observed after 72 hours 1 nM H2-relaxin, higher doses did not augment this effect. The overall effect is a shift in the fibrotic balance to a more collagen degrading phenotype.

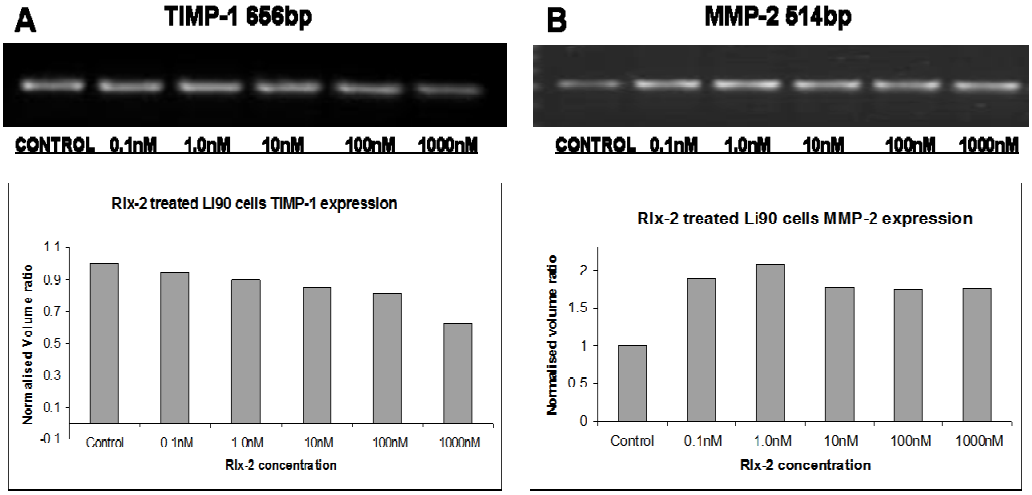

Figure 2. (A) Expression of TIMP-1 in Li90 cells that have been treated with a dose response for H2-relaxin for 72 hours, assessed by RT-PCR (n=1). TIMP-1 expression is

reduced, in a dose dependent manner, by over 30% after 72 hours 1 μM H2-relaxin treatment. **(B)** Expression of MMP-2 in Li90 cells that have been treated with a dose response for H2-relaxin for 72 hours, assessed by RT-PCR (n=1). MMP-2 expression increases in all of the treatment groups and dose not appear to be dose dependent. The greatest increase was after 72 hours 1 nM H2-relaxin treatment which induced a 2-fold increase in expression.

Appendix 2

Buffers, primers and siRNA sequences

Appendix 2 - Buffers and reaction components

Western Buffers

Western running Buffer

20x NuPAGE SDS Running Buffer MOPS (Invitrogen) was diluted to prepare 1x NuPAGE SDS Running Buffer. 50 ml NuPAGE SDS Running Buffer 20x MOPS was added to 950 ml of Ultra-pure Water making a total volume of 1000 ml. 600 ml of the 1x NuPAGE SDS Running Buffer was needed in the outer buffer chamber. Immediately prior to loading the samples, 500 µl of the NuPAGE Antioxidant (Invitrogen) was added to the remaining 200 ml of the 1x NuPAGE SDS Running Buffer and mixed thoroughly. This was for use in the inner running chamber.

Western Transfer Buffer

1 litre of 1x NuPAGE Transfer Buffers was prepared as follows:

Contents	Amount
Ultrapure Water	749 ml
20X NuPAGE Transfer Buffer	50 ml
NuPAGE Antioxidant	1 ml
Methanol	200 ml

Table 9. Contents of western transfer buffer (because there was transfer of two gels within a blot unit, the methanol content was 20% (200 ml) to ensure even and efficient transfer of both gels; it was reduced to 10% if only one gel was transferred).

Immunohistochemistry/immunocytochemistry buffers

Tris buffered Saline

Sodium chloride (sigma)	80 grams
Tris	6.05 grams
1M hydrochloric acid (sigma)	38 ml
Distilled water	10 Litres

The buffer salts and acid were mixed in 1 litre of distilled water. The pH was then adjusted to pH 7.65 and then the remaining 9 litres of water was added, which gave a final pH of 7.6.

Endogenous peroxidise inhibitor-paraffin

Methanol (romil)	5.9 ml
Hydrogen peroxide	0.1 ml

Blocking culture media (gibco)

Dulbecco's modified Eagles medium	80 ml
Fetal calf serum	20 ml
Bovine serum albumin	1 gram

BSA was dissolved in the DMEM and FCS then aliquoted and stored at -20˚C until required.

0.01M Citrate buffer formula

Citric Acid crystals	2.1grams
Distilled water	1000 ml

Mixed and pH adjusted to pH 6.0 with 1M sodium hydroxide (approximately 25 ml)

RT-PCR primer sequences

RXFP-1- 317bp

Sense: 5'-CAGCTTGTAGGATCTTTGGCC-3'

Antisense: 5'- GCGGCCAAATTAATACCAAG-3'

RXFP-2- 200bp

Sense: 5'-AGATATTGGAAGCAAAGGGT-3'

Antisense: 5'-TGGCATCAGAGAACACTATA-3'

RXFP-3 - 288bp

Sense: 5'-CGGAGACTGTCGAAGGTCAC-3'

Antisense: 5'-GCTGGTGATCGAAGGAGACG-3'

RXFP-4 - 356bp

Sense: 5'-CCTTTGCCTGCTGCGTTTCC-3'

Antisense: 5'-GCACAGGGTTGAGGCAGCTA-3'

Procollagen-1- 651bp

Sense: 5'-AACATGACCAAAAACCAAAAG-3'

Antisense: 5'-CATTGTTTCCTGTGTCTTCTGG-3'

MMP-2 - 514 bp

Sense: 5'-GCTGGCCCTGGCTCCCACAGG-3'

Antisense: 5'-ATACAAAGCAAACTGCTAATG-3'

MMP-1 -243 bp

Sense: 5'-ATGCTGAAACCCTGAAGGTG-3'

Antisense: 5'-CTGCTTGACCCTCAGAGACC-3'

TIMP-1 - 656 bp

Sense: 5'-TGTTGTTGCTGTGGCTGATAG-3'

Antisense: 5'-CGGAAGAAAGATGGGTGTGGG-3'

H2-relaxin- 247bp

Sense: 5'-CCTGGAGCAAAAGGTCTCTG-3'

Antisense: 5'-CTTCAGCTCCTGTGGCAAAT-3'

Endothelin-1 receptor A- 233bp

Sense: 5'-TATCCTGGCCATTCCTGAAG-3'

Antisense: 5'-TTCTCAAGCTGCCATTCCTT-3'

Endothelin-1 receptor B- 231bp

Sense: 5'-TCCCGTTCAGAAGACAGCTT-3'

Antisense: 5'-CAGAGGCAAAGACAAGGAC-3'

GAPDH-240bp

Sense: 5'-GGAGTCAACGGATTTGGTCGTA-3'

Antisense: 5'-CTTGATTTTGGAGGGATCTCGC-3'

β-actin- 674bp

Sense: 5'-ACCAGGGCGTGATGGTGGGCATGGGTCAGAA-3'

Antisense: 5'-TCCATAGGCTGGAAGAGTGCCTCAG-3'

qRT-PCR primer sequences

RXFP-1- 99bp

Sense: 5'-GCTGTATGCCATGTCAATCATT-3'

Antisense: 5'-TCTCCACGAAACTTTAGGTCAA-3'

TIMP-1- 81bp

Sense: 5'-GCAATTCCGACCTCGTCATC-3'

Antisense: 5'-TCTTGATCTCATAACGCTGGTATAA-3'

MMP-1- 127bp

Sense: 5'-GCACTGAGAAAGAAGACAAAGG-3'

Antisense: 5'-CTAAGTCCACATCTTGCTCTTG-3'

TGF-β1- 83bp

Sense: 5'-CACTCCCACTCCCTCTCTC-3'

Antisense: 5'-GTCCCCTGTGCCTTGATG-3'

α-SMA- 76bp

Sense: 5'-AAGCACAGAGCAAAAGAGGAAT-3'

Antisense: 5'-ATGTCGTCCCAGTTGGTGAT-3'

MMP-2- 90bp

Sense: 5'-CATACAGGATCATTGGCTACAC

Antisense: 5'-TCACATCGCTCCAGACTTG

Procollagen-1- 130bp

Sense: 5'-AGACAGTGATTGAATACAAAACCA-3'

Antisense: 5'-GGAGTTTACAGGAAGCAGACA-3'

CTGF- 113bp

Sense: 5'-CCCAGACCCAACTATGATTAGAG-3'

Antisense: 5'-AGGCGTTGTCATTGGTAACC-3'

Short interfering RNA (siRNA) sequences

RXFP-1 siRNA (1)

Sense: 5'-GCCUAGAAGGGAUUGAAAUtt-3'

Antisense: 5'-AUUCAAUCCCUUCUAGGCtg-3'

RXFP-1 siRNA (2)

Sense: 5'-GGAUGUUUAGACCUCUUAUtt-3'

Antisense: 5'-AUAAGAGGUCUAAACAUCCtt-3'

RXFP-1 siRNA (3)

Sense: 5'CCACAAGACCAUUUAAAGAtt-3'

Antisense: 5'-UCUUUAAAUGGUCUUGUGGtc-3'

-ve control scrambled

Sense: 5'-AAGCAUGGAUGCUGAAGUAtt-3'

Antisense: 5'-UACUUCAGCAUCCAUGCUUtg-3'

Ambion predesigned –ve control #1

Commercial product no sequence available

List of References

List of References

Abraldes, J.G., M.Pasarin, and J.C.Garcia-Pagan. 2006. Animal models of portal hypertension. *World J. Gastroenterol.* 12:6577-6584.

Aikin, R., L.Rosenberg, S.Paraskevas, and D.Maysinger. 2004. Inhibition of caspase-mediated PARP-1 cleavage results in increased necrosis in isolated islets of Langerhans. *J. Mol. Med.* 82:389-397.

Alderton, W.K., C.E.Cooper, and R.G.Knowles. 2001. Nitric oxide synthases: structure, function and inhibition. *Biochem. J.* 357:593-615.

Alison, M.R., P.Vig, F.Russo, B.W.Bigger, E.Amofah, M.Themis, and S.Forbes. 2004. Hepatic stem cells: from inside and outside the liver? *Cell Prolif.* 37:1-21.

Antunes, F., A.Boveris, and E.Cadenas. 2004. On the mechanism and biology of cytochrome oxidase inhibition by nitric oxide. *Proc. Natl. Acad. Sci. U. S. A* 101:16774-16779.

Arendt, E., U.Ueberham, R.Bittner, R.Gebhardt, and E.Ueberham. 2005. Enhanced matrix degradation after withdrawal of TGF-beta1 triggers hepatocytes from apoptosis to proliferation and regeneration. *Cell Prolif.* 38:287-299.

Arroyo, V. 2002. Pathophysiology, diagnosis and treatment of ascites in cirrhosis. *Ann. Hepatol.* 1:72-79.

Arthur, M.J., S.L.Friedman, F.J.Roll, and D.M.Bissell. 1989. Lipocytes from normal rat liver release a neutral metalloproteinase that degrades basement membrane (type IV) collagen. *J. Clin. Invest* 84:1076-1085.

Asanuma, K., E.Yanagida-Asanuma, M.Takagi, F.Kodama, and Y.Tomino. 2007. The role of podocytes in proteinuria. *Nephrology. (Carlton.)* 12 Suppl 3:S15-S20.

Avrameas, S. and J.Uriel. 1966. [Method of antigen and antibody labelling with enzymes and its immunodiffusion application]. *C. R. Acad. Sci. Hebd. Seances Acad. Sci. D.* 262:2543-2545.

Bahcecioglu, I.H., S.S.Koca, O.K.Poyrazoglu, M.Yalniz, I.H.Ozercan, B.Ustundag, K.Sahin, A.F.Dagli, and A.Isik. 2008. Hepatoprotective effect of infliximab, an anti-TNF-alpha agent, on carbon tetrachloride-induced hepatic fibrosis. *Inflammation* 31:215-221.

Bani, D., M.C.Baccari, S.Nistri, F.Calamai, M.Bigazzi, and T.B.Sacchi. 1999. Relaxin up-regulates the nitric oxide biosynthetic pathway in the mouse uterus: involvement in the inhibition of myometrial contractility. *Endocrinology* 140:4434-4441.

Bani, D., E.Masini, M.G.Bello, M.Bigazzi, and T.B.Sacchi. 1998. Relaxin protects against myocardial injury caused by ischemia and reperfusion in rat heart. *Am J Pathol.* 152:1367-1376.

Bani, D., S.Nistri, S.Quattrone, M.Bigazzi, and S.T.Bani. 2001. The vasorelaxant hormone relaxin induces changes in liver sinusoid microcirculation: a morphologic study in the rat. *J. Endocrinol.* 171:541-549.

Bataller, R. and D.A.Brenner. 2005. Liver fibrosis. *J Clin Invest.* 115:209-218.

Bataller, R. and P.Gines. 2002. [New therapeutic strategies in liver fibrosis: pathogenic basis]. *Med Clin (Barc.)* 118:339-346.

Bataller, R., J.M.Nicolas, P.Gines, A.Esteve, G.M.Nieves, E.Garcia-Ramallo, M.Pinzani, J.Ros, W.Jimenez, A.P.Thomas, V.Arroyo, and J.Rodes. 1997. Arginine vasopressin induces contraction and stimulates growth of cultured human hepatic stellate cells. *Gastroenterology* 113:615-624.

Bathgate, R.A., R.Ivell, B.M.Sanborn, O.D.Sherwood, and R.J.Summers. 2005. Receptors for relaxin family peptides. *Ann. N. Y. Acad. Sci.* 1041:61-76.

Bathgate, R.A., R.Ivell, B.M.Sanborn, O.D.Sherwood, and R.J.Summers. 2006. International Union of Pharmacology LVII: recommendations for the nomenclature of receptors for relaxin family peptides. *Pharmacol. Rev.* 58:7-31.

Bathgate, R.A., C.S.Samuel, T.C.Burazin, S.Layfield, A.A.Claasz, I.G.Reytomas, N.F.Dawson, C.Zhao, C.Bond, R.J.Summers, L.J.Parry, J.D.Wade, and G.W.Tregear. 2002. Human relaxin gene 3 (H3) and the equivalent mouse relaxin (M3) gene. Novel members of the relaxin peptide family. *J. Biol. Chem.* 277:1148-1157.

Bazzoni, G. and E.Dejana. 2004. Endothelial cell-to-cell junctions: molecular organization and role in vascular homeostasis. *Physiol Rev.* 84:869-901.

Becker, F.F. 1970. The normal hepatocyte in division: regeneration of the mammalian liver. *Prog. Liver Dis.* 3:60-76.

Becker, F.F. and B.P.Lane. 1968. Regeneration of the mammalian liver. VI. Retention of phenobarbital-induced cytoplasmic alterations in dividing hepatocytes. *Am. J. Pathol.* 52:211-226.

Bell, E., B.Ivarsson, and C.Merrill. 1979. Production of a tissue-like structure by contraction of collagen lattices by human fibroblasts of different proliferative potential in vitro. *Proc. Natl. Acad. Sci. U. S. A* 76:1274-1278.

Bennett, R.G., S.R.Dalton, K.J.Mahan, M.J.Gentry-Nielsen, F.G.Hamel, and D.J.Tuma. 2007. Relaxin receptors in hepatic stellate cells and cirrhotic liver. *Biochem. Pharmacol.* 73:1033-1040.

Bennett, R.G., K.K.Kharbanda, and D.J.Tuma. 2003. Inhibition of markers of hepatic stellate cell activation by the hormone relaxin. *Biochem Pharmacol.* 66:867-874.

Bennett, R.G., K.J.Mahan, M.J.Gentry-Nielsen, and D.J.Tuma. 2005. Relaxin receptor expression in hepatic stellate cells and in cirrhotic rat liver tissue. *Ann. N Y. Acad. Sci.* 1041:185-189.

Benyon, R.C., J.P.Iredale, S.Goddard, P.J.Winwood, and M.J.Arthur. 1996. Expression of tissue inhibitor of metalloproteinases 1 and 2 is increased in fibrotic human liver. *Gastroenterology* 110:821-831.

Berridge, M.V. and A.S.Tan. 1993. Characterization of the cellular reduction of 3-(4,5-dimethylthiazol-2-yl)-2,5-diphenyltetrazolium bromide (MTT): subcellular localization, substrate dependence, and involvement of mitochondrial electron transport in MTT reduction. *Arch. Biochem. Biophys.* 303:474-482.

Billack, B. 2006. Macrophage activation: role of toll-like receptors, nitric oxide, and nuclear factor kappa B. *Am. J. Pharm. Educ.* 70:102.

Bilzer, M., F.Roggel, and A.L.Gerbes. 2006. Role of Kupffer cells in host defense and liver disease. *Liver Int.* 26:1175-1186.

Binder, C., T.Hagemann, B.Husen, M.Schulz, and A.Einspanier. 2002. Relaxin enhances in-vitro invasiveness of breast cancer cell lines by up-regulation of matrix metalloproteases. *Mol. Hum. Reprod.* 8:789-796.

Bleul, C.C., R.C.Fuhlbrigge, J.M.Casasnovas, A.Aiuti, and T.A.Springer. 1996. A highly efficacious lymphocyte chemoattractant, stromal cell-derived factor 1 (SDF-1). *J. Exp. Med.* 184:1101-1109.

Blomhoff, R. and K.Wake. 1991. Perisinusoidal stellate cells of the liver: important roles in retinol metabolism and fibrosis. *FASEB J.* 5:271-277.

Bogdan, C. 2001. Nitric oxide and the immune response. *Nat. Immunol.* 2:907-916.

Bonis, P.A., S.L.Friedman, and M.M.Kaplan. 2001. Is liver fibrosis reversible? *N. Engl. J. Med.* 344:452-454.

Bosch, J., J.G.Abraldes, and R.Groszmann. 2003. Current management of portal hypertension. *J Hepatol.* 38 Suppl 1:S54-S68.

Bosch, J. and J.C.Garcia-Pagan. 2000. Complications of cirrhosis. I. Portal hypertension. *J. Hepatol.* 32:141-156.

Boyer, T.D. 2008. Transjugular intrahepatic portosystemic shunt in the management of complications of portal hypertension. *Curr. Gastroenterol. Rep.* 10:30-35.

Boyer, T.D., J.M.Henderson, A.M.Heerey, S.Arrigain, V.Konig, J.Connor, K.bu-Elmagd, J.Galloway, L.F.Rikkers, and L.Jeffers. 2008. Cost of preventing variceal rebleeding with transjugular intrahepatic portal systemic shunt and distal splenorenal shunt. *J. Hepatol.* 48:407-414.

Bradshaw, A.D. and E.H.Sage. 2001. SPARC, a matricellular protein that functions in cellular differentiation and tissue response to injury. *J. Clin. Invest* 107:1049-1054.

Breitkopf, K., C.Roeyen, I.Sawitza, L.Wickert, J.Floege, and A.M.Gressner. 2005. Expression patterns of PDGF-A, -B, -C and -D and the PDGF-receptors alpha and beta in activated rat hepatic stellate cells (HSC). *Cytokine* 31:349-357.

Brune, B. 2003. Nitric oxide: NO apoptosis or turning it ON? *Cell Death. Differ.* 10:864-869.

Carmeliet, P. 2003. Angiogenesis in health and disease. *Nat. Med.* 9:653-660.

Cassiman, D., C.Denef, V.J.Desmet, and T.Roskams. 2001. Human and rat hepatic stellate cells express neurotrophins and neurotrophin receptors. *Hepatology* 33:148-158.

CASTEN, G.G. and R.J.BOUCEK. 1958. Use of relaxin in the treatment of scleroderma. *J Am Med Assoc.* 166:319-324.

Cattran, D.C. 2003. Outcomes research in glomerulonephritis. *Semin. Nephrol.* 23:340-354.

Chien, A., D.B.Edgar, and J.M.Trela. 1976. Deoxyribonucleic acid polymerase from the extreme thermophile Thermus aquaticus. *J. Bacteriol.* 127:1550-1557.

Chinnaiyan, A.M., K.O'Rourke, M.Tewari, and V.M.Dixit. 1995. FADD, a novel death domain-containing protein, interacts with the death domain of Fas and initiates apoptosis. *Cell* 81:505-512.

Chisari, F.V. 2000. Rous-Whipple Award Lecture. Viruses, immunity, and cancer: lessons from hepatitis B. *Am. J. Pathol.* 156:1117-1132.

Cho, J.H., T.Itoh, Y.Sendai, and H.Hoshi. 2008. Fibroblast growth factor 7 stimulates in vitro growth of oocytes originating from bovine early antral follicles. *Mol. Reprod. Dev.*

Clark, J.M., F.L.Brancati, and A.M.Diehl. 2002. Nonalcoholic fatty liver disease. *Gastroenterology* 122:1649-1657.

Conrad, K.P., A.Jeyabalan, L.A.Danielson, L.J.Kerchner, and J.Novak. 2005. Role of relaxin in maternal renal vasodilation of pregnancy. *Ann. N. Y. Acad. Sci.* 1041:147-154.

COONS, A.H. and M.H.KAPLAN. 1950. Localization of antigen in tissue cells; improvements in a method for the detection of antigen by means of fluorescent antibody. *J. Exp. Med.* 91:1-13.

Cory, A.H., T.C.Owen, J.A.Barltrop, and J.G.Cory. 1991. Use of an aqueous soluble tetrazolium/formazan assay for cell growth assays in culture. *Cancer Commun.* 3:207-212.

Crawford, J.M. 2002. Development of the intrahepatic biliary tree. *Semin. Liver Dis.* 22:213-226.

Csukai, M. and D.Mochly-Rosen. 1999. Pharmacologic modulation of protein kinase C isozymes: the role of RACKs and subcellular localisation. *Pharmacol. Res.* 39:253-259.

Cuthbert, J.A. 2001. Hepatitis A: old and new. *Clin. Microbiol. Rev.* 14:38-58.

Czochra, P., B.Klopcic, E.Meyer, J.Herkel, J.F.Garcia-Lazaro, F.Thieringer, P.Schirmacher, S.Biesterfeld, P.R.Galle, A.W.Lohse, and S.Kanzler. 2006. Liver fibrosis induced by hepatic overexpression of PDGF-B in transgenic mice. *J. Hepatol.* 45:419-428.

Dajak, M., S.Ignjatovic, S.Jovicic, and N.Majkic-Singh. 2008. The values of estimated glomerular filtration rate calculated with creatinine and cystatin C based equations in healthy adults. *Clin. Lab* 54:153-159.

Daskalakis, N. and M.P.Winn. 2006. Focal and segmental glomerulosclerosis. *Cell Mol. Life Sci.* 63:2506-2511.

Dayanithi, G., M.Cazalis, and J.J.Nordmann. 1987. Relaxin affects the release of oxytocin and vasopressin from the neurohypophysis. *Nature* 325:813-816.

Dempsey, E.C., A.C.Newton, D.Mochly-Rosen, A.P.Fields, M.E.Reyland, P.A.Insel, and R.O.Messing. 2000. Protein kinase C isozymes and the regulation of diverse cell responses. *Am. J. Physiol Lung Cell Mol. Physiol* 279:L429-L438.

Dessauer, C.W. and B.T.Nguyen. 2005. Relaxin stimulates multiple signaling pathways: activation of cAMP, PI3K, and PKCzeta in THP-1 cells. *Ann. N. Y. Acad. Sci.* 1041:272-279.

Diehl, A.M. 2000. Cytokine regulation of liver injury and repair. *Immunol. Rev.* 174:160-171.

Dooley, S., B.Delvoux, B.Lahme, K.Mangasser-Stephan, and A.M.Gressner. 2000. Modulation of transforming growth factor beta response and signaling during transdifferentiation of rat hepatic stellate cells to myofibroblasts. *Hepatology* 31:1094-1106.

Dooley, S., J.Hamzavi, K.Breitkopf, E.Wiercinska, H.M.Said, J.Lorenzen, D.P.Ten, and A.M.Gressner. 2003. Smad7 prevents activation of hepatic stellate cells and liver fibrosis in rats. *Gastroenterology* 125:178-191.

Dooley, S., J.Hamzavi, L.Ciuclan, P.Godoy, I.Ilkavets, S.Ehnert, E.Ueberham, R.Gebhardt, S.Kanzler, A.Geier, K.Breitkopf, H.Weng, and P.R.Mertens. 2008. Hepatocyte-specific Smad7 expression attenuates TGF-beta-mediated fibrogenesis and protects against liver damage. *Gastroenterology* 135:642-659.

Downing, S.J. and M.Hollingsworth. 1993. Action of relaxin on uterine contractions--a review. *J. Reprod. Fertil.* 99:275-282.

Drexler, H.G. and H.Quentmeier. 2004. FLT3: receptor and ligand. *Growth Factors* 22:71-73.

Dschietzig, T., C.Bartsch, M.Greinwald, G.Baumann, and K.Stangl. 2005. The pregnancy hormone relaxin binds to and activates the human glucocorticoid receptor. *Ann. N Y. Acad. Sci.* 1041:256-271.

Dschietzig, T., C.Bartsch, C.Richter, M.Laule, G.Baumann, and K.Stangl. 2003. Relaxin, a pregnancy hormone, is a functional endothelin-1 antagonist: attenuation of endothelin-1-mediated vasoconstriction by stimulation of endothelin type-B receptor expression via ERK-1/2 and nuclear factor-kappaB. *Circ. Res.* 92:32-40.

Dschietzig, T., C.Bartsch, V.Stangl, G.Baumann, and K.Stangl. 2004. Identification of the pregnancy hormone relaxin as glucocorticoid receptor agonist. *FASEB J.* 18:1536-1538.

Du, X.J. 2004. Gender modulates cardiac phenotype development in genetically modified mice. *Cardiovasc. Res.* 63:510-519.

Dvorak, H.F. 2000. VPF/VEGF and the angiogenic response. *Semin. Perinatol.* 24:75-78.

Eigenbrot, C., M.Randal, C.Quan, J.Burnier, L.O'Connell, E.Rinderknecht, and A.A.Kossiakoff. 1991. X-ray structure of human relaxin at 1.5 A. Comparison to insulin and implications for receptor binding determinants. *J. Mol. Biol.* 221:15-21.

Einspanier, A., R.Nubbemeyer, S.Schlote, M.Schumacher, R.Ivell, K.Fuhrmann, and A.Marten. 1999. Relaxin in the marmoset monkey: secretion pattern in the ovarian cycle and early pregnancy. *Biol. Reprod.* 61:512-520.

Einspanier, A., M.R.Zarreh-Hoshyari-Khah, M.Balvers, L.Kerr, K.Fuhrmann, and R.Ivell. 1997. Local relaxin biosynthesis in the ovary and uterus through the oestrous cycle and early pregnancy in the female marmoset monkey (Callithrix jacchus). *Hum. Reprod.* 12:1325-1337.

Eknoyan, G., N.Lameire, R.Barsoum, K.U.Eckardt, A.Levin, N.Levin, F.Locatelli, A.Macleod, R.Vanholder, R.Walker, and H.Wang. 2004. The burden of kidney disease: improving global outcomes. *Kidney Int.* 66:1310-1314.

Evans, B.A., M.John, K.J.Fowler, R.J.Summers, M.Cronk, J.Shine, and G.W.Tregear. 1993. The mouse relaxin gene: nucleotide sequence and expression. *J. Mol. Endocrinol.* 10:15-23.

Fabris, P., D.Infantolino, M.R.Biasin, G.Marchelle, E.Venza, W.M.Terribile, V, P.Benedetti, G.Tositti, V.Manfrin, and F.De Lalla. 1999. High prevalence of HCV-RNA in the saliva cell fraction of patients with chronic hepatitis C but no evidence of HCV transmission among sexual partners. *Infection.* 27:86-91.

Failli, P., S.Nistri, S.Quattrone, L.Mazzetti, M.Bigazzi, T.B.Sacchi, and D.Bani. 2002. Relaxin up-regulates inducible nitric oxide synthase expression and nitric oxide generation in rat coronary endothelial cells. *FASEB J.* 16:252-254.

Fairbanks, K.D. and A.S.Tavill. 2008. Liver disease in alpha 1-antitrypsin deficiency: a review. *Am. J. Gastroenterol.* 103:2136-2141.

Farci P,P.RH. Clinical significance of hepatitis C virus genotypes and quasispecies. Semin.Liver Dis. 20[1], 103-126. 2008.
Ref Type: Generic

Faul, C., K.Asanuma, E.Yanagida-Asanuma, K.Kim, and P.Mundel. 2007. Actin up: regulation of podocyte structure and function by components of the actin cytoskeleton. *Trends Cell Biol.* 17:428-437.

Fausto, N. 2000. Liver regeneration. *J. Hepatol.* 32:19-31.

Fausto, N. 2001. Liver regeneration: from laboratory to clinic. *Liver Transpl.* 7:835-844.

Fausto, N. and J.S.Campbell. 2003. The role of hepatocytes and oval cells in liver regeneration and repopulation. *Mech. Dev.* 120:117-130.

Feng, S., I.U.Agoulnik, N.V.Bogatcheva, A.A.Kamat, B.Kwabi-Addo, R.Li, G.Ayala, M.M.Ittmann, and A.I.Agoulnik. 2007. Relaxin promotes prostate cancer progression. *Clin. Cancer Res.* 13:1695-1702.

Fernandez-Patron, C., M.W.Radomski, and S.T.Davidge. 1999. Vascular matrix metalloproteinase-2 cleaves big endothelin-1 yielding a novel vasoconstrictor. *Circ. Res.* 85:906-911.

Fevold, H.L., F.L. Hisaw and R.K. Meyer. 1930. The relaxative hormone of the corpus luteum. Its purification and concentration. J. Am. Chem. Soc. 52:3340-3348.

Fields, P.A. 2005. Is relaxin a calcium transporter/buffer? *Ann. N Y. Acad. Sci.* 1041:328-331.

Filonzi, M., L.C.Cardoso, M.T.Pimenta, D.B.Queiroz, M.C.Avellar, C.S.Porto, and M.F.Lazari. 2007. Relaxin family peptide receptors Rxfp1 and Rxfp2: mapping of the mRNA and protein distribution in the reproductive tract of the male rat. *Reprod. Biol. Endocrinol.* 5:29.

Fire, A., S.Xu, M.K.Montgomery, S.A.Kostas, S.E.Driver, and C.C.Mello. 1998. Potent and specific genetic interference by double-stranded RNA in Caenorhabditis elegans. *Nature* 391:806-811.

Fletcher, L.M. and J.W.Halliday. 2002. Haemochromatosis: understanding the mechanism of disease and implications for diagnosis and patient management following the recent cloning of novel genes involved in iron metabolism. *J. Intern. Med.* 251:181-192.

Forbes, S.J., F.P.Russo, V.Rey, P.Burra, M.Rugge, N.A.Wright, and M.R.Alison. 2004. A significant proportion of myofibroblasts are of bone marrow origin in human liver fibrosis. *Gastroenterology* 126:955-963.

Friedman, S.L. 1993. Seminars in medicine of the Beth Israel Hospital, Boston. The cellular basis of hepatic fibrosis. Mechanisms and treatment strategies. *N. Engl. J. Med.* 328:1828-1835.

Friedman, S.L. 2008. Hepatic fibrosis-Overview. *Toxicology*.

Friedman, S.L. and M.J.Arthur. 1989. Activation of cultured rat hepatic lipocytes by Kupffer cell conditioned medium. Direct enhancement of matrix synthesis and stimulation of cell proliferation via induction of platelet-derived growth factor receptors. *J. Clin. Invest* 84:1780-1785.

Friedman, S.L., D.C.Rockey, R.F.McGuire, J.J.Maher, J.K.Boyles, and G.Yamasaki. 1992. Isolated hepatic lipocytes and Kupffer cells from normal human liver: morphological and functional characteristics in primary culture. *Hepatology* 15:234-243.

Friedman, S.L. and F.J.Roll. 1987. Isolation and culture of hepatic lipocytes, Kupffer cells, and sinusoidal endothelial cells by density gradient centrifugation with Stractan. *Anal. Biochem.* 161:207-218.

Friedman, S.L., F.J.Roll, J.Boyles, and D.M.Bissell. 1985. Hepatic lipocytes: the principal collagen-producing cells of normal rat liver. *Proc. Natl. Acad. Sci. U. S. A* 82:8681-8685.

Friedman, S.L., S.Wei, and W.S.Blaner. 1993. Retinol release by activated rat hepatic lipocytes: regulation by Kupffer cell-conditioned medium and PDGF. *Am J Physiol* 264:G947-G952.

Furchgott, R.F., P.D.Cherry, J.V.Zawadzki, and D.Jothianandan. 1984. Endothelial cells as mediators of vasodilation of arteries. *J. Cardiovasc. Pharmacol.* 6 Suppl 2:S336-S343.

Furchgott, R.F. and P.M.Vanhoutte. 1989. Endothelium-derived relaxing and contracting factors. *FASEB J.* 3:2007-2018.

Furchgott, R.F. and J.V.Zawadzki. 1980. The obligatory role of endothelial cells in the relaxation of arterial smooth muscle by acetylcholine. *Nature* 288:373-376.

Gaca, M.D., X.Zhou, R.Issa, K.Kiriella, J.P.Iredale, and R.C.Benyon. 2003. Basement membrane-like matrix inhibits proliferation and collagen synthesis by activated rat hepatic stellate cells: evidence for matrix-dependent deactivation of stellate cells. *Matrix Biol.* 22:229-239.

Ganem, D. and A.M.Prince. 2004. Hepatitis B virus infection--natural history and clinical consequences. *N. Engl. J. Med.* 350:1118-1129.

Gao, Y., S.Dhanakoti, J.F.Tolsa, and J.U.Raj. 1999. Role of protein kinase G in nitric oxide- and cGMP-induced relaxation of newborn ovine pulmonary veins. *J. Appl. Physiol* 87:993-998.

Garber, S.L., Y.Mirochnik, C.S.Brecklin, E.N.Unemori, A.K.Singh, L.Slobodskoy, B.H.Grove, J.A.Arruda, and G.Dunea. 2001. Relaxin decreases renal interstitial fibrosis and slows progression of renal disease. *Kidney Int.* 59:876-882.

Gast, M.J. 1983. Characterization of preprorelaxin by tryptic digestion and inhibition of its conversion to prorelaxin by amino acid analogs. *J. Biol. Chem.* 258:9001-9004.

Geerts, A.M., E.Vanheule, M.Praet, V.H.Van, V.M.De, and I.Colle. 2008. Comparison of three research models of portal hypertension in mice:

macroscopic, histological and portal pressure evaluation. *Int. J. Exp. Pathol.* 89:251-263.

Giannelli, G., V.Quaranta, and S.Antonaci. 2003. Tissue remodelling in liver diseases. *Histol. Histopathol.* 18:1267-1274.

Ginn, F.L., P.Hochstein, and B.F.Trump. 1969. Membrane alterations in hemolysis: Internalization of plasmalemma induced by primaquine. *Science* 164:843-845.

Gomis-Ruth, F.X., K.Maskos, M.Betz, A.Bergner, R.Huber, K.Suzuki, N.Yoshida, H.Nagase, K.Brew, G.P.Bourenkov, H.Bartunik, and W.Bode. 1997. Mechanism of inhibition of the human matrix metalloproteinase stromelysin-1 by TIMP-1. *Nature* 389:77-81.

Gong, W., A.Pecci, S.Roth, B.Lahme, M.Beato, and A.M.Gressner. 1998. Transformation-dependent susceptibility of rat hepatic stellate cells to apoptosis induced by soluble Fas ligand. *Hepatology* 28:492-502.

Gorrell, M.D., X.M.Wang, M.T.Levy, E.Kable, G.Marinos, G.Cox, and G.W.McCaughan. 2003. Intrahepatic expression of collagen and fibroblast activation protein (FAP) in hepatitis C virus infection. *Adv. Exp. Med Biol* 524:235-243.

Gospodarowicz, D. and J.S.Moran. 1975. Mitogenic effect of fibroblast growth factor on early passage cultures of human and murine fibroblasts. *J. Cell Biol.* 66:451-457.

Gospodarowicz, D., J.S.Moran, and D.L.Braun. 1977. Control of proliferation of bovine vascular endothelial cells. *J. Cell Physiol* 91:377-385.

Goss, J.A., M.J.Mangino, and M.W.Flye. 1992a. Kupffer cell autoregulation of IL-1 production by PGE2 during hepatic regeneration. *J. Surg. Res.* 52:422-428.

Goss, J.A., M.J.Mangino, and M.W.Flye. 1992b. Prostaglandin E2 production during hepatic regeneration downregulates Kupffer cell IL-6 production. *Ann. Surg.* 215:553-559.

Gressner, A.M. and M.G.Bachem. 1990. Cellular sources of noncollagenous matrix proteins: role of fat-storing cells in fibrogenesis. *Semin. Liver Dis.* 10:30-46.

Gressner, A.M., B.Polzar, B.Lahme, and H.G.Mannherz. 1996. Induction of rat liver parenchymal cell apoptosis by hepatic myofibroblasts via transforming growth factor beta. *Hepatology* 23:571-581.

Gressner, A.M. and R.Weiskirchen. 2006. Modern pathogenetic concepts of liver fibrosis suggest stellate cells and TGF-beta as major players and therapeutic targets. *J. Cell Mol. Med.* 10:76-99.

Gressner, A.M., R.Weiskirchen, K.Breitkopf, and S.Dooley. 2002. Roles of TGF-beta in hepatic fibrosis. *Front Biosci.* 7:d793-d807.

Gunnersen, J.M., P.Fu, P.J.Roche, and G.W.Tregear. 1996. Expression of human relaxin genes: characterization of a novel alternatively-spliced human relaxin mRNA species. *Mol. Cell Endocrinol.* 118:85-94.

Hadjantonakis, A. and V.Papaioannou. 2001. The stem cells of early embryos. *Differentiation* 68:159-166.

Halls, M.L., R.A.Bathgate, P.J.Roche, and R.J.Summers. 2005a. Signaling pathways of the LGR7 and LGR8 receptors determined by reporter genes. *Ann. N. Y. Acad. Sci.* 1041:292-295.

Halls, M.L., R.A.Bathgate, S.Sudo, J.Kumagai, C.P.Bond, and R.J.Summers. 2005b. Identification of Binding Sites with Differing Affinity and Potency for Relaxin Analogues on LGR7 and LGR8 Receptors. *Ann. N Y. Acad. Sci.* 1041:17-21.

Halls, M.L., R.A.Bathgate, and R.J.Summers. 2006. Relaxin family peptide receptors, RXFP1 and RXFP2, modulate cAMP signalling by distinct mechanisms. *Mol Pharmacol*.

Halls, M.L., C.P.Bond, S.Sudo, J.Kumagai, T.Ferraro, S.Layfield, R.A.Bathgate, and R.J.Summers. 2005c. Multiple binding sites revealed by interaction of relaxin family peptides with native and chimeric relaxin family peptide receptors 1 and 2 (LGR7 and LGR8). *J Pharmacol. Exp. Ther* 313:677-687.

Han, Y.P., C.Yan, L.Zhou, L.Qin, and H.Tsukamoto. 2007. A matrix metalloproteinase-9 activation cascade by hepatic stellate cells in trans-differentiation in the three-dimensional extracellular matrix. *J. Biol. Chem.* 282:12928-12939.

Harty, M.W., E.F.Papa, H.M.Huddleston, E.Young, S.Nazareth, C.A.Riley, G.A.Ramm, S.H.Gregory, and T.F.Tracy, Jr. 2008. Hepatic macrophages promote the neutrophil-dependent resolution of fibrosis in repairing cholestatic rat livers. *Surgery* 143:667-678.

Heeg, M.H., M.J.Koziolek, R.Vasko, L.Schaefer, K.Sharma, G.A.Muller, and F.Strutz. 2005. The antifibrotic effects of relaxin in human renal fibroblasts are mediated in part by inhibition of the Smad2 pathway. *Kidney Int* 68:96-109.

Heidaran, M.A., J.H.Pierce, J.C.Yu, D.Lombardi, J.E.Artrip, T.P.Fleming, A.Thomason, and S.A.Aaronson. 1991. Role of alpha beta receptor heterodimer formation in beta platelet-derived growth factor (PDGF) receptor activation by PDGF-AB. *J. Biol. Chem.* 266:20232-20237.

Heldin, C.H., K.Miyazono, and D.P.Ten. 1997. TGF-beta signalling from cell membrane to nucleus through SMAD proteins. *Nature* 390:465-471.

Hemmann, S., J.Graf, M.Roderfeld, and E.Roeb. 2007. Expression of MMPs and TIMPs in liver fibrosis - a systematic review with special emphasis on anti-fibrotic strategies. *J. Hepatol.* 46:955-975.

Henderson, N.C. and J.P.Iredale. 2007. Liver fibrosis: cellular mechanisms of progression and resolution. *Clin. Sci. (Lond)* 112:265-280.

Henry, G. and W.L.Garner. 2003. Inflammatory mediators in wound healing. *Surg. Clin. North Am.* 83:483-507.

Hess, D.T., A.Matsumoto, S.O.Kim, H.E.Marshall, and J.S.Stamler. 2005. Protein S-nitrosylation: purview and parameters. *Nat. Rev. Mol. Cell Biol.* 6:150-166.

Hinz, B., V.Dugina, C.Ballestrem, B.Wehrle-Haller, and C.Chaponnier. 2003. Alpha-smooth muscle actin is crucial for focal adhesion maturation in myofibroblasts. *Mol. Biol. Cell* 14:2508-2519.

Hinz, B. and G.Gabbiani. 2003. Mechanisms of force generation and transmission by myofibroblasts. *Curr. Opin. Biotechnol.* 14:538-546.

Hinz, B., G.Gabbiani, and C.Chaponnier. 2002. The NH2-terminal peptide of alpha-smooth muscle actin inhibits force generation by the myofibroblast in vitro and in vivo. *J. Cell Biol.* 157:657-663.

Hisaw, F. 1926. Proc Soc Exp Biol med. *Experimental relaxation of the pelvic ligament of the guinea pig* 23:661-663.

Ho, T.Y., W.Yan, and C.A.Bagnell. 2007. Relaxin-induced matrix metalloproteinase-9 expression is associated with activation of the NF-kappaB pathway in human THP-1 cells. *J. Leukoc. Biol.* 81:1303-1310.

Hombach-Klonisch, S., J.Bialek, B.Trojanowicz, E.Weber, H.J.Holzhausen, J.D.Silvertown, A.J.Summerlee, H.Dralle, C.Hoang-Vu, and T.Klonisch. 2006. Relaxin enhances the oncogenic potential of human thyroid carcinoma cells. *Am. J. Pathol.* 169:617-632.

Hoofnagle, J.H. 1989. Type D (delta) hepatitis. *JAMA* 261:1321-1325.

Horuk, R. and S.C.Peiper. 1996. Chemokines: molecular double agents. *Curr. Biol.* 6:1581-1582.

Houglum, K., P.Bedossa, and M.Chojkier. 1994. TGF-beta and collagen-alpha 1 (I) gene expression are increased in hepatic acinar zone 1 of rats with iron overload. *Am J Physiol* 267:G908-G913.

Houglum, K., K.S.Lee, and M.Chojkier. 1997. Proliferation of hepatic stellate cells is inhibited by phosphorylation of CREB on serine 133. *J. Clin. Invest* 99:1322-1328.

Housset, C., D.C.Rockey, and D.M.Bissell. 1993. Endothelin receptors in rat liver: lipocytes as a contractile target for endothelin 1. *Proc. Natl. Acad. Sci. U. S. A* 90:9266-9270.

Housset, C.N., D.C.Rockey, S.L.Friedman, and D.M.Bissell. 1995. Hepatic lipocytes: a major target for endothelin-1. *J. Hepatol.* 22:55-60.

Hsu, S.Y., K.Nakabayashi, S.Nishi, J.Kumagai, M.Kudo, O.D.Sherwood, and A.J.Hsueh. 2002. Activation of orphan receptors by the hormone relaxin. *Science* 295:671-674.

Hudson, P., J.Haley, M.John, M.Cronk, R.Crawford, J.Haralambidis, G.Tregear, J.Shine, and H.Niall. 1983. Structure of a genomic clone encoding biologically active human relaxin. *Nature* 301:628-631.

Hudson, P., M.John, R.Crawford, J.Haralambidis, D.Scanlon, J.Gorman, G.Tregear, J.Shine, and H.Niall. 1984. Relaxin gene expression in human ovaries and the predicted structure of a human preprorelaxin by analysis of cDNA clones. *EMBO J.* 3:2333-2339.

Hynes, R.O. 2002. Integrins: bidirectional, allosteric signaling machines. *Cell* 110:673-687.

Ignarro, L.J., R.E.Byrns, G.M.Buga, K.S.Wood, and G.Chaudhuri. 1988. Pharmacological evidence that endothelium-derived relaxing factor is nitric oxide: use of pyrogallol and superoxide dismutase to study endothelium-dependent and nitric oxide-elicited vascular smooth muscle relaxation. *J. Pharmacol. Exp. Ther.* 244:181-189.

Imai, K., M.Sato, T.Sato, N.Kojima, M.Miura, N.Higashi, D.R.Wang, S.Suzuki, and H.Senoo. 2004. Intercellular Adhesive Structures Between Stellate Cells - An Analysis in Cultured Human Hepatic Stellate Cells. *Comp. Hepatol.* 3 Suppl 1:S13.

Imai, K., T.Sato, and H.Senoo. 2000. Adhesion between cells and extracellular matrix with special reference to hepatic stellate cell adhesion to three-dimensional collagen fibers. *Cell Struct. Funct.* 25:329-336.

Ip, N.Y., C.F.Ibanez, S.H.Nye, J.McClain, P.F.Jones, D.R.Gies, L.Belluscio, M.M.Le Beau, R.Espinosa, III, S.P.Squinto, and . 1992. Mammalian neurotrophin-4: structure, chromosomal localization, tissue distribution, and receptor specificity. *Proc. Natl. Acad. Sci. U. S. A* 89:3060-3064.

Iredale, J. 2008. Defining therapeutic targets for liver fibrosis: Exploiting the biology of inflammation and repair. *Pharmacol. Res.*

Iredale, J.P. 1996. Matrix turnover in fibrogenesis. *Hepatogastroenterology* 43:56-71.

Iredale, J.P. 1997. Tissue inhibitors of metalloproteinases in liver fibrosis. *Int J Biochem Cell Biol* 29:43-54.

Iredale, J.P. 2003. Cirrhosis: new research provides a basis for rational and targeted treatments. *BMJ.* 327:143-147.

Iredale, J.P. 2007. Models of liver fibrosis: exploring the dynamic nature of inflammation and repair in a solid organ. *J. Clin. Invest* 117:539-548.

Iredale, J.P., R.C.Benyon, M.J.Arthur, W.F.Ferris, R.Alcolado, P.J.Winwood, N.Clark, and G.Murphy. 1996. Tissue inhibitor of metalloproteinase-1 messenger RNA expression is enhanced relative to interstitial collagenase messenger RNA in experimental liver injury and fibrosis. *Hepatology* 24:176-184.

Iredale, J.P., R.C.Benyon, J.Pickering, M.McCullen, M.Northrop, S.Pawley, C.Hovell, and M.J.Arthur. 1998. Mechanisms of spontaneous resolution of rat liver fibrosis. Hepatic stellate cell apoptosis and reduced hepatic expression of metalloproteinase inhibitors. *J Clin Invest.* 102:538-549.

Iredale, J.P., G.Murphy, R.M.Hembry, S.L.Friedman, and M.J.Arthur. 1992. Human hepatic lipocytes synthesize tissue inhibitor of metalloproteinases-1. Implications for regulation of matrix degradation in liver. *J Clin Invest.* 90:282-287.

Issa, R., X.Zhou, C.M.Constandinou, J.Fallowfield, H.Millward-Sadler, M.D.Gaca, E.Sands, I.Suliman, N.Trim, A.Knorr, M.J.Arthur, R.C.Benyon, and J.P.Iredale. 2004. Spontaneous recovery from micronodular cirrhosis: evidence for incomplete resolution associated with matrix cross-linking. *Gastroenterology* 126:1795-1808.

Jeyabalan, A. and K.P.Conrad. 2007. Renal function during normal pregnancy and preeclampsia. *Front Biosci.* 12:2425-2437.

Jeyabalan, A., J.Novak, L.A.Danielson, L.J.Kerchner, S.L.Opett, and K.P.Conrad. 2003. Essential role for vascular gelatinase activity in relaxin-induced renal vasodilation, hyperfiltration, and reduced myogenic reactivity of small arteries. *Circ. Res* 93:1249-1257.

Jeyabalan, A., S.G.Shroff, J.Novak, and K.P.Conrad. 2007. The vascular actions of relaxin. *Adv. Exp. Med. Biol.* 612:65-87.

Jiang, Y., B.N.Jahagirdar, R.L.Reinhardt, R.E.Schwartz, C.D.Keene, X.R.Ortiz-Gonzalez, M.Reyes, T.Lenvik, T.Lund, M.Blackstad, J.Du, S.Aldrich, A.Lisberg, W.C.Low, D.A.Largaespada, and C.M.Verfaillie. 2002a. Pluripotency of mesenchymal stem cells derived from adult marrow. *Nature* 418:41-49.

Jiang, Y., B.Vaessen, T.Lenvik, M.Blackstad, M.Reyes, and C.M.Verfaillie. 2002b. Multipotent progenitor cells can be isolated from postnatal murine bone marrow, muscle, and brain. *Exp. Hematol.* 30:896-904.

John, M.J., B.W.Borjesson, J.R.Walsh, and H.D.Niall. 1981. Limited sequence homology between porcine and rat relaxins: implications for physiological studies. *Endocrinology* 108:726-729.

Juan, T.S., I.K.McNiece, G.Van, D.Lacey, C.Hartley, P.McElroy, Y.Sun, J.Argento, D.Hill, X.Q.Yan, and F.A.Fletcher. 1997. Chronic expression of

murine flt3 ligand in mice results in increased circulating white blood cell levels and abnormal cellular infiltrates associated with splenic fibrosis. *Blood* 90:76-84.

Jung, Y., J.Wang, A.Havens, Y.Sun, J.Wang, T.Jin, and R.S.Taichman. 2005. Cell-to-cell contact is critical for the survival of hematopoietic progenitor cells on osteoblasts. *Cytokine* 32:155-162.

Junqueira, L.C., G.Bignolas, and R.R.Brentani. 1979. Picrosirius staining plus polarization microscopy, a specific method for collagen detection in tissue sections. *Histochem. J.* 11:447-455.

Junqueira, L.C., W.Cossermelli, and R.Brentani. 1978. Differential staining of collagens type I, II and III by Sirius Red and polarization microscopy. *Arch. Histol. Jpn.* 41:267-274.

Kaissling, B., M.Le Hir, 2008. The renal cortical intersitium morphological and functional aspects. *Hitochem Cell Biol.* Aug:130:247-262.

Kamat, A.A., S.Feng, I.U.Agoulnik, F.Kheradmand, N.V.Bogatcheva, D.Coffey, A.K.Sood, and A.I.Agoulnik. 2006. The role of relaxin in endometrial cancer. *Cancer Biol. Ther.* 5:71-77.

Kanda, T., O.Yokosuka, and Y.Suzuki. 2005. Prolonged hepatitis caused by cytomegalovirus and non-alcoholic steatohepatitis in 16-year-old obese boy. *Eur J Pediatr* 164:212-215.

Kato, K., T.Takada, and T.Fukusato. 2007. Expression of vascular endothelial-cadherin in human hepatocellular carcinoma tissues. *Hepatol. Res.* 37:444-453.

Kaufmann, S.H., S.Desnoyers, Y.Ottaviano, N.E.Davidson, and G.G.Poirier. 1993. Specific proteolytic cleavage of poly(ADP-ribose) polymerase: an early marker of chemotherapy-induced apoptosis. *Cancer Res.* 53:3976-3985.

Kerchner, L.J., J.Novak, K.Hanley-Yanez, K.D.Doty, L.A.Danielson, and K.P.Conrad. 2005. Evidence against the hypothesis that endothelial endothelin B receptor expression is regulated by relaxin and pregnancy. *Endocrinology* 146:2791-2797.

Kern, A., A.I.Agoulnik, and G.D.Bryant-Greenwood. 2007. The low-density lipoprotein class A module of the relaxin receptor (leucine-rich repeat containing G-protein coupled receptor 7): its role in signaling and trafficking to the cell membrane. *Endocrinology* 148:1181-1194.

Kerr, J.F. and J.Searle. 1973. Deletion of cells by apoptosis during castration-induced involution of the rat prostate. *Virchows Arch. B Cell Pathol.* 13:87-102.

Kerr, J.F., A.H.Wyllie, and A.R.Currie. 1972. Apoptosis: a basic biological phenomenon with wide-ranging implications in tissue kinetics. *Br. J. Cancer* 26:239-257.

Khan, S., A.Dodson, F.Campbell, A.Kawesha, J.S.Grime, M.Critchley, and R.Sutton. 2005. Prognostic potential of hepatocyte volume and cytokine expression in cirrhotic portal hypertension. *J. Gastroenterol. Hepatol.* 20:1519-1526.

Kharbanda, K.K., D.D.Rogers, T.A.Wyatt, M.F.Sorrell, and D.J.Tuma. 2004. Transforming growth factor-beta induces contraction of activated hepatic stellate cells. *J. Hepatol.* 41:60-66.

Kheradmand, F. and Z.Werb. 2002. Shedding light on sheddases: role in growth and development. *Bioessays* 24:8-12.

Kim, W.R. 2002. The burden of hepatitis C in the United States. *Hepatology* 36:S30-S34.

Knittel, T., M.Mehde, A.Grundmann, B.Saile, J.G.Scharf, and G.Ramadori. 2000. Expression of matrix metalloproteinases and their inhibitors during hepatic tissue repair in the rat. *Histochem. Cell Biol.* 113:443-453.

Knittel, T., M.Mehde, D.Kobold, B.Saile, C.Dinter, and G.Ramadori. 1999. Expression patterns of matrix metalloproteinases and their inhibitors in parenchymal and non-parenchymal cells of rat liver: regulation by TNF-alpha and TGF-beta1. *J. Hepatol.* 30:48-60.

Kone, B.C., T.Kuncewicz, W.Zhang, and Z.Y.Yu. 2003. Protein interactions with nitric oxide synthases: controlling the right time, the right place, and the right amount of nitric oxide. *Am. J. Physiol Renal Physiol* 285:F178-F190.

Korbling, M. and Z.Estrov. 2003. Adult stem cells for tissue repair - a new therapeutic concept? *N. Engl. J. Med.* 349:570-582.

Korzeniewski, C. and D.M.Callewaert. 1983. An enzyme-release assay for natural cytotoxicity. *J. Immunol. Methods* 64:313-320.

Krajnc-Franken, M.A., A.J.van Disseldorp, J.E.Koenders, S.Mosselman, D.M.van, and J.A.Gossen. 2004. Impaired nipple development and parturition in LGR7 knockout mice. *Mol. Cell Biol.* 24:687-696.

Krizhanovsky, V., M.Yon, R.A.Dickins, S.Hearn, J.Simon, C.Miething, H.Yee, L.Zender, and S.W.Lowe. 2008. Senescence of activated stellate cells limits liver fibrosis. *Cell* 134:657-667.

Kroemer, G. 1997. The proto-oncogene Bcl-2 and its role in regulating apoptosis. *Nat. Med.* 3:614-620.

Kubista, M., J.M.Andrade, M.Bengtsson, A.Forootan, J.Jonak, K.Lind, R.Sindelka, R.Sjoback, B.Sjogreen, L.Strombom, A.Stahlberg, and N.Zoric. 2006. The real-time polymerase chain reaction. *Mol. Aspects Med.* 27:95-125.

Kumar, P.D. and K.G.Chandrasekharan. 1994. Encysted ascites caused by entamoeba histolytica. *J Assoc. Physicians. India.* 42:168.

Laemmli, U.K. 1970. Cleavage of structural proteins during the assembly of the head of bacteriophage T4. *Nature* 227:680-685.

Lagasse, E., H.Connors, M.Al-Dhalimy, M.Reitsma, M.Dohse, L.Osborne, X.Wang, M.Finegold, I.L.Weissman, and M.Grompe. 2000. Purified hematopoietic stem cells can differentiate into hepatocytes in vivo. *Nat. Med.* 6:1229-1234.

Lai, M.M. 1995. The molecular biology of hepatitis delta virus. *Annu. Rev. Biochem.* 64:259-286.

Lampugnani, M.G., M.Resnati, M.Raiteri, R.Pigott, A.Pisacane, G.Houen, L.P.Ruco, and E.Dejana. 1992. A novel endothelial-specific membrane protein is a marker of cell-cell contacts. *J. Cell Biol.* 118:1511-1522.

Lands, W.E. 1995a. Alcohol and energy intake. *Am. J. Clin. Nutr.* 62:1101S-1106S.

Lands, W.E. 1995b. Cellular signals in alcohol-induced liver injury: a review. *Alcohol Clin. Exp. Res.* 19:928-938.

Lapidot, T. 2001. Mechanism of human stem cell migration and repopulation of NOD/SCID and B2mnull NOD/SCID mice. The role of SDF-1/CXCR4 interactions. *Ann. N. Y. Acad. Sci.* 938:83-95.

Laurent, G.J. 1987. Dynamic state of collagen: pathways of collagen degradation in vivo and their possible role in regulation of collagen mass. *Am. J. Physiol* 252:C1-C9.

Lavker, R.M. and T.T.Sun. 2000. Epidermal stem cells: properties, markers, and location. *Proc. Natl. Acad. Sci. U. S. A* 97:13473-13475.

Lawyer, F.C., S.Stoffel, R.K.Saiki, S.Y.Chang, P.A.Landre, R.D.Abramson, and D.H.Gelfand. 1993. High-level expression, purification, and enzymatic characterization of full-length Thermus aquaticus DNA polymerase and a truncated form deficient in 5' to 3' exonuclease activity. *PCR Methods Appl.* 2:275-287.

Le, B.B., P.Bioulac-Sage, R.Senuita, A.Quinton, J.Saric, and C.Balabaud. 1990. Fine structure of hepatic sinusoids and sinusoidal cells in disease. *J. Electron Microsc. Tech.* 14:257-282.

Lekgabe, E.D., H.Kiriazis, C.Zhao, Q.Xu, X.L.Moore, Y.Su, R.A.Bathgate, X.J.Du, and C.S.Samuel. 2005. Relaxin reverses cardiac and renal fibrosis in spontaneously hypertensive rats. *Hypertension* 46:412-418.

Leung, R.K. and P.A.Whittaker. 2005. RNA interference: from gene silencing to gene-specific therapeutics. *Pharmacol. Ther.* 107:222-239.

Li, D. and S.L.Friedman. 1999. Liver fibrogenesis and the role of hepatic stellate cells: new insights and prospects for therapy. *J. Gastroenterol. Hepatol.* 14:618-633.

Libbrecht, L. and T.Roskams. 2002. Hepatic progenitor cells in human liver diseases. *Semin. Cell Dev. Biol.* 13:389-396.

Lichtinghagen, R., D.Michels, C.I.Haberkorn, B.Arndt, M.Bahr, P.Flemming, M.P.Manns, and K.H.Boeker. 2001. Matrix metalloproteinase (MMP)-2, MMP-7, and tissue inhibitor of metalloproteinase-1 are closely related to the fibroproliferative process in the liver during chronic hepatitis C. *J. Hepatol.* 34:239-247.

Lincoln, T.M., K.B.Pryzwansky, T.L.Cornwell, T.A.Wyatt, and L.A.MacMillan. 1993. Cyclic-GMP-dependent protein kinase in smooth muscle and neutrophils. *Adv. Second Messenger Phosphoprotein Res.* 28:121-132.

Liu, C., J.Chen, C.Kuei, S.Sutton, D.Nepomuceno, P.Bonaventure, and T.W.Lovenberg. 2005a. Relaxin-3/insulin-like peptide 5 chimeric peptide, a selective ligand for G protein-coupled receptor (GPCR)135 and GPCR142 over leucine-rich repeat-containing G protein-coupled receptor 7. *Mol. Pharmacol.* 67:231-240.

Liu, C., E.Eriste, S.Sutton, J.Chen, B.Roland, C.Kuei, N.Farmer, H.Jornvall, R.Sillard, and T.W.Lovenberg. 2003. Identification of relaxin-3/INSL7 as an endogenous ligand for the orphan G-protein-coupled receptor GPCR135. *J. Biol. Chem.* 278:50754-50764.

Liu, C., C.Kuei, S.Sutton, J.Chen, P.Bonaventure, J.Wu, D.Nepomuceno, F.Kamme, D.T.Tran, J.Zhu, T.Wilkinson, R.Bathgate, E.Eriste, R.Sillard, and T.W.Lovenberg. 2005b. INSL5 is a high affinity specific agonist for GPCR142 (GPR100). *J. Biol. Chem.* 280:292-300.

Llanos, R.M. and J.F.Mercer. 2002. The molecular basis of copper homeostasis copper-related disorders. *DNA Cell Biol.* 21:259-270.

Lo, R., A.Austin, and J.Freeman. 2008. Vasopressin in liver disease - should we turn on or off? *Curr. Clin. Pharmacol.* 3:156-165.

LONG, C. and M.F.MAGUIRE. 1954. The structure of the naturally occurring phosphoglycerides. II. Evidence derived from a study of the action of phospholipase C. *Biochem. J.* 57:223-226.

Machesky, L.M. and A.Hall. 1997. Role of actin polymerization and adhesion to extracellular matrix in Rac- and Rho-induced cytoskeletal reorganization. *J. Cell Biol.* 138:913-926.

Madsen, K.M., W.L.Clapp, and J.W.Verlander. 1988a. Structure and function of the inner medullary collecting duct. *Kidney Int.* 34:441-454.

Madsen, K.M., J.W.Verlander, and C.C.Tisher. 1988b. Relationship between structure and function in distal tubule and collecting duct. *J. Electron Microsc. Tech.* 9:187-208.

Maisonpierre, P.C., C.Suri, P.F.Jones, S.Bartunkova, S.J.Wiegand, C.Radziejewski, D.Compton, J.McClain, T.H.Aldrich, N.Papadopoulos, T.J.Daly, S.Davis, T.N.Sato, and G.D.Yancopoulos. 1997. Angiopoietin-2, a natural antagonist for Tie2 that disrupts in vivo angiogenesis. *Science* 277:55-60.

Mallat, A. 1998. Hepatic stellate cells and intrahepatic modulation of portal pressure. *Digestion* 59:416-419.

Marshman, E., C.Booth, and C.S.Potten. 2002. The intestinal epithelial stem cell. *Bioessays* 24:91-98.

Martin, G.R. 1981. Isolation of a pluripotent cell line from early mouse embryos cultured in medium conditioned by teratocarcinoma stem cells. *Proc. Natl. Acad. Sci. U. S. A* 78:7634-7638.

Martin, S.J. and D.R.Green. 1995. Protease activation during apoptosis: death by a thousand cuts? *Cell* 82:349-352.

Mason, D.Y. and R.Sammons. 1978. Alkaline phosphatase and peroxidase for double immunoenzymatic labelling of cellular constituents. *J. Clin. Pathol.* 31:454-460.

Massaous, J. and A.Hata. 1997. TGF-beta signalling through the Smad pathway. *Trends Cell Biol.* 7:187-192.

Mast, E.E., M.J.Alter, and H.S.Margolis. 1999. Strategies to prevent and control hepatitis B and C virus infections: a global perspective. *Vaccine.* 17:1730-1733.

Mast, E.E. and K.Krawczynski. 1996. Hepatitis E: an overview. *Annu. Rev. Med.* 47:257-266.

Masterson, R., T.D.Hewitson, K.Kelynack, M.Martic, L.Parry, R.Bathgate, I.Darby, and G.Becker. 2004. Relaxin down-regulates renal fibroblast function and promotes matrix remodelling in vitro. *Nephrol. Dial. Transplant.* 19:544-552.

Mathieson, P.W. 2007. Minimal change nephropathy and focal segmental glomerulosclerosis. *Semin. Immunopathol.* 29:415-426.

Matrisian, L.M. 1990. Metalloproteinases and their inhibitors in matrix remodelling. *Trends Genet.* 6:121-125.

Matsui, T., M.Heidaran, T.Miki, N.Popescu, R.W.La, M.Kraus, J.Pierce, and S.Aaronson. 1989a. Isolation of a novel receptor cDNA establishes the existence of two PDGF receptor genes. *Science* 243:800-804.

Matsui, T., J.H.Pierce, T.P.Fleming, J.S.Greenberger, W.J.LaRochelle, M.Ruggiero, and S.A.Aaronson. 1989b. Independent expression of human alpha or beta platelet-derived growth factor receptor cDNAs in a naive hematopoietic cell leads to functional coupling with mitogenic and chemotactic signaling pathways. *Proc. Natl. Acad. Sci. U. S. A* 86:8314-8318.

McCawley, L.J. and L.M.Matrisian. 2001. Matrix metalloproteinases: they're not just for matrix anymore! *Curr. Opin. Cell Biol.* 13:534-540.

McGuire, R.F., D.M.Bissell, J.Boyles, and F.J.Roll. 1992. Role of extracellular matrix in regulating fenestrations of sinusoidal endothelial cells isolated from normal rat liver. *Hepatology* 15:989-997.

Medema, J.P., C.Scaffidi, F.C.Kischkel, A.Shevchenko, M.Mann, P.H.Krammer, and M.E.Peter. 1997. FLICE is activated by association with the CD95 death-inducing signaling complex (DISC). *EMBO J.* 16:2794-2804.

Meindl-Beinker, N.M. and S.Dooley. 2008. Transforming growth factor-beta and hepatocyte transdifferentiation in liver fibrogenesis. *J. Gastroenterol. Hepatol.* 23 Suppl 1:S122-S127.

Meyer-ter-Vehn, T., B.Katzenberger, H.Han, F.Grehn, and G.Schlunck. 2008. Lovastatin inhibits TGF-beta-induced myofibroblast transdifferentiation in human tenon fibroblasts. *Invest Ophthalmol. Vis. Sci.* 49:3955-3960.

Michalopoulos, G.K. and M.C.DeFrances. 1997. Liver regeneration. *Science* 276:60-66.

Milewicz, D.M., Z.Urban, and C.Boyd. 2000. Genetic disorders of the elastic fiber system. *Matrix Biol.* 19:471-480.

Miner, J.H. 1999. Renal basement membrane components. *Kidney Int.* 56:2016-2024.

Mizuguchi, H., M.Nakatsuji, S.Fujiwara, M.Takagi, and T.Imanaka. 1999. Characterization and application to hot start PCR of neutralizing monoclonal antibodies against KOD DNA polymerase. *J. Biochem.* 126:762-768.

Mookerjee, I., M.L.Tang, N.Solly, G.W.Tregear, and C.S.Samuel. 2005a. Investigating the role of relaxin in the regulation of airway fibrosis in animal models of acute and chronic allergic airway disease. *Ann. N Y. Acad. Sci.* 1041:194-196.

Mookerjee, I., E.N.Unemori, X.J.Du, G.W.Tregear, and C.S.Samuel. 2005b. Relaxin modulates fibroblast function, collagen production, and matrix metalloproteinase-2 expression by cardiac fibroblasts. *Ann N Y. Acad Sci.* 1041:190-193.

Morales, J., E.Moitinho, J.G.Abraldes, M.Fernandez, and J.Bosch. 2003. Effects of the V1a vasopressin agonist F-180 on portal hypertension-related bleeding in portal hypertensive rats. *Hepatology* 38:1378-1383.

Mullauer, L., P.Gruber, D.Sebinger, J.Buch, S.Wohlfart, and A.Chott. 2001. Mutations in apoptosis genes: a pathogenetic factor for human disease. *Mutat. Res.* 488:211-231.

Murakami, K., T.Abe, M.Miyazawa, M.Yamaguchi, T.Masuda, T.Matsuura, S.Nagamori, K.Takeuchi, K.Abe, and M.Kyogoku. 1995. Establishment of a new human cell line, LI90, exhibiting characteristics of hepatic Ito (fat-storing) cells. *Lab Invest* 72:731-739.

Murphy, F.R., R.Issa, X.Zhou, S.Ratnarajah, H.Nagase, M.J.Arthur, C.Benyon, and J.P.Iredale. 2002. Inhibition of apoptosis of activated hepatic stellate cells by tissue inhibitor of metalloproteinase-1 is mediated via effects on matrix metalloproteinase inhibition: implications for reversibility of liver fibrosis. *J Biol Chem.* 277:11069-11076.

Myllyharju, J. and K.I.Kivirikko. 2001. Collagens and collagen-related diseases. *Ann. Med.* 33:7-21.

Nakane, P.K. and G.B.Pierce, Jr. 1966. Enzyme-labeled antibodies: preparation and application for the localization of antigens. *J. Histochem. Cytochem.* 14:929-931.

Natoli, G., A.Ianni, A.Costanzo, P.G.De, I.Ilari, P.Chirillo, C.Balsano, and M.Levrero. 1995. Resistance to Fas-mediated apoptosis in human hepatoma cells. *Oncogene* 11:1157-1164.

Negulescu, O., I.Bognar, J.Lei, P.Devarajan, S.Silbiger, and J.Neugarten. 2002. Estradiol reverses TGF-beta1-induced mesangial cell apoptosis by a casein kinase 2-dependent mechanism. *Kidney Int.* 62:1989-1998.

Neugarten, J., I.Medve, J.Lei, and S.R.Silbiger. 1999. Estradiol suppresses mesangial cell type I collagen synthesis via activation of the MAP kinase cascade. *Am. J. Physiol* 277:F875-F881.

Ngo, P., P.Ramalingam, J.A.Phillips, and G.T.Furuta. 2006. Collagen gel contraction assay. *Methods Mol. Biol.* 341:103-109.

Nguyen, B.T., L.Yang, B.M.Sanborn, and C.W.Dessauer. 2003. Phosphoinositide 3-kinase activity is required for biphasic stimulation of cyclic adenosine 3',5'-monophosphate by relaxin. *Mol. Endocrinol.* 17:1075-1084.

Nistri, S. and D.Bani. 2003. Relaxin receptors and nitric oxide synthases: search for the missing link. *Reprod. Biol. Endocrinol.* 1:5.

Nolte, W., J.Wiltfang, C.Schindler, H.Munke, K.Unterberg, U.Zumhasch, H.R.Figulla, G.Werner, H.Hartmann, and G.Ramadori. 1998. Portosystemic hepatic encephalopathy after transjugular intrahepatic portosystemic shunt in patients with cirrhosis: clinical, laboratory, psychometric, and electroencephalographic investigations. *Hepatology* 28:1215-1225.

O'Connell, J., A.Houston, M.W.Bennett, G.C.O'Sullivan, and F.Shanahan. 2001. Immune privilege or inflammation? Insights into the Fas ligand enigma. *Nat. Med.* 7:271-274.

Oakley, F., J.Mann, S.Nailard, D.E.Smart, N.Mungalsingh, C.Constandinou, S.Ali, S.J.Wilson, H.Millward-Sadler, J.P.Iredale, and D.A.Mann. 2005. Nuclear factor-kappaB1 (p50) limits the inflammatory and fibrogenic responses to chronic injury. *Am. J. Pathol.* 166:695-708.

Oakley, F., N.Trim, C.M.Constandinou, W.Ye, A.M.Gray, G.Frantz, K.Hillan, T.Kendall, R.C.Benyon, D.A.Mann, and J.P.Iredale. 2003. Hepatocytes express nerve growth factor during liver injury: evidence for paracrine regulation of hepatic stellate cell apoptosis. *Am J Pathol.* 163:1849-1858.

Okuno, M., K.Akita, H.Moriwaki, N.Kawada, K.Ikeda, K.Kaneda, Y.Suzuki, and S.Kojima. 2001. Prevention of rat hepatic fibrosis by the protease inhibitor, camostat mesilate, via reduced generation of active TGF-beta. *Gastroenterology* 120:1784-1800.

Oldham, R.K., J.R.Ortaldo, H.T.Holden, and R.B.Herberman. 1977. Cytotoxicity inhibition assay: cryopreservation and standardization: brief communication. *J. Natl. Cancer Inst.* 59:1321-1323.

Oppenheim, J.J., C.O.Zachariae, N.Mukaida, and K.Matsushima. 1991. Properties of the novel proinflammatory supergene "intercrine" cytokine family. *Annu. Rev. Immunol.* 9:617-648.

Pang, I.H., D.L.Shade, E.Tamm, and L.DeSantis. 1993. Single-cell contraction assay for human ciliary muscle cells. Effect of carbachol. *Invest Ophthalmol. Vis. Sci.* 34:1876-1879.

Parry, L.J. and L.A.Vodstrcil. 2007. Relaxin physiology in the female reproductive tract during pregnancy. *Adv. Exp. Med. Biol.* 612:34-48.

Pawlina, W., L.H.Larkin, and S.C.Frost. 1989. Effect of relaxin on differentiation of 3T3-L1 preadipocytes. *Endocrinology* 125:2049-2055.

Perlmutter, D.H. 2002. Liver injury in alpha1-antitrypsin deficiency: an aggregated protein induces mitochondrial injury. *J. Clin. Invest* 110:1579-1583.

Perri, R.E., D.A.Langer, S.Chatterjee, S.J.Gibbons, J.Gadgil, S.Cao, G.Farrugia, and V.H.Shah. 2006. Defects in cGMP-PKG pathway contribute to impaired NO-dependent responses in hepatic stellate cells upon activation. *Am. J. Physiol Gastrointest. Liver Physiol* 290:G535-G542.

Philpott, C.C. 2002. Molecular aspects of iron absorption: Insights into the role of HFE in hemochromatosis. *Hepatology* 35:993-1001.

Pietrangelo, A. 2002. Physiology of iron transport and the hemochromatosis gene. *Am. J. Physiol Gastrointest. Liver Physiol* 282:G403-G414.

Pinzani, M., L.Gesualdo, G.M.Sabbah, and H.E.Abboud. 1989. Effects of platelet-derived growth factor and other polypeptide mitogens on DNA synthesis and growth of cultured rat liver fat-storing cells. *J. Clin. Invest* 84:1786-1793.

Pinzani, M., S.Milani, F.R.De, C.Grappone, A.Caligiuri, A.Gentilini, C.Tosti-Guerra, M.Maggi, P.Failli, C.Ruocco, and P.Gentilini. 1996. Endothelin 1 is overexpressed in human cirrhotic liver and exerts multiple effects on activated hepatic stellate cells. *Gastroenterology* 110:534-548.

Pomerantz, R.J. and G.Nunnari. 2004. HIV and GB virus C--can two viruses be better than one? *N. Engl. J. Med.* 350:963-965.

Ponta, H., L.Sherman, and P.A.Herrlich. 2003. CD44: from adhesion molecules to signalling regulators. *Nat. Rev. Mol. Cell Biol.* 4:33-45.

Priya, S. and P.R.Sudhakaran. 2008. Cell survival, activation and apoptosis of hepatic stellate cells: modulation by extracellular matrix proteins. *Hepatol. Res.*

Prockop, D.J. and K.I.Kivirikko. 1995. Collagens: molecular biology, diseases, and potentials for therapy. *Annu. Rev. Biochem.* 64:403-434.

Quenet, D., R.R.El, V.Schreiber, and F.Dantzer. 2008. The role of poly(ADP-ribosyl)ation in epigenetic events. *Int. J. Biochem. Cell Biol.*

Radestock, Y., C.Hoang-Vu, and S.Hombach-Klonisch. 2008. Relaxin reduces xenograft tumour growth of human MDA-MB-231 breast cancer cells. *Breast Cancer Res.* 10:R71.

Ramadori, G. 1991. The stellate cell (Ito-cell, fat-storing cell, lipocyte, perisinusoidal cell) of the liver. New insights into pathophysiology of an intriguing cell. *Virchows Arch. B Cell Pathol. Incl. Mol. Pathol.* 61:147-158.

Rameshwar, P., H.S.Oh, C.Yook, P.Gascon, and V.T.Chang. 2003. Substance p-fibronectin-cytokine interactions in myeloproliferative disorders with bone marrow fibrosis. *Acta Haematol.* 109:1-10.

RAPPAPORT, A.M. 1958. The structural and functional unit in the human liver (liver acinus). *Anat. Rec.* 130:673-689.

Reynaert, H., M.G.Thompson, T.Thomas, and A.Geerts. 2002. Hepatic stellate cells: role in microcirculation and pathophysiology of portal hypertension. *Gut* 50:571-581.

Rockey, D.C. 1997. New concepts in the pathogenesis of portal hypertension: hepatic wounding and stellate cell contractility. *Clin. Liver Dis.* 1:13-29.

Rockey, D.C. 2001. Hepatic blood flow regulation by stellate cells in normal and injured liver. *Semin. Liver Dis.* 21:337-349.

Rockey, D.C., J.K.Boyles, G.Gabbiani, and S.L.Friedman. 1992. Rat hepatic lipocytes express smooth muscle actin upon activation in vivo and in culture. *J. Submicrosc. Cytol. Pathol.* 24:193-203.

Rockey, D.C., C.N.Housset, and S.L.Friedman. 1993. Activation-dependent contractility of rat hepatic lipocytes in culture and in vivo. *J. Clin. Invest* 92:1795-1804.

Rockey, D.C. and R.A.Weisiger. 1996. Endothelin induced contractility of stellate cells from normal and cirrhotic rat liver: implications for regulation of portal pressure and resistance. *Hepatology* 24:233-240.

Roderfeld, M., R.Weiskirchen, S.Wagner, M.L.Berres, C.Henkel, J.Grotzinger, A.M.Gressner, S.Matern, and E.Roeb. 2006. Inhibition of hepatic fibrogenesis by matrix metalloproteinase-9 mutants in mice. *FASEB J.* 20:444-454.

Roderick, P. 2004. Liver function tests: defining what's normal. *BMJ* 328:987.

Rogers, E.L. 1985. Hepatic encephalopathy. *Crit Care Clin.* 1:313-325.

Rolla, R., D.Vay, E.Mottaran, M.Parodi, N.Traverso, S.Arico, M.Sartori, G.Bellomo, L.W.Klassen, G.M.Thiele, D.J.Tuma, and E.Albano. 2000. Detection of circulating antibodies against malondialdehyde-acetaldehyde adducts in patients with alcohol-induced liver disease. *Hepatology* 31:878-884.

Roncalli, M., M.Borzio, and T.L.Di. 2008. Hepatocellular dysplastic nodules. *Ann. Ital. Chir* 79:81-89.

Saha, T.C. and H.Singh. 2006. Minimal change disease: a review. *South. Med. J.* 99:1264-1270.

Samah, B., F.Porcheray, and G.Gras. 2008. Neurotrophins modulate monocyte chemotaxis without affecting macrophage function. *Clin. Exp. Immunol.* 151:476-486.

Samuel, C.S. 2005b. Relaxin: antifibrotic properties and effects in models of disease. *Clin. Med. Res.* 3:241-249.

Samuel, C.S. and T.D.Hewitson. 2006. Relaxin in cardiovascular and renal disease. *Kidney Int* 69:1498-1502.

Samuel, C.S., I.Mookerjee, R.Masterson, G.W.Tregear, and T.D.Hewitson. 2005a. Relaxin regulates collagen overproduction associated with experimental progressive renal fibrosis. *Ann. N. Y. Acad. Sci.* 1041:182-184.

Samuel, C.S., H.Tian, L.Zhao, and E.P.Amento. 2003. Relaxin is a key mediator of prostate growth and male reproductive tract development. *Lab Invest* 83:1055-1067.

Samuel, C.S., E.N.Unemori, I.Mookerjee, R.A.Bathgate, S.L.Layfield, J.Mak, G.W.Tregear, and X.J.Du. 2004. Relaxin modulates cardiac fibroblast proliferation, differentiation, and collagen production and reverses cardiac fibrosis in vivo. *Endocrinology* 145:4125-4133.

Samuel, C.S., C.Zhao, R.A.Bathgate, X.J.Du, R.J.Summers, E.P.Amento, L.L.Walker, M.McBurnie, L.Zhao, and G.W.Tregear. 2005b. The relaxin gene-knockout mouse: a model of progressive fibrosis. *Ann. N Y. Acad. Sci.* 1041:173-181.

Samuel, C.S., C.Zhao, Q.Yang, H.Wang, H.Tian, G.W.Tregear, and E.P.Amento. 2005c. The relaxin gene knockout mouse: a model of progressive scleroderma. *J Invest. Dermatol.* 125:692-699.

Sanborn, B.M. 2001. Hormones and calcium: mechanisms controlling uterine smooth muscle contractile activity. The Litchfield Lecture. *Exp. Physiol* 86:223-237.

Sanderson, N., V.Factor, P.Nagy, J.Kopp, P.Kondaiah, L.Wakefield, A.B.Roberts, M.B.Sporn, and S.S.Thorgeirsson. 1995. Hepatic expression of

mature transforming growth factor beta 1 in transgenic mice results in multiple tissue lesions. *Proc. Natl. Acad. Sci. U. S. A* 92:2572-2576.

Sanes, J.R. 2003. The basement membrane/basal lamina of skeletal muscle. *J. Biol. Chem.* 278:12601-12604.

Sato, Y., R.Tsuboi, R.Lyons, H.Moses, and D.B.Rifkin. 1990. Characterization of the activation of latent TGF-beta by co-cultures of endothelial cells and pericytes or smooth muscle cells: a self-regulating system. *J. Cell Biol.* 111:757-763.

Saxena, R., N.D.Theise, and J.M.Crawford. 1999. Microanatomy of the human liver-exploring the hidden interfaces. *Hepatology* 30:1339-1346.

Schaefer, M., R.G.Hopkins, M.L.Failla, and J.D.Gitlin. 1999. Hepatocyte-specific localization and copper-dependent trafficking of the Wilson's disease protein in the liver. *Am J Physiol* 276:G639-G646.

Schnaper, H.W., T.Hayashida, S.C.Hubchak, and A.C.Poncelet. 2003. TGF-beta signal transduction and mesangial cell fibrogenesis. *Am. J. Physiol Renal Physiol* 284:F243-F252.

Schofield, B.M. 1957. The hormonal control of myometrial function during pregnancy. *J. Physiol* 138:1-10.

Schofield, B.M. and C.WOOD. 1964. LENGTH-TENSION RELATION IN RABBIT AND HUMAN MYOMETRIUM. *J. Physiol* 175:125-133.

Schuppan, D., M.Ruehl, R.Somasundaram, and E.G.Hahn. 2001. Matrix as a modulator of hepatic fibrogenesis. *Semin. Liver Dis.* 21:351-372.

Schwabe, C. and J.K.McDonald. 1977. Primary structure of the B-chain of porcine relaxin. *Biochem. Biophys. Res. Commun.* 75:503-510.

Schwabe, C., J.K.McDonald, and B.G.Steinetz. 1976. Primary structure of the A chain of porcine relaxin. *Biochem. Biophys. Res. Commun.* 70:397-405.

Scoazec, J.Y. and G.Feldmann. 1994. The cell adhesion molecules of hepatic sinusoidal endothelial cells. *J. Hepatol.* 20:296-300.

Scoazec, J.Y., L.Racine, A.Couvelard, J.F.Flejou, and G.Feldmann. 1994. Endothelial cell heterogeneity in the normal human liver acinus: in situ immunohistochemical demonstration. *Liver* 14:113-123.

Seamon, K.B., W.Padgett, and J.W.Daly. 1981. Forskolin: unique diterpene activator of adenylate cyclase in membranes and in intact cells. *Proc. Natl. Acad. Sci. U. S. A* 78:3363-3367.

Searle, J., J.F.Kerr, and C.J.Bishop. 1982. Necrosis and apoptosis: distinct modes of cell death with fundamentally different significance. *Pathol. Annu.* 17 Pt 2:229-259.

Seibold, J.R., J.H.Korn, R.Simms, P.J.Clements, L.W.Moreland, M.D.Mayes, D.E.Furst, N.Rothfield, V.Steen, M.Weisman, D.Collier, F.M.Wigley, P.A.Merkel, M.E.Csuka, V.Hsu, S.Rocco, M.Erikson, J.Hannigan, W.S.Harkonen, and M.E.Sanders. 2000b. Recombinant human relaxin in the treatment of scleroderma. A randomized, double-blind, placebo-controlled trial. *Ann Intern. Med* 132:871-879.

Seibold, J.R., J.H.Korn, R.Simms, P.J.Clements, L.W.Moreland, M.D.Mayes, D.E.Furst, N.Rothfield, V.Steen, M.Weisman, D.Collier, F.M.Wigley, P.A.Merkel, M.E.Csuka, V.Hsu, S.Rocco, M.Erikson, J.Hannigan, W.S.Harkonen, and M.E.Sanders. 2000a. Recombinant human relaxin in the treatment of scleroderma. A randomized, double-blind, placebo-controlled trial. *Ann Intern. Med* 132:871-879.

Servillo, G., M.A.la Fazia, and P.Sassone-Corsi. 2002. Coupling cAMP signaling to transcription in the liver: pivotal role of CREB and CREM. *Exp. Cell Res.* 275:143-154.

Shaulian, E. and M.Karin. 2002. AP-1 as a regulator of cell life and death. *Nat. Cell Biol.* 4:E131-E136.

Sheahan, S., C.O.Bellamy, S.N.Harland, D.J.Harrison, and S.Prost. 2008. TGFbeta induces apoptosis and EMT in primary mouse hepatocytes independently of p53, p21Cip1 or Rb status. *BMC. Cancer* 8:191.

Sheikh, S., W.B.Gratzer, J.C.Pinder, and G.B.Nash. 1997. Actin polymerisation regulates integrin-mediated adhesion as well as rigidity of neutrophils. *Biochem. Biophys. Res. Commun.* 238:910-915.

Sherwood, O.D. 2004b. Relaxin's physiological roles and other diverse actions. *Endocr Rev.* 25:205-234.

Sherwood, O.D. 2004a. Relaxin's physiological roles and other diverse actions. *Endocr Rev.* 25:205-234.

Smith, M., J.Davison, K.Conrad, and L.Danielson. 2005. Renal hemodynamic effects of relaxin in humans. *Ann. N. Y. Acad. Sci.* 1041:163-172.

Sodek, J., B.Zhu, M.H.Huynh, T.J.Brown, and M.Ringuette. 2002. Novel functions of the matricellular proteins osteopontin and osteonectin/SPARC. *Connect. Tissue Res.* 43:308-319.

Somerville, R.P., S.A.Oblander, and S.S.Apte. 2003. Matrix metalloproteinases: old dogs with new tricks. *Genome Biol.* 4:216.

Stahlberg, A., N.Zoric, P.Aman, and M.Kubista. 2005. Quantitative real-time PCR for cancer detection: the lymphoma case. *Expert. Rev. Mol. Diagn.* 5:221-230.

Sterzel, R.B., E.Schulze-Lohoff, and M.Marx. 1993. Cytokines and mesangial cells. *Kidney Int. Suppl* 39:S26-S31.

Sterzel, R.B., E.Schulze-Lohoff, M.Weber, and S.L.Goodman. 1992. Interactions between glomerular mesangial cells, cytokines, and extracellular matrix. *J. Am. Soc. Nephrol.* 2:S126-S131.

Stupack, D.G. and D.A.Cheresh. 2002. Get a ligand, get a life: integrins, signaling and cell survival. *J. Cell Sci.* 115:3729-3738.

Su, A.I., L.G.Guidotti, J.P.Pezacki, F.V.Chisari, and P.G.Schultz. 2002. Gene expression during the priming phase of liver regeneration after partial hepatectomy in mice. *Proc. Natl. Acad. Sci. U. S. A* 99:11181-11186.

Sudo, S., J.Kumagai, S.Nishi, S.Layfield, T.Ferraro, R.A.Bathgate, and A.J.Hsueh. 2003. H3 relaxin is a specific ligand for LGR7 and activates the receptor by interacting with both the ectodomain and the exoloop 2. *J. Biol. Chem.* 278:7855-7862.

Sugahara, K. and H.Kitagawa. 2000. Recent advances in the study of the biosynthesis and functions of sulfated glycosaminoglycans. *Curr. Opin. Struct. Biol.* 10:518-527.

Suzuki, S., K.Sano, and H.Tanihara. 1991. Diversity of the cadherin family: evidence for eight new cadherins in nervous tissue. *Cell Regul.* 2:261-270.

SWEAT, F., H.PUCHTLER, and S.I.ROSENTHAL. 1964. SIRIUS RED F3BA AS A STAIN FOR CONNECTIVE TISSUE. *Arch. Pathol.* 78:69-72.

Tacke, F., C.Liedtke, S.Bocklage, M.P.Manns, and C.Trautwein. 2005. CREB/PKA sensitive signalling pathways activate and maintain expression levels of the hepatitis B virus pre-S2/S promoter. *Gut* 54:1309-1317.

Takahra, T., D.E.Smart, F.Oakley, and D.A.Mann. 2004. Induction of myofibroblast MMP-9 transcription in three-dimensional collagen I gel cultures: regulation by NF-kappaB, AP-1 and Sp1. *Int. J. Biochem. Cell Biol.* 36:353-363.

Takashi, M., M.Igarashi, S.Hino, H.Musha, K.Takayasu, M.Arakawa, T.Nakashima, K.Ohnishi, and K.Okuda. 1985. Esophageal varices: correlation of left gastric venography and endoscopy in patients with portal hypertension. *Radiology* 155:327-331.

Teckman, J.H., J.K.An, S.Loethen, and D.H.Perlmutter. 2002. Fasting in alpha1-antitrypsin deficient liver: constitutive [correction of consultative] activation of autophagy. *Am. J. Physiol Gastrointest. Liver Physiol* 283:G1156-G1165.

Thurman, R.G. 2000. Sex-related liver injury due to alcohol involves activation of Kupffer cells by endotoxin. *Can. J Gastroenterol.* 14 Suppl D:129D-135D.

Tilg, H. 2001. Cytokines and liver diseases. *Can. J. Gastroenterol.* 15:661-668.

Timpl, R. 1996. Macromolecular organization of basement membranes. *Curr. Opin. Cell Biol.* 8:618-624.

Timpl, R. and J.C.Brown. 1996. Supramolecular assembly of basement membranes. *Bioessays* 18:123-132.

Toole, B.P., T.N.Wight, and M.I.Tammi. 2002. Hyaluronan-cell interactions in cancer and vascular disease. *J. Biol. Chem.* 277:4593-4596.

Toubia, N. and A.J.Sanyal. 2008. Portal hypertension and variceal hemorrhage. *Med. Clin. North Am.* 92:551-74, viii.

Trump, B.F., P.J.Goldblatt, and R.E.Stowell. 1965. Studies of necrosis in vitro of mouse hepatic parenchymal cells. Ultrastructural alterations in endoplasmic

reticulum, Golgi apparatus, plasma membrane, and lipid droplets. *Lab Invest* 14:2000-2028.

Tsukada, N., C.A.Ackerley, and M.J.Phillips. 1995. The structure and organization of the bile canalicular cytoskeleton with special reference to actin and actin-binding proteins. *Hepatology* 21:1106-1113.

Tsukamoto, H. and S.C.Lu. 2001. Current concepts in the pathogenesis of alcoholic liver injury. *FASEB J.* 15:1335-1349.

Turtinen, L.W., D.N.Prall, L.A.Bremer, R.E.Nauss, and S.C.Hartsel. 2004. Antibody array-generated profiles of cytokine release from THP-1 leukemic monocytes exposed to different amphotericin B formulations. *Antimicrob. Agents Chemother.* 48:396-403.

Ueberham, E., R.Low, U.Ueberham, K.Schonig, H.Bujard, and R.Gebhardt. 2003. Conditional tetracycline-regulated expression of TGF-beta1 in liver of transgenic mice leads to reversible intermediary fibrosis. *Hepatology* 37:1067-1078.

Ueno, T., P.Bioulac-Sage, C.Balabaud, and J.Rosenbaum. 2004. Innervation of the sinusoidal wall: regulation of the sinusoidal diameter. *Anat. Rec. A Discov. Mol. Cell Evol. Biol.* 280:868-873.

Ueno, T., M.Sata, R.Sakata, T.Torimura, M.Sakamoto, H.Sugawara, and K.Tanikawa. 1997. Hepatic stellate cells and intralobular innervation in human liver cirrhosis. *Hum. Pathol.* 28:953-959.

Ueno, T. and K.Tanikawa. 1997. Intralobular innervation and lipocyte contractility in the liver. *Nutrition* 13:141-148.

Unemori, E.N. and E.P.Amento. 1990. Relaxin modulates synthesis and secretion of procollagenase and collagen by human dermal fibroblasts. *J Biol Chem.* 265:10681-10685.

Unemori, E.N., L.B.Pickford, A.L.Salles, C.E.Piercy, B.H.Grove, M.E.Erikson, and E.P.Amento. 1996. Relaxin induces an extracellular matrix-degrading phenotype in human lung fibroblasts in vitro and inhibits lung fibrosis in a murine model in vivo. *J Clin Invest.* 98:2739-2745.

Urashima, S., M.Tsutsumi, K.Nakase, J.S.Wang, and A.Takada. 1993. Studies on capillarization of the hepatic sinusoids in alcoholic liver disease. *Alcohol Alcohol Suppl* 1B:77-84.

Van den Berg, G.B., T.J.Van Berkel, and J.F.Koster. 1980. The role of Ca2+ and cyclic AMP in the phosphorylation of rat-liver soluble proteins by endogenous protein kinases. *Eur. J. Biochem.* 113:131-140.

Vernon, R.B. and M.D.Gooden. 2002. An improved method for the collagen gel contraction assay. *In Vitro Cell Dev. Biol. Anim* 38:97-101.

Viitala, K., K.Makkonen, Y.Israel, T.Lehtimaki, O.Jaakkola, T.Koivula, J.E.Blake, and O.Niemela. 2000. Autoimmune responses against oxidant stress and acetaldehyde-derived epitopes in human alcohol consumers. *Alcohol Clin. Exp. Res.* 24:1103-1109.

Vu, T.H. and Z.Werb. 2000. Matrix metalloproteinases: effectors of development and normal physiology. *Genes Dev.* 14:2123-2133.

Walsh, M.P., G.J.Kargacin, J.Kendrick-Jones, and T.M.Lincoln. 1995. Intracellular mechanisms involved in the regulation of vascular smooth muscle tone. *Can. J. Physiol Pharmacol.* 73:565-573.

Wang, X.M., D.M.Yu, G.W.McCaughan, and M.D.Gorrell. 2005. Fibroblast activation protein increases apoptosis, cell adhesion, and migration by the LX-2 human stellate cell line. *Hepatology* 42:935-945.

Watson, M.R., K.Wallace, R.G.Gieling, D.M.Manas, E.Jaffray, R.T.Hay, D.A.Mann, and F.Oakley. 2008. NF-kappaB is a critical regulator of the survival of rodent and human hepatic myofibroblasts. *J. Hepatol.* 48:589-597.

Watt, F.M. and B.L.Hogan. 2000. Out of Eden: stem cells and their niches. *Science* 287:1427-1430.

Weissman, I.L. 2000. Stem cells: units of development, units of regeneration, and units in evolution. *Cell* 100:157-168.

Weissman, I.L., D.J.Anderson, and F.Gage. 2001. Stem and progenitor cells: origins, phenotypes, lineage commitments, and transdifferentiations. *Annu. Rev. Cell Dev. Biol.* 17:387-403.

Werner, S. and R.Grose. 2003. Regulation of wound healing by growth factors and cytokines. *Physiol Rev.* 83:835-870.

Whittaker, P., R.A.Kloner, D.R.Boughner, and J.G.Pickering. 1994. Quantitative assessment of myocardial collagen with picrosirius red staining and circularly polarized light. *Basic Res. Cardiol.* 89:397-410.

Williams, E.J., R.C.Benyon, N.Trim, R.Hadwin, B.H.Grove, M.J.Arthur, E.N.Unemori, and J.P.Iredale. 2001. Relaxin inhibits effective collagen deposition by cultured hepatic stellate cells and decreases rat liver fibrosis in vivo. *Gut* 49:577-583.

Williams, E.J. and J.P.Iredale. 1998. Liver cirrhosis. *Postgrad. Med J* 74:193-202.

Wilson, B.C. and A.J.Summerlee. 1994. Effects of exogenous relaxin on oxytocin and vasopressin release and the intramammary pressure response to central hyperosmotic challenge. *J Endocrinol* 141:75-80.

Wimalawansa, S.J. 2008. Nitric oxide: new evidence for novel therapeutic indications. *Expert. Opin. Pharmacother.* 9:1935-1954.

Winchester, G. 1983. p53 protein and control of growth. *Nature* 303:660-661.

Wyatt, T.A., J.H.Sisson, M.A.Forget, R.G.Bennett, F.G.Hamel, and J.R.Spurzem. 2002. Relaxin stimulates bronchial epithelial cell PKA activation, migration, and ciliary beating. *Exp. Biol. Med. (Maywood.)* 227:1047-1053.

Xu, L., A.Y.Hui, E.Albanis, M.J.Arthur, S.M.O'Byrne, W.S.Blaner, P.Mukherjee, S.L.Friedman, and F.J.Eng. 2005. Human hepatic stellate cell lines, LX-1 and LX-2: new tools for analysis of hepatic fibrosis. *Gut* 54:142-151.

Yanai, M., N.Tatsumi, N.Hasunuma, K.Katsu, F.Endo, and Y.Yokouchi. 2008. FGF signaling segregates biliary cell-lineage from chick hepatoblasts cooperatively with BMP4 and ECM components in vitro. *Dev. Dyn.* 237:1268-1283.

Yu, J.C., W.Li, L.M.Wang, A.Uren, J.H.Pierce, and M.A.Heidaran. 1995. Differential requirement of a motif within the carboxyl-terminal domain of alpha-platelet-derived growth factor (alpha PDGF) receptor for PDGF focus forming activity chemotaxis, or growth. *J. Biol. Chem.* 270:7033-7036.

Yuan, H.T., S.Venkatesha, B.Chan, U.Deutsch, T.Mammoto, V.P.Sukhatme, A.S.Woolf, and S.A.Karumanchi. 2007. Activation of the orphan endothelial receptor Tie1 modifies Tie2-mediated intracellular signaling and cell survival. *FASEB J.* 21:3171-3183.

Yuhas, J.M., R.E.Toya, and N.H.Pazmino. 1974. Neuraminidase and cell viability: failure to detect cytotoxic effects with dye-exclusion techniques. *J. Natl. Cancer Inst.* 53:465-468.

Zakhari, S. and T.K.Li. 2007. Determinants of alcohol use and abuse: Impact of quantity and frequency patterns on liver disease. *Hepatology* 46:2032-2039.

Zhang, J.X., W.Pegoli, Jr., and M.G.Clemens. 1994. Endothelin-1 induces direct constriction of hepatic sinusoids. *Am. J. Physiol* 266:G624-G632.

Zhao, L., P.J.Roche, J.M.Gunnersen, V.E.Hammond, G.W.Tregear, E.M.Wintour, and F.Beck. 1999. Mice without a functional relaxin gene are unable to deliver milk to their pups. *Endocrinology* 140:445-453.

Zhao, L., C.S.Samuel, G.W.Tregear, F.Beck, and E.M.Wintour. 2000. Collagen studies in late pregnant relaxin null mice. *Biol. Reprod.* 63:697-703.

Zhong, M., C.Y.Ku, and B.M.Sanborn. 2005. Pathways used by relaxin to regulate myometrial phospholipase C. *Ann. N. Y. Acad. Sci.* 1041:300-304.

Zhou, Q., T.Desta, M.Fenton, D.T.Graves, and S.Amar. 2005. Cytokine profiling of macrophages exposed to Porphyromonas gingivalis, its lipopolysaccharide, or its FimA protein. *Infect. Immun.* 73:935-943.

Zhou, X., F.R.Murphy, N.Gehdu, J.Zhang, J.P.Iredale, and R.C.Benyon. 2004. Engagement of alphavbeta3 integrin regulates proliferation and apoptosis of hepatic stellate cells. *J. Biol. Chem.* 279:23996-24006.

Bibliography

Annual Report of the Chief Medical Officer (2001), Department of Health.

Byers, P.H. 2000. The Metabolic and Molecular Basis of Inherited Disease, 8th edition, CR. Scriver, AL. Beaudet, WS. Sly, D Valle, B Childs, B Vogelstein, editors. McGraw-Hill, New York.

Chandrasoma, P. and C.Taylor. 1998. Concise Pathology. Lange.

Clark, R.A.F. 1996. The molecular and cellular biology of wound repair. R.A.F.Clark, editor. Plenum Press, New York.

Goss, R.J. 1992. Regeneration versus repair. WB Saunders, Philedelphia.

Kumar, V., A.K.Abbas, N.Fausto. 2005. Robbins and Cotran Pathologic Basis of Disease. WB Saunders, Philedelphia.